DEPARTMENT OF THE INTERIOR
UNITED STATES GEOLOGICAL SURVEY

1990 PROCEEDINGS OF THE

NATIONAL EARTHQUAKE PREDICTION EVALUATION COUNCIL

January 11-12, 1990
Berkeley, California

April 30 - May 1, 1990
Menlo Park, California

June 6, 1990
Menlo Park, California

by
Randall G. Updike

Open-File Report 90-722

This report is preliminary and has not been edited or reviewed for conformity with U.S. Geological Survey publication standards.

1990

TABLE OF CONTENTS

PREFACE

The National Earthquake Prediction Evaluation Council (NEPEC) was established in 1979 pursuant to the Earthquake Hazards Reduction Act of 1977 to advise the Director of the U.S. Geological Survey (USGS) in issuing any formal predictions or other information pertinent to the potential for the occurrence of a significant earthquake. It is the Director of the USGS who is responsible for the decision whether and when to issue such a prediction or information.

NEPEC, also referred to in this document as the Council, according to its charter is comprised of a Chairman, Vice-Chairman, and from 8 to 12 other members appointed by the Director of the USGS. The Chairman shall not be a USGS employee and at least one-half of the membership shall be other than USGS employees.

The USGS has published the proceedings of previous NEPEC meetings as open-file reports; these reports are available from the USGS Open-File Distribution Center in Denver, Colorado.

NATIONAL EARTHQUAKE PREDICTION EVALUATION COUNCIL

APPENDICES

NATIONAL EARTHQUAKE PREDICTION EVALUATION COUNCIL

PROCEEDINGS OF THE MEETING OF JANUARY 11-12, 1990

Berkeley, California

Council Members Present

Thomas McEvilly, Chairman	University of California
Robert Wesson, Vice-Chairman	USGS, Reston
Keiiti Aki	University of Southern California
William Bakun	USGS, Menlo Park
James Davis	California Division of Mines and Geology
James Dieterich	USGS, Menlo Park
Thomas Heaton	USGS, Pasadena
Arch Johnston	Memphis State University
Hiroo Kanamori	California Institute of Technology
William Prescott	USGS, Menlo Park
Kaye Shedlock	USGS, Golden
Ray Weldon	University of Oregon
Randall Updike, Exec. Secy.	USGS, Reston

Invited Participants

A. Bernardi	Teknekron Communications, Berkeley
Allin Cornell	Stanford University
Jack Healy	USGS, Menlo Park
David Hill	USGS, Menlo Park
Lucy Jones	USGS, Pasadena
John Langbein	USGS, Menlo Park
Al Lindh	USGS, Menlo Park
Paul Reasenberg	USGS, Menlo Park
David Schwartz	USGS, Menlo Park

JANUARY 11, 1990
Morning Session

T.McEVILLY, the new chairman of the National Earthquake Prediction Evaluation Council (NEPEC), opened the Council meeting by welcoming the new members as well as those continuing as members of the Council. All members were in attendance except J.Stock and J.Davies.

R.WESSON began the meeting by providing members with a brief history of NEPEC. The Council was formed was a direct outgrowth of the National Earthquake Hazards Reduction Program and specifically serves as an advisory council responsive to the Director of the U.S. Geological Survey (USGS). In the early years of its existence (late 1970's - early 1980's), the Council was primarily focused on reviewing earthquake predictions and quasi-predictions, under the chairmanship of Clarence Allen. Later, under the leadership of Lynn Sykes, NEPEC became more oriented to reviewing developments in earthquake predictions, both in terms of regional focus and topical work. Four regions were examined in detail: northern California, southern California, Alaska, and the Pacific Northwest. In addition, two outstanding roles played by NEPEC were in reviewing and recommending implementation of the Parkfield Prediction Experiment and the California Earthquake Probabilities Report (USGS Open-file Report 88-398).

Now entering its third era, under the leadership of Tom McEvilly, the newly convened Council is being asked to decide how active it should be. Should it review topical problems or continue to do regional studies? Should NEPEC consider public policy issues associated with earthquake predictions, and perhaps look at related hazards such as Mammoth Mountain, California? Should it begin to focus on another experiment in southern California along the pattern of the Parkfield array? We are beginning to see some real encouragement that we are gaining ground on earthquake predictions, based in part upon the experience we have had with the Loma Prieta earthquake. It is becoming more technologically feasible for us to make time-variable statements about earthquakes in specific regions.

T.McEVILLY thanked Wesson for the helpful summary. He made the point that, because of the Loma Prieta earthquake, the 1988 probabilities report, and the USGS stating a successful forecast of the event, NEPEC was now being put in a position of taking aggressive new steps in earthquake prediction evaluation.

K.AKI reminded the Council that NEPEC is an <u>evaluation</u> council, not a research or operational organization.

R.WESSON agreed. Predictions are formulated by researchers somewhere else, and NEPEC evaluates, e.g., the evaluation efforts of the Working Group for California Earthquake Probabilities. Meanwhile, operational kinds of things will have to be done by the USGS and other institutions. NEPEC will need to look at issues, scenarios, and documents that are concerned with time scales of years to months.

J.DAVIS believes that from the State of California perspective, NEPEC has been very successful. NEPEC can effectively assess what is being published in the technical literature. NEPEC played a key role in advising the USGS on what is needed to be done to make Parkfield operational. However, NEPEC cannot deal with short-term predictions, i.e., on a scale of hours to days in an extemporaneous manner; the Council is not geared for that.

J.DIETERICH agreed. One of the values of regional evaluations is that it brought NEPEC up to speed so that it can respond to predictions as they come up. NEPEC could not have undertaken the Working Group Report if it had not had the extensive background regional understanding. He felt that regional reviews should be continued.

T.HEATON felt it would be exceedingly helpful to the USGS and State of California to have some prearranged policy on how to respond in southern California in a manner similar to Parkfield. How to respond and what should be said need to be developed in advance instead of in an ad hoc manner during the crisis. There are still some long-term geologic problems on which NEPEC could offer some advice, e.g., the Los Angeles Basin deformation issue and how to deal with the Cascadia Subduction zone; particularly, NEPEC could help in dealing with local governments.

B.BAKUN reminded NEPEC that it has a lot of power in advising the USGS Director's office. It can offer good ideas and force actions to be taken by the USGS, e.g., Parkfield. Also, as a result of Parkfield, we have made a lot of progress in communicating with the public, the California Office of Emergency Services, and the local emergency-response community.

J.DAVIS recalled that NEPEC did review the Parkfield prediction in 1984, and the California Earthquake Prediction Evaluation Council also did so in 1985. Advisories from NEPEC stated that we should attempt to make a real-time prediction at Parkfield. We need to get ready for predictions that may be developed for other fault segments, and we need to preplan our advisories.

K.SHEDLOCK felt we need to be conscious of both our proactive function and reactive function. We review conclusions from studies in a particular region and then try to motivate further work to resolve questions. Also, she was curious about the results of the NEPEC review of Pacific Northwest which occurred over 2 years ago.

R.WESSON said that there was not sufficiently compelling evidence at that time to issue a statement for public concern for a major subduction zone earthquake.

R.WELDON indicated that Oregon needs to have some guidance from NEPEC on how to respond to the individual statements of researchers indicating specific risks in the State.

R.WESSON agreed, there has been a lot of new evidence that has come about since 1987 to make it appropriate to revisit the question of a major subduction zone earthquake in the Pacific Northwest.

A.JOHNSTON indicated that there is also a need to look at the Central United States. He suggests that as you go from West to East, from California to Wasatch to New Madrid, the data ranges from very good to very limited.

R.WESSON reminded NEPEC that from 1978 to present, several millions of dollars of effort have resulted in our ability to write the California probability report. So far, probability estimates in the Eastern United States are based on very limited research expenditures.

H.KANAMORI reiterated that NEPEC's traditional role has been to review regional earthquake predictions and that it is becoming more difficult, especially outside of California, for the Council to have sufficient expertise to do these reviews. He thinks we need to rely more on working groups in the various regions being addressed. Also, can we make our long-term and intermediate-term predictions more useful to hazard reduction, e.g., more practical applications, such as for engineers? How should we be using earthquake predictions to reduce the risk?

T.HEATON agreed that NEPEC has the opportunity to make policy statements based upon predictions and forecasts, i.e., to advise practicing engineers erecting buildings whose design lives are within the prediction time window.

J.DAVIS pointed out that NEPEC also can have an effect on the decisionmakers at Federal, State, and local levels.

R.WELDON would like to see an evaluation of current earthquake prediction methodologies. Just how good are our understandings of processes? What research is needed? What should be done to improve our abilities to issue forecasts or predictions?

J.HEALY was invited to give a summary of his views on the question, "Did the Soviets predict the Loma Prieta Earthquake?" He provided NEPEC with some supporting documentation (appendix A). He opened his presentation by summarizing the organization of the new Soviet research group "International Institute for the Theory of Earthquake Prediction and Mathematical Geophysics" which is led by V.Keilis-Borok (see NEPEC Proceedings, USGS Open-file Report 89-144). After extensive interaction with his Soviet colleagues, particularly V.Kossobokov, Healy felt he was able to give a summary of the Soviet prediction methodology known as "M8." If he were asked the question, "Did the Soviets predict the Loma Prieta earthquake?" he would answer in the affirmative, but felt we must be careful of terminology. The methods of the United States and Soviet Union are quite distinct. In the United States, all of our predictions are based on the concept that we first know the fault and the size of the potential earthquake before we attempt a prediction. The Soviets begin from an entirely different starting point; they predict the time without knowing the location. Therefore, we would generally not accept their work as a prediction.

The Soviet method depends upon an existing catalogue of earthquakes for a region. The Western United States probably has the best data set available anywhere in the world. Once the data is entered into the computer with the proper program, you give the magnitude you want to predict, and the algorithm gives you a radius. For example, at magnitude 7, the radius is 282 km. Then, we process the data for a series of diagnostic traits (the Soviets currently use 7). When 6 of the 7 traits are anomalous, a Time of Increased Probability (TIP) is declared, and this TIP remains on for 5 years or until the earthquake "closes" the TIP.

Next, Healy showed a series of viewgraphs which indicate: 1975, no TIP; 1976, no TIP; 1977, a TIP in northern California; 1978, TIP remains on; 1979, TIP remains on, and a second TIP appears in southern California; this TIP closed the same year by Imperial Valley earthquake; 1980, northern California TIP closed by Cape Mendocino earthquake; 1981, no TIP; 1982, no TIP; 1983, no TIP; 1984, no TIP; 1985, a TIP in northern California, region 5; 1986, TIP continues; 1987, TIP continues; 1988, TIP in region 6 added to continued TIP in region 5; 1989, both TIP's closed by Loma Prieta earthquake.

What Healy is suggesting is that he thinks the Soviets predicted three large earthquakes in California. If this method is used in conjunction with the U.S. methodology, the area of concern could be more focused in time and location. He doesn't know what to suggest about magnitude because various measures of magnitude (e.g., moment, surface) are used from the catalogue. Aftershock clusters are filtered out. The 1977 TIP in northern California was declared retrospectively in 1986, using the algorithm which was trained outside of California. The southern California TIP was declared by an earthquake that was questionably not large enough. The northern California TIP was declared before Loma Prieta, in 1985, (although there seemed to be some discussion by NEPEC members as to how this was actually publicized). For every 6 months, the computer program is run to review the existing TIPs. At the present time, there are no TIPs in California for M8.

There are two algorithms, M8 and CN. CN is more sophisticated, and Healy was not prepared to discuss it. The CN areas are so large that it is not a prediction for public response but a research prediction.

Healy has prepared a document for M8 which consists of a floppy disk plus the NEIS catalogue plus program documentation which he is offering to NEPEC. Regarding the question of probabilities, we cannot attach a definite probability to M8 predictions, but the Soviets claim about 80 percent success worldwide on retrospective tests and that they predicted in advance both Loma Prieta and Armenia. NEPEC members still question the actual successes of this method.

The traits used in the algorithm include:

1) Average of the 10 largest earthquakes/year.

2) Average of the 20 largest earthquakes/year.

3) Cumulative number of earthquakes (a moment deficit parameter).

4) A larger catalogue of the cumulative number of earthquakes.

5) A measure of the concentration of earthquakes.

6) A larger catalogue of trait #5.

7) A count of aftershocks.

At present, there is no M8 TIP in California for magnitude 7. For magnitude 7.5 there is a TIP, but Healy is not satisfied with it because the area is significantly larger (427 km radius) and application is unsatisfactory.

R.WESSON thanked J.Healy for his review and our Soviet colleagues for their diligence in working with us. NEPEC is glad to accept the documentation provided. He proposes that the document and disk be published as a USGS open-file report for U.S. scientists to individually test.

T.HEATON made the statement that there is no M8 magnitude 7 TIP, which says that no earthquake of this magnitude will occur in California this year or until such time as a TIP is declared.

A.LINDH believes that the algorithm and TIPs should be published in "Nature" or elsewhere so that the methodology is documented and can be tested.

B.BAKUN was invited to present a summary of the Loma Prieta earthquake; he used figures found in USGS Circular 1045, "Lessons Learned from the Loma Prieta, California, Earthquake of October 17, 1989." Some points he made were:

- Southern 45 km of 1906 break.
- First break to occur on the 1906 rupture zone.
- Largest earthquake on the San Andreas fault since 1906.

- o Right lateral slip, southwest dipping with 1.9 m right lateral displacement and 1.3 m southwest thrust over northeast side.
- o Occurs on a jog in the fault trace which tends to cause the southwest side to ride up over the northeast side.
- o Mainshock at the base and in the middle of the rupture zone and rupture was bilateral and upward.
- o Aftershock zone dips 75 degrees southwest.
- o Rupture zone extends from a depth of 18 km up to within 4-5 km of the surface.
- o The rupture was over a wide zone and may involve the Sargent and Zyante faults.
- o Seismicity along the San Andreas fault prior to this earthquake showed a gap in seismicity similar to Parkfield; this zone filled in by earthquake and may be a future tool for looking at other parts of faults in the Bay area.
- o Focal mechanisms of aftershocks are in all different directions suggesting they may be off the main fault.

R.WESSON suggested looking retrospectively at this earthquake, back past the Lake Elsman I and II, back to 1906. The Corralitos earthquakes in the 1960's to the south of Loma Prieta were, at the time, the most northern significant earthquakes of the San Andreas fault as far back as the 1906 event. If we had been capable of making short-term forecasts at that time, would we have issued advisories after those events too? If we had, there would have been no follow-on events; thus, we should not become too overconfident of our current abilities.

A.LINDH was asked to give a brief presentation to address the question: Did we forecast the Loma Prieta earthquake? He began by showing space-time plots for northern California which indicate that the seismic cycle is still very valid, and he points to the significant difference in regional seismicity before and after 1906. He asks, does the increased seismicity in the past 10 years indicate that there is an increased likelihood of a big earthquake in the next 10 years, as per seismic cycle? He points to several significant earthquakes in the last 10 years in a region where no 5.5 or larger earthquake had previously occurred back to 1914. He reiterated Bakun by making the point that microseismicity is a very valuable tool for defining segments of Bay area faults.

T.HEATON questioned whether we know confidently that the Loma Prieta earthquake was actually on the San Andreas or may instead have been on a steeply dipping subsidiary fault. For example, Loma Prieta could have been a thousand-year event on some other fault rather than the characteristic Santa Cruz segment earthquake.

A discussion followed regarding rates of uplift and erosion relative to the displacement observed in this earthquake. Are we clinging a bit too hard to the characteristic earthquake idea for a given fault segment? Specifically, can the earthquakes of 1865 and 1989 be compared? The distinct characteristics attributed to Parkfield earthquakes are not a concept being rigidly applied elsewhere.

J.DIETERICH reiterated that this was complicated fault movement, and it is not hard to imagine slip through this zone occurring along a lot of subsidiary faults.

T.HEATON restated the point he was making was that this was not necessarily on the primary San Andreas fault but instead on a subsidiary oblique slip fault.

J.DAVIS and **J.DIETERICH** agreed that the point is that strain release along this segment of the fault zone has been accomplished, and strain release is the most important issue.

H.KANAMORI felt we should face the possibility of variability in style of rupture which bears that the characteristic slip may be different, and this could have bearing on our probability of recurrence. We may not be able to rely on our simple model arguments.

A.LINDH pointed to the Thatcher diagram of the 1906 earthquake showing strain along the fault and indicated that the important data point is the Wright Tunnel. He compared drawing the end points of the segment according to Sykes, Nishenko, and Scholz versus Thatcher and Lisowski. He felt that the only valid number for measured offset is Wright Tunnel, and when you divide offset by slip rate, you get the estimate of when Loma Prieta occurred.

W.PRESCOTT questioned why Wright Tunnel is given more credible weight than surface features. Wright Tunnel is only one data point, and it could have been a landslide.

A.LINDH presented figures to show that Loma Prieta falls into his proposed seismic cycle. Using the Berkeley Catalogue, there was an increase of seismic activity beginning in the 1950's. He showed a series of illustrations of various researchers showing the evolution of probability estimates of an earthquake on this segment over the past 2 decades.

W.PRESCOTT disputed that the slip measurement from 1906 was accurate because Wright Tunnel should be considered a surface value. We may have ended up with the right interpretation for the wrong reasons.

J.DAVIS reminded the Council that in the Working Group Report, this segment is given a level E quality; the quality of our success might also be judged as E.

JANUARY 11, 1990
Afternoon Session

A.BERNARDI (Teknekron Communications, Berkeley) was invited to summarize ultra-low frequency (ULF) electromagnetic observations he made prior to the Loma Prieta earthquake. His research is supported by the Office of Naval Research for possible application to Submarine Observational systems. Particularly, he is measuring electromagnetic noise or "atmospherichess." Two observational stations are in operation: 10 hertz to 32 kilohertz (Stanford campus) and 0.01 hertz to 10 hertz (Corralitos). They have been operating the Corralitos station for about 2 years. Normally what is measured are very weak signals caused by the incidence of solar wind which causes changes in the magnetic field of the Earth. The daily variation is generally in a predictable range. This monitoring system is simple, consisting of an electromagnetic coil about 2 m long with a data logging system which records information every half hour. The record anomalies began in mid-September when irregularities were noted in two frequency bands. On October 5, substantial increase in noise was recorded over the entire range of ULF operation. One day before the earthquake there was an anomalous drop in background noise in the range of 0.2 to 5 Hz. At the preassigned recording time, at 3 hours before the earthquake, there was an exceptionally large increase in noise in the 0.01 to 0.5 Hz range. Thereafter, power went down after 5:00 p.m. due to the earthquake. Nothing seems to have been happening in the upper atmosphere that could account for this anomalous activity in terms of magnetic field fluctuations from solar sources. When the system was brought back on line, records were examined for aftershock correlation; none was observed. The suggestion is made that the observation 3 hours before the earthquake could have been an electromagnetic precursor.

This is a low-budget system costing about $6,000 per station. The USGS is interested in acquiring and testing this system and hopes to deploy three at Parkfield.

J.LANGBEIN presented a status report on the geodetic array deployed across the San Andreas fault after the Loma Prieta earthquake. One week following the earthquake, he deployed an array in the Los Gatos-Saratoga area to look for post-seismic slip. The net is not particularly robust because of geographic and vegetation limitations of line-of-sight for the 2-color geodimeter. So far there have been two sets of measurements, one at installation, the other last week. The two sets indicate that the south line has shortened by about 4 mm, the northwest directed line extended by about 4 mm, which together are a raw slip rate equal to 30 mm/year. The line perpendicular to the fault shows no change.

W.PRESCOTT said that the Black Mountain geodetic network has not been remeasured but soon will be. The accuracy of the Loma Prieta network is not as precise as Langbein's, and preliminary data does not show this strain. He finds this new data very surprising, and it appears to be strain not creep. The concern is whether this is a coseismic event or whether this segment decided to start creeping and loading the Peninsula segment. If it is simply a coseismic creep event, we won't be able to do much with it; if it indicates a creep rate change, it will be very significant for future study.

W.THATCHER emphasized that John's net is within a few kilometers of the northern end of the rupture zone of Loma Prieta.

J.LANGBEIN said he will probably resurvey these lines every 2-3 months.

J.DIETERICH was asked to give a status report on the new Working Group for San Francisco Bay area earthquake probabilities. The Working Group was organized in the aftermath of the Loma Prieta earthquake. A list of participants on the Working Group was given (see appendix). The group's charge was to review and revise the probabilities for the Bay area as presented in Open-file Report 88-398. Some questions the Working Group will address are:

1) Has the occurrence of Loma Prieta changed any interpretations we had that pertain to probabilities in the Bay area?

2) Has the earthquake caused any physical changes that would alter the probabilities, e.g., has the probability for the Santa Cruz segment been lowered?

3) Was there a stress change in the area?

4) Some new data have been generated for faults in the Bay area since the previous report and need to be incorporated.

5) Are there any improvements we can make in our methodology?

The group has had three meetings to date, December 1 & 19, 1989, and January 8, 1990. No preliminary report is available; this meeting will be a progress report.

A.CORNELL (Stanford University) discussed revisions of the Working Group methodology. Two basic considerations in evaluating the methodology are:

1) What probabilistic models are available?

2) What are the statistical (parametric) uncertainties of those models?

He followed by offering a discussion of the statistical model used by the previous Working Group and some improvements that are being made with the kind of information we have on Bay area segments, i.e., one previous event, the dominant uncertainty is the slip in the last event. In contrast to the previous method, which basically divides "previous slip" by "slip rate" to estimate time to next event, a stronger model is the "time predictable model" which says, if you can tell me the amount of slip since the last event, I can tell you the time to the next event.

Since we have rather large parametric uncertainties of long-term slip rates, there is probably not much difference in using the simple model or time-predictable model.

There are some limitations in our models because segments interact (overlap, may trigger one another), and stress may be loaded or released by adjacent segments, i.e., mechanics of system may interfere with the model. The time-predictable model fails to capture these interaction effects. He then discussed criticisms offered by Davis, Jackson, and Kagan (BSSA, October 1989) and Savage (draft, 1990) of the Working Group methodology.

The Working Group will be using some improvements in the statistical model. The group will:

1) Be more careful about the assumptions used.

2) Employ logic trees, which is a way to try to display the debate going on in the group in which they do not know for sure which hypothesis holds about the elements of the problem being discussed.

3) Deal with the parametric uncertainties being employed.

4) Make some effort to consider the interaction of segments.

D.SCHWARTZ gave preliminary results of where we stand in our understanding of the faults in the Bay area. He reviewed interpretations used in the 1988 report. Since then, Lienkaemper and Williams have been working on the Hayward fault. The earthquake of 1868 ruptured a 40-km segment. At the north end of this rupture, at Lake Chabot, a bend in the fault may account for the end of rupture. From San Leandro to Warm Springs, there was continuous rupture in 1868. The 1836 earthquake may have involved the Hayward fault north from the northern end of the 1868 rupture.

J.DIETERICH mentioned there may be some historic information from Spanish archives about the 1836 event which has not been studied.

D.SCHWARTZ said Lienkaemper suggests stopping the 1836 and 1868 ruptures at the bend. Segmentation in the 1988 report simply split the 100-km length of fault into two equal parts. At the southern end, there is a change in complexity of the Hayward fault, becoming broader and more diffuse, and Lienkaemper does not see evidence of creep south of there. He estimates creep of 5-6 mm/year, up to 8-10 mm/year at the south end (Warm Springs) and south of there, no evidence of creep. He also sees no surface fault south of Warm Springs.

R.WELDON questioned the uncertainty of the segmentation model of the Hayward fault, which was followed by Council discussion of the various uncertainties of magnitude, length of previous rupture, amount of offsets in 1868, etc.

D.SCHWARTZ believes we can hang our hat on the 1868 rupture length and summarize J.Lienkaemper's work on displaced alluvial fans. The initial results suggest slip rates for

14,000 years of 7-10 mm/year. This is the first firm estimate of geologic slip rate. Combined with a creep rate of 0-10 mm/year to the south and geodetic data of 10 mm/year, the group selected 9 mm/year, which is a step up in our understanding of the Hayward fault. The Rogers Creek fault is an extension of the Hayward fault to the north, on the north side of San Pablo Bay and up to Santa Rosa. It shows:

1) No surface creep.

2) About 6 km of stepover from Hayward fault.

3) Absence of microearthquake activity.

Karen Budding and Schwartz have been working on this fault, which they conclude is a locked fault. Results of their work at trench sites are:

Minimum slip rate:	4-5.5 mm/year (over 1270 years)
Slip per event:	2 m/event (but we don't know when)
Recurrence interval:	256-620 years
Minimum elapsed time since last earthquake:	181 years

He then made some comments regarding the Bay area San Andreas fault segments.

The 1988 report used the following parameters:

	Peninsula segment:	Santa Cruz:
1906 slip	2.5 ± 0.6	2.0 ± 0.5
Length	90 km	30 km
Slip rate	16 ± 2.5	16 ± 2.5

One of the important new concerns regards the model of segmentation. He pointed to the importance of the Crystal Springs reservoir on this question. The geometry, structure, slip step, geodetic data, and microseismicity make this a segment boundary, but it may continue to Daly City. Also, perhaps a segment exists from Lexington Reservoir to Black Mountain.

T.HEATON asked if the North Coast segment is being reevaluated.

D.SCHWARTZ said they are not going to look at it again.

T.HEATON was concerned about saying that the probability is so low for that segment that it is not worth worrying about.

R.WELDON agreed that there could be a repeat of large events in a relatively short time interval.

A discussion of various aspects of the Bay area fault segments followed.

H.KANAMORI opened a discussion of uncertainties of slip rates. He questioned whether there should be a new representation of the uncertainties in the report in the form of error bars, which he followed by comments on the real usefulness of the Probability approach in a report for public consumption.

J.DIETERICH then summarized similarities and differences of new probabilities compared with the 1988 report. A guiding philosophy has been that we do not want the probabilities to bounce around over the years because of a difference of composition of the Working Group. We are looking for good reasons to make a change from the 1988 report. The probabilities comparisons are provided in the handout (see appendix), but keep in mind these are preliminary and may change in coming weeks.

The significant changes in the new review are:

1) Southern Hayward probability was pushed up by the new slip rates.

2) Aggregate probability included Peninsula, San Andreas, N. Hayward, S. Hayward in 1988, and now has the Rogers Creek fault added in.

We are pushing the data and the model to their limits. One of the things that drove the Working Group to work on an emergency basis has been the historic earthquakes of the 1800's which occurred in pairs:

1836 Hayward	1838 San Andreas
1865 San Andreas	1868 Hayward

Probabilities may be higher if there is a validity to the pairing pattern in the 1800's.

Preliminary conclusions are given in the appendix.

R.WESSON asked two basic questions:

1) Is the expectation of completion of the preliminary report within the next 2 months acceptable?

2) What is the desire of NEPEC for a more detailed study prompted by the

preliminary report?

B.BAKUN asked if the report is going to say something about the concept of how the Loma Prieta earthquake has possibly loaded the Peninsula segment. There is a need to address the question in the report.

A discussion followed with the general agreement and anticipation that something will be said about the stress on adjacent segments and paired events.

J.DIETERICH suggested that we might need to have a standing Working Group to deal with the Bay area as new data and concepts develop.

JANUARY 12, 1990
Morning Session

P.REASENBERG was invited to give a summary of the statistical model for the aftershock probabilities technique and how it can be applied. There have been three applications of the model in 1989:

1) The Brawley swarm (described in Science handout).

2) Lake Elsman earthquake in August with advisory issued by the State.

3) Loma Prieta sequence.

He offered some comments about Loma Prieta. The smoothness of forecasts through time was interrupted by a couple of jumps due to:

1) Artificial effect of analyzing a numerical function used within the method at 1, 3, 10 days; this will be changed to a continuous adjustment.

2) The calculated magnitude of the mainshock changed the day after the earthquake.

3) Aftershock sequence characteristics changed, starting off quietly followed by a surge of moderate aftershocks.

4) Our choice of how to portray forecasts changed, started out with 1-day interval for M5 and M6 earthquakes during the first 4 days, then switched to 1 day and next 2 months for the next 25 days. He suggests a uniform forecasting of 1 week and 2-3 months.

He offered several applications of the method:

1) After a moderate earthquake, the probability of a larger earthquake (e.g., Brawley swarm).

2) After a strong earthquake, the probability of strong aftershocks.

3) After a strong earthquake, the probability of an even stronger follow-on earthquake.

4) Following a strong earthquake, the expectations for further activity for planning, field studies, and instrument deployment.

5) The generic model can be a contribution to response plan scenarios.

Some policy issues were raised:

1) In what situation should short-term probability be released, and to whom?

2) How should forecasts be issued; what kind of timing, wording, and frequency?

3) How should we issue them consistently and with sufficient explanation?

4) When do we stop issuing forecasts?

R.WESSON raised a concern about utilizing a real-time model that is changing with the events versus a generic model, as it affects public awareness in terms of consistency through time.

P.REASENBERG said that if we had stayed with the generic model, our forecasts of large aftershocks would have been about 5 times higher.

R.WESSON suggested that maybe we haven't trained the model enough on large magnitude earthquakes to use the real-time model and should stick with the more robust generic model.

T.HEATON asked what the long-term Loma Prieta aftershock probability given to State?

P.REASENBERG
M7 in 1 year, based on Loma Prieta model=1.0%, beginning 1/1/90.
M7 in 1 year, based on generic model=1.5%, beginning 1/1/90.
M7 20% in 30 years, or 0.67% per year.

J.DIETERICH found this model was very useful for the public in the aftermath of the earthquake.

A discussion followed on the merits of the generic versus the real-time models.

J.DAVIS briefly described the findings of D.Mileti regarding the social impact of these advisories. Three groups of public reaction:

1) Disregarded because already saturated with information.

2) Assimilation of this information into a form personally useful.

3) Denied because didn't want to acknowledge continued hazard.

R.WESSON recommended we:

1) Continue to do what we have been doing.

2) Decide on a policy of what we are going to say during event.

3) Run the model further; discuss again at the next NEPEC meeting, and fine tune the approach.

NEPEC was in general agreement that this was a very useful model to be applying in significant earthquakes and concluded that Reasenberg should come up with a standardized advisory, get review/comments, then bring it back to the next NEPEC meeting for discussion.

B.BAKUN summarized his concerns regarding earthquake alerts and response plans. The success of the plan developed for Parkfield is prompting use in other areas. Can we use the same terms and methodology in other areas so that there can be some consistency of message and understanding by the public? He reviewed the development of the Parkfield Plan. An important question in developing a plan is who are you writing it for? Write it for yourself. It must be clear and specific so it can be operated without mistake. Use of alert levels is an effective way of triggering a certain response. In terms of using response plans in other areas, how are we going to design the alert levels for consistency?

At Parkfield, only "A" level triggers a public warning, that is, a prediction occurs. At "B" level, there is only a scientific warning. To date, neither "A" nor "B" levels have occurred. When you do a plan, are you doing a probability alert or a response? We have had about 60 "D" and 20 "C" level alerts to date at Parkfield.

L.JONES was invited to explain her method of formulating prediction probabilities from foreshocks. She uses foreshocks within 3 days of the mainshock. She recognizes three types of events in the probability theory:

1) Background earthquakes.

2) Foreshocks of mainshock.

3) Characteristic mainshock.

She presented a summary of the probability statistics methodology she is using for foreshock predictions (see appendix H). For southern California, she lists the probability of the characteristic earthquake occurring within 3 days of what is potentially a foreshock. Three different foreshock magnitudes for each southern San Andreas fault segment are listed:

Segment	Probability level		
	10-30%	1-10%	0.1-1%
(suggested alert level)	(B)	(C)	(D)
San Bernardino	5.9	4.9	3.8
San Gorginio	6.4	5.3	4.2
Coachella Valley	5.9	4.7	3.6

And magnitudes for potential foreshocks for the San Jacinto fault:

Segment	Probability level		
	10-30%	1-10%	0.1-1%
(suggested alert level)	(B)	(C)	(D)
San Bernardino	5.8	4.8	3.8
San Jacinto Valley	5.7	4.6	3.6
Anza	6.1	5.0	3.9
Borrego	5.5	4.5	3.5

And for Parkfield:

Segment	Probability level		
	10-30%	1-10%	0.1-1%
(suggested alert level)	(B)	(C)	(D)
Parkfield	4.6	3.8	2.3

Characteristic earthquakes followed those given in the 1988 Working Group report. The larger the magnitude of a background earthquake, the more likely it is a foreshock of a mainshock and, therefore, the higher probability and alert level results.

J.DIETERICH was concerned that foreshocks to characteristic earthquakes are a separate class to background earthquakes.

T.HEATON replied that this is a statistical function, not a physical function; there is a population of background earthquakes that turn out to be foreshocks and no physical difference is inferred.

L.JONES said the alert levels being used are tied to probabilities. There are other physical circumstances where activity could change months before the mainshock, but that is a different phenomenon than is being considered here (references to Australian earthquakes and Loma Prieta-Lake Elsman). She is only dealing with immediate foreshocks as part of a foreshock-mainshock-aftershock cluster.

R.WESSON asked if we should move toward using this technique as an alert plan for OES's use or should it continue as a research effort?

B.BAKUN questioned if we can use this approach in a response plan since it is tied to probabilities rather than to specific signals. He is concerned that there is not a consistency of what alert levels mean; they mean different things in different methods.

R.WELDON wondered if the intent of the alerts is strictly to advise the public or if it is also intended to notify the scientists so that they can make special plans in advance of the earthquake.

B.BAKUN said that the scientific aspect is built into the alerts but is not the main reason.

D.HILL came to address NEPEC about the Long Valley volcanic problem and ask how the experience of Parkfield-type alerts can perhaps be employed at Long Valley. Since 1979 there has been a high level of activity at Long Valley. He summarized the seismic activity of the caldera and surrounding region which is one of the most productive earthquake areas in California. Accompanying the earthquakes is uplift from 1979, up to 25 cm in one year. They saw no activity prior to the last decade. He summarized the warnings beginning in the 1980 earthquakes; after the third M6, the USGS issued a "watch." Activity of the area continued, and the USGS issued the lowest level of "notice of volcanic activity." The local officials are now asking for an alert system that they can use more effectively. Hill is trying to adapt Parkfield to a volcanic area that we have never seen erupt. It is difficult to establish the criteria for alert levels. What do we do for an "A" level alert? We can get some information from the other volcanic centers, but we have never seen a caldera-type eruption like this any place in the world.

The alerts applied to this area may serve as a template for other volcanic centers.

R.WESSON said we have some informal systems working at the Cascades and in Alaska but nothing like what we are after at Long Valley.

H.KANAMORI cautioned we may be making up alert levels which are based on no prior activity to use as data. Can we really use the Parkfield approach? We are dealing with a very different situation.

J.DAVIS suggested that volcanologists use a sequence that goes from repose to unrest to eruption. It seems that the transition criteria to go to from unrest to eruption is important. We will be forced to use a group of criteria which are approximate and qualitative. Discussion followed on how alerts on earthquakes and volcanoes are similar and different.

B.BAKUN reiterated that we need advice from NEPEC as to whether a uniform alert level can be applied to the various hazard areas.

JANUARY 12, 1990
Afternoon Session

R.WESSON raised the issue of whether we should focus on other regions including New Madrid, Wasatch of Utah, Hawaii, and perhaps the Northeast. There are perplexing issues arising regarding the midcontinent.

J.DIETERICH would like to make a case from Hawaii. After Alaska and California, it is one of the most active areas in the country. There are some forecasts in print. An alternative may be a USGS "Red Book" conference.

R.WESSON will explore the possibility of convening a Red Book conference on the earthquake hazards and predictions of Hawaii.

After extensive discussion there was general agreement that the future agenda for NEPEC will tentatively be:

Spring 1990
Review of Bay area probability report revision from the Working Group.

Fall 1990
Focus on items of investigation which could be pursued to add light on a probabilistic evaluation of the New Madrid region.

Winter 1990-91
Southern California and Los Angeles basin.

Mid-year 1991
Hawaiian Red Book Conference

Fall 1991
Wasatch fault, Utah

J.DIETERICH summarized the issues related to the Bay area Working Group and sought guidance from NEPEC regarding recommendations to take back to the group. He offered the following considerations:

1) Revised interpretations of data as a result of the Loma Prieta earthquake.

2) Physical changes in the Bay area resulting from the earthquake.

3) Seismicity patterns of the 1800's and the issue of paired earthquakes.

4) New data on faults of the San Francisco Bay region obtained since the 1988 report was produced.

5) Consider possible improvements in the methodology used by the group such as the logic tree approach.

Items 1, 3, and 4 are the easiest to address.

R.WESSON was somewhat disappointed that the Working Group is not going to be able to convey our concern for increased hazards in the Bay area as a result of the Loma Prieta earthquake. Can the Working Group make some kind of qualitative statement?

A.JOHNSTON thought it would be a mistake to push the report through without looking at a possible increase in earthquake probability for the Peninsula segment.

J.DIETERICH said the Working Group is divided between those who are mildly of the view of an elevated hazard because of Loma Prieta and those who are of the strong opinion that there is no increase in probability. Actually, for the entire Bay area, the probability will remain as it was reported yesterday. We don't want to revise the original report without good evidence to support it.

R.WESSON asked if there was a way to use the logic tree approach to look at the paired events issue and the question of stress changes related to Loma Prieta?

J.DIETERICH suggested that one way to approach this is that NEPEC request the Working Group to address:

1) Truncated logic tree to look at our perception of the existing data on the Peninsula segment in light of what we learned from the Loma Prieta earthquake.

2) Truncated logic tree to capture the sense of probability change as a result of Loma Prieta (stress effects and paired events).

3) Recommendations about what work should be done next.

Tentatively, the deadline for the draft report will coincide with the scheduling of the next NEPEC meeting, mid-March to beginning of April. It would be most valuable if we could have a rough draft report before the Congressional hearings where Loma Prieta will be discussed.

R.WESSON sought views on how to proceed on earthquake alert protocols including Coachella Valley, Long Valley, and the Bay area. Is it premature to have a Parkfield-type response plan? Or follow ideas suggested by L.Jones?

Extended discussion followed which generally supported the idea that the alerts should be for response purposes. The characteristics may be different for various fault segments, but the implications will be the same for each alert level.

R.WESSON asked if it was possible to prepare a draft plan for Coachella Valley based on a cross-fertilization of the Parkfield methodology with the L.Jones - D.Agnew Working Group methodology which employs probabilities in alert levels.

B.BAKUN thought it might be possible.

R.WESSON announced that E.Roeloffs, USGS Branch of Tectonophysics in Menlo Park, will take over as chief scientist of the Parkfield prediction experiment, replacing A.Lindh, who is becoming more involved in the Bay area faults. T.McEvilly tentatively set the time for the next NEPEC meeting to be the first week in April in Menlo Park.

NATIONAL EARTHQUAKE PREDICTION EVALUATION COUNCIL

PROCEEDINGS OF THE MEETING OF APRIL 30 - MAY 1, 1990

Menlo Park, California

Council Members Present

Thomas McEvilly, Chairman	University of California
Robert Wesson, Vice-Chairman	USGS, Reston
William Bakun	USGS, Menlo Park
James Davis	California Division of Mines and Geology
John Davies	University of Alaska, Geophysical Institute
James Dieterich	USGS, Menlo Park
Thomas Heaton	USGS, Pasadena
Arch Johnston	Memphis State University
Hiroo Kanamori	California Institute of Technology
Kaye Shedlock	USGS, Golden
Joann Stock	Harvard University
Ray Weldon	University of Oregon
Randall Updike, Exec. Secy.	USGS, Reston

Invited Participants

Allin Cornell	Stanford University
Richard Eisner	Bay Area Regional Earthquake Preparedness Project
William Ellsworth	USGS, Menlo Park
Al Lindh	USGS, Menlo Park
Nicholas Nikas	FEMA, Region IX
John Savage	USGS, Menlo Park
David Schwartz	USGS, Menlo Park
Wayne Thatcher	USGS, Menlo Park
Thomas Tobin	California Seismic Safety Commission

APRIL 30, 1990
Morning Session

T.McEVILLY opened the meeting by noting that all members of the Council were present with the exception of W.Prescott and K.Aki. A.Lindh, D.Schwartz, A.Cornell, W.Ellsworth, and W.Thatcher were in attendance representing the Working Group on Bay Area Earthquake Probabilities.

J.DIETERICH, chairman of the Working Group, began the meeting by discussing the "bottom line" conclusions of the Working Group, which was charged with conducting a new evaluation of the probabilities for earthquakes in the San Francisco Bay region. The segments considered were:

1) North Coast segment, San Andreas fault.

2) San Francisco Peninsula segment, San Andreas fault (considering both rupture of entire segment and broken into two subsegments).

3) Southern Santa Cruz Mountain segment, San Andreas fault.

4) Southern East Bay segment, Hayward fault.

5) Northern East Bay segment, Hayward fault.

6) Rodgers Creek fault.

(Note: A draft of the report was distributed to the Council prior to the meeting.)

The Working Group was charged with this new evaluation due to:

1) New data that has been obtained on various fault segments in the past 2 years since the release of the first probabilities report.

2) The concern that regional stress patterns may have changed due to the Loma Prieta earthquake in 1989.

3) Historic seismicity patterns of the 1800's as contrasted and compared with current activity.

4) New information and methods for evaluating the existing data.

The principal revisions include:

1) San Andreas fault slip rate was revised upward from 16 to 19 mm/year.

2) Logic tree analyses used.

3) Consideration of increased stress on the San Andreas fault resulting from the Loma Prieta earthquake.

4) Hayward fault slip rate was revised upward from 7.5 to 9 mm/year.

5) Rodgers Creek was evaluated.

6) Incorporated uncertainties into probability determinations.

A discussion followed as to the function of NEPEC with respect to the current report and its relationship to the previous report. NEPEC is to review the new report and provide recommendations to the Director of the USGS regarding its release and use by the public.

J.DAVIS suggested that, as was the case with the first report, the California Earthquake Prediction Evaluation Council (CEPEC) should also review this new report in order to advise the State of California. The Council agreed that this should happen within the next month.

A.CORNELL presented a discussion of the methodology used in the new report, emphasizing that the approach is the same as the previous report with some substantial enhancements of that approach. He discussed in some detail the statistics used, particularly focusing on the intrinsic and parametric uncertainties. There was an extended interaction of Cornell with the Council on details of the use of data and the methodology. The methodology is summarized in appendix L.

J.DIETERICH summarized the logic tree method used for the San Andreas fault (SAF), which was an outgrowth of recommendations at the last NEPEC meeting. The logic tree approach allowed weighting of different interpretations on three aspects of the probabilities calculations:

1) Segmentation models.

2) Recurrence time models.

3) Effect of stress changes on elapsed time.

Details of this part of the report are provided in appendix M.

R.WELDON questioned the slip rates used by the Working Group and how serious an impact the uncertainties in slip rates have upon the weighting of the logic tree and the resulting calculations.

J.DIETERICH went through the details of the logic tree (appendix M, figure B-1). He then discussed the stress calculations which he did with R.Simpson (USGS-Menlo Park). These calculations were originally going to be incorporated as an appendix to the current report, but it has been decided that these calculations will be published by Dieterich and Simpson as a separate open-file report, which will be released prior to release of the probabilities report. He emphasized that there are uncertainties in the stressing rate on the individual fault segments (Mid-Peninsula, northern Santa Cruz Mountains, and San Francisco Peninsula segment models). Several members of the Council discussed the implications of the weighting of the logic tree based upon the stress calculations.

Dieterich then discussed how the final probabilities resulting from the logic tree approach were affected by various weighting factors (appendix M). Extensive discussion by the Council focused on the concern that breaking out smaller fault segments of the San Andreas can reduce the probabilities for large earthquakes on major segments. Dieterich showed that the report will provide the quartile probabilities on the conditional probability for each segment (table C-2).

For the Hayward fault, the major revision was in slip rate, from 7.5 to 9 mm/year based on J.Lienkaemper data. An extended discussion by the Council followed, focused on the assumptions in segmentation of the fault and decisions on selection of slip rates, based upon surface creep rates. They assumed that the fault is creeping at the surface but locked at depth. Alternatively, maybe the Hayward fault is in some type of afterslip mechanism from the 1868 event.

R.WESSON introduced the contrasts between the Rodgers Creek and Hayward fault, including no observed creep or seismicity on the Rodgers Creek and the apparent stepover from the Hayward to Rodgers Creek fault in the San Pablo Bay area.

The Council discussed the Hayward fault, including surface rupture in the 1800's and changes in the segmentation of the fault used in the current study.

W.BAKUN introduced his concern regarding the Working Group's seemingly arbitrary change in the relative lengths of the two segments of the Hayward fault as compared to the previous report. He feels some statement is needed to indicate why that change was made.

R.WELDON raised the question of the validity of the strain rate that was used for the Rodgers Creek fault as an extension of the value determined for the southern Hayward fault. Discussion of the validity and supporting evidence followed.

J.DIETERICH presented the "bottom line" comparison of the 1988 report with the present report:

	M	5yr	10yr	20yr	30yr
1988					
San Francisco Peninsula segment of the San Andreas, North and South East Bay segments of the Hayward fault	7	0.1	0.2	0.3	0.5
1990					
Same as above plus the Rodgers Creek fault	7	0.1	0.3	0.5	0.7

D. SCHWARTZ summarized what is currently known about the Rodgers Creek fault, particularly what has been found since the previous report was prepared.

T.McEVILLY asked what the essence of changes are in the new report, which, if dropped, would take us back to the 1988 probabilities.

J.DIETERICH summarized that we would be back to the 1988 values if:

1) Change the San Andreas fault slip rate from 19 back to 16 mm/yr.

2) Change the Hayward fault slip rate from 9 back to 7.5 mm/yr.

3) Displacement from 1.5 back to 1.4 m for Hayward fault.

4) Drop the Rodgers Creek fault.

About half of that difference is due to the Rodgers Creek fault and the remainder due to the other factors. One final issue is that we now have 19 plus 9 mm of slip that we are accounting for in the Bay area across the SAF zone. There is some additional amount of slip that is not accounted for by these two values (total should by 33 to 44 mm/yr), so we should consider these as lower bound probabilities.

W.BAKUN suggests that a section should be added to the report that is a statement which would outline what kinds of data could improve the probability estimates.

APRIL 30, 1990
Afternoon Session

J.SAVAGE presented a critique of the probability report. He provided a draft document to NEPEC (appendix N), which summarized his concerns. He questioned the validity of the probabilities as presented in the 1988 open-file report, and by association of the same methodology, the probabilities that will be presented in the new report. He raised three separate arguments:

1) The distributions of recurrence times of the four best-observed characteristic earthquake sequences (i.e., Miyagi-oki, Japan; Parkfield, CA; Conception, Chile; Valparaiso, Chile) are only marginally consistent with the Nishenko-Buland log normal distribution (used by the Working Group).

2) The range of possible 30-year conditional probabilities for many of the fault segments is so great, due to uncertainty in the average recurrence time for that segment, that the assigned probability is meaningless.

3) The 1988 forecasts not subject to the foregoing objection are those in which there is a low probability of an earthquake in the near future (North Coast segment and Carrizo segment). However, the same reasoning would assign only a 5 percent probability before mid-1993 to the southern Santa Cruz Mountains segment which ruptured in 1989, i.e., the Loma Prieta earthquake came too soon.

The Council, Working Group representatives, and Savage held an extended discussion regarding his criticisms, particularly focused on the use of the mean, the mode, and the entire distribution as representations of the uncertainties.

R.WESSON felt that NEPEC must resolve two issues:

1) The challenge offered by Savage, that is, that there is so much breadth in these distributions that we cannot say we know anything.

2) We should identify what key issues have been raised by the discussions and how these issues should be resolved.

H.KANAMORI questioned how the previous report has been used and whether the reliability was incorporated in the use of the probability numbers.

T.TOBIN said the information prompted significant use by State and local governments and by insurance companies for risk evaluation.

R.EISNER thought that most users understood the level of reliability of the probabilities due to limitations in the data. He thought the numbers were extremely valuable.

J.DAVIS did not think that there was a great deal of change in State policy before and after the 1988 report and cautioned overemphasis of its impact. In contrast, as a result of Loma Prieta, there will be greater attention paid to the current report.

A.JOHNSTON believes it is extremely important to express numerically what is already an intuitive risk for the Bay area.

W.BAKUN asked if there was an actual use of the reliability factors attached to the numbers.

R.EISNER said that the numbers were the primary focus. The aggregate numbers were most commonly used so that the lack of use of the reliability factors was minimized.

T.HEATON raised the point that prior to 1906, we had an 80-year period where we had 5 large earthquakes in the Bay area, and in the 80 years after 1906, we had none, so are we confident that we are now back in a period similar to the 1800's?

T.McEVILLY asked that each member of the Council offer a few brief comments regarding his or her opinion of the report draft. The comments included:

1) We must resolve the issue of statistics, as raised by Savage.

2) The reliability of each number must be emphasized.

3) The report itself is very good but far too detailed for general consumption; either the Executive Summary must be carefully prepared or a separate document is needed.

4) There is a need to specify what has changed since 1988 that determines the new probabilities.

5) The summary perspective diagram has problems; reliability needs to be added.

6) The proper line of decision science has been used, and we should go with it; Savage's comments reflect the underlying uncertainty but does not negate the effort and current results.

7) The current report should provide the direct contrast with the equivalent segments discussed in the 1988 report.

8) Should the Working Group add the probability for a 6.5 magnitude on the possible northern Santa Cruz Mountains segment?

The representatives of the Working Group were excused to discuss the recommendations of NEPEC.

A.LINDH provided NEPEC with a brief summary of recent seismicity in the San Francisco Bay region, including Monterey Bay, the Chittenden earthquake (a 5.5

aftershock at the south end of the Loma Prieta rupture zone), the Danville swarm and the Alamo swarm in the East Bay.

MAY 1, 1990
Morning Session

The session began with a discussion of what action NEPEC should take on the Working Group Report, as presented to the Council and discussed on the previous day.

J.DIETERICH brought forward his compiled list of seven main issues that need to be resolved by NEPEC so that the Working Group can take action.

1) The criticism of the report and, specifically, the methodology as brought forward by J.Savage. It appears that Savage will present his criticisms in the scientific literature and so NEPEC must be prepared to deal with that. If the Working Group goes ahead to publish this report, the Group needs to know that NEPEC is behind the Working Group.

2) With regard to the northern Santa Cruz segment, there was concern that it was downgraded and then pushed aside. Would NEPEC be satisfied, assuming the segmentation is correct, to state that the segment is included with the 0.4 probability, given that the Working Group was split 50-50 on this issue resulting in a 0.2 probability? The aggregated Bay area probability will probably stay at 0.7. We should more prominently flag the potential for this earthquake. The Council felt that the issue of heightened probability as a result of Loma Prieta is important enough that it should be included.

3) The question was raised regarding the aggregated probabilities and a tie-in between the 1988 and 1990 reports. The problem is how to include the Rodgers Creek fault. R.Wesson suggested that the Working Group recalculate the 1988 probability by including the southern Santa Cruz Mountain segment and adding what we know about the Rodgers Creek fault to have an "expanded Bay area aggregate probability," which we could then compare to the 1990 probability (to which the northern Santa Cruz segment is being added). Then we are in a better position to state how Loma Prieta has affected the aggregated probability.

4) The summary figures in the tables could be rounded or left to two decimal places; also the figures could be presented as percents or decimals.

5) The question came up in reference to the Hayward fault and changing the prior displacement from 1.4 to 1.5 m. The Working Group felt that the number should change even though it appears arbitrary.

6) There is a need for a publication plan. The Group would accept a popular version of the report as a USGS circular, the technical version as an open-file report, and the ability to publish the results in a peer-reviewed scientific journal.

7) There is a question of the release and use of the document. Perhaps J.Evernden could prepare a separate document based on his intensity models which would show what might happen in various selected localities as a result of an earthquake on each segment.

L.JONES was asked to present a summary of the revised version of a report entitled "Short-Term Earthquake Alerts for the Southern San Andreas Fault," which was prepared by a Working Group for southern California earthquakes (appendix P). The first version of this report was presented to NEPEC at its January 1990 meeting. The recommendations of NEPEC at the previous meeting have been incorporated into the radically rewritten current version, which include alert responses patterned after the alert model used at Parkfield. The alert levels from D (lowest) to A (highest) are based primarily upon the observation of foreshocks within 10 km of one of four segments of the southern San Andreas fault, as well as creep events (rapid aseismic surficial slip on faults) and anomalous strain events.

After some questions from various NEPEC members, it was agreed that the Council members will review the report subsequent to this meeting and forward comments to the Council chairman within the next few weeks. In addition, the report will be forwarded to CEPEC for review and comments.

P.REASENBERG presented a summary of the USGS aftershock sequence model and particularly addressed a question raised at the last NEPEC meeting regarding the establishment of guidelines for the use of the model in drafting aftershock forecasts. He recommended that the forecasts focus only on potentially damaging aftershocks (magnitude 5 and larger). Regarding time intervals for forecast statements, he recommended in the document short-term (1 week) and long-term (3 months) time intervals; since writing the document, he recommends only a 1-month window. As far as the frequency of issuing these forecast advisories, he suggests daily forecasts at first, then 2-3 times per week, and when the probability of a magnitude 5 decreases to 20 percent or less, the forecasts should be stopped. These advisories should be distributed to the media after a half-hour delay to allow time to notify various government agencies such as the Office of Emergency Services. He also discussed the options of the generic model versus the real-time model and revisions he has made.

J.DIETERICH emphasized the usefulness of issuing advisories on the short-term likelihood for moderate aftershocks, particularly as demonstrated by the Loma Prieta earthquake.

T.McEVILLY will draft a letter of endorsement of the aftershock forecast methodology with reference to both its technical merit and utility in post-earthquake response.

R.WESSON returned the discussion to the Working Group Report and offered a number of suggestions:

1) NEPEC has offered a few minor suggestions for modifications; the Working Group should go ahead and finish the report.

2) In parallel to the above effort, further consideration by appropriate experts in statistics of the concerns raised to confirm or negate the methodology being used by the Working Group.

3) In cooperation with the California Division of Mines and Geology (CDMG) and the Bay Area Regional Earthquake Preparedness Project (BAREPP), begin work on a series of maps that will link the Working Group Report to expected intensity patterns in the Bay region.

4) Within the USGS, begin the preparation of a popular report which would distill the essence of the Working Group Report and possibly include the intensity work.

5) Suggest that NEPEC reconvene in June to review these various items as available at that time.

The members of the Council were asked to individually comment on the Working Group Report. Some individual concerns were reiterated, with particular emphasis on resolving the J.Savage issue. However, in general, the Council will be in support of this document. The review by appropriate decision scientists was highly recommended.

In review of R.Wesson's suggestions, the Council agreed with the actions but with concern that action proceed as quickly as possible. It was agreed that the final revisions of the Working Group Report can be completed by June and that a review of the methodology should be completed by that time. The intensity mapping effort should proceed independently and will not be completed in the short-time window. As for a popular version of the report, the USGS will initiate efforts to draft a document that can come out at the same time as the Working Group Report. An interim letter will be prepared by T.McEvilly for the USGS Director to inform him of the progress on this entire effort. The final Working Group Report and the "popular" document will move forward on parallel tracks with the intent that the formal report will be released first with a press release and the popular report will follow within a week.

NATIONAL EARTHQUAKE PREDICTION EVALUATION COUNCIL

PROCEEDINGS OF THE MEETING OF JUNE 6, 1990

Menlo Park, California

Council Members Present

Thomas McEvilly, Chairman	University of California
Robert Wesson, Vice-Chairman	USGS, Reston
William Bakun	USGS, Menlo Park
James Davis	California Division of Mines and Geology
James Dieterich	USGS, Menlo Park
Thomas Heaton	USGS, Pasadena
Arch Johnston	Memphis State University
Hiroo Kanamori	California Institute of Technology
William Prescott	USGS, Menlo Park
Kaye Shedlock	USGS, Golden
Ray Weldon	University of Oregon
Randall Updike, Exec. Secy.	USGS, Reston

Invited Participants

Richard Eisner	Bay Area Regional Earthquake Preparedness Project
Al Lindh	USGS, Menlo Park
John Savage	USGS, Menlo Park
David Schwartz	USGS, Menlo Park
Peter Ward	USGS, Menlo Park

JUNE 6, 1990
Morning Session

NEPEC reconvened at the same location as the April 30 - May 1 meeting to continue review and prepare final recommendations regarding the San Francisco Bay area Working Group Report.

The first item discussed by the Council was the aftershock forecast model of P.Reasenberg. Hearing no objection from the members of NEPEC, T.McEvilly will draft a letter to the Director of the USGS recommending adoption of this methodology by the USGS.

The second item was the implementation of the foreshock earthquake alert report as presented by L.Jones at the May 1, 1990, meeting.

W.BAKUN indicated that there is some immediacy for NEPEC action before September and to have this plan in place in the event of near-future activity in southern California.

T.HEATON felt that we need to use the report plan. Although the report needs an introduction, it is basically pretty clean. L.Jones will be giving a presentation to the Southern California Earthquake Preparedness Project (SCEPP) and would like NEPEC's endorsement. If the Coachella segment were to "go" in the near future, would NEPEC endorse the use of this plan?

J.DIETERICH cautioned that the approach is new and novel and has not been rigorously tested.

R.WESSON reminded NEPEC that the Director of the USGS is identified by law as the person responsible for issuing earthquake predictions. NEPEC could recommend to the Director that he agree in advance that USGS-Pasadena can issue predictions based upon this model.

After extended discussion of the implications of the alert plan, the Council agreed to adopt this report on an interim basis and make this recommendation to the USGS Director. It is suggested that the word "Proposed" be added to the title of the report, and after review by CEPEC, USGS move quickly toward publishing the report as a open-file report.

T.McEVILLY informed NEPEC that he had received a letter from the Central United States Earthquake Consortium (CUSEC) regarding an earthquake prediction on or about December 3, 1990, for the Central United States. The Council was asked to advise CUSEC on the prediction. The prediction is not appropriately documented but is apparently based upon tidal forces. Local governments and the media are taking the prediction seriously and are initiating preparation plans. The letter should not have been directed to NEPEC directly but to the Director of the USGS. It was agreed that T.McEvilly will draft a letter back to CUSEC which indicates the proper procedures for NEPEC evaluation of predictions, indicate NEPEC's interest in focusing on the Central United States in the near future, and invite CUSEC to meet with NEPEC regarding earthquake probabilities in the Central United States.

T.McEVILLY provided a brief summary of the progress and decisions thus far regarding the report of the Working Group on Bay Area Earthquake Probabilities. The revisions of the report have been completed. Three individuals have been asked, as experts in decision science statistics, to review the report methodology. They have responded, and their reviews are attached as appendices Q, R, and S. A "popular version" of the report has been initiated, under the guidance of P.Ward. The draft was sent to CEPEC for their comments in their May 11 meeting; comments from CEPEC have been received by the Working Group (appendix T). Additional comments on the methodology used in the Working Group Report are provided in appendices U, V, and W.

J.DIETERICH summarized changes of the Working Group Report (appendix X) as recommended by NEPEC including:

1) Regarding the reporting of probability numbers, the Working Group decided not to round but report as 2 decimal places; however, differences of less than 0.1 are not significant.

2) On summary figures, the other faults are added, and various changes are included to clarify the data presentation.

3) The report now has an executive summary.

The members of NEPEC offered several additional comments on specific points within the report. These points included:

1) Comments on earthquakes of less than maximum magnitude.

2) Changes in the length of North and South Bay segments of the Hayward fault.

3) Possibility of an earthquake on the North Coast segment.

4) Clear use of reliability letters and use of "uncertainty words."

5) Difference in opinion on slip estimates for various fault segments.

6) Use of quartiles in probability tables.

7) Clarification on the role of the Loma Prieta earthquake/southern Santa Cruz

Mountains segment and its involvement in the Bay area faulting.

8) Some indication that these probabilities are actually on the low side and aggregate probabilities could be larger than those reported.

T.McEVILLY concluded that NEPEC is accepting the report with the exception of what may be discussed later with J.Savage, i.e., statistics of the methodology.

J.SAVAGE presented a rebuttal presentation of his criticisms of the methodology used in the Working Group Report. Discussion centered around difference of opinion on use of statements of uncertainty on reported probabilities which Savage asserts are needed in order to judge the validity of the probability estimate. For a period of 2 hours, NEPEC and representative Working Group members debated the various differences of opinion on the use of probability distributions and what details of the statistics are meaningful to report. Savage felt that the uncertainties are so significant that the Working Group does not know enough to make a meaningful probability statement. If the confidence intervals were put into the report, a lot of people would look at the report and say, "They don't know very much." NEPEC members felt that the A through E reliability letters give the reader a relative assessment of the data reliability and, therefore, of the probability estimates.

R.WESSON suggests that a paragraph could be added to appendix stating the concerns and issues raised by Savage.

T.McEVILLY will draft a letter to Dallas Peck, Director of the USGS, indicating that NEPEC is in unanimous agreement that they endorse the new probabilities report, and it should be issued as a public document. NEPEC suggests that the report should appear as an open-file report or a circular with late June or early July as a target for release.

R.WESSON outlined the procedure that should occur. The Working Group Report would be submitted to Bakun who will act as the manuscript reviewer, followed by review by Wesson and the Director. In contrast, the public interest document will be discussed today by NEPEC. P.Ward will incorporate suggestions from NEPEC; he will then go through an approval process with State and local groups and go to press with the final manuscript. The target for release of the formal report should be mid-July with a briefing of the public officials 24 hours prior to the official press conference and release. The public interest document will be available then or be distributed broadly within a week.

P.WARD welcomed the input of NEPEC regarding the scope and format of the public interest document (appendix Y). The document should not just summarize the hazard but tell people what they can do to reduce their personal risk. Therefore, the approach being taken is to briefly summarize the results of the new report, then tell what it means to the public, tell what the public can do to prepare for the earthquake, and then document how the hazard was determined. A map will be included to show the relative hazard across the Bay region. The brochure must get wide distribution to be effective; options of mailing or newspapers are being considered. The goal is to print on the order of 2 million copies of the brochure with various underwriting agencies.

Members of NEPEC offered a variety of suggestions on the content and layout of the brochure. Some Council members felt that the draft did not contain enough of the science from the Working Group Report. Ward emphasized that numerous USGS scientists have reviewed the manuscript and provided construction improvements.

R.WESSON announced that out of the Dire Emergency Appropriation to the USGS as a result of the Loma Prieta earthquake, the USGS has set aside about $1 million to focus on the hazard from future Bay region earthquakes. A new "megaproject" has been established called the "Bay Region Future Earthquake Project." That project will be headed by a chief scientist; Bill Bakun has been named to fill that responsibility. An integrated program will be developed which will include studies of what the effects of future earthquakes will be, as well as anticipating those earthquakes.

T.McEVILLY led a discussion to select the region that should be the topic of the next NEPEC meeting. The two areas needing attention are the midcontinent region and Utah. It was decided that the midcontinent region should be the topic of the next meeting and probably should convene in the fall or early winter of 1990.

Appendix A

Document provided by J.Healy to accompany presentation to NEPEC, January 11, 1990.

SOVIET EARTHQUAKE PREDICTIONS

Presented to NEPEC on January 11. 1990

John H. Healy

Soviet scientists visited Menlo Park after the Loma Prieta Earthquake and presented their work on Earthquake Prediction. One of their algorithms, M8, configured to predict earthquakes of magnitude 7 or larger, gave a before-the-fact warning of this earthquake.

Prediction Terminology

Some confusion has arisen over differences in terminology between the U. S. "official" terminology and general usage in the Soviet Union. Implicit in American terminology is the assumption that we will predict the location and magnitude of an earthquake before we can make an intermediate-term or short-term prediction of the time of occurrence. The Soviet prediction research is based on the assumption that the timing of an earthquake can be predicted by changes in the pattern of regional seismicity without specific knowledge of an earthquake's location.

We recommend the term research prediction to identify predictions made for the purpose of formulating and testing an hypothesis. In viewgraph 1 we show a prediction model in which we try to encompass many different uses of the term prediction. We make many predictions in our daily activities. For example, we make hundreds of predictions when we drive our cars through traffic. These predictions are so natural and intuitive that we don't think about them as predictions in a formal sense. Astrologers make predictions, Psychics make predictions, gamblers make predictions, and Doctors make predictions. To cover all these varied uses of term prediction the general terminology is necessarily broad and imprecise. We add some precision by considering the range of actions we may take as a result of the prediction. Many predictions are not taken seriously. They may be used in the news media primarily for their entertainment value on days when no significant news is available. Other predictions are taken very seriously and have a great impact on human behavior.

When we make formal earthquake predictions they must be precise and go through a process of formal evaluation and testing. In my judgment the method used to make these predictions should be formulated as a computer algorithm with fixed parameters so that it can be tested as a "black box" by a number of investigators. At a minimum the investigator trying to evaluate a prediction algorithm should be able to vary the data base and observe the changes in the predictions without excessive effort.

NEPEC's task, in the terminology of viewgraph 1, is to determine when a method of prediction is sufficiently reliable to pass from the category of research to the stage where it is used as part of a public warning. This decision obviously requires a much more intensive review than is normally required for publication in leading scientific journals. In turn it is reasonable for NEPEC and the reviewers who are assisting them to expect that the authors of prediction schemes assume the burden of presenting their material in a form that facilitates evaluation.

Soviet Scientists

Our Soviet colleagues have made a considerable effort to make their algorithms and data available to us and to explain their methods. In viewgraph 2 we list some of the Soviet scientists who are participating in this cooperation. Volodya Kossobokov is currently in Menlo Park, and with his aid we have implemented the algorithm M8 on IBM PC-compatible computers. This algorithm, set to predict magnitude 7 or greater earthquakes, successfully predicted the Loma Prieta Earthquake. This prediction was made before the earthquake, but the presentation of the prediction may have been confused by the simultaneous presentation of other Soviet predictions.

The M8 Algorithm

The M8 algorithm can be set to predict earthquakes of different magnitudes. When the magnitude and a point of investigation is chosen the algorithm selects a radius of investigation and examines all the earthquakes within a circle centered on the chosen point. When set to predict a magnitude 7 earthquake the radius of the circle is 280 kilometers. The algorithm removes the aftershocks from the data and then calculates seven measures of seismic activity. Six of these measures are an average of activity for the preceding six years in the circle of investigation. The seventh measure is a count of the number of aftershocks in the first two days after each main shock.

When six of the seven measures are in the top ten percent of their historic range an alert or Time of Increased Probability (TIP) is declared. Once declared a TIP lasts for five years or until it is terminated by an earthquake.

The Loma Prieta Prediction

With the aid of Volodya Kossobokov we have prepared plots that show the predictions of the M8 algorithm configured to predict magnitude 7 earthquakes in California. The algorithm was run in eight overlapping circles of investigation, figure 1. The two circles of investigation relevant to the Loma Prieta Earthquake are shown in an expanded view, figure 2. Figures 3 through 17 show the areas where alerts were declared and the earthquakes of magnitude seven or greater for the years 1975 through 1989. Four alerts were declared in this period. An alert in region four was closed by the Eureka Earthquake. An alert in region 8 was closed by the Imperial Valley earthquake (this earthquake has reported magnitudes ranging from 6.5 to 7.0). Alerts in regions five and six were closed by the Loma Prieta Earthquake which occurred in the overlap of the two regions. During the 15 year interval from 1975 through 1989 there were four alerts which preceded earthquakes and no false alarms.

Other Predictions

The Soviet researchers also reported TIPs from two other algorithms. They run an algorithm known as CN and they run the algorithm M8 configured to predict magnitude 7.5 earthquakes. These algorithms have both produced results that are interesting for research, but in my judgment their reliability and specificity is not adequate for use in a public warning system at this time.

The algorithm CN is designed to make predictions for two large regions in California and Nevada figure 18. The size of these regions is so large that it is hard to envision a useful public response even if the predictions were very reliable. The territory covered by the algorithm CN includes about 30,000,000 people. Divided in two parts the number of people affected by a prediction will be more than 10,000,000. False predictions that affect such large populations can do serious damage to our credibility.

We have not run this algorithm successfully in Menlo Park. I recommend that NEPEC not accept this algorithm for evaluation until it can be run successfully by independent American investigators. By success I mean duplicating the Soviet results exactly.

The algorithm M8 configured to predict magnitude 7.5 has produced ambiguous results in California. It produced a TIP in the region including the Eureka Earthquake. It produced a TIP in Central California in a region that included the Loma Prieta Earthquake. This TIP will remain in force until the middle of 1992. No other TIP's were produced between 1975 and 1990.

These results suggest that the TIPs for magnitude 7.5 may have been set by activity associated with the smaller earthquakes at Eureka and Loma Prieta. A magnitude 7.5 or larger earthquake in Central California would probably require a repeat of the 1906 rupture. If we interpret these results literally they suggest that the 1906 earthquake would repeat before the middle of 1992. Based on other evidence I believe that this is very unlikely, and I conclude that the M8 algorithm set to predict magnitude 7.5 earthquakes is not producing reliable TIPs in California. There are a number of reasons why the reliability of the algorithm might be dependent on the magnitude threshold chosen for prediction. This question will be investigated in future research.

The algorithms CN and M8 set to to predict magnitude 7.5 earthquakes are both producing research predictions that have considerable scientific interest, but the predictions of these algorithms do not have the demonstrated reliability needed for use in a public warning system at this time.

Conclusion

The algorithm M8 set to predict magnitude 7.0 earthquakes appears to be generating reliable alerts in California, and this algorithm may be useful as part of a public warning system. We will run this algorithm in Menlo Park and in Moscow, and we will report the TIPs generated by this algorithm to NEPEC.

After-thoughts

In addition to the NEPEC presentation I presented this talk in a seminar, and I have discussed it individually with other thoughtful people. I have received many good suggestions for further research, but most of these suggestions don't deal directly with the more difficult question of evaluating the reliability of this particular algorithm.

Consider the development and testing of a new drug as an analog that may provide some insight for this problem. Research laboratories may use very sophisticated methods to develop a new drug. When the a drug appears to have great promise it starts a long and costly period of testing which must be completed before it is released for prescription to the general public. This testing process is very different from the research needed to the develop the drug. Testing is carried out by specialists in testing who have different skills than the research scientists who developed the drug. Once the drug goes into the testing process its composition cannot be changed. Results on similar drugs and theoretical considerations do not play an important part in the testing process. Drug testing involves a search for unfavorable side effects, and many drugs are rejected or restricted because of these side effects. If a drug cures 25% of the patients or even 10% of the patients with no negative side affects then it will be accepted. If a drug cures 25% of the patients and kills 10% of the patients it will be rejected.

In my judgment the M8 algorithm configured to predict magnitude 7 earthquakes in California has passed from the stage of research to the stage where we must design a test program to evaluate its reliability for public earthquake predictions.

A Test Plan

We have fixed the algorithm and the control parameters. The algorithm uses the National Earthquake Information Center Global Hypocenter Data Base, which is available to all researchers. We will run this algorithm in the future and report the results. If it continues to perform in the future as it has in the past with no missed predictions and no false alarms it would take about 15 years to establish the reliability of this algorithm.

The challenge is to design test procedures that will shorten the time for evaluation. With the control parameters fixed the only parameter that can be varied is the center of the circle of investigation. The algorithm is now configured to investigate eight overlapping circles in California. We can increase the data base by choosing additional circles of investigation. In fact we can run it everywhere in the world where the NEIC Global Hypocenter Data Base has a low enough magnitude threshold to run the algorithm. Unfortunately, the data is not adequate to run the algorithm in many areas with high seismicity, but we will search the data base and run the algorithm at all possible sites.

We believe that the algorithm may not produce reliable results in some regions. We will search for regions where the algorithm has a good record on past data and then test the algorithm in the future in these regions.

We need to define the criteria for acceptance or rejection of the algorithm. The negative side effects in our case are the false predictions. If any algorithm could predict 25% of the earthquakes with no false alarms it would be very useful. False alarms at this stage of our research can be very costly because they threaten our credibility not only for future earthquake predictions but for all statements which we make about earthquakes. Loss of public confidence in our recommendations about mitigating the earthquake hazard will have serious consequences for years in the future. Thus we will make false alarms the main criteria for rejecting the algorithm.

We will run the algorithm with centers of the circles of investigation spaced at 20-kilometer intervals everywhere in the Western United States where the data permit. If we generate any clear false alarms in this test we will reject the algorithm as unsuitable for public earthquake predictions.

If the algorithm generated a TIP for a magnitude 7.0 earthquake that was followed by an earthquake of 6.5 or larger we would not regard that case as a "clear false alarm". Similarly if the algorithm produced a TIP in a circle of investigation and the earthquake occurred just outside the circle in an overlapping circle that also had a TIP we would not regard that case as a "clear false alarm".

If the algorithm generates no false alarms in the Western United States and if there are favorable results in some other areas in the world then we will recommend that NEPEC use this algorithm in combination with other data for future earthquake alerts.

Appendix B

Handouts provided by A.Lindh to accompany presentation to NEPEC, January 11, 1990.

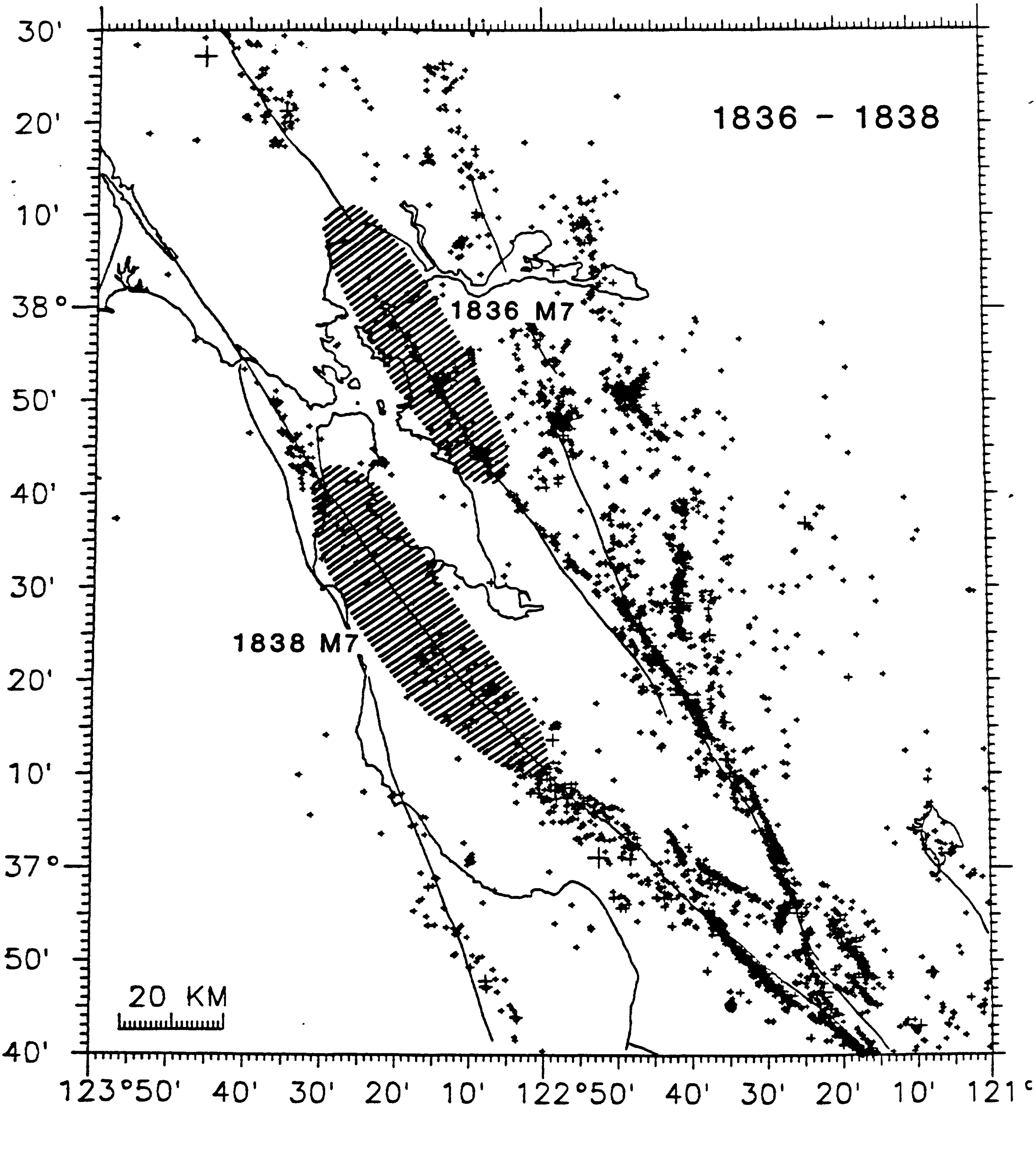
1836 - 1838
1836 M7
1838 M7
20 KM
30'
20'
10'
38°
50'
40'
30'
20'
10'
37°
50'
40'
123°50'
40'
30'
20'
10'
122°50'
40'
30'
20'
10'
121°

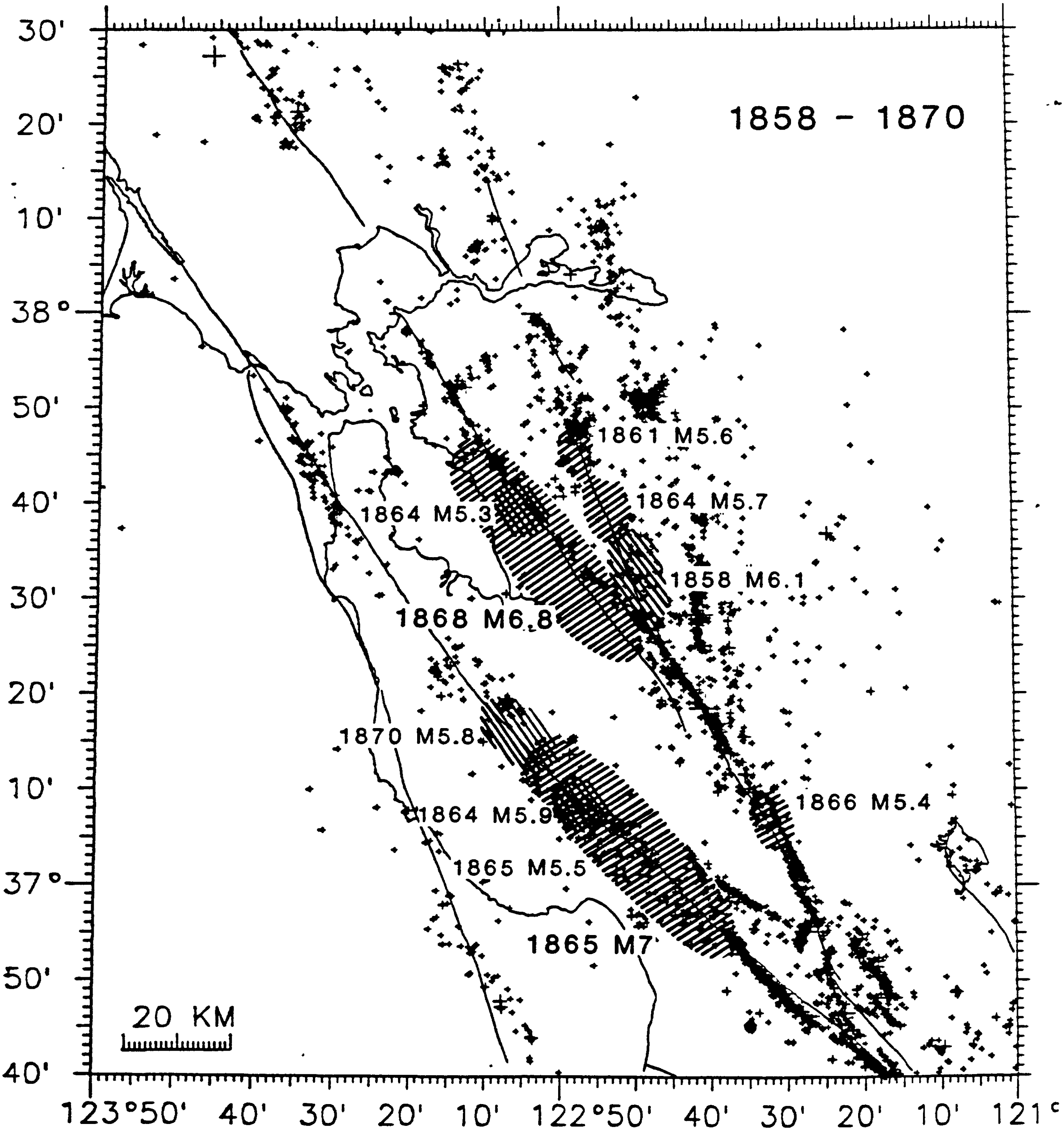
1858 - 1870
1861 M5.6
1864 M5.7
1864 M5.3
1858 M6.1
1868 M6.8
1870 M5.8
1866 M5.4
1864 M5.9
1865 M5.5
1865 M7
20 KM
30'
20'
10'
38°
50'
40'
30'
20'
10'
37°
50'
40'
123°50'
40'
30'
20'
10'
122°50'
40'
30'
20'
10'
121°

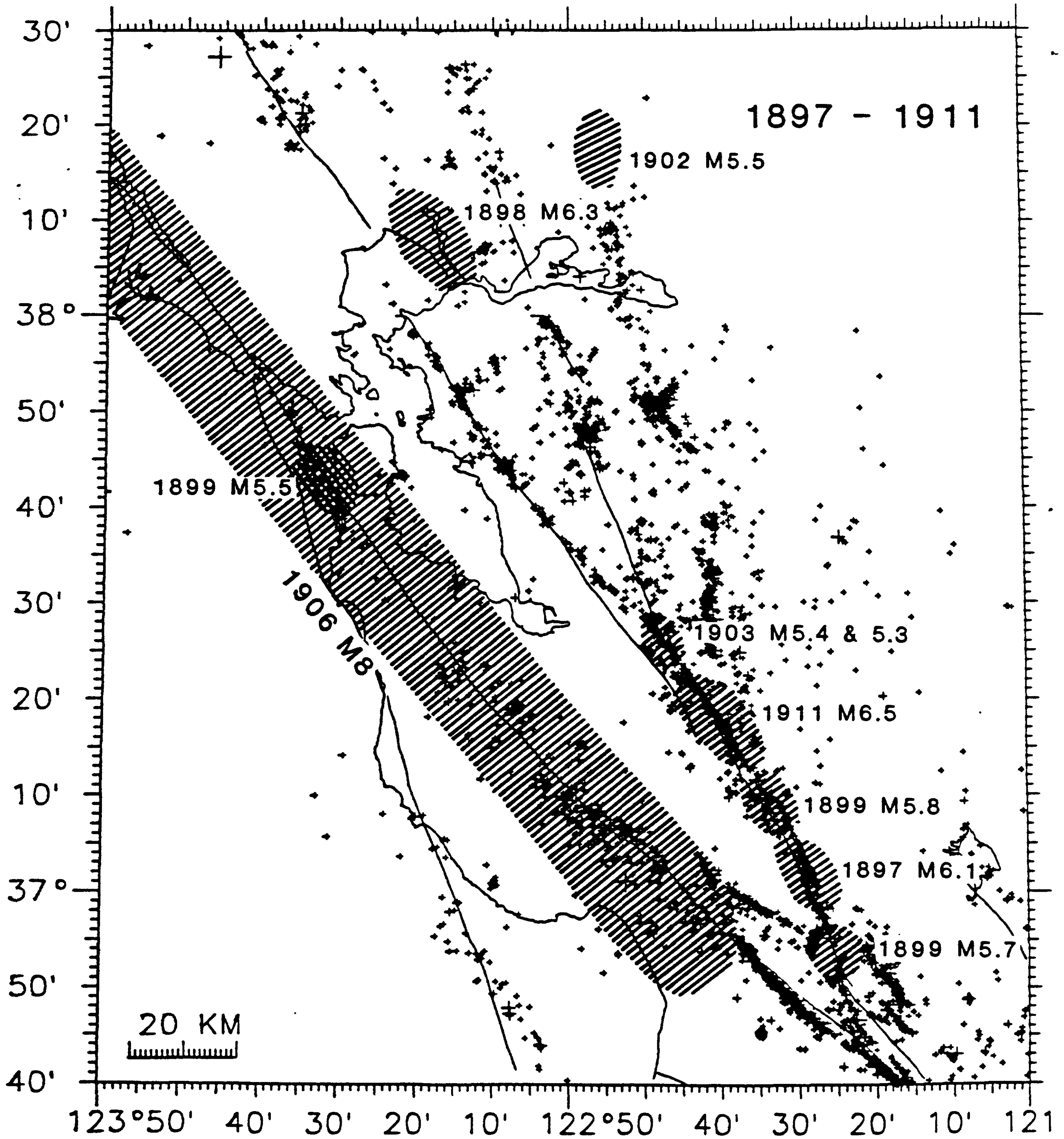

1897 - 1911
1902 M5.5
1898 M6.3
1899 M5.5
1906 M8
1903 M5.4 & 5.3
1911 M6.5
1899 M5.8
1897 M6.1
1899 M5.7
20 KM
30'
20'
10'
38°
50'
40'
30'
20'
10'
37°
50'
40'
123°50'
40'
30'
20'
10'
122°50'
40'
30'
20'
10'
121°

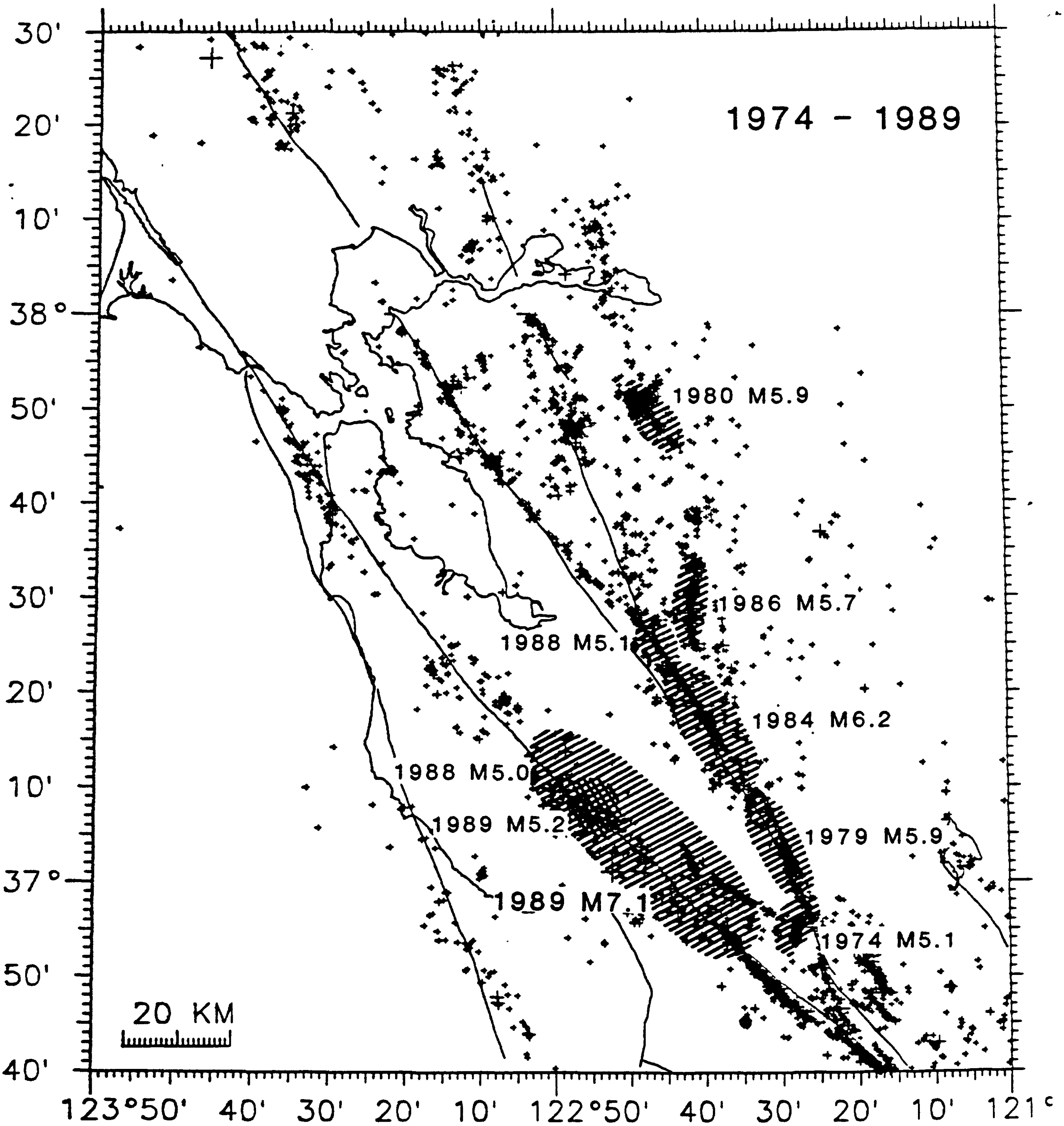
1974 - 1989
1980 M5.9
1986 M5.7
1988 M5.1
1984 M6.2
1988 M5.0
1989 M5.2
1979 M5.9
1989 M7.1
1974 M5.1
20 KM
30'
20'
10'
38°
50'
40'
30'
20'
10'
37°
50'
40'
123°50' 40' 30' 20' 10' 122°50' 40' 30' 20' 10' 121°

PROCEEDINGS OF THE

SECOND JOINT MEETING OF THE U.S.-JAPAN CONFERENCE

ON NATURAL RESOURCES

(UJNR) PANEL ON EARTHQUAKE PREDICTION TECHNOLOGY

JULY 13-17, 1981

Panel Chairmen:

David P. Hill
U.S. Geological Survey
Menlo Park, California 94025
U.S.A.

Keiji Nishimura
Geographical Survey Institute
Ibaraki-Ken 305
Japan

U.S. Geological Survey

Open-File Report 82-180

HISTORIC SEISMICITY OF THE SAN JUAN BAUTISTA, CALIFORNIA REGION

A. G. Lindh, B. L. Moths, W. L. Ellsworth, and J. Olson
U.S. Geological Survey
Menlo Park, California 94025, U.S.A.

The 430-km-long segment of the San Andreas fault that ruptured in the great 1906 earthquake (M 8) has been seismically quiet at the M 6 level for the last 75 years (Ellsworth et al., 1981). The historic record of earthquakes in the 19th century for the southernmost 100 km of the rupture, extending from San Francisco to just north of San Juan Bautista, indicates that it was the site of three or four M 6 or greater earthquakes in the 110 years preceding 1906: 1800?; 1838, M 7?; 1865, M 6.5; 1890, M 5.9 (Toppozada, 1980). We believe that these earthquakes are plausibly accounted for by repeated slip on the southernmost 50 km of fault, just to the northwest of San Juan Bautista (Fig. 1).

Geodetic data indicate that strain is currently accumulating across this zone at a rate (0.6 μstrain/a; Prescott, 1980) which can be explained if the right lateral displacement across the fault is 2 cm/a, and the upper 10 km of the fault are locked. This rate of strain accumulation is consistant with short and long term geologic determinations of displacement rates in the region, and is sufficient to account for a M 6.5 earthquake every 30 years (Fig. 2), a close approximation to this segment's behavior in the nineteenth century. The long interval without a large event since 1906 can plausibly be accounted for by the 1.5 m of slip that occurred on this portion of the fault in the 1906 earthquake. If this model (Bufe et al., 1977; Shimazaki and Nakata, 1980; Sykes and Quittmeyer, 1981) is correct, it suggests that a large (>M 6) earthquake could occur in this region at any time. This idea is reinforced somewhat by the pattern of lower magnitude seismicity following 1906. Quiescence extending down to the M 4.5 level lasted for 40 years, with activity resuming in the mid-1940's (Fig. 2). These variations are suggestive of a small scale, stress modulated "seismic cycle".

Since 1979, a sequence of M 4 earthquakes have occurred on the San Andreas in the region northwest of San Juan Bautista. Microearthquake hypocenters associated with each of these larger events map out nonoverlapping areas on the fault plane and highlight two portions of the fault where future large events might reasonably be expected (top, Fig. 3). One is a 10-15-km-long zone between San Juan Bautista and Pajaro (0-15 km on the horizontal scale at the top of Figure 3) that has not ruptured in the past twelve years. The other is a 40 km zone northwest of Pajaro (15-55 km, top Fig. 3), which not only has been anomalously quiet in the last twelve years, as compared to the preceding eighteen (Fig. 2), but also was the probable location of at least some of the large earthquakes of the nineteenth century.

In cross section, the pattern of microseismicity on the fault plane at San Juan Bautista strongly resembles that at Parkfield, some 150 km to the southeast (bottom, Fig. 3). Lindh and Boore (1980) have determined that fault slip during the M 5.5-6 1966 Parkfield earthquake, (dashed line, bottom, Fig. 3), started near a dense cluster of activity at the leading edge of the seismically active zone (left side, bottom, Fig. 3), and propagated 20-25 km southeast to a single deep cluster (right side, bottom, Fig. 3). By analogy, we speculate that the 1865 earthquake near San Juan Bautista occurred within the dashed line shown in the top of Figure 3. Furthermore, several of the recent M 4 earthquakes have occurred at the ends of the 40-km-long zone on which we believe a >M 6 event is possible today.

Further similarities exist between the San Juan Bautista and Parkfield regions. Each region contains the terminus of a historic rupture zone for a great earthquake on the San Andreas fault, 1906 to the north and 1857 to the south. In both cases the transition from locked to creeping behavior is accompanied on the east side of the San Andreas by a change from a high-density, high-velocity basement (gabbroic and/or greenstones) to a low-velocity, low-density crustal section of predominantly graywacke character. The transition from locked to creeping behavior is also accompanied by the appearance of a high level of microseismicity on the fault plane that persists along the length of the creeping zone, by geometrical complexities in the fault zone, and by the occurence of moderate (M 5-6) earthquakes. We believe that the distribution of rock types along the fault plays a major role in determining whether or not a given section of fault slips seismically or aseismically, in determining the character of the microseismicity, and in determining where large earthquakes will occur. Thus we believe an integrated study of the geology, tectonics, seismic velocities, densities, and seismicity of a region forms a rational basis on which to build an earthquake prediction program.

References

Bufe, C. G., Harsh, P. W., and Burford, R. O., 1977, Steady-state seismic slip—a precise recurrence model: Geophysical Research Letters, v. 4, p. 91-94.

Ellsworth, W. L., Lindh, A. G., Prescott, W. H., and Herd, D. G., 1981, The 1906 San Francisco earthquake and the seismic cycle, in Simpson, D. W., and Richards, P. G., eds, Earthquake prediction: an international review: American Geophysical Union Maurice Ewing Series 4, p. 127-140.

Lindh, A. G., and Boore, D. M., 1981, Control of rupture by fault geometry during the 1966 Parkfield earthquake: Seismological Society of America Bulletin, v. 71, no. 1, p. 95-116.

Prescott, W. H., 1980, The accommodation of relative motion along the San Andreas fault system in California: Ph.D. Thesis, Stanford University, 195 p.

Shimazaki, K., and Nakata, T., 1980, Time-predictable recurrence model for large earthquakes: Geophysical Research Letters, v. 7, no. 4, p. 279-282.

Sykes, L. R., and Quittmeyer, R. C., 1981, Repeat times of great earthquakes along simple plate boundaries, in Simpson, D. W., and Richards, P. G., eds., Earthquake prediction: an international review: American Geophysical Union Maurice Ewing Series 4, p. 217-247.

Toppozada, T. R., Real, C. R., Bezore, S. P., and Parke, D. L., 1980, Preparation of isoseismal maps and summaries of reported effects for pre-1900 California earthquakes: California Division of Mines and Geology Open-File Release 80-15, 78 p.

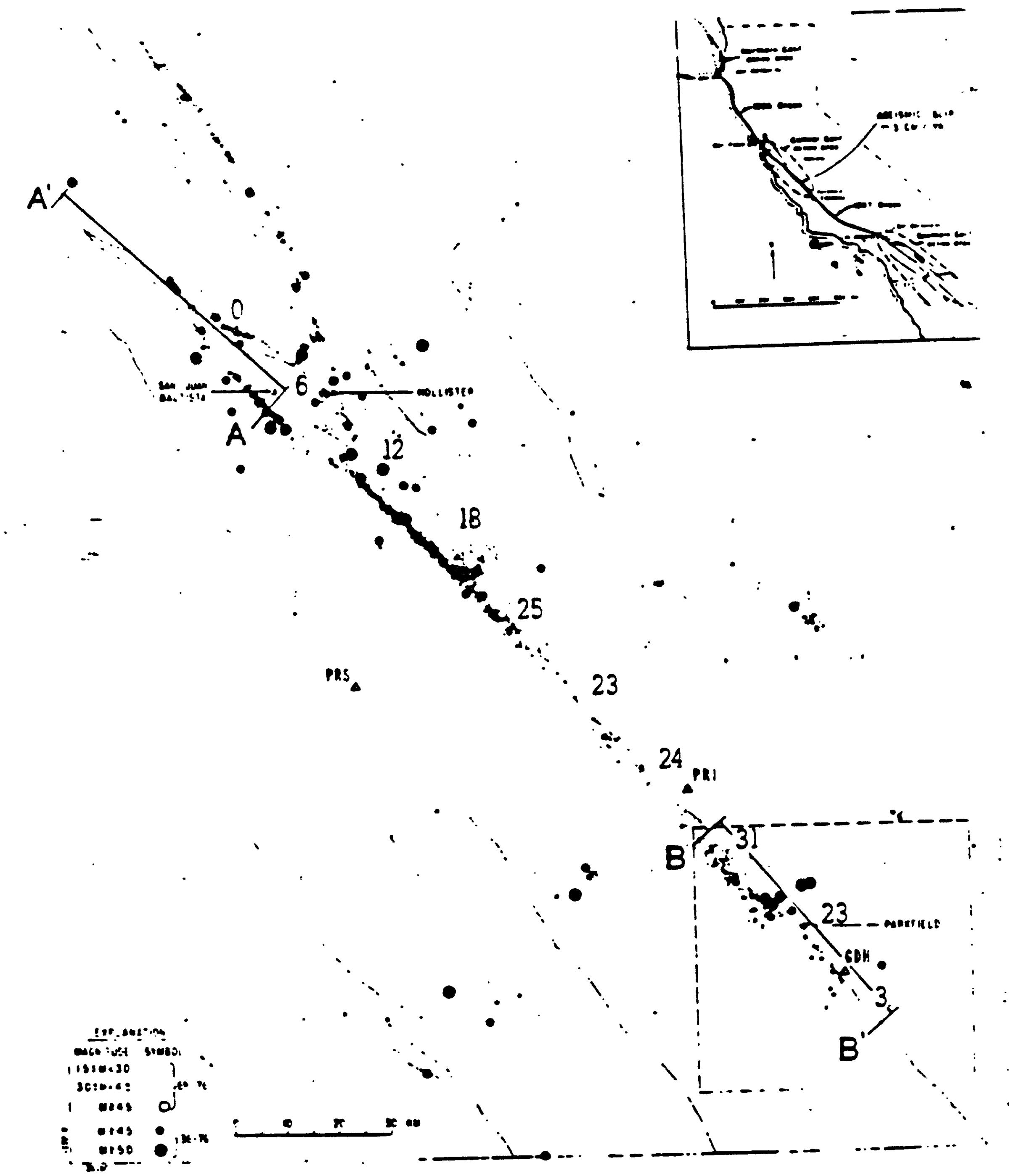

Fig. 1. Map showing the recent microseismicity (small dots) and the moderate earthquakes since 1936 (solid dots). The aseismic slip rate along the central portion of the San Andreas is shown by large numerals (mm/A).

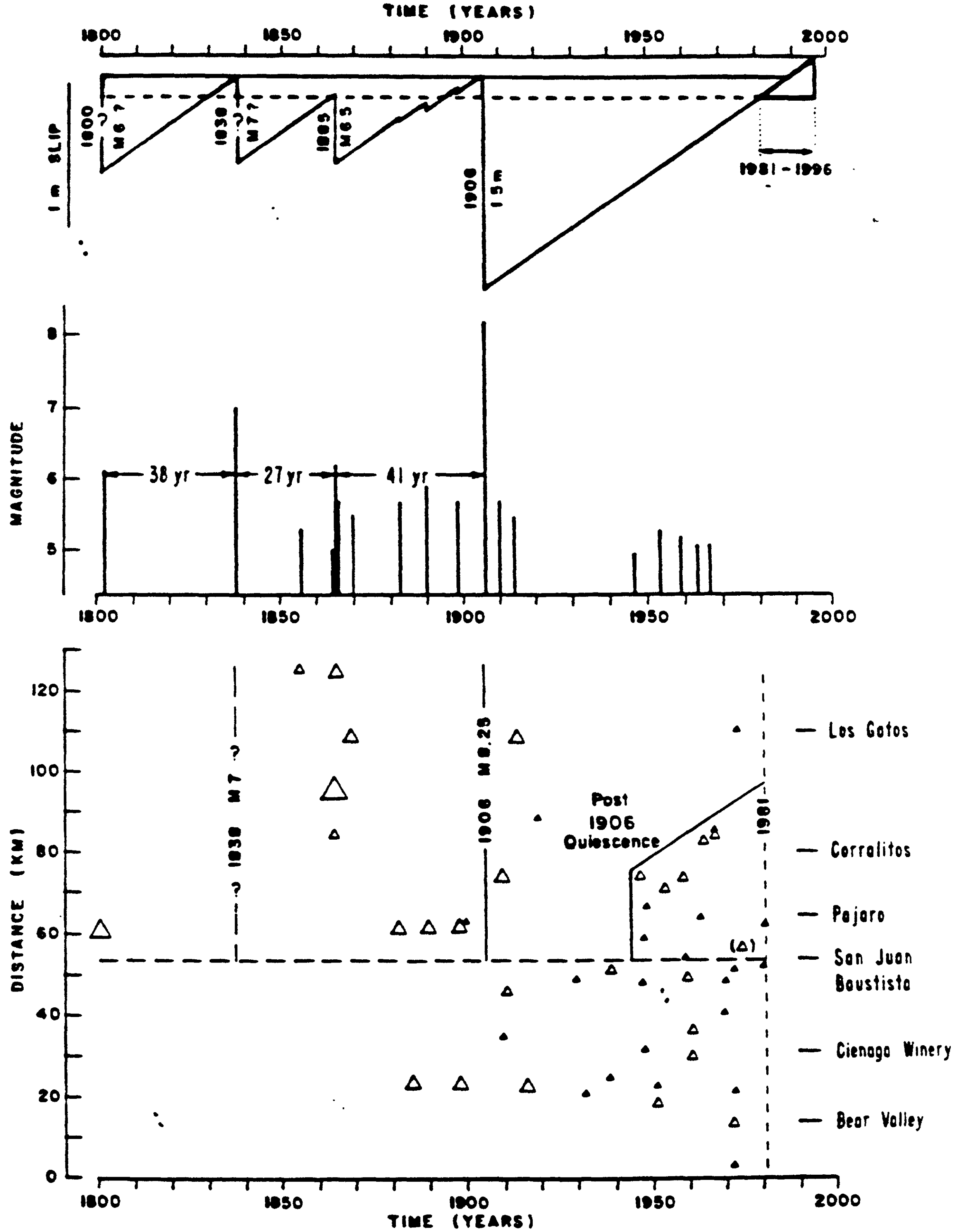

Fig. 2. (top) Equivalent slip plot of the events of M 5.5 from the middle figure. Magnitudes converted to moment by the usual relation log $M_o = 16 + 1.5\ M_L$, equivalent slip (u) based on a fault plane of area 10 x 40 km (A) and $M_o = Au$.

(middle) Stick figure of the events above the dashed line in the space time plot. This represents activity at the southern end of the 1906 break.

(bottom) Space time plot of the seismicity along the San Andreas from Bear Valley to Los Gatos. M 5 prior to 1900, M 4.5 since that time.

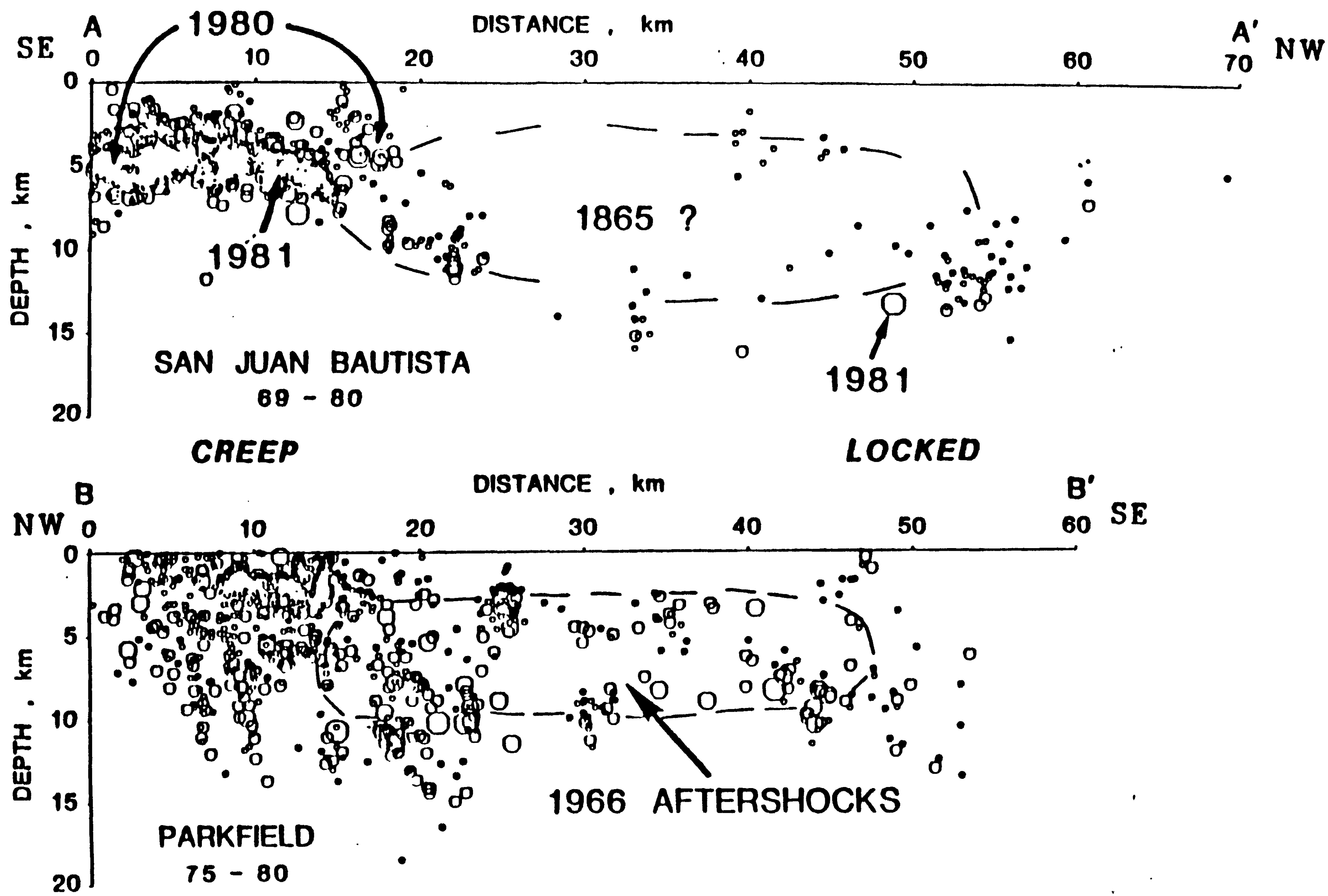

Fig. 3. (bottom) Cross section in the plane of the San Andreas, of the seismicity in the Parkfield area since 1975. (top) Similar plot of the activity in the San Juan Bautista region since 1969. Arrows identify hypocenters of M 4 earthquakes from 1980-81. Note that NW is to the right in the top figure, but to the left at the bottom; thus both cross sections are oriented such that the creeping portions of the fault are to the left in each case, and the locked portions to the right. The locations of the two cross sections are shown in Figure 1.

PREDICTION

DATA
BLACK BOX
PREDICTION
EVALUATION

ACTION

IGNORE
LAUGH
WORRY
CRITICIZE
RESEARCH
PUBLIC ACTION

View Graph 1

US-Soviet Cooperation in Earthquake Prediction
(Some important Soviet participants)

Academy of Sciences of the USSR

International Institute for the Theory of Earthquake Prediction and Mathematical Geophysics

Address: Warshavskoe Sh., 79 k.2, Moscow 113556, USSR

Phone: (095)110 77 95

FAX #: (095) 310 70 32

Telex: 411 628 IFZWA SU

V.I.Keilis-Borok - Director

I.M.Rotwain - author of the CN algorithm
V.G.Kossobokov - author of the M8 algorithm
G.M.Molchan - leading statistician
A.M.Gabrielov - mechanical models
I.V.Kouznetsov - author of software for analysis of catalogues
A.Lander - geophysicist
T.A.Levshina - physicist
I.Vorobieva - applied mathematician

View Graph 2

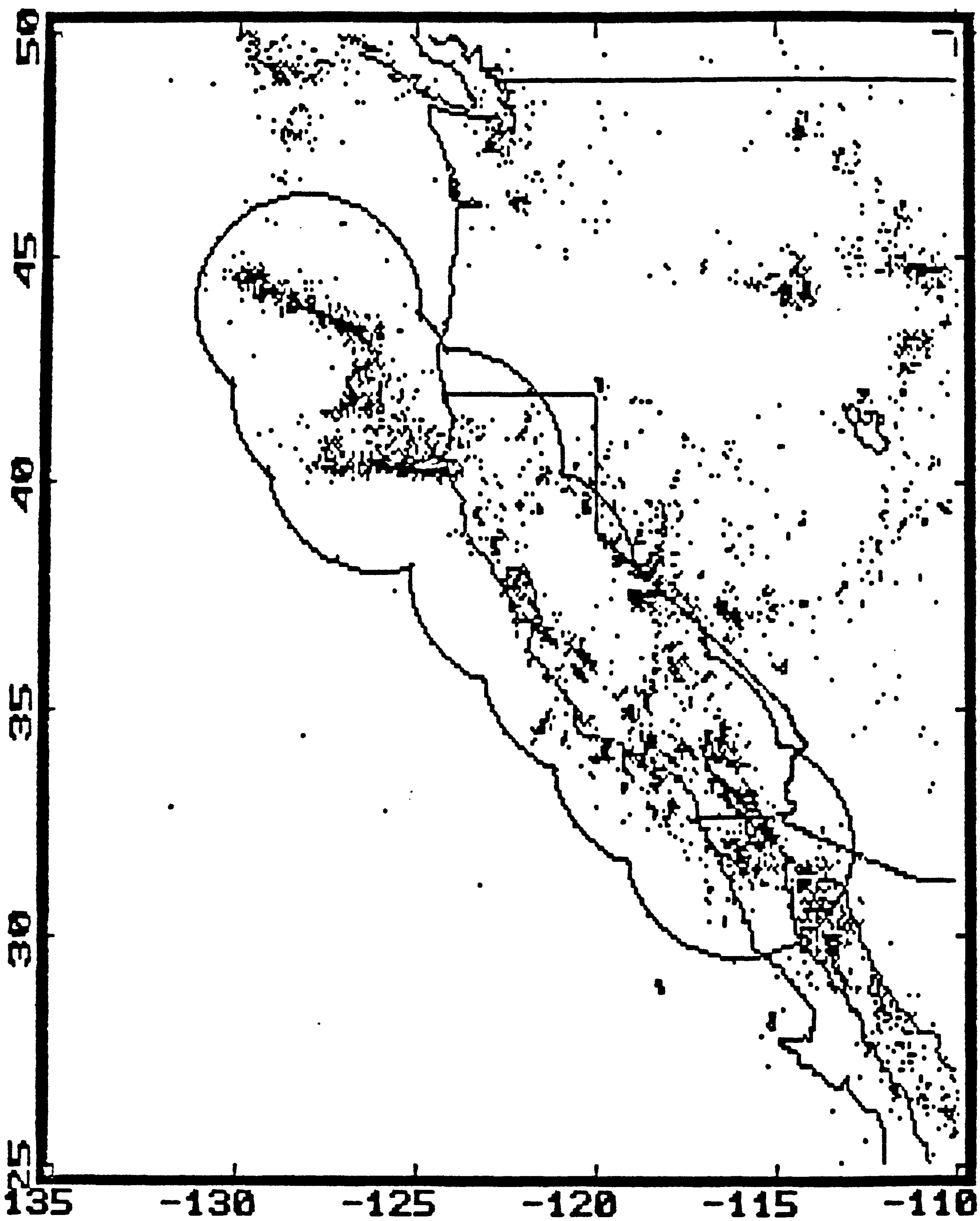

FIGURE 1

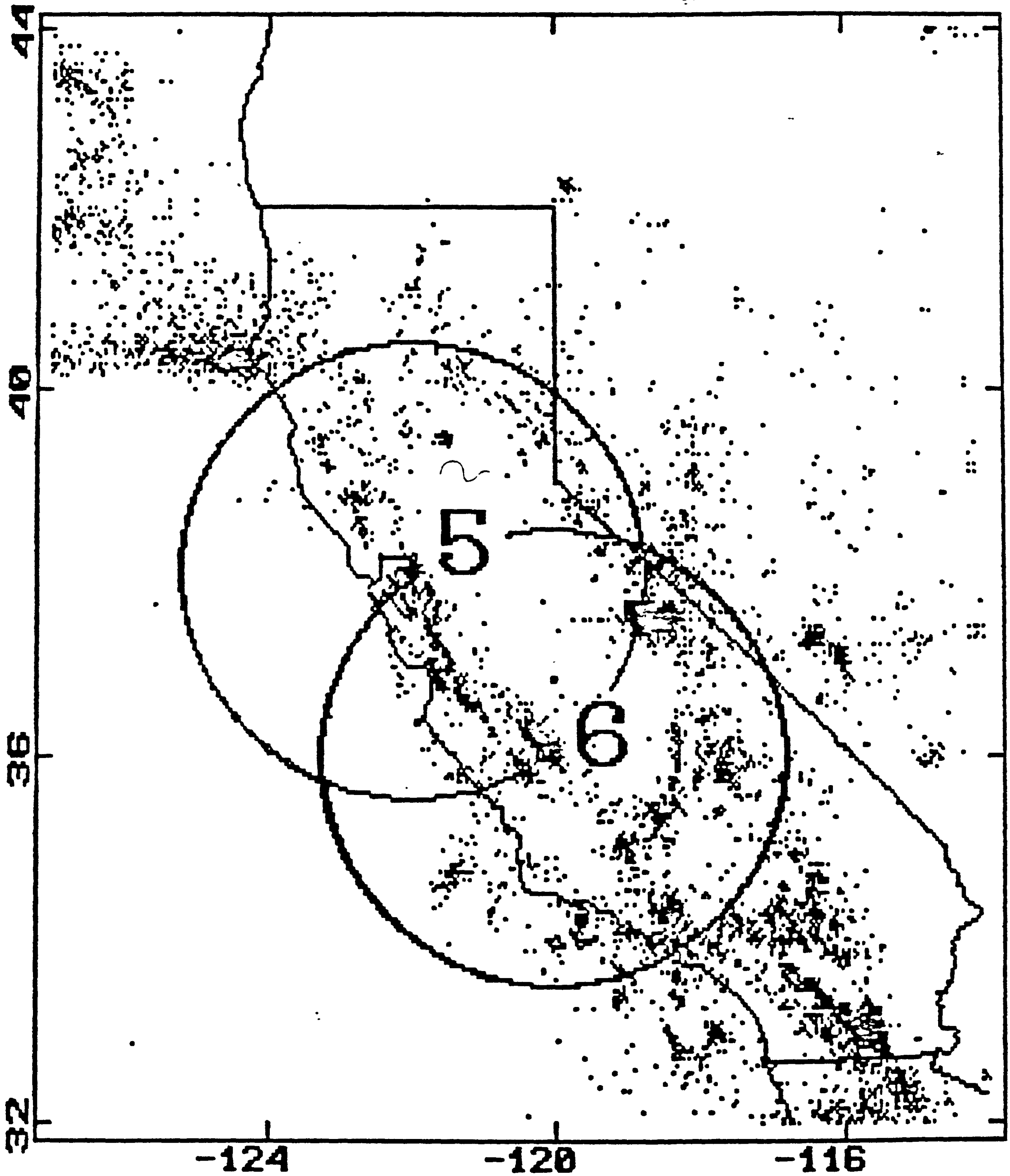

FIGURE 2

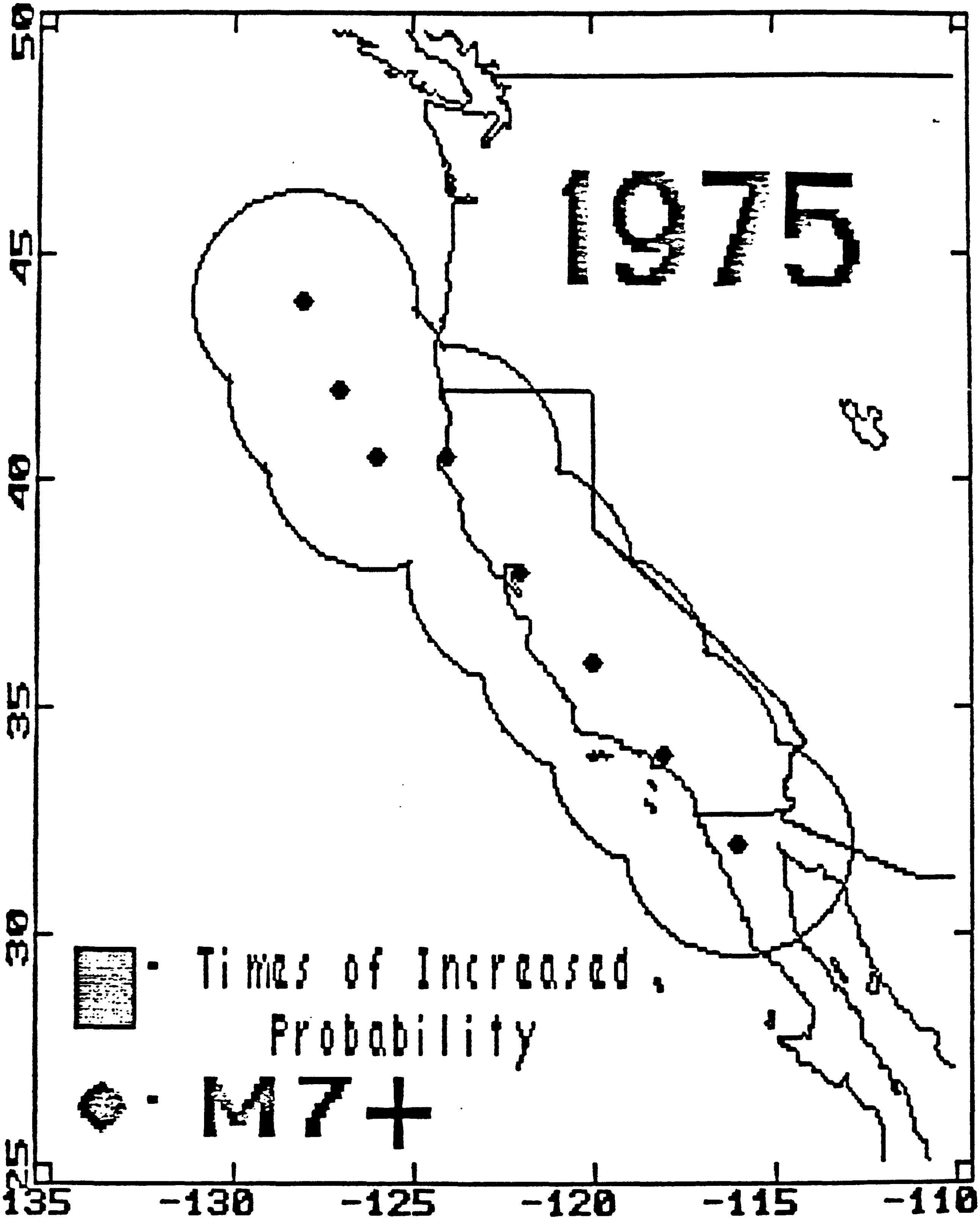

1975
Times of Increased, Probability
M7+
50
45
40
35
30
25
135
-130
-125
-120
-115
-110

FIGURE 3

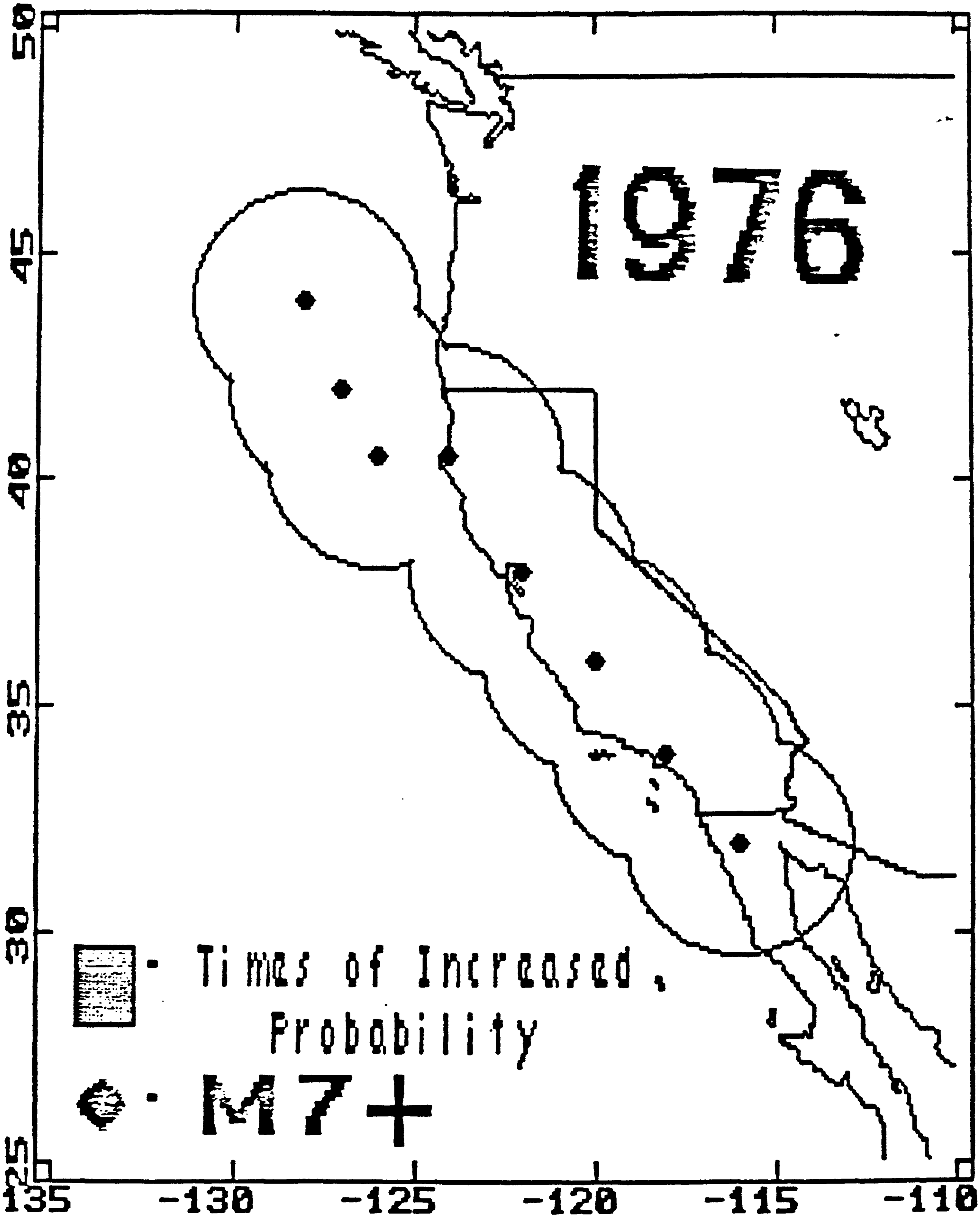
1976
Times of Increased Probability
M7+
50
45
40
35
30
25
135
-130
-125
-120
-115
-110

FIGURE 4

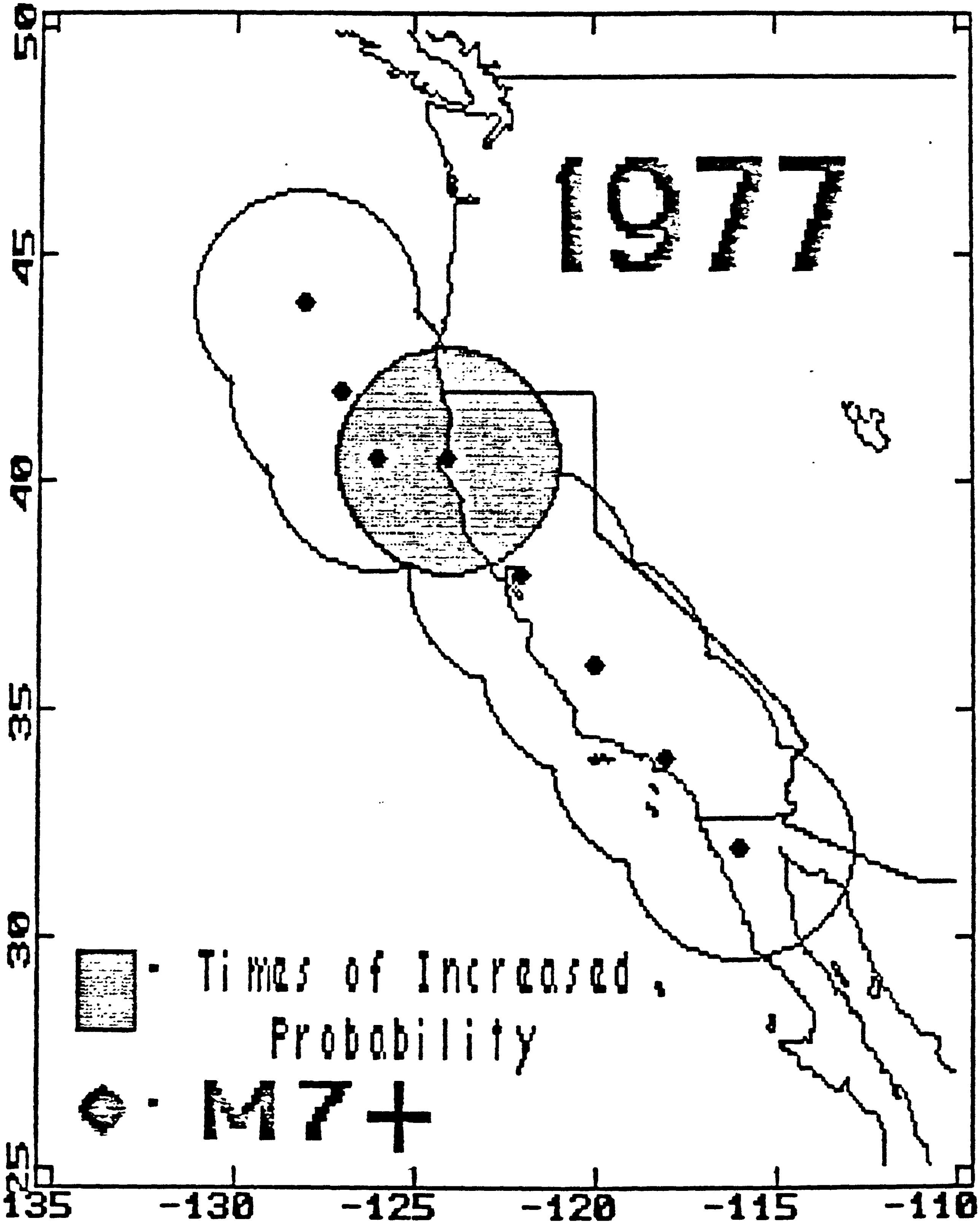
1977
Times of Increased Probability
M7+
50
45
40
35
30
25
135
-130
-125
-120
-115
-110

FIGURE 5

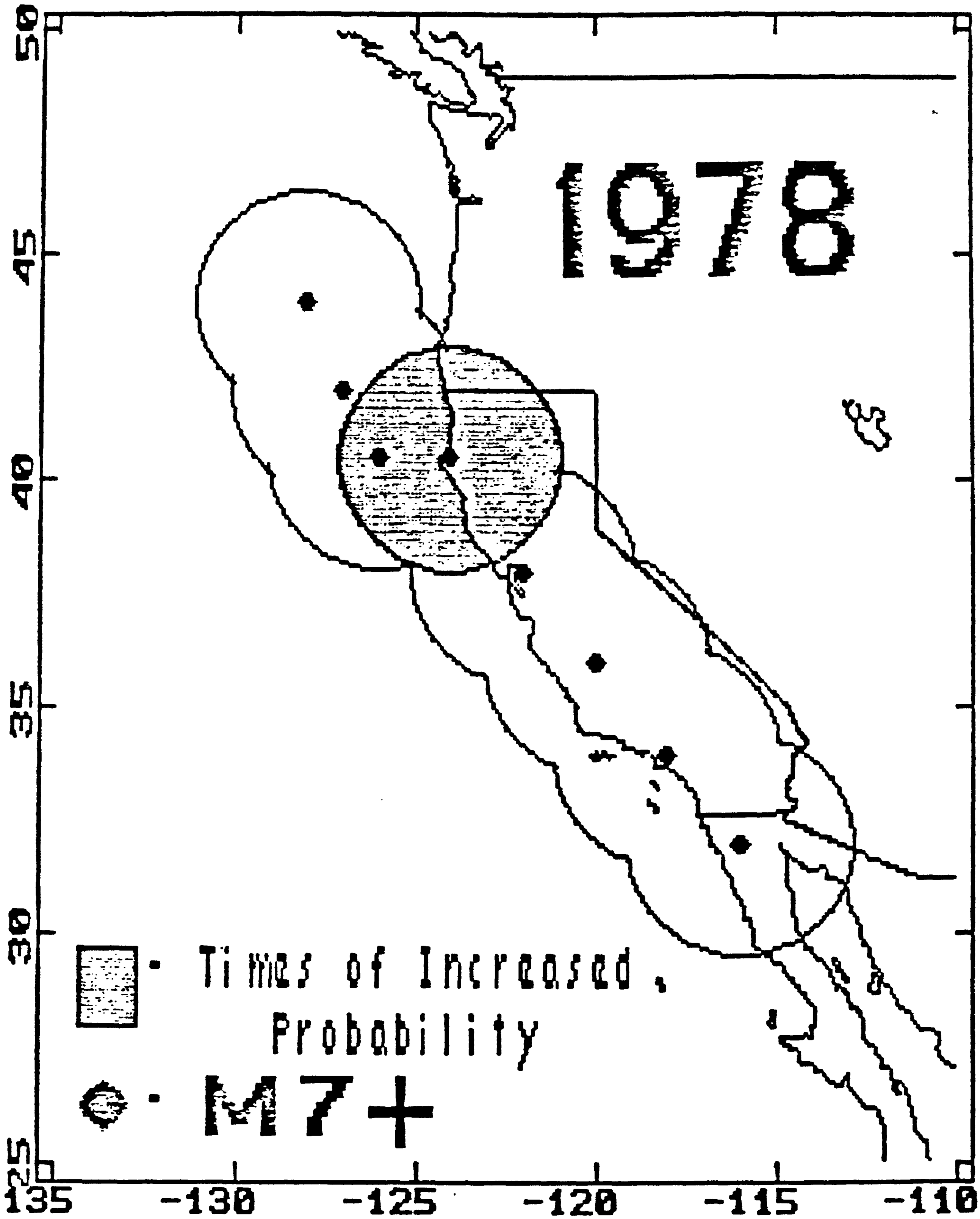

1978
50
45
40
35
30
25
135
-130
-125
-120
-115
-110
- Times of Increased Probability
- M7+

FIGURE 6

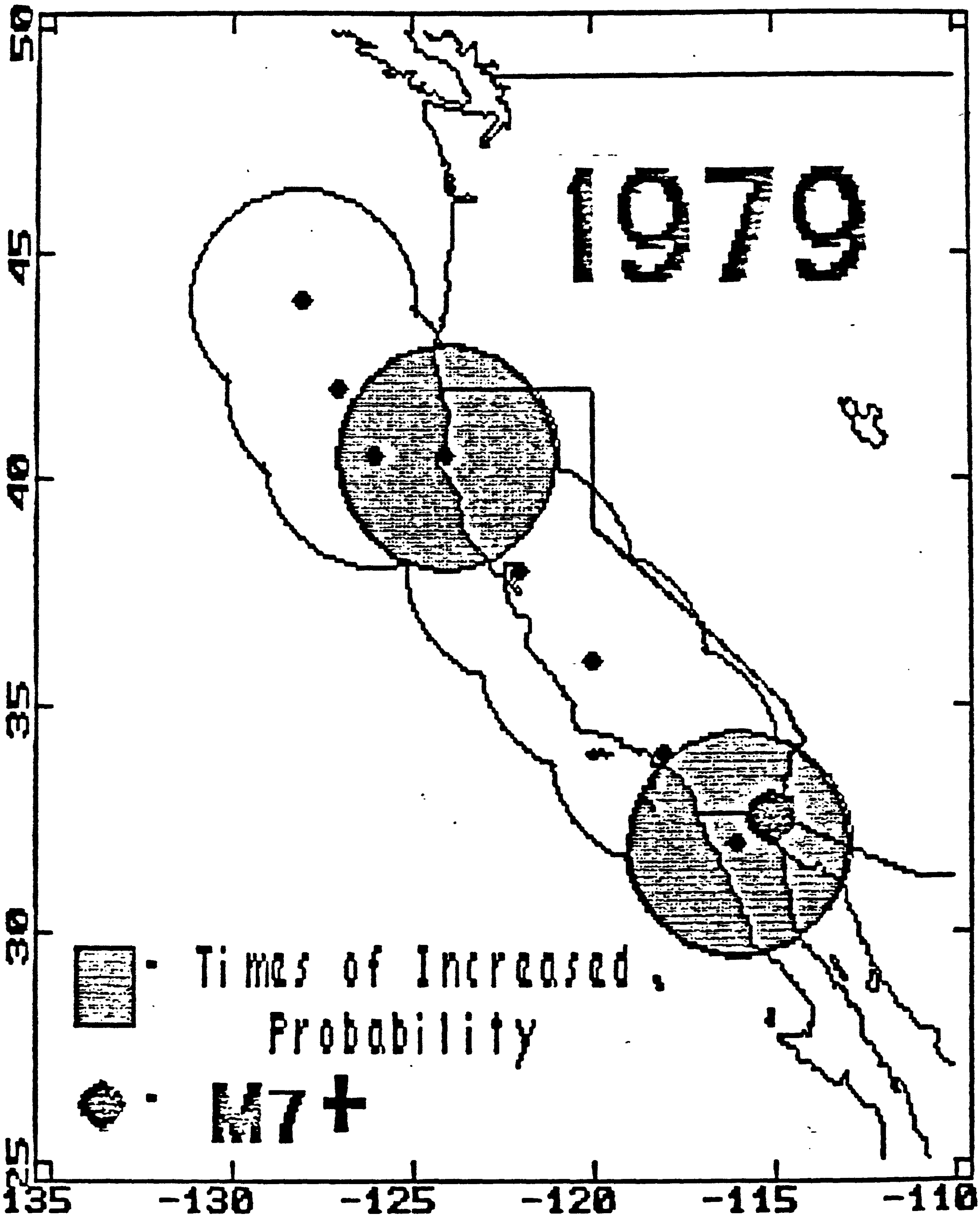
1979
50
45
40
35
30
25
135
-130
-125
-120
-115
-110
Times of Increased Probability
M7+

FIGURE 7

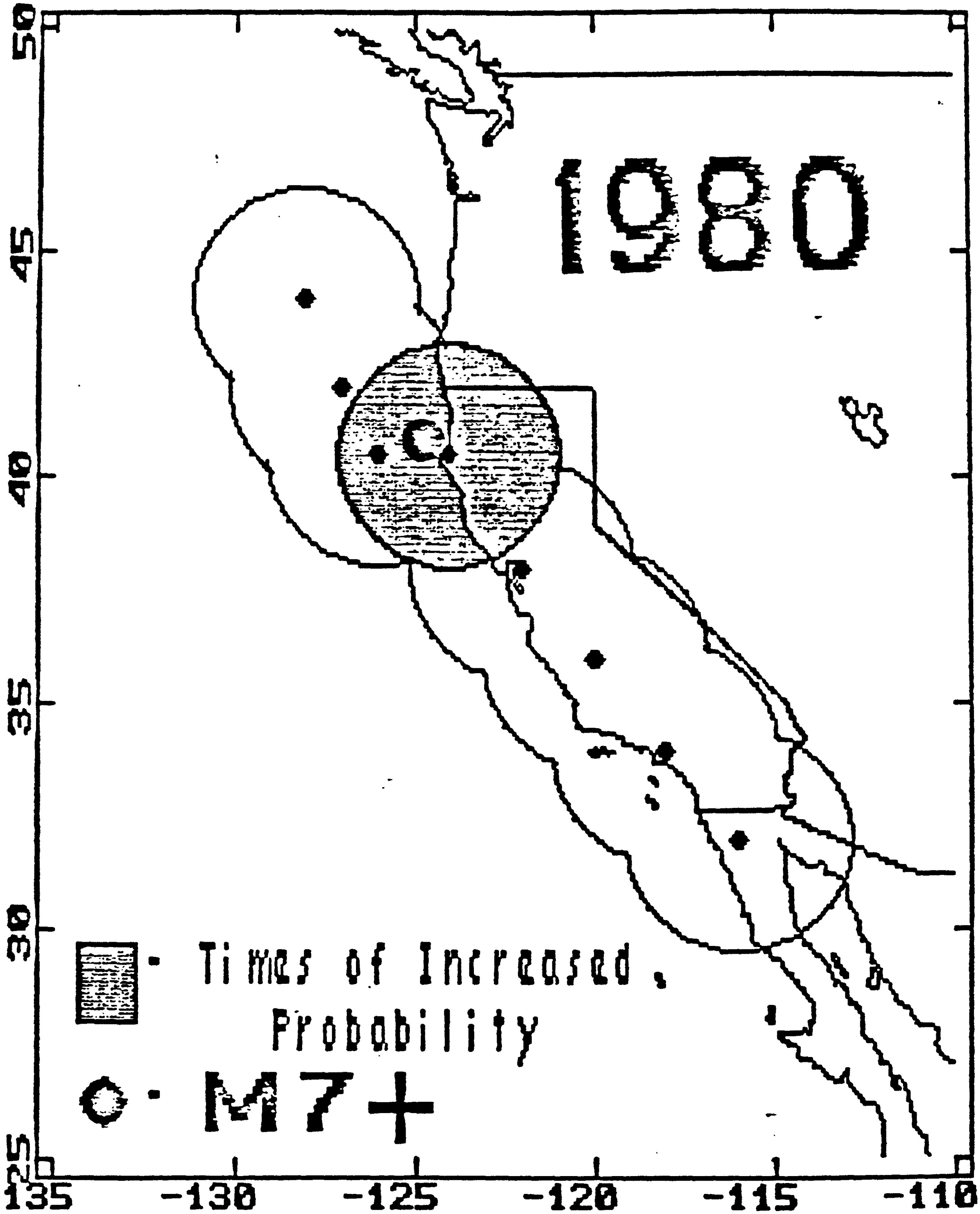

1980
Times of Increased Probability
M7+
50
45
40
35
30
25
135
-130
-125
-120
-115
-110

FIGURE 8

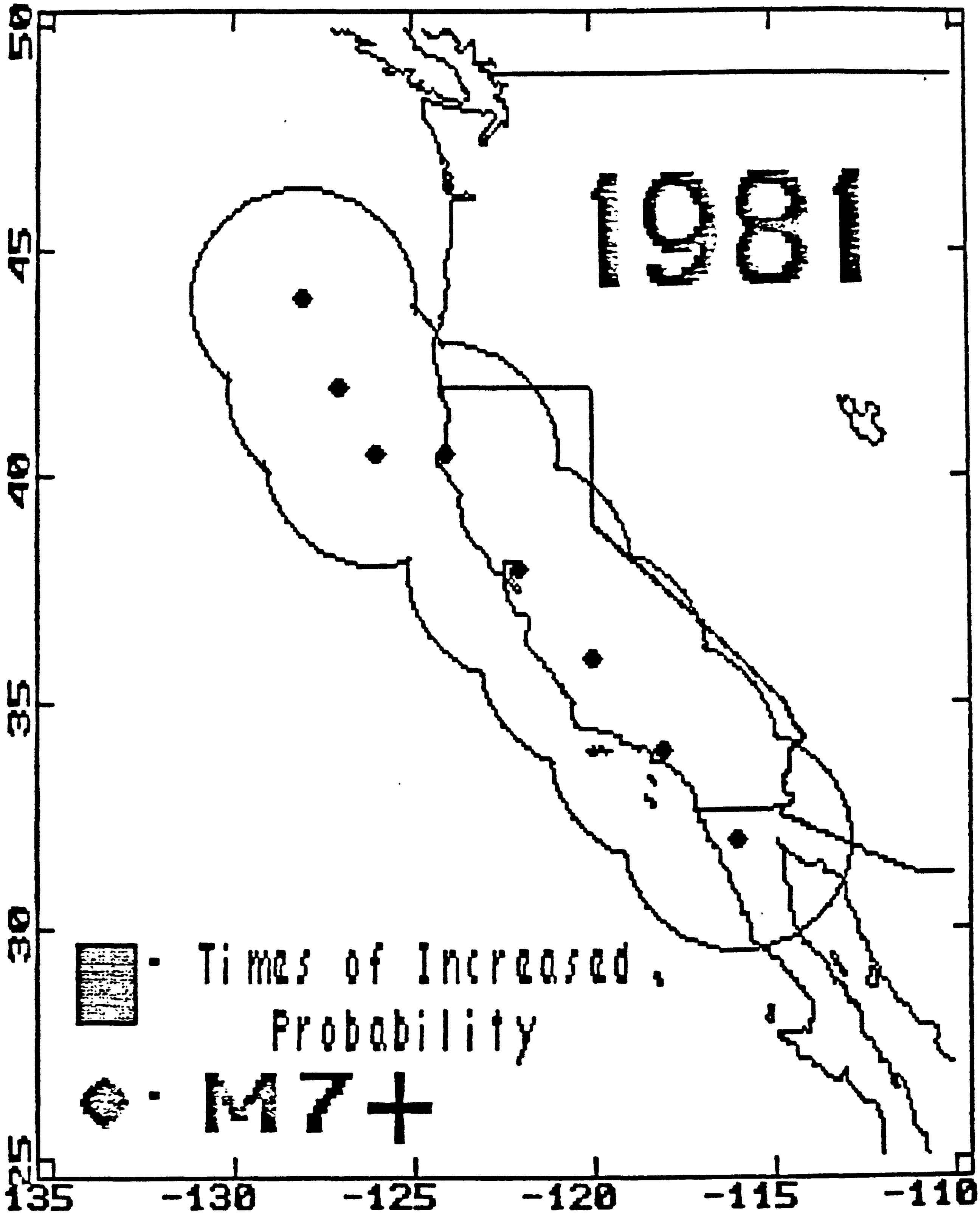
1981
Times of Increased Probability
M7+
50
45
40
35
30
25
135
-130
-125
-120
-115
-110

FIGURE 9

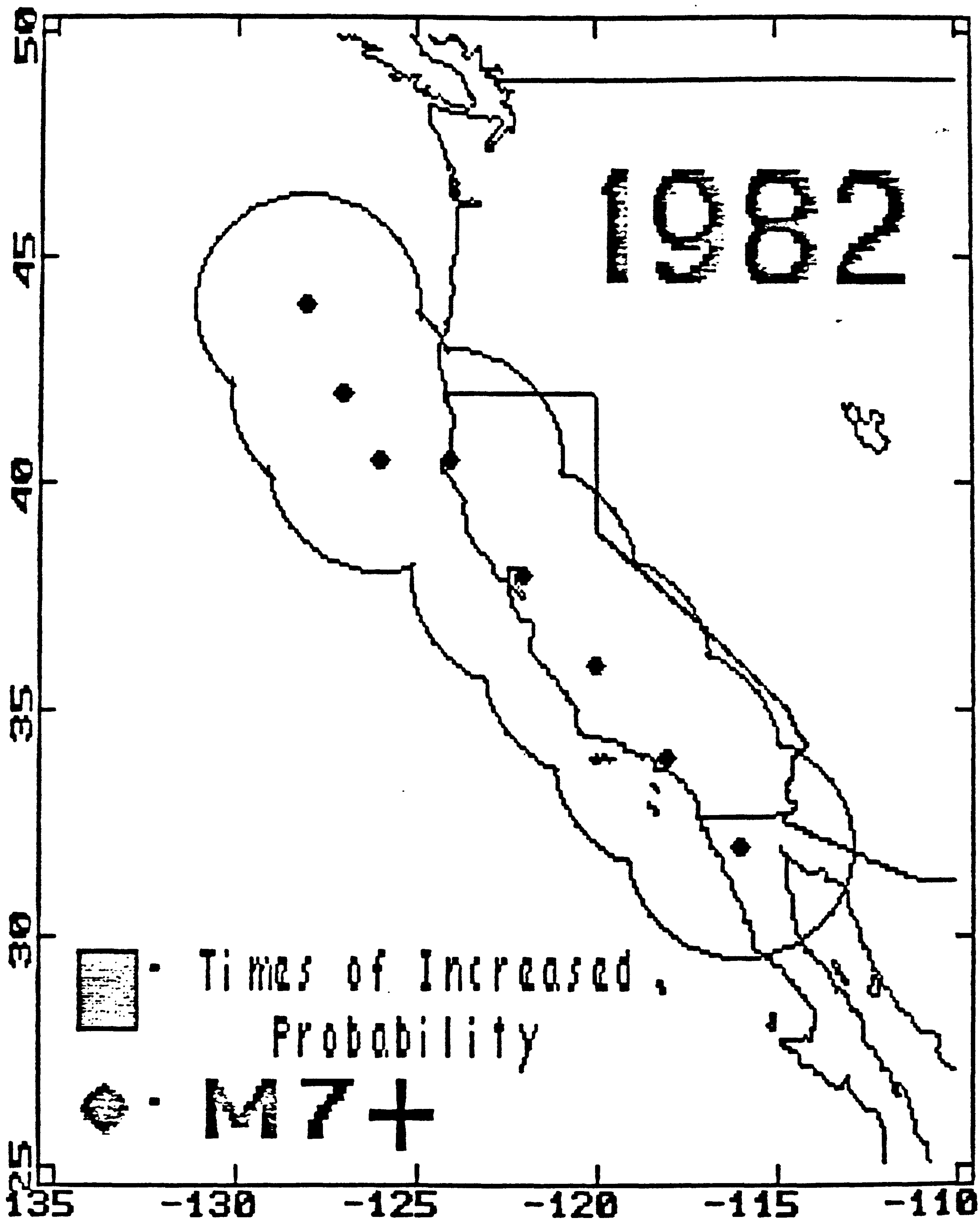

1982
Times of Increased Probability
M7+
50
45
40
35
30
25
135
-130
-125
-120
-115
-110

FIGURE 10

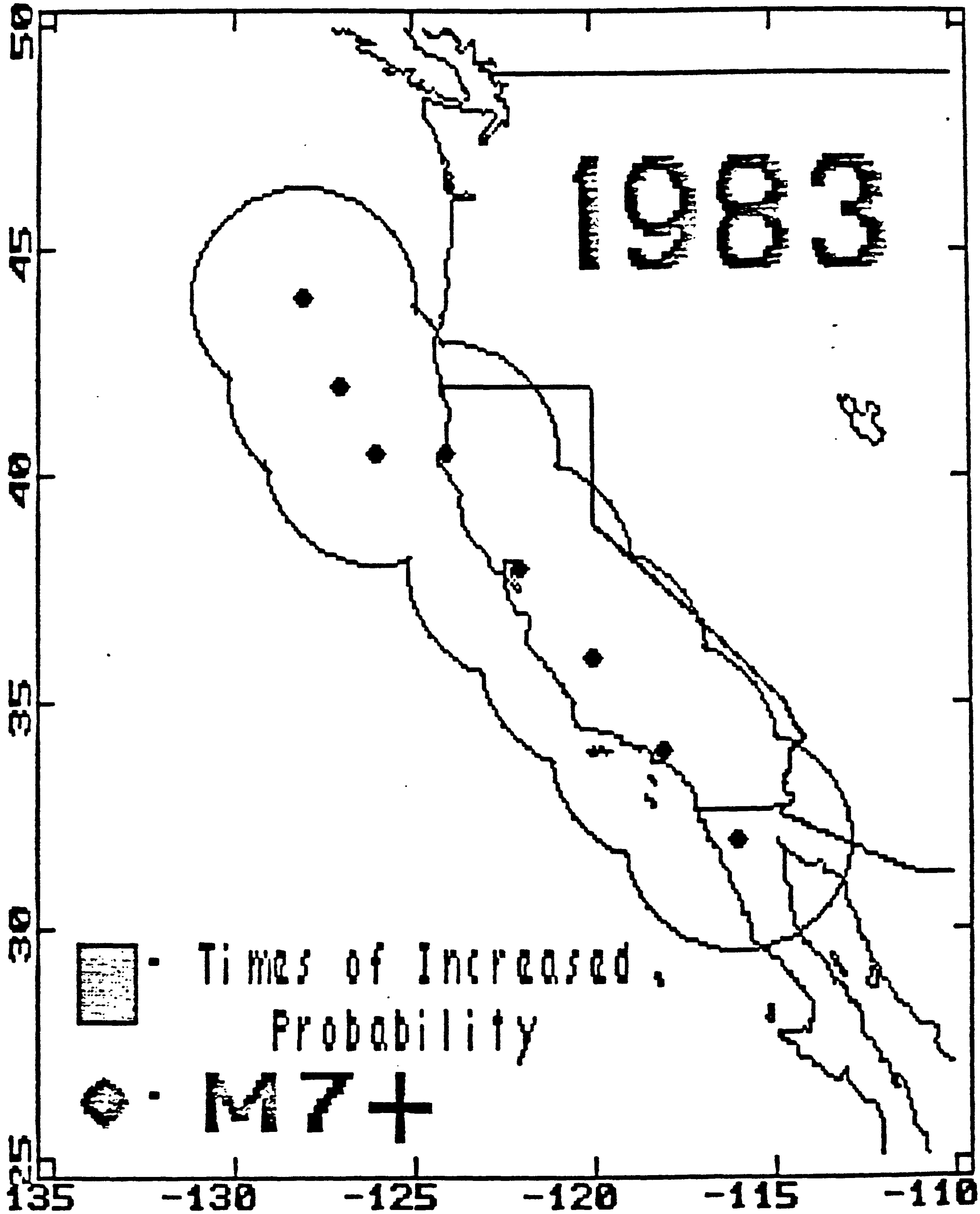
1983
Times of Increased Probability
M7+
50
45
40
35
30
25
135
-130
-125
-120
-115
-110

FIGURE 11

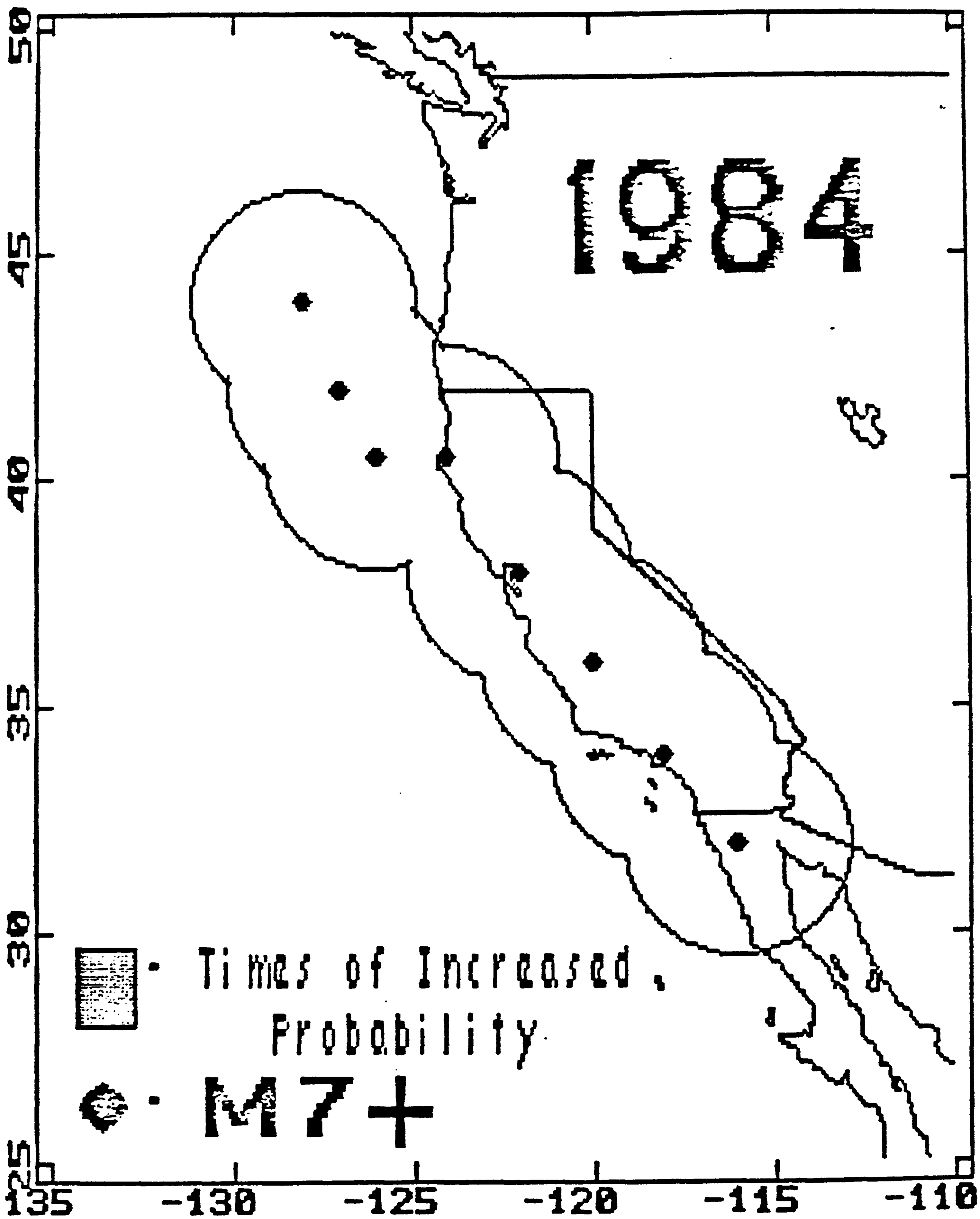
1984
50
45
40
35
30
25
135
-130
-125
-120
-115
-110
- Times of Increased Probability
- M7+

FIGURE 12

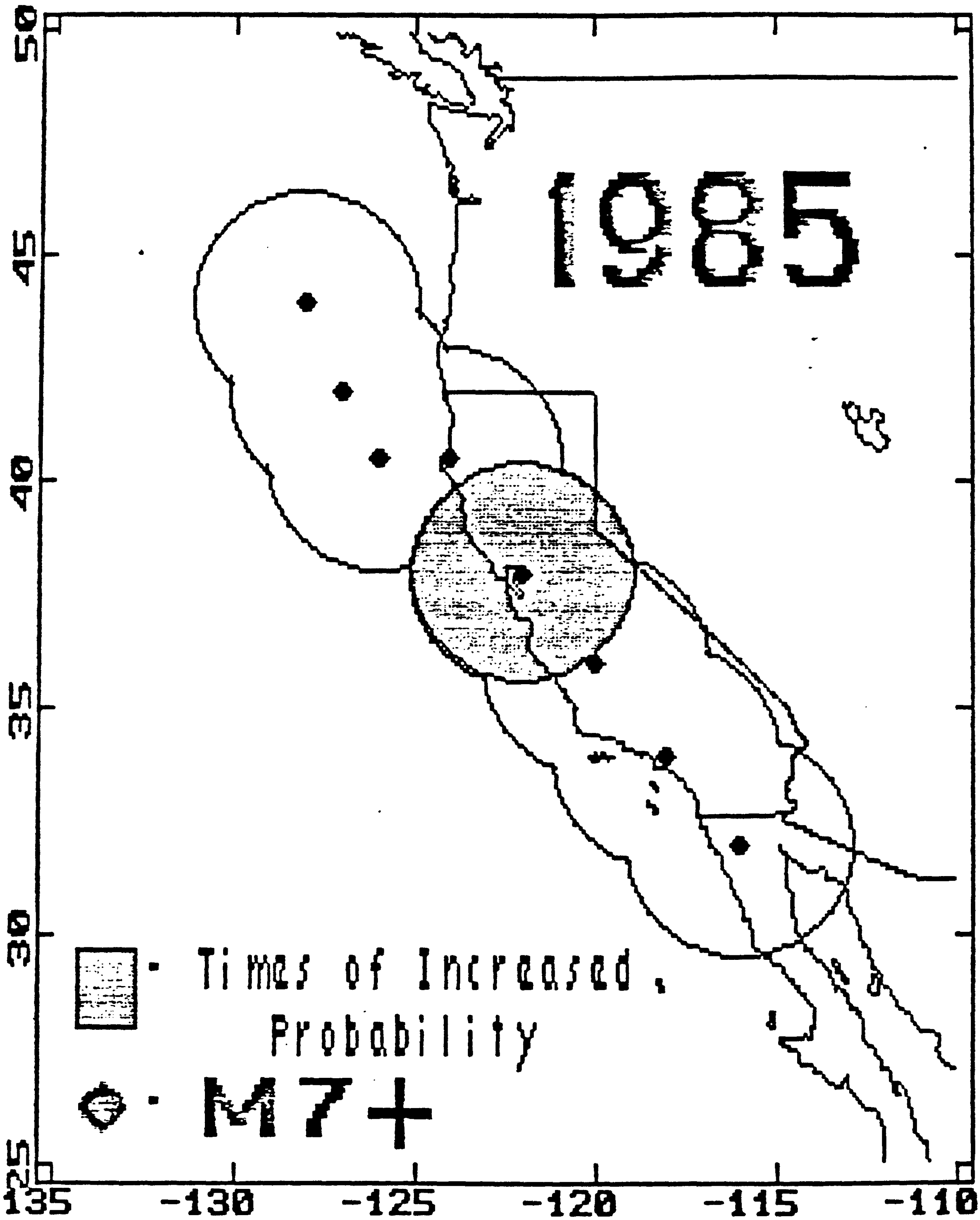

1985
Times of Increased, Probability
M7+
50
45
40
35
30
25
135
-130
-125
-120
-115
-110

FIGURE 13

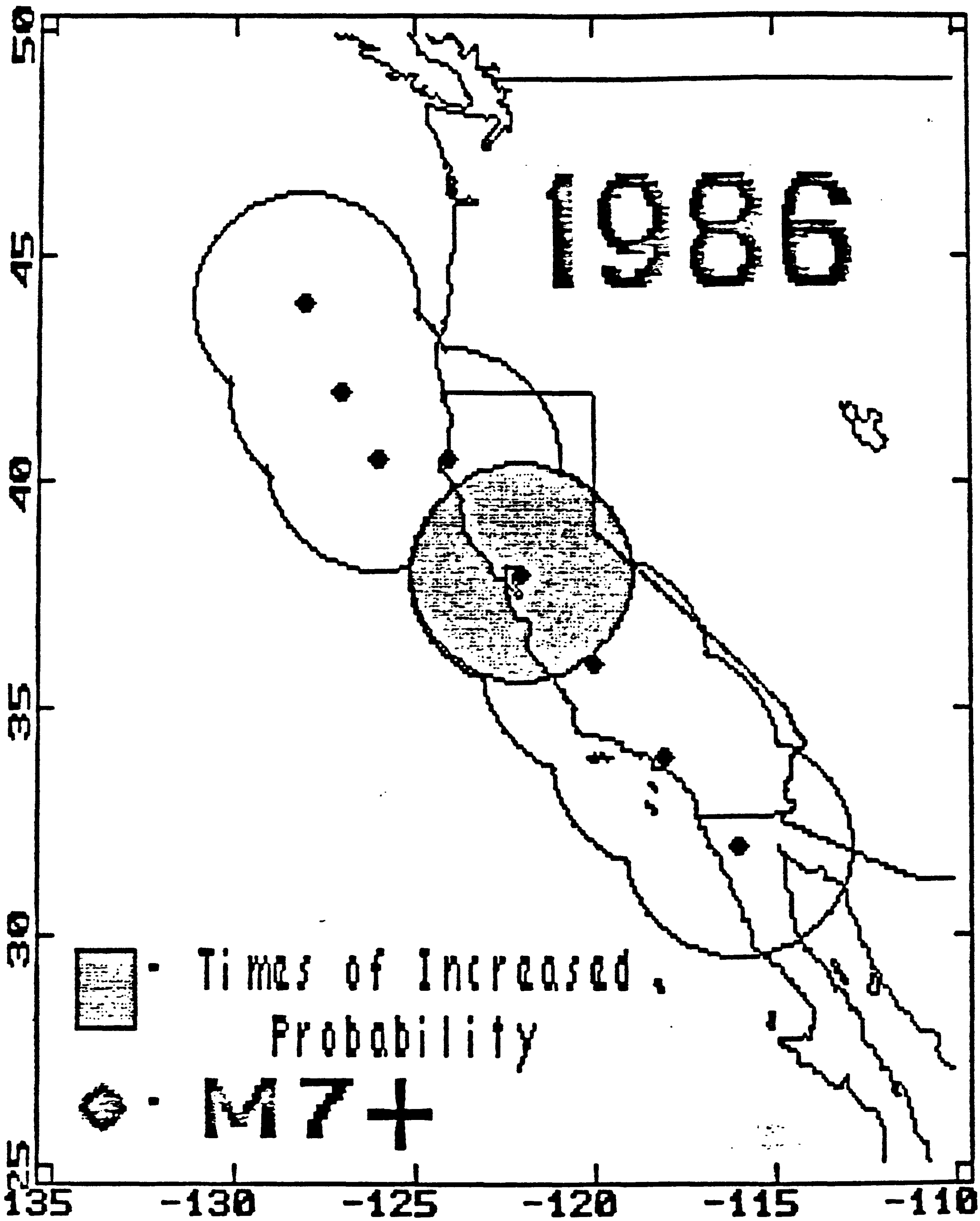

1986
Times of Increased Probability
M7+
50
45
40
35
30
25
135
-130
-125
-120
-115
-110

FIGURE 14

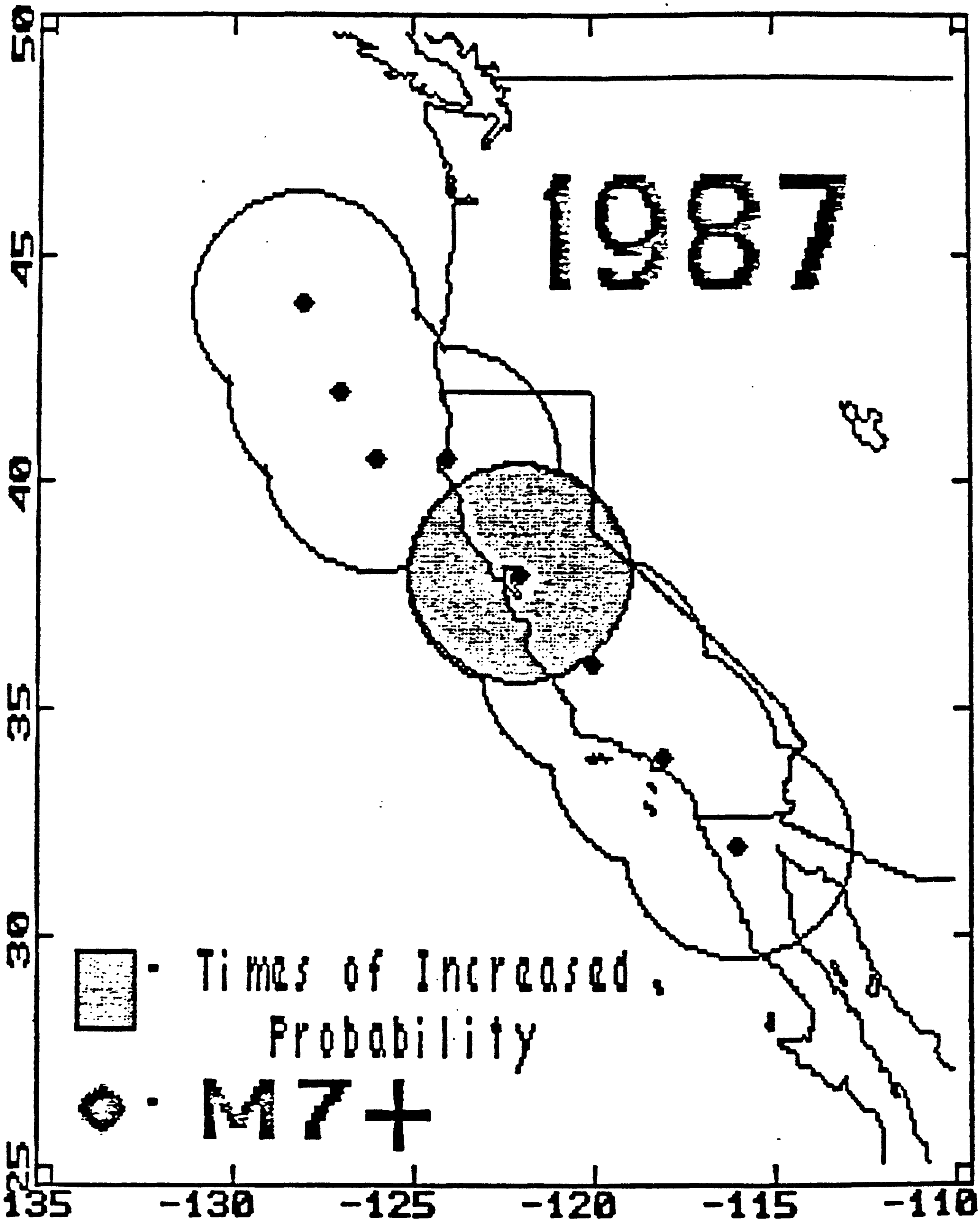
1987
Times of Increased
Probability
M7+
50
45
40
35
30
25
135
-130
-125
-120
-115
-110

FIGURE 15

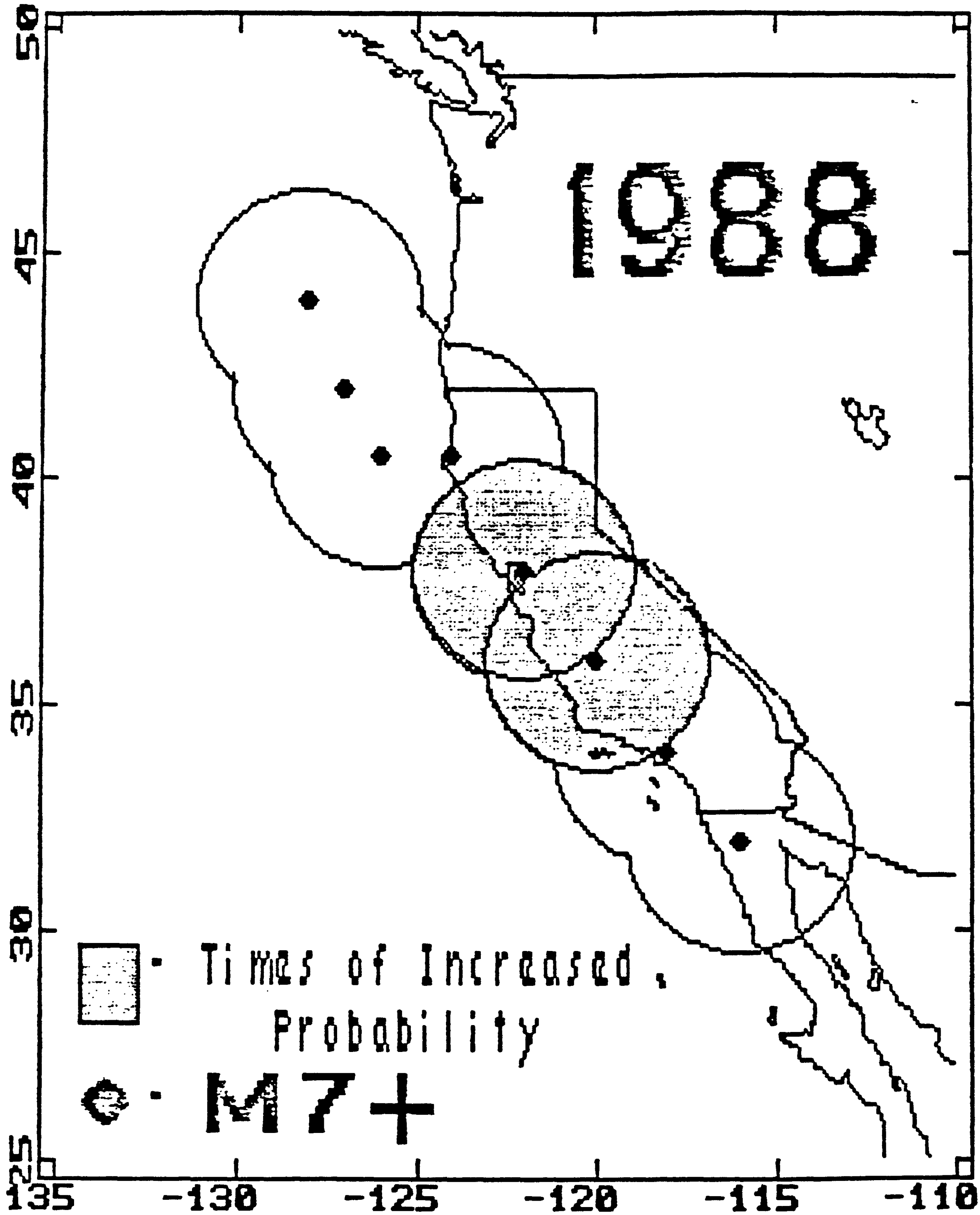
1988
Times of Increased Probability
M7+
50
45
40
35
30
25
135
-130
-125
-120
-115
-110

FIGURE 16

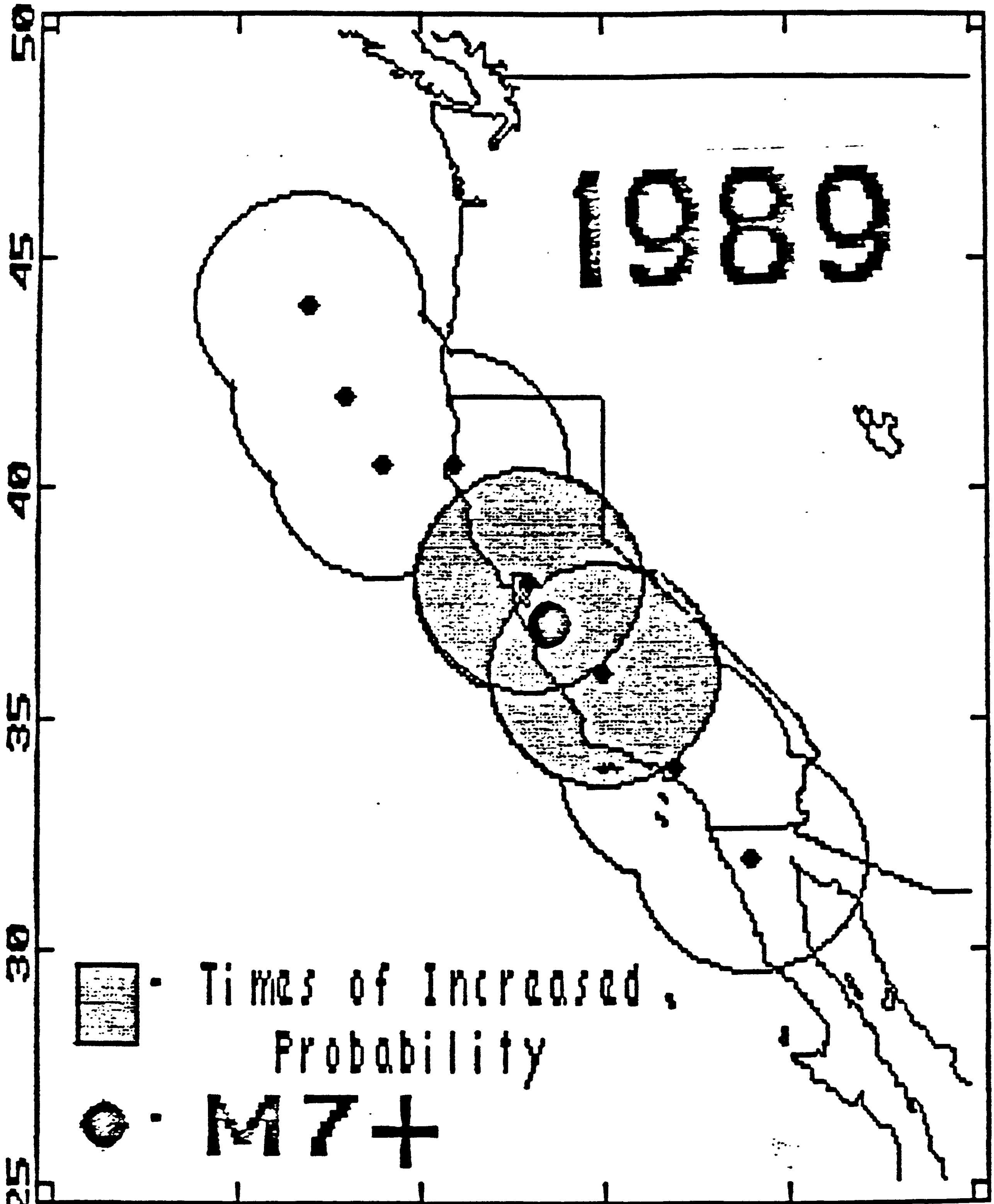
1989
Times of Increased Probability
M7+
50
45
40
35
30
25
135
-130
-125
-120
-115
-110

FIGURE 17

Appendix C

Reprints provided by A.Bernardi to accompany presentation to NEPEC, January 11, 1990.

Proc. 1985 IEEE Internat. Symp. on Electromag. Compatability, Wakefield, Mass., Aug. 1985

THE STANFORD UNIVERSITY ELF/VLF RADIOMETER PROJECT: MEASUREMENT OF THE GLOBAL DISTRIBUTION OF ELF/VLF ELECTROMAGNETIC NOISE

A.C. Fraser-Smith and R.A. Helliwell
Space, Telecommunications and Radioscience Laboratory
Stanford University, Stanford, CA 94305

Abstract. Stanford University is currently conducting a global survey of electromagnetic noise in the 10 - 32,000 Hz (ELF/VLF) frequency band using a network of eight computer-controlled receiving systems, or 'radiometers.' One goal of this measurement program is to improve communication in the ELF/VLF band by providing more up-to-date and complete information about the properties of ELF/VLF noise (both natural and man-made) than is currently available--the last extensive survey of noise in the same frequency band was made over two decades ago. In this presentation we describe the Stanford ELF/VLF noise measurement project, including the instrumentation comprising each of the radiometers, the form of their analog and digital measurements (which are made under the control of a minicomputer), and the data processing techniques that will be used. The results of previous noise surveys are briefly reviewed and the significance of the overall decline of noise power with increasing frequency revealed by these surveys and other studies is discussed in the context of the scientific applications of the noise data obtained by the radiometer network.

Introduction

The Stanford University ELF/VLF Radiometer is a new dual-channel computer-controlled system that provides quantitative measurements of electromagnetic activity in the frequency range 10 Hz to 32 kHz. Both analog and digital recording are used, the latter covering 16 narrowband channels (5% bandwidths) distributed throughout the specified frequency range; the actual frequencies are listed in Table 1. Synoptic recordings of wideband ELF/VLF analog data (200 Hz to 32 kHz) are made on a routine basis, usually in the format of 1 minute of recording every 30 minutes. However, during periods of unusual activity, or during intervals of cooperative measurements, it is possible for the operator to record the analog data continuously. Synoptic recordings of wideband lower-ELF data (10-400 Hz) are also made, but in this case the data are recorded digitally. Further technical details of the radiometer are provided below.

The radiometer project was undertaken in response to several different requirements in ELF/VLF studies. Perhaps the most important of these requirements is the need for accessible well-calibrated data with continuous high time and amplitude resolution over a wide range of frequencies. This need led to the adoption of the predominantly digital recording capability in the design of the radiometer, and the inclusion of automatic calibration circuitry. The analog recording capability provides an essential check on the digital data, a backup in case of failure of the digital system, and wideband data for a variety of special studies and cooperative observations. Another important requirement in ELF/VLF research is information about the global distribution of ELF/VLF noise, and this need will be satisfied by locating up to eight of the radiometers at widely-separated locations over the earth's surface.

The present actual and planned locations for the radiometers are: (1) Thule, Geenland, (2) Sondre Stromfjord, Greenland, (3) New Hampshire (i.e., East-Coast USA), (4) L'Aquila, Italy, (5) Stanford, California (i.e. West-Coast USA), (6) Kochi, Japan, (7) Dunedin, New Zealand, and (8) Arrival Heights, adjacent to McMurdo Station, Antarctica. The geographical coordinates of the locations are tabulated in Table 2 and their distribution is shown in Figure 1.

Operation of the radiometers is largely automatic. However, tape changes are necessary every 2 - 7 days, depending on the adopted recording schedule (currently changes every two days are required), and a daily check of the system operation lasting for approximately 30 minutes is also required. With the exception of the Stanford and Arrival Heights radiometers, which are operated either by Stanford scientists or by scientists and technicians located at McMurdo Station, operation of the radiometers is the responsibility of local scientists involved in ELF/VLF studies, who assume responsibility for the operation of the radiometers on a cooperative basis. We should also point out the opportunities for other cooperative work. In particular, independent observations at the frequencies indicated in Table 1, or at other frequencies in the overall range 10 Hz to 32 kHz, could

Table 1: Center frequencies and bandwidths for the 16 narrowband channels of the ELF/VLF radiometer.

Channel	Center Frequency	Bandwidth (5%)
ELF system 1	10 Hz	0.5 Hz
2	30	1.5
3	80	4.0
4	135	6.75
5	275	13.75
6	380	19.0
VLF system 1	500	25.0
2	750 Hz	37.5
3	1 kHz	50
4	1.5	75
5	2	100
6	3	150
7	4	200
8	8	400
9	10.2	510
10	32 kHz	1600 Hz

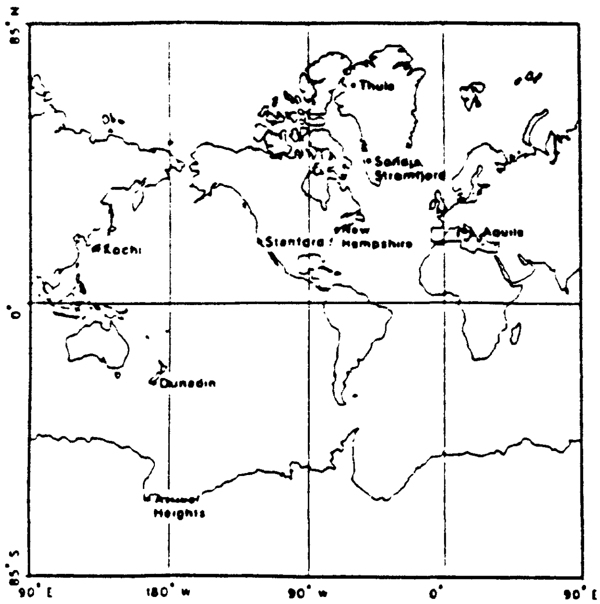

Figure 1: Locations of the eight radiometer installations.

be mutually beneficial. It is anticipated that the radiometers will be operated simultaneously for at least a year following the completion of their deployment, *i.e.*, until approximately the end of 1986.

Fortuitously, the radiometers in California, Italy, Japan, and New Zealand are located either in or close to seismically active regions and their continuous operation for up to a year may make possible a study of the relationship that has been reported between ELF/VLF electromagnetic wave emissions and the occurrence of earthquakes [*e.g.*, 7, 10, 11]. The feasibility of conducting this study will depend on the earthquake activity that occurs during the ELF/VLF data aquisition period.

Frequency Designation

From the point of view of its signal input, the radiometer consists of two independent receivers, one for the frequency range 200 Hz - 32 kHz and the other for the range 10 - 400 Hz. These frequency ranges straddle the VLF (3 - 30 kHz) and ELF (5 Hz - 3 kHz) frequency ranges, as well as extending slightly above the official VLF range, which causes some difficulty in nomenclature. For simplicity, throughout the remainder of this communication, we will refer to the radiometer's upper frequency range (200 Hz - 32 kHz) as VLF and we will refer to its lower frequency range (10 - 400 Hz) as ELF.

Some Technical Details of the Radiometer

A block diagram showing the various subsystems comprising the radiometer is given in Figure 2; the following discussion of the radiometer is essentially a guided tour of the block diagram, starting at the input end (*i.e.*, at the antennas) and working through the system to the output end (*i.e.*, to the tape recorders). As noted above, the radiometer consists initially of two independent receivers, one for the frequency range 200 Hz - 32 kHz (referred to as VLF) and the other for the range 10 - 400 Hz (referred to as ELF). Note further that each of the receiving systems is dual channel, i.e., both North-South (N-S) and East-West (E-W) data are measured simultaneously. The total electric power required to operate the system lies in the range 1 - 2 kW, with the largest power usage occurring when all the systems, including the two tape recorders in particular, are all operating.

Antennas. There are two pairs of crossed antennas, one pair for VLF signals and the other for ELF signals. Within each pair, one antenna is oriented in a N-S direction and the other in an E-W direction (these directions could change if strong local interference is encountered). The VLF antennas are conventional single-turn triangular loop antennas. They are 9 m in height and 18 m across at the base, with an area of 81 m^2; their resistance is 0.062 ohms and their inductance 65 microhenries. Antennas of this type have been used extensively at Stanford installations for many years. The ELF antennas are specially designed and constructed loop antennas of circular cross-section with a mean radius of about 0.49 m. To control their electrical characteristics, the coils were wound in 12 segments of 97 turns, giving a total of 1164 turns. Their resistance is 75 ohms, their inductance 2.7 henries, and they weigh roughly 30 kgm (65 lb). The VLF antennas can be supported above ground by means of a mast, but to avoid wind-induced noise the ELF antennas must either be buried or carefully shielded from the wind with an appropriate structure.

Preamplifiers and Line Receivers. The preamplifiers and line receivers were designed and constructed at Stanford. They are of conventional design, but extensive use was made of circuits and components that would ensure stable, reliable, low-noise operation. Notch filters are built-in to remove up to four power-line frequencies. The four frequencies are 60, 120, 180, and 300 Hz for locations with 60 Hz local power systems, or 50, 100, 150, and 250 Hz for locations with 50 Hz local power systems. Individual filters can be inserted or omitted as desired.

Mixer/Monitor. The mixer/monitor is an interface between the VLF line receiver and the analog tape recorder. It has a 4 channel capability (although not all channels will be used initially) and provision is made for voice annotation on the tapes. While the design of the mixer/monitor is largely conventional, an important innovation is the inclusion of a capability for it to feed information on all the front panel settings to the computer, so that the settings can be included automatically in the log.

Table 2: Geographical coordinates for the eight radiometer sites.

Station	Coordinates
Arrival Heights, Antarctica	78°S, 167°E
Sondre Stromfjord, Greenland	67°N, 50°W
Thule, Greenland	80°N, 60°W
Dunedin, New Zealand	46°S, 170°E
Kochi, Japan	33°N, 133°E
Stanford, California	37°N, 122°W
New Hampshire	43°N, 72°W
L'Aquila, Italy	42°N, 13°E

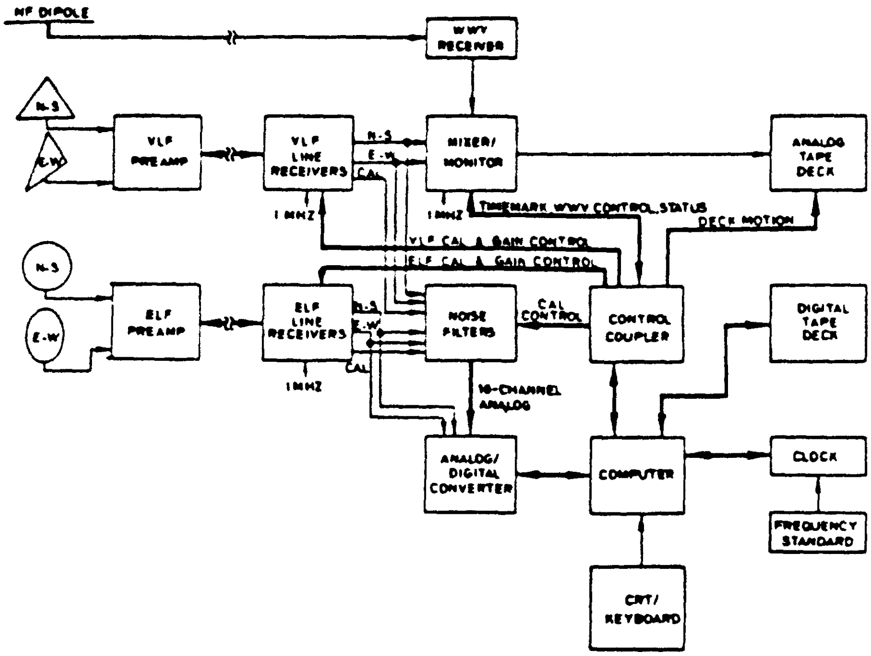

Figure 2: Block diagram of the Stanford ELF/VLF radiometer.

Noise Filter Unit. The purpose of this unit is to provide the 16-frequency filtered data for input to the analog-to-digital (A/D) converter. The unit contains 16 dual bandpass filters and rms detectors, with one pair of filters and detectors assigned to each frequency channel. Because of their dual characteristics, each pair of filters and detectors can simultaneously process both North-South and East-West data. The center frequencies for the 16 filters are listed in Table 1 and their bandwidths, as has already been described, are 5%. For each frequency channel there are two analog outputs giving the N-S and E-W detected data. These analog data are then sent to the A/D converter.

Analog-to-Digital Converter. The A/D converter is manufactured by Computer Products Inc. (Model RTP 7431/30). It digitizes input samples in any order under the control of the computer that will be described in the next section. It has 14-bit resolution and it will digitize up to 4,000 samples/second in our system. The input range is ±10.24 V, but there is a programmable gain of either 1, 2, 4, or 8, giving a minimum input range of ±1.28 V. In the present configuration the A/D converter has 32 single-ended input channels and 8 differential-input channels. The 32 single-ended input channels will be used for the analog data from the noise filters and two of the differential-input channels will be used to digitize the ELF broadband signal (sampled at a 1000 sample/sec rate); the remaining six differential-input channels are uncommitted at the present time.

Computer. The radiometer is computer controlled, and its data measurement capability is greatly enhanced as a result. We use a MicroNova MP/100 minicomputer with 64 kbytes of memory, in the form of 32 kbytes of RAM, and 32 kbytes of EPROM (erasable programmable memory). In addition to monitoring and controlling the operation of the radiometer, the computer will have some time available for data processing. One of its data processing tasks will be to compute the total rms signal in each of the 16 frequency channels by taking the square-root of the sum of the squares of the digitized N-S and E-W narrowband data. It will also calculate minimum, maximum, and average signal level statistics from the narrowband data.

Control Coupler. This unit was designed and constructed at Stanford. Its function is to allow the computer to read and control the status of all of the important subsystems in the radiometer (except for the A/D converter, clock, and digital tape deck, which are controlled directly by the computer). The computer will write control coupler status information onto the digital magnetic tape at regular intervals, thus providing a continuous log of the system operation.

Video Display Terminal (CRT/Keyboard). The system operator can communicate with the computer through a video display terminal. Status information can also be displayed and certain modifications to the system operation can be made by means of commands entered through the keyboard. We are using Zenith Z19 and Z29 terminals for this purpose.

Clock/Frequency Standard. A Stanford designed and constructed clock is used in conjunction with a 1 MHz commercial frequency standard (Spectracom) to provide accurate time information. The clock is read by the computer and in addition to giving standard time of day and day of year information it also provides (1) a two-character station code, (2) 10 msec interrupts to the computer for timing the operation of the digitizing system, and (3) synchronizing pulses to the A/D converter. The clock and frequency standard automatically switch to battery power during power failures, thus maintaining correct time information. Further, if the external frequency standard should fail, the clock has an internal crystal standard of reduced accuracy which automatically takes over.

Tape Recorders. Each radiometer has both an analog (Ampex 440C or TASCAM 42, 1/4-inch 1/2-track) and a digital tape recorder (Kennedy 9000, 800/1600 bpi), whose operations are controlled by the computer. The number of times fresh tapes must be loaded will depend on the sampling rate (digital data) and on the format adopted for the synoptic recordings (analog data), which can be varied by the operator. According to our current mode of operation, fresh tapes are required every two days for the analog data and every four days for the digital.

Format of the Digital Data on Tape. The digital data acquired by the radiometer will be written onto the digital data tape in 4096 32-bit-word blocks. These digital data will include system status information (*i.e.*, the system log), operator messages entered via the video terminal, the broadband ELF synoptic data, and the digital samples of the 16-channel narrowband data. The latter data can be written onto the tape at a variety of operator-selectable rates in the range of 0.1 - 5 samples/second; we are using a rate of 1 sample/second as the standard for our current data acquisition.

The dynamic range of the narrowband digital data is approximately 90 db. This range can be improved by further processing, but the standard 90 db range is expected to be adequate for most purposes.

Calibration. As is indicated in the block diagram (Figure 2), calibration signals ultimately derived from the clock/frequency standard are inserted into the ELF/VLF data stream by the computer at all the important stages of the data processing.

Size of the Radiometer. The radiometer modules fill two standard equipment racks, with the video terminal located on a separate stand (or table). The terminal could be incorporated into the racks to save space if necessary, but it is more convenient for the operator to use when it is separate from the racks.

Previous ELF/VLF Noise Measurements

The present standard atmospheric radio noise reference is Report 322 of the International Radio Consultative Committee (C.C.I.R.) [1]. This report summarizes atmospheric noise measurements from 16 stations distributed over the earth's surface and it makes worldwide predictions of noise level values. However, the data are limited to the range 10 kHz to 20 MHz and therefore provide no information about ELF noise or about VLF noise in the lower part of the VLF range. Furthermore, the data are over two decades old and may no longer be completely applicable.

More specifically relevant to our noise measurement project are the data provided by *Watt and Maxwell* [18, 19], *Maxwell and Stone* [12], and *Maxwell* [13]. The data displays in the latter reference are particularly pertinent, since they cover much the same frequency range as will ours and both temporal and geographic variations are indicated. Figure 3 shows an illustrative example of these data. Our noise data will differ from Maxwell's in many details (for example, we measure the magnetic field of the noise, whereas Maxwell measured the electric field, and we will have much higher time resolution), but in the initial stage of our data processing it will desirable and comparatively simple for us to display similar noise spectra and their temporal and geographic variations. From this start, we will expand our analysis to include computations of V_d (defined as the ratio of the noise envelope to its mean value, expressed in db), which is a direct measure of the impulsiveness of the noise, and the amplitude probability distribution.

While there do not appear to have been any wideband measurements of ELF/VLF noise since the work of Watt, Maxwell, and Stone referenced above, there have been a number of studies of specific sections of the ULF (frequencies

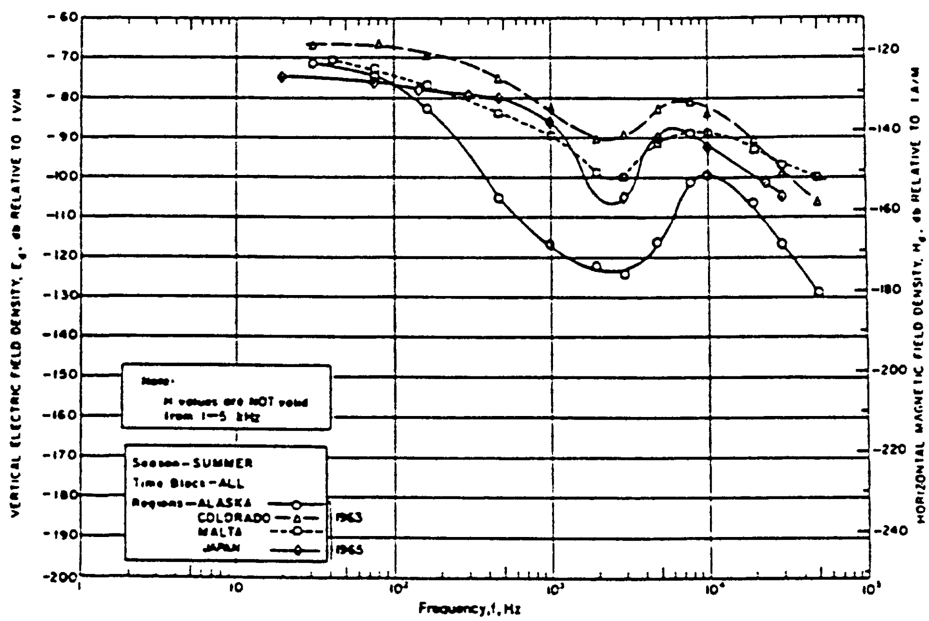

Figure 3: Curves showing the geographical dependence of radio noise in the frequency range 10 Hz to 10 kHz [13].

less than 5 Hz), ELF, VLF, and LF (frequencies in the range 30 - 300 kHz) bands that have implications for our ELF/VLF measurements. For example, superconducting magnetometer measurements of magnetic noise in the frequency range 0.1 - 14 Hz by *Fraser-Smith and Buxton* [4] provide information about the noise background at the low frequency end of the ELF/VLF range, while measurements by *Gurnett* [8] and others help define the characteristics of auroral kilometric radiation (AKR), which is observed in space near the earth and which influences the noise background there at frequencies just above the upper end of the ELF/VLF range. Within the ELF/VLF range the measurements of *Dinger et al.* [2] are noteworthy for the detailed information they give about noise in the 1.0 to 4.0 kHz frequency band.

When an attempt is made to obtain an overall picture of the frequency dependence of natural electromagnetic noise over a broad frequency range that includes the ULF, ELF, VLF, and LF bands as sub-ranges, an interesting and suggestive picture of the general trend of the noise becomes apparent. This trend is illustrated in Figures 4 and 5. The first of these figures is taken from *Spaulding and Hagn* [15], and it shows the variation of their external noise figure F_a with frequency. F_a is a measure of the available noise power (in units of dB above kT_0B, where k is Boltzman's constant (1.381×10^{-23} J/°K), T_0 is a reference temperature taken, in this case, to be 288 °K, and B is the bandwidth in Hz). As can be seen, there is a general downward trend of the noise power over the frequency range covered by the display (0.1 Hz to 10 kHz), which includes most of the range of our radiometer measurements. Other displays by the same authors (also see the review by *Flock and Smith* [3]), covering higher frequencies, indicate that the downward trend continues until the frequency reaches about 1 GHz. The noise data in Figure 5 are taken from *Lanzerotti and Southward* [9]. Despite the different units used for noise power and the emphasis given in the display to the dominant varieties of noise at various frequencies, the same downward trend of noise power with increasing frequency is clearly evident.

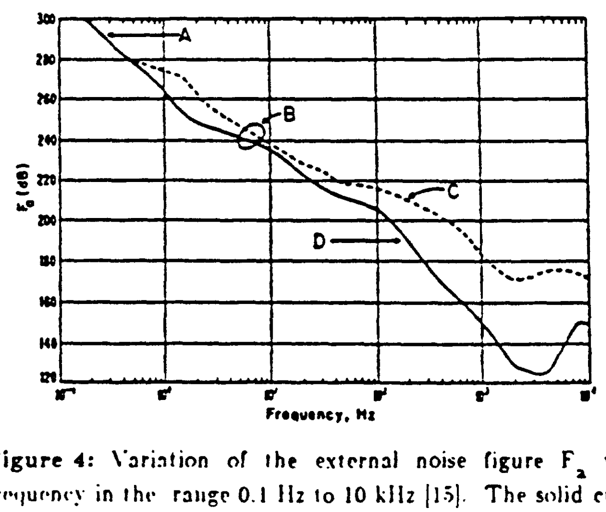

Figure 4: Variation of the external noise figure F_a with frequency in the range 0.1 Hz to 10 kHz [15]. The solid curve (D) shows minimum expected values of F_a at the earth's surface and the dashed curve (C) shows maximum expected values. Section A of the two curves denotes geomagnetic pulsations and section B the location of the first earth-ionosphere cavity resonance.

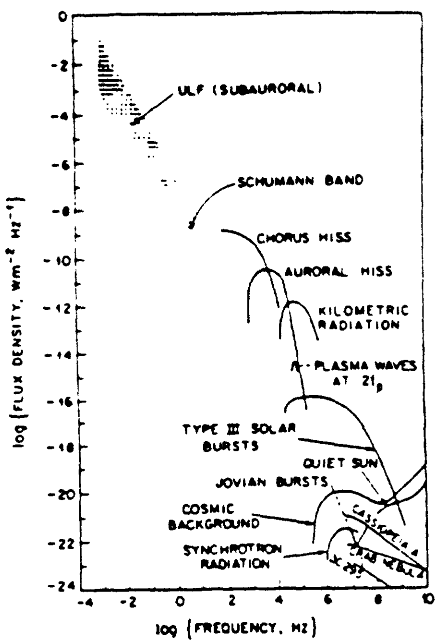

Figure 5: Power flux levels for various frequency ranges of naturally-occurring electromagnetic and plasma waves in the earth's environment and in astrophysical sources as observed at the earth [9].

A possible clue to the form of this downward trend, together with a framework for the interpretation of the noise data, is provided by the ULF/ELF measurements of *Fraser-Smith and Buxton* [4]. After analyzing their measurements, *Fraser-Smith and Buxton* tentatively concluded that geomagnetic noise on the earth's surface could be divided into two components as follows: (1) a class of comparatively stable background activity, where the magnetic field amplitudes drop off with frequency as f^{-n}, where n is in the range 1.0 to 1.3, and (2) a class of comparatively transient events with center frequencies, bandwidths, and durations that vary widely on an event to event basis. The transient events in the latter class grow out of the stable background activity, reach a maximum field strength that can be large in comparison to the background level, and then decay until they finally disappear back into the background activity. There can of course be spatial and temporal variations of the background activity. For example, the measurements of *Fraser-Smith and Buxton* indicated that their ULF/ELF background activity was stronger during the day and during times of geomagnetic disturbance (the measurements were only made at one middle latitude location, so they gave no information about the spatial variation of the background activity). Extrapolating these measurements slightly in frequency, Figure 6 provides a model for the background noise in the frequency range 0.001 - 100 Hz: the magnetic field amplitude, in units of pT/Hz$^{1/2}$, can be written $B=B_0/f$, where the constant B_0 has values 2, 4, and 8 for nighttime quiet, average, or disturbed periods, respectively, or 4, 8, and 16 for daytime quiet, average, or disturbed periods, respectively.

Returning now to the general declining trend of noise power with increasing frequency exemplified in the work of *Spaulding and Hagn* [15] and *Lanzerotti and Southward* [9],

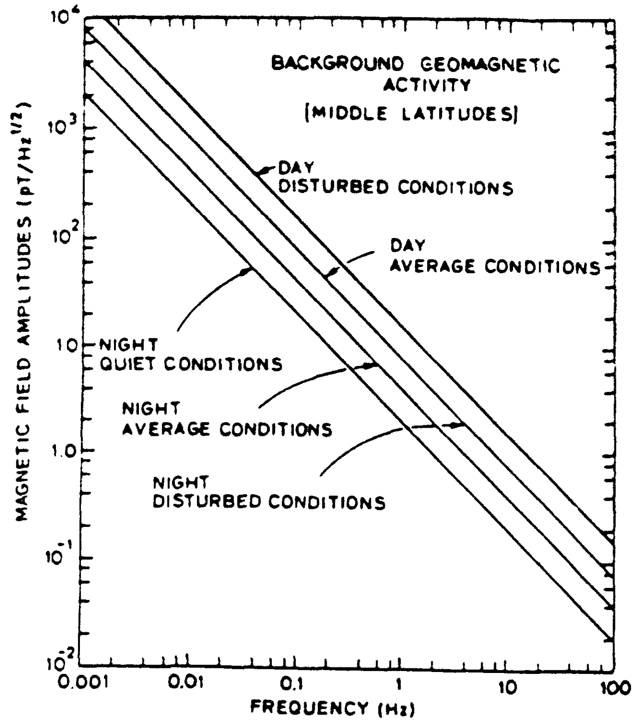

Figure 6: A projection of background geomagnetic noise in the frequency range 0.001-100 Hz, based on the measurements in [4]. An inverse relation between magnetic field amplitude and frequency is assumed.

we have prepared a display similar to that of *Lanzerotti and Southward*, but with f^{-1} and f^{-2} trend lines drawn in (see Figure 7). Since it is now power that is displayed, the background noise should have an f^{-2} decline with increasing frequency if the trend shown for amplitudes in Figure 6 were to be continued at higher frequencies. As can be seen, the f^{-2} trend line fits the data quite well, particularly when it is remembered that the fit is to the background activity - the comparatively stable and continuous level of activity out of which grow the more transient varieties of activity, such as Pc 1 pulsations, VLF chorus, plasmaspheric and auroral hiss, and AKR. Thus, the best fitting trend line for the background activity should appear as a base to the other forms of activity.

The background noise described above, and its frequency dependence, is of interest for several reasons. First, and foremost in our work, it is of interest because it is the source of the minimum level of non-instrumental noise in any communication band and thus has important implications for communication. Second, the source (or sources) of the background noise are not known. *Fraser-Smith and Buxton* [4] speculated that the source of their background ULF/ELF magnetic field fluctuations was interplanetary magnetic field fluctuations; however, there is no reason at this time to expect that the entire spectrum of background noise (up to frequencies near 1 GHz) originates in the interplanetary field. Studies of the frequency dependence of the background noise may help determine its origin. Finally, as described in particular by *Voss and Clarke* [16, 17], although there are many different forms of noise encountered in nature and in our society, a large proportion of fluctuating physical variables have a spectral density that is "1/f-like," *i.e.*, the power spectrum varies as f^{-n}, where n lies in the approximate range 0.5 - 1.5. The background noise discussed in this communication does not appear to be $1/f$-like (the f^{-1} trend line in Figure 7 is clearly an inferior fit to the noise compared with the f^{-2} line), but instead it appears to belong to a less widespread class of noise that is variously described as being "correlated," "Brownian," or "brown" [*e.g.*, 6] and which is characterized by a $1/f^2$ variation of spectral density. Studies of the background noise in the more-general context of correlated noise could provide new insight into its origin and properties.

Applications of the Noise Data

The Stanford University ELF/VLF noise survey will provide new information about the global distribution and temporal variation of ELF/VLF noise. An immediate practical application of the noise measurements is to communication in the ELF/VLF band. Another possible practical application, still speculative at this stage, is to earthquake prediction, based on the reported observation of ELF/VLF signals as precursors to earthquakes. Among the many potential scientific applications of the data, in addition to the obvious application in studies of electromagnetic noise in the earth's environment, specific reference may be made to applications in (1) the study of wave-particle interactions in the magnetosphere (which produce a number of the transient varieties of noise shown in Figures 6 and 7, and which may contribute to the background noise), (2) studies of the ionosphere (which influences the noise both as a transmission and absorbing medium and as the upper region in the earth-ionosphere waveguide), (3) studies of the effects of man on the electromagnetic environment, by using digital processing of the noise data to detect "weekend effects" [5] and other possible indicators of human influence, and (4) studies of the general characteristics of noise [*e.g.*, 16, 17].

Acknowledgements. Evans W. Paschal designed the radiometer and prepared its computer software. Construction and deployment of the radiometers has been the responsibility of Bruce R. Fortnam.

Support for the ELF/VLF noise survey is provided by the Office of Naval Research, through Contract No. N00014-81-K-0382 and Grant No. N00014-84-G-0202, by Rome Air Development Center, partly through ONR Contract No. N00014-81-K-0382 and partly through Contract No. F19628-84-K-0043, and by the National Science Foundation, Division of Polar Programs, through Grant No. DPP-8316641.

References

[1] C.C.I.R., "World distribution and characteristics of atmospheric radio noise," Report 322, published by the International Telecommunication Union, Geneva, 1963.

[2] R.J. Dinger, W.D. Meyers, and J.R. Davis, "Experimental investigation of ambient electromagnetic noise from 1.0 to 4.0 kHz in Italy and Norway," Radio Sci., vol. 17, pp. 285-302, 1982.

[3] W.L. Flock and E.K. Smith, "Natural radio noise - a mini-review," IEEE Trans. Antennas Prop., vol. AP-32, pp. 762-767, 1984.

[4] A.C. Fraser-Smith and J.L. Buxton, "Superconducting magnetometer measurements of geomagnetic activity in

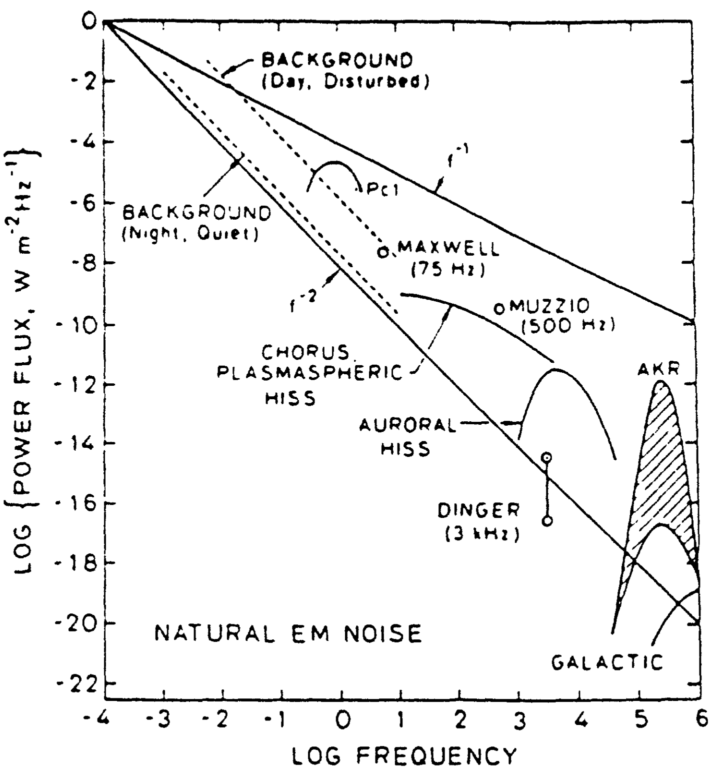

Figure 7: A summary plot of power flux levels for noise in the broad frequency range 10^{-4} to 10^{6} Hz. Two trend lines, showing f^{-2} and f^{-1} frequency variations have been inserted; their common point of intersection on the power axis was chosen arbitrarily, but it nevertheless represents a reasonable preliminary choice for the f^{-2} trend line if an attempt is made to fit a f^{-2} variation to the background noise. The two dashed lines are taken from Figure 6 and some specific data points taken from [2], [13], and [14] are circled.

the 0.1- to 14-Hz frequency range," J. Geophys Res., vol. 80, pp. 3141-3147, 1975.

[5] A.C. Fraser-Smith, "Effects of man on geomagnetic activity and pulsations," Adv. Space Res., vol. 1, pp. 455-466, 1981.

[6] M. Gardner, "Mathematical games: White and brown noise, fractal curves and one-over-f fluctuations," Sci. American, vol. 238, pp. 16-32, April 1978.

[7] M.B. Gokhberg, V.A. Morgounov, T. Yoshino, and I. Tomizawa, "Experimental measurement of electromagnetic emissions possibly related to earthquakes in Japan," J. Geophys. Res., vol. 87, pp. 7824-7828, 1982.

[8] D.A. Gurnett, "The earth as a radio source," pp. 197-208 in Magnetospheric Particles and Fields, Ed. B.M. McCormac, D. Reidel, Dordrecht-Holland, 1976.

[9] L.J. Lanzerotti and D.J. Southwood, "Hydromagnetic waves," Ch. III.1.3 in Solar System Plasma Physics, vol. 3, Ed. L.J. Lanzerotti, C.F. Kennel, and E.N. Parker, North-Holland, New York, 1979.

[10] V.I. Larkina, A.V. Nalivayko, N.I. Gershenzon, M.B. Gokhberg, V.A. Liperovskiy, and S.L. Shalimov, "Observations of VLF emission, related with seismic activity, on the Interkosmos-19 satellite," Geomagn. Aeron., Engl. Transl., vol. 23, pp. 684-687, 1983.

[11] K. Maki and T. Ogawa, "ELF emissions associated with earthquakes," Res. Letts. Atmos. Elec., vol. 3, pp. 41-44, 1983.

[12] E.L. Maxwell and D.L. Stone, "Natural noise fields from 1 cps to 100 kc," IEEE Trans. Antennas Prop., vol. AP-11, pp. 339-343, 1963.

[13] E.L. Maxwell, "Atmospheric noise from 20 Hz to 30 kHz," pp. 557-593 in Sub-Surface Communications, AGARD Conf. Proceedings No. 20, 1966.

[14] J.L.R. Muzzio and J.J. Angerami, "Ogo 4 observations of extremely low frequency hiss," J. Geophys. Res., vol. 77, pp. 1157-1173, 1972.

[15] Spaulding, A.D., and G.H. Hagn, "Worldwide minimum environmental radio noise levels (0.1 Hz to 100 GHz)," pp. 177-182 in Proceedings: Effects of the Ionosphere on Space and Terrestrial Systems, Ed. J.M. Goodwin, ONR/NRL, Arlington, Virginia, 1978.

[16] R.F. Voss and J. Clarke, "'1/f noise' in music and speech," Nature, vol. 258, pp. 317-318, 1975.

[17] R.F. Voss and J. Clarke, "'1/f noise' in music: Music from 1/f noise," J. Acoust. Soc. Am., vol. 63, pp. 258-263, 1978.

[18] A.D. Watt and E.L. Maxwell, "Measured statistical characteristics of VLF atmospheric radio noise," Proc. IRE, vol. 45, pp. 55-62, 1957a.

[19] A.D. Watt and E.L. Maxwell, "Characteristics of atmospheric noise from 1 to 100 Kc," Proc. IEEE, vol. 45, pp. 787-794, 1957b.

Measurements of BART Magnetic Fields with an Automatic Geomagnetic Pulsation Index Generator

A. BERNARDI, A. C. FRASER-SMITH, AND O. G. VILLARD, JR

Abstract—**Measurements of the large-amplitude magnetic field fluctuations produced by the San Francisco Bay Area Rapid Transit (BART) system using an automatic computer-based geomagnetic pulsation index generator located on the Stanford campus, which is approximately 40 km from the center of the BART system, are described. Because the temporal variation of the fluctuations is well defined on an hour-to-hour and day-to-day basis, due to the transit system scheduling, they provide a convenient means for evaluating the performance of the index generator. The index generator, in turn, provides new information about the frequency content of the BART field fluctuations, and it can be used, in a general sense, to monitor activity on the BART system.**

I. Introduction

City and suburban environments are notorious for the variety and strength of their low-frequency electromagnetic noise sources, which force those interested in making measurements of the natural noise background to remote locations. Even then, it may be difficult to avoid some man-made low-frequency noise from widely distributed systems such as electric railroads, telephone lines, and power transmission lines. There is even a possibility, which is still speculative at this stage, that the man-made sources of low-frequency noise are now sufficiently intense to influence some of the sources of the natural noise (see, e.g., [1]).

Some years ago, our research group drew attention to the large-amplitude ultra-low frequency (ULF—frequencies less than 5 Hz) electromagnetic fields being produced by the new dc-powered Bay Area Rapid Transit (BART) system that had been constructed in the San Francisco Bay area [2]-[4]. We showed that the BART system could generate magnetic field fluctuations at Stanford University, which is roughly 40 km from the center of the BART tracks, that were an order of magnitude or more larger than the natural geomagnetic noise background in the same frequency range. Further, the energy of the ULF signals was found to be concentrated below about 0.3 Hz, although it was still easily detectable above the natural background noise at 1 Hz.

Manuscript received April 6, 1989; revised June 10, 1989. This work was supported by the Office of Naval Research under Contract N00014-83-K-0390.

The authors are with STAR Laboratory, Stanford University, Stanford, CA 94305.

IEEE Log Number 8930255.

0018-9375/89/1100-0413$01.00

Since our research interest is primarily natural ULF geomagnetic field fluctuations, our ultimate response to the presence of the BART magnetic field fluctuations on the Stanford campus and throughout the San Francisco Bay area and its vicinity was typical of geomagnetic field researchers during this last century: we moved our measuring equipment to a more remote location. Thus, we ceased making measurements of the BART fields. However, in 1986, as part of the evaluation of a new geomagnetic activity monitoring system we were developing, we set up one of the systems in an isolated area of the campus and measured the BART magnetic fields for several months. The new ULF measurement system (which we will refer to as a magnetic activity index (MAI) generation system) differed from the systems used for the earlier measurements primarily through its use of a small computer to run the system and to compute half-hour indices of the geomagnetic activity in nine narrow nonoverlapping bands covering the frequency range 0.01-10 Hz. Since the index generation system is calibrated and each index is proportional to the logarithm to the base two of the average power in its corresponding frequency band, the indices provide a new quantitative measurement of the BART magnetic fields. As we will show, they closely follow the level of service being provided by the BART system.

II. Description of the Index Generation System

Each MAI generation system has two main sections that are connected to each other via a 500-ft shielded cable. The first section consists of the computer that operates the system and its associated signal receiving and sending circuitry. This section is normally housed in a shed or other shelter that is equipped with ac power and a telephone line. The telephone line gives authorized users remote access to the indices via a modem linked to the computer, and it also enables users with the correct priority to initiate certain system operations. For example, a self-calibration procedure can be either initiated or turned off by telephone commands. The second section of the index generator consists of its magnetic field sensor and associated high-gain low-noise amplifiers, which are located as far away from the first section as the connecting cable and measurement site will allow in order to prevent the pickup of electromagnetic interference from the computer and other electronic and electrical equipment housed in the shed. Fig. 1 shows a block diagram of the system as a whole.

The sensor used in the MAI generation system is made up of a pair of solenoidal coils of aluminum wire connected in series and enclosing a high-permeability steel core (see Fig. 1). A single-turn calibration coil is inserted between the two sense coils; it can be used to inject a known magnetic field variation into the sensor either automatically under the control of the computer or in response to commands given to the computer over the telephone.

The small voltages produced at the terminals of the coils by variations of the magnetic field in the core are amplified by low-noise amplifiers with an overall voltage gain of approximately 118 dB (800 000 times) that are located immediately adjacent to the coils. The amplified signals are then sent back to the second section of the system (in the shed) by a set of differential line drivers, which are used to minimize external noise pickup in the cable.

A differential line amplifier in the second section is used to receive the transmitted differential signals. The difference signal can be further amplified at this stage if necessary (the additional amplification is optional; no extra amplification is required at either of the two middle latitude locations at which we have been operating MAI generation systems), after which the signal is passed through a sharp antialiasing filter before being sampled. An 8-bit analog-to-digital converter is used for the sampling, which takes place at a rate of 30 samples per second. Finally, the digital stream of data is sent to the computer for processing. Although we use a relatively simple computer, it has adequate speed to continually process the incoming data samples without loss of any of the incoming data.

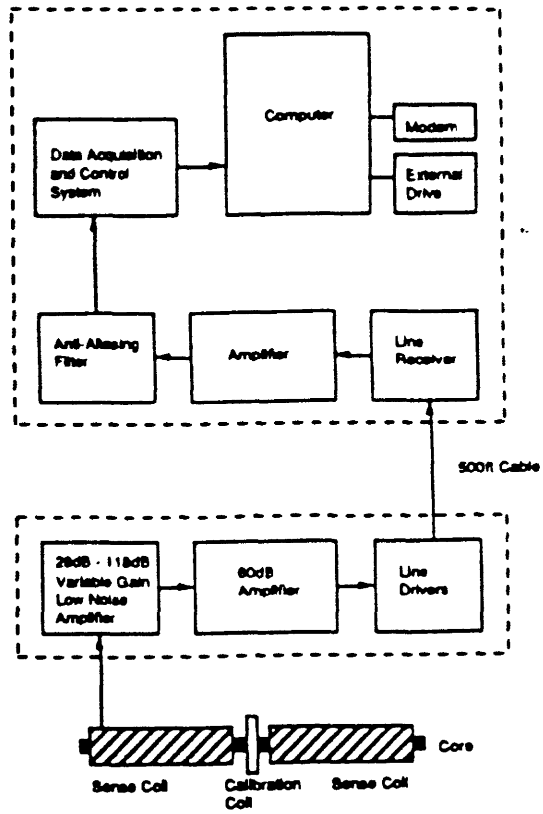

Fig. 1. Block diagram of the MAI generation system. It consists of two main sections separated by a 500-ft cable.

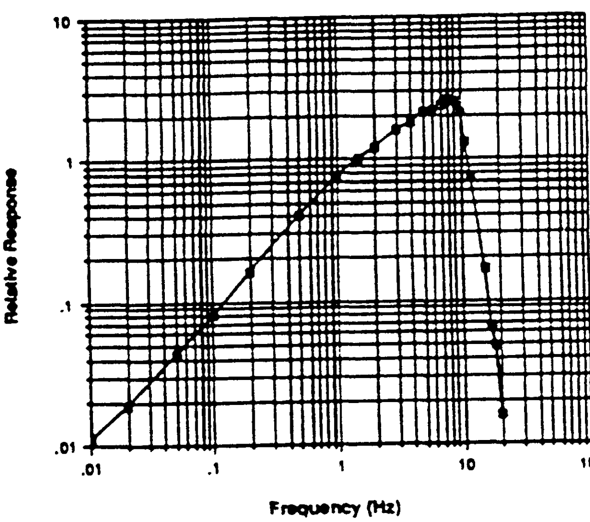

Fig. 2. Relative response of the analog section of the MAI generation system. In practice, a 100-pT peak-to-peak sinusoidal variation of the magnetic field at the sensor will produce a 2.6-V peak-to-peak output from the analog section at 8 Hz (the point of maximum response). Measured values are shown by hollow boxes and interpolated values are shown by solid boxes. The sharp drop in the response above 10 Hz is caused by the antialiasing filter in the system.

The relative response of the analog section of the MAI generation system to a fixed amplitude sinusoidal variation of the magnetic field is shown in Fig. 2. The data were obtained by applying a known sinusoidally varying magnetic field from another large air-cored coil as part of an absolute calibration process and stepping through the frequency range of the system. At frequencies less than 0.1 Hz, the response of the system is interpolated. Above 10 Hz, the sharp drop in response of the system is produced by the low-pass antialiasing filter. In general, and as may be seen below 10 Hz, the relative response of the system increases with frequency due to the increase in the induced voltage across the solenoidal sensor as the frequency of the incident magnetic field is increased. That is, if the magnetic field applied to the coil sensor is

$$B(t) = B_0 \sin(\omega t) \tag{1}$$

the voltage induced across the coil terminals is

$$V(t) = \mu_r A_e N \frac{dB(t)}{dt} = \mu_r A_e N B_0 \omega \cos(\omega t) \tag{2}$$

where N is the total number of turns of wire in the coils, and A_e is the *effective* cross sectional area of the coil. The relative permeability of the core material is denoted by μ_r, and it is in general a nonlinear quantity that can depend both on the frequency and amplitude of the applied magnetic field. The core material can saturate at large signal levels, but such large signal levels are not expected from exposure to natural geomagnetic activity.

In the MAI generation system, the value of μ_r lies in the 10-20 range, depending on the core used, and it remains constant over the frequency range of the system. We can rewrite (2) as

$$V(t) = C\omega \cos(\omega t) \tag{3}$$

where C is defined as

$$C = \mu_r A_e N B_0. \tag{4}$$

Thus, the amplitude of the induced voltage increases linearly as the frequency is increased, with the slope being approximately equal to 1 on a log-log plot (Fig. 2).

The digitized stream of data from the analog-to-digital converter is processed continuously by the computer. The data are collected in blocks of 4096 samples (136 seconds of data) multiplied by a 4096-point Hamming window and frequency analyzed using a fast Fourier transform (FFT), after which the average power in each of the desired frequency bands is calculated. The use of the Hamming window (which smooths the spectral estimates at each frequency), combined with the averaging over each frequency band, reduces the statistical variance of the power spectrum estimates for the bands. This process is constantly repeated, and it generates a set of spectral estimates every 136 seconds. The statistical variance of the spectral estimates is further reduced by the method of averaging nonoverlapped modified periodograms [5]. The averaging is performed over half-hour intervals, which include 13 or 14 spectral estimates (depending on the exact timing of the transform operations), and the final results of these computations, consisting of logarithms to the base 2 of the averages, are stored every half hour.

The information stored in the MAI generation system therefore consists of a collection of logarithms to the base two of the half-hourly average of the average power in the various frequency bands. These numbers comprise our magnetic activity (MA) indices, and currently, we compute at least nine basic half-hour indices MA3-MA11 for nine nonoverlapping frequency bands in the 0.01-10-Hz range. Table I lists the nine frequency bands, together with the FFT bins that are used in calculating each MA index. Notice that the bands span the 0.01-10-Hz frequency range without gaps as well as without overlapping.

To limit the quantity of data stored by the computer, we do not at this time convert the power in the various frequency bands to system-

TABLE I
FREQUENCY BANDS COVERED BY THE MA INDICES AND THEIR ASSOCIATED FFT BINS

MA Index	Frequency Band (Hz)	FFT Bins
MA3*	0.015	2
MA4	0.022-0.044	3-6
MA5	0.051-0.095	7-13
MA6	0.103-0.198	14-27
MA7	0.205-0.498	28-68
MA8	0.505-0.996	69-136
MA9	1.003-2.000	137-273
MA10	2.007-4.995	274-682
MA11	5.002-9.998	683-1365

*Only one FFT bin included.

TABLE II
CONVERSION OF MA INDICES TO MAGNETIC FIELD UNITS. TO CONVERT A PARTICULAR MA INDEX VALUE M TO A CORRESPONDING AVERAGE MAGNETIC FIELD AMPLITUDE a IN $pT/\sqrt{Hz}$, SUBSTITUTE M AND THE APPROPRIATE CONVERSION FACTOR C IN THE EXPRESSION $a = \sqrt{2M} \times C$ $pT/\sqrt{Hz}$

MA Index	Center Frequency (Hz)	Conversion Factor (C)
MA3	0.015	$2.704 \times 10^{+2}$
MA4	0.033	$4.790 \times 10^{+1}$
MA5	0.073	$1.070 \times 10^{+1}$
MA6	0.150	2.645×10^{0}
MA7	0.352	4.992×10^{-1}
MA8	0.751	1.213×10^{-1}
MA9	1.502	3.698×10^{-2}
MA10	3.501	1.368×10^{-2}
MA11	7.500	7.129×10^{-3}

independent units, e.g., to power measured in (magnetic field unit)^2/Hz. Thus, quantitative comparison of the indices measured in the different bands must be done cautiously. It is of course possible to convert the indices to more absolute units by using the calibration data in Fig. 2 and by allowing for the different bandwidths used for the indices. When this is done, the conversion factors given in Table II are obtained.

Unlike the other indices, the MA3 index is derived from only one frequency bin of the frequency transform, and it is comparatively strongly influenced by the spectral estimates in the two adjacent frequency bins as a result of the use of the Hamming window. Thus, the values of MA3 should not be given as high a significance as the values of the other indices. The power spectral estimate for this single bin has been included as an MAI primarily to allow for the study of the activity in frequency bands extending up from 0.01 Hz to optional higher limits within the overall operating range of the index generation system.

Data collection by each MAI generation system is entirely automatic, and no operator is needed. A visit is required roughly once every seven months to change the magnetic disk on which the half-hourly MAI's are stored. All other system-related operations can be performed remotely by communicating with the MAI generation system via computer terminal, modem, and telephone line.

III. BART MEASUREMENTS

Following completion of our first MAI generation system, a series of testing and calibration measurements were made on the Stanford

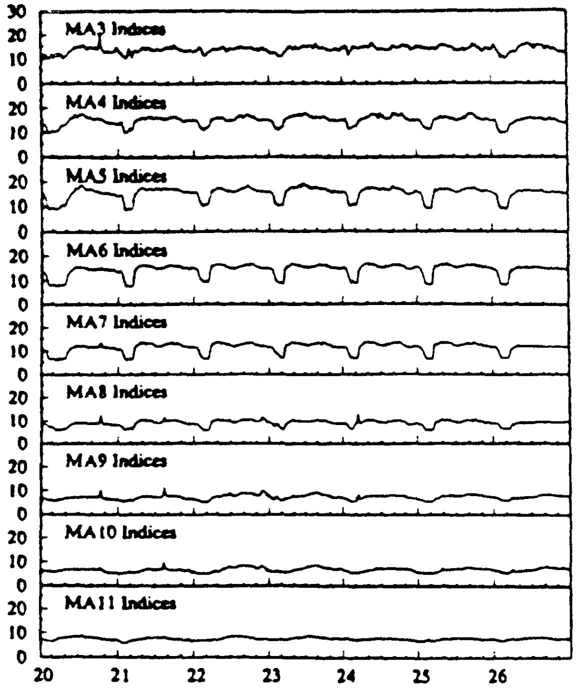

Fig. 3. The MAI's measured at Stanford during the week of April 20-26, 1986. The repetitive pattern we associate with BART is evident in most bands, but it is concentrated in the 0.10-0.20-Hz band, for which the corresponding index is MA6. Note that April 20 was a Sunday, and April 26 was a Saturday.

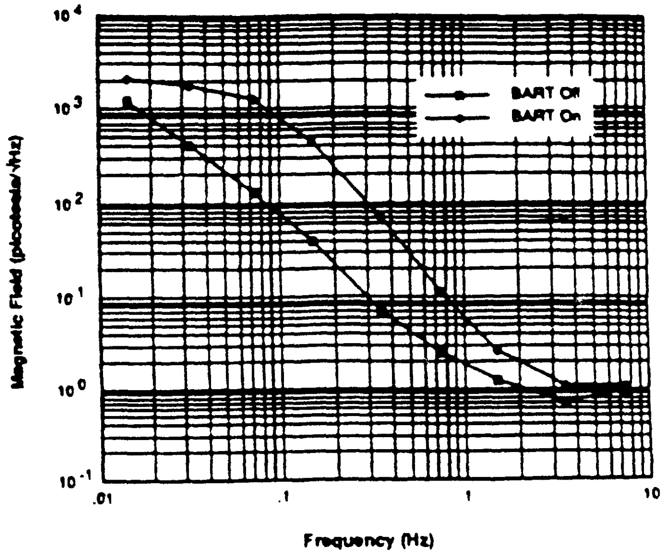

Fig. 4. Comparison of the magnetic field amplitudes measured on April 20, 1986 when BART was on (6:00-9:00 AM) with those when BART was off (2:00-4:30 AM). Note that the picotesla unit we use here is equivalent to the older milligamma unit (1 pT = 1mγ).

campus prior to the relocation of the system to a remote site for measurements of natural magnetic field variations. By March 1986, the system was running well, and it was left in operation until June 1986. The data described here were obtained during that four-month interval between March and June 1986.

Fig. 3 shows a plot of the indices generated by the index generator during the week beginning Sunday, April 20, 1986. The data are typical of the indices that were generated during other weeks of the measurement interval. It can be seen that the variation of the indices follows a repetitive daily pattern from Monday through Friday, with a similar, but slightly different, pattern on Saturday and Sunday. Following our earlier work, we did not hesitate to ascribe the magnetic field variations to BART, and indeed, as we will describe, the variation of the indices conforms closely to use of the BART system. It will be noticed that the repetitive BART activity is strongest in the MA6 band, which corresponds to the 0.10-0.20-Hz frequency range. It is only weakly evident in the MA3 index (0.01 Hz) and in the MA9-MA11 indices (1-10 Hz). Thus, the activity is concentrated in the frequency range 0.02-1 Hz, with a peak around 0.1-0.2 Hz. This frequency variation is in accord with our earlier measurements at Stanford [2].

To quantify the BART magnetic fields in greater detail, Fig. 4 shows two plots of average Stanford magnetic field amplitudes against frequency for Tuesday, April 22, 1986. The amplitude data were derived from the index measurements made during the intervals between 2:00 and 4:30 AM (BART off) and 6:00 and 9:00 AM (BART on) by converting the indices to magnetic field amplitudes, using the conversion data in Table II and averaging the amplitudes for each interval. The measurements made when BART was not operating correspond very closely to those made over a decade ago at the same location with an entirely different system [6]. Furthermore, other measurements we have made in Northern California at a location well away from the San Francisco Bay area indicate that the background noise measurements made during the time interval between 2:00 and 4:30 AM remain typical through 6:00 and 9:00 AM, except possibly for a small enhancement in the range between 0.015 and 0.2 Hz corresponding to the commencement of daytime Pc 3 pulsation activity. By comparison with these BART off data, the measurements made when BART was operating are approximately an order of magnitude larger for frequencies in the 0.07-0.40-Hz range. Although these particular measurements apply only to a specific day, the BART magnetic field fluctuations are highly predictable when averaged over intervals of the order of an hour or more, and thus, the amplitude data in Fig. 4 can be considered typical.

To extend this quantitative comparison of our index measurements with activity in the BART system, we obtained information from BART's public affairs office on the total number of cars operating on the tracks as a function of the time of day [8]. Because the BART system, like other similar transit systems, adds and removes cars to their trains as demand varies during the day, it is the number of cars in use that provides a measure of the activity in the system, as opposed to the number of trains. Following our earlier conclusion that the magnetic field fluctuations generated by BART has amplitudes proportional to the changes in the dc current drawn by the trains as they accelerate or decelerate, and noting that the power spectrum of the magnetic field is proportional to the square of the magnetic field, we decided to use the logarithm to the base two of the total number of cars operating on the BART tracks as a measure of BART activity to compare with our logarithmic MA indices.

Fig. 5 compares the variation of the MA6 index during the week of April 20-26, 1986, with the variation of our logarithmic measure of BART activity. To compare the two variations on the same scale without overlapping, we have added 20 to the BART logarithms, and at times when BART is not in operation (during the early morning hours), we have avoided having to take the logarithm of zero by setting the BART activity index to 20. The two variations are very similar. Both show the same variation from Monday through Friday, with the morning and afternoon rush hours being clearly evident as maximums, and the reduced service during the day, further reduced service during the evening, and end of service late at night are also easily identifiable. On Saturdays, BART begins its service at the same time as on Mondays through Fridays, but it only provides two

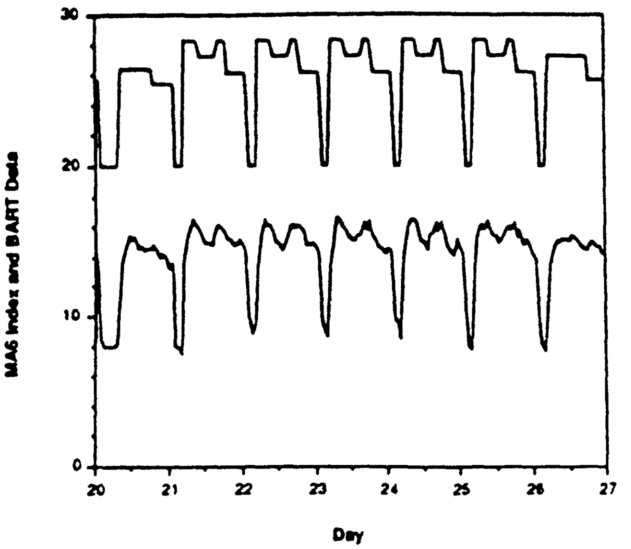

Fig. 5. Comparison of the MA6 indices (0.1–0.2 Hz) measured at Stanford during the week of April 20-26, 1986, with the number of BART cars in use during the week. The lower plots shows that variation of the MA6 indices, and the upper plot shows the simultaneous variation of the quantity (20 + $\log_2$(total number of BART cars in operation)).

levels of service during the day. On Sundays, BART starts its service later than the usual time, and again provides only two levels of service. All these features of BART weekend activity are also mirrored by the MA6 indices.

IV. Discussion

Even though our measurements of the BART magnetic fields are made at some distance from the center of the BART system, the indices we computed nevertheless followed the level of service being provided by BART very closely, and they could be used to monitor overall activity on the BART system, if there was a need for such an application. The frequency content of the BART magnetic field fluctuations probably also relates to the level of service, although we have not been able to investigate this aspect of the field variations in any detail. In the measurements reported here, the field fluctuations are concentrated in the 0.02-1-Hz range with a peak of activity in the 0.07-0.4-Hz range. We broadly relate these frequency ranges to the number of accelerations and decelerations per unit time of the trains in the BART system taken as a whole; if it was possible for this number to be doubled, we would expect to see the frequencies doubled as well.

Our results have one interesting practical implication. The center of the growing Washington, DC Metro system, which closely resembles the BART system in the use of dc power and other related features, is located roughly 80 km from the Fredericksburg geomagnetic observatory, whose measurements are incorporated into the widely used K_p and A_p indices of planetary geomagnetic activity [7]. Our measurements suggest that the observatory may be becoming significantly exposed to magnetic field fluctuations from the Metro system. Fortunately, the magnetic measurement specifically incorporated into the geomagnetic indices is the three-hourly range of one of the magnetic field components, and that measurement is relatively immune to the Metro magnetic fields at this time. However, let us consider the implications of magnetic noise similar to that produced by BART for magnetic field measurements by a conventional observatory analog magnetometer at Fredericksburg.

If typical, the magnetometer will be capable of responding to magnetic field fluctuations with periods in the 10–100-s range, where the Metro activity is likely to be concentrated, but the time resolution of its magnetograms will only be on the order of 1 min. As a result, the magnetometer trace will be thickened, thus giving somewhat greater maximums and lower minimums than would otherwise be recorded, and consequently, a slightly greater three-hourly range will be measured. Assuming a noise amplitude of about 2000 $pT/\sqrt{Hz}$, as is the case for BART in the 10-100-s period band (Fig. 4), the amplitude of the thickening will be roughly 1000 pT, or 1 γ. This latter amplitude is only just measurable in a conventional observatory magnetometer, and thus, we can conclude that the Metro magnetic noise is unlikely to be a threat to the integrity of the Fredericksburg magnetic field measurements at this time, but it may be on the point of becoming a threat. The Metro signals can be removed by filtering, and new digital magnetometers being introduced at Fredericksburg will make such filtering possible, but this will also limit the response of the magnetometers to natural activity in the same frequency range. As a result of these considerations, it appears evident that the continued growth of Metro can only have negative long-term implications for the Fredericksburg measurements.

Acknowledgment

The authors thank P. McGill for assistance during the design and development of the index generators and Dr. A. Philips of ETAK Inc. for his design of one of the low-frequency amplifiers used in the systems. Dr. O. Heinz of the Naval Postgraduate School provided important support during the initial stages of the project.

References

[1] A. C. Fraser-Smith, "Effects of man on geomagnetic activity and pulsations," *Adv. Space Res.*, vol. 1, pp. 455–466, 1981.

[2] A. C. Fraser-Smith and D. B. Coates, "Large-amplitude ULF electromagnetic fields from BART," *Radio Sci.*, vol. 13, pp. 661-668, 1978.

[3] A. M. -H. Ho, A. C. Fraser-Smith, and O. G. Villard, Jr., "Large-amplitude ULF magnetic fields produced by a rapid transit system: Close-rage measurements," *Radio Sci.*, vol. 14, pp. 1011-1015, 1979.

[4] R. Samadani, A. C. Fraser-Smith, and O. G. Villard, Jr., "Possible changes in natural Pc 1 pulsation activity caused by BART," *J. Geophys. Res.*, vol. 86, pp. 9211-9214, 1981.

[5] P. D. Welch, "The use of fast Fourier transform for the estimation of power spectra: A method based on time averaging over short, modified periodograms," *IEEE Trans. Audio Electroacoust.*, vol. AU-15, pp. 70–73, 1967.

[6] A. C. Fraser-Smith and J. L. Buxton, "Superconducting magnetometer measurements of geomagnetic activity in the 0.1- to 14-Hz frequency range," *J. Geophys. Res.*, vol. 80, pp. 3141-3147, 1975.

[7] P. N. Mayaud *Derivation, Meaning, and Use of Geomagnetic Indices*. Washington, DC, American, Geophys. Union, 1980.

[8] P. Patubo, BART Public Affairs Office, Private Communication, 1986.

ABSTRACT: American Geophysical Union Meeting, December 1989

ULF, ELF, and VLF Electromagnetic Field Observations Close to the Epicenter of the M_S 7.1 Loma Prieta Earthquake: Possible ULF Precursors

A.C. Fraser-Smith, A. Bernardi*, P.R. McGill, M.E. Ladd, R.A. Helliwell, and O.G. Villard, Jr. (STAR Laboratory, Stanford University, Stanford, CA 94305)

Our Laboratory has been operating two independent electromagnetic noise monitoring systems in the general vicinity of Stanford University for several years. Both systems made measurements right up until the occurrence of the Loma Prieta earthquake of 17 October 1989. As a result, we have a uniquely detailed record of the electromagnetic noise background variations prior to the earthquake. Specifically, our measurements cover 25 narrow frequency bands in the more than five-decade frequency range 0.01 Hz - 32 kHz, with a time resolution varying from a half hour in the ULF range (0.01 - 10 Hz) to one second for the ELF and VLF ranges (10 Hz - 32 kHz). The ULF system is located near Corralitos, and it was within about 7 km of the epicenter. The Corralitos system was therefore nearly vertically above the focus, which was about 18 km deep. The ELF/VLF system, one of a global array of eight identical systems, is located on the Stanford campus, and it is 52 km from the epicenter.

Analysis of the ELF/VLF data has revealed no precursor activity that we can identify at this time. However, the ULF data have several distinctive and anomalous features that may prove to be precursors. First, there was a substantial increase in the noise background starting on 5 October and covering the entire range of operation of the ULF system. Second, there was an anomalous drop in the noise background in the range 0.2 - 5 Hz, starting one day ahead of the earthquake. Third, and perhaps most compelling, there was an exceptionally large increase of activity in the range 0.01 - 0.5 Hz starting approximately three hours before the earthquake. There do not appear to have been any magnetic field fluctuations originating in the upper atmosphere that can account for this increase. Further, while our systems are sensitive to motion, seismic measurements indicate that there were no significant shocks preceding the quake. Thus, the large-amplitude increase in activity starting three hours before the quake appears to have been an electromagnetic precursor.

---

* Present Address: Teknekron Communications Systems, Berkeley, CA 94704

Appendix D

Viewgraphs used by J.Langbein to accompany presentation to NEPEC, January 11, 1990.

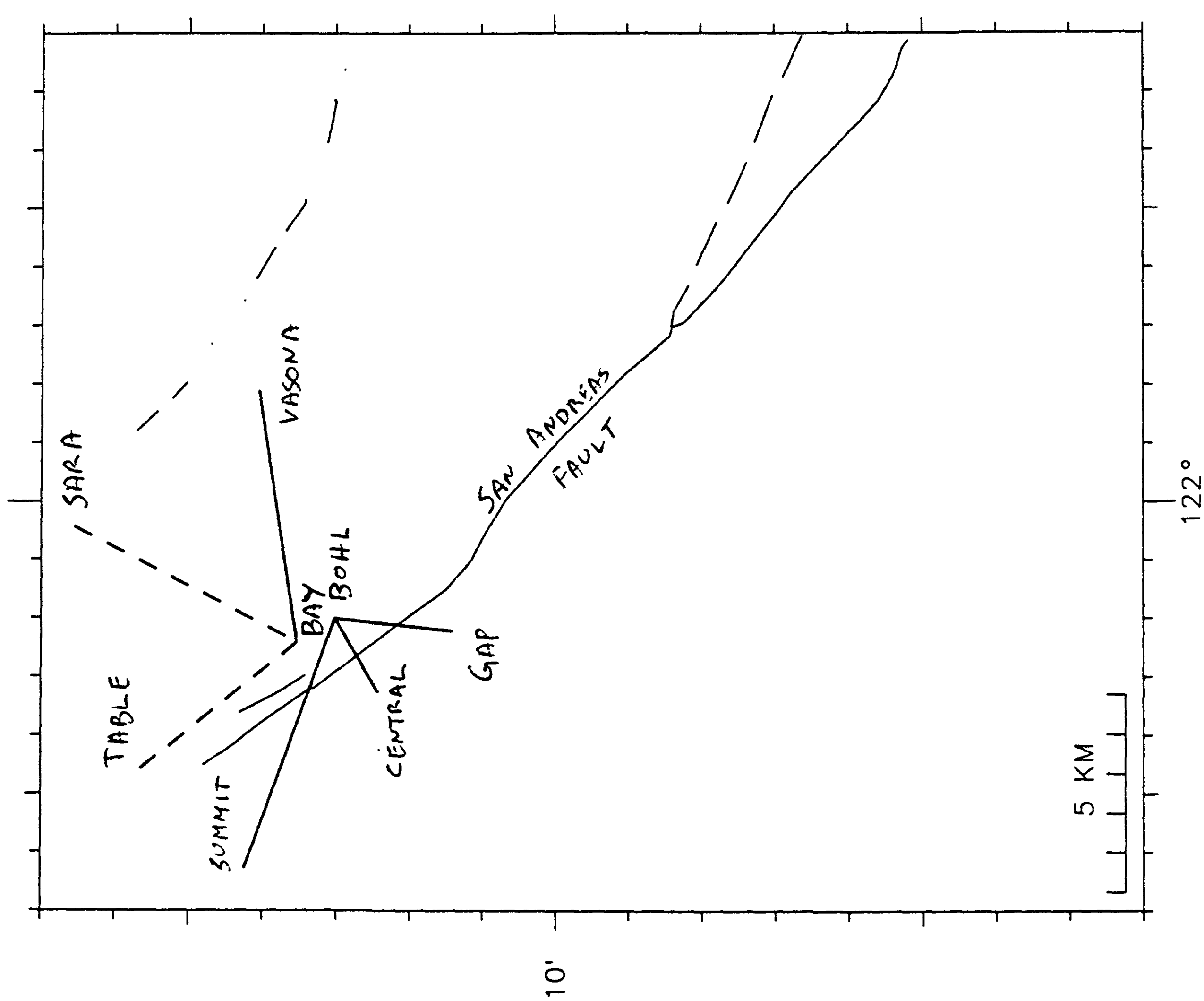
SARA
VASONA
TABLE
SUMMIT
BAY
BOHL
CENTRAL
GAP
SAN ANDREAS
FAULT
5 KM
122°
10'

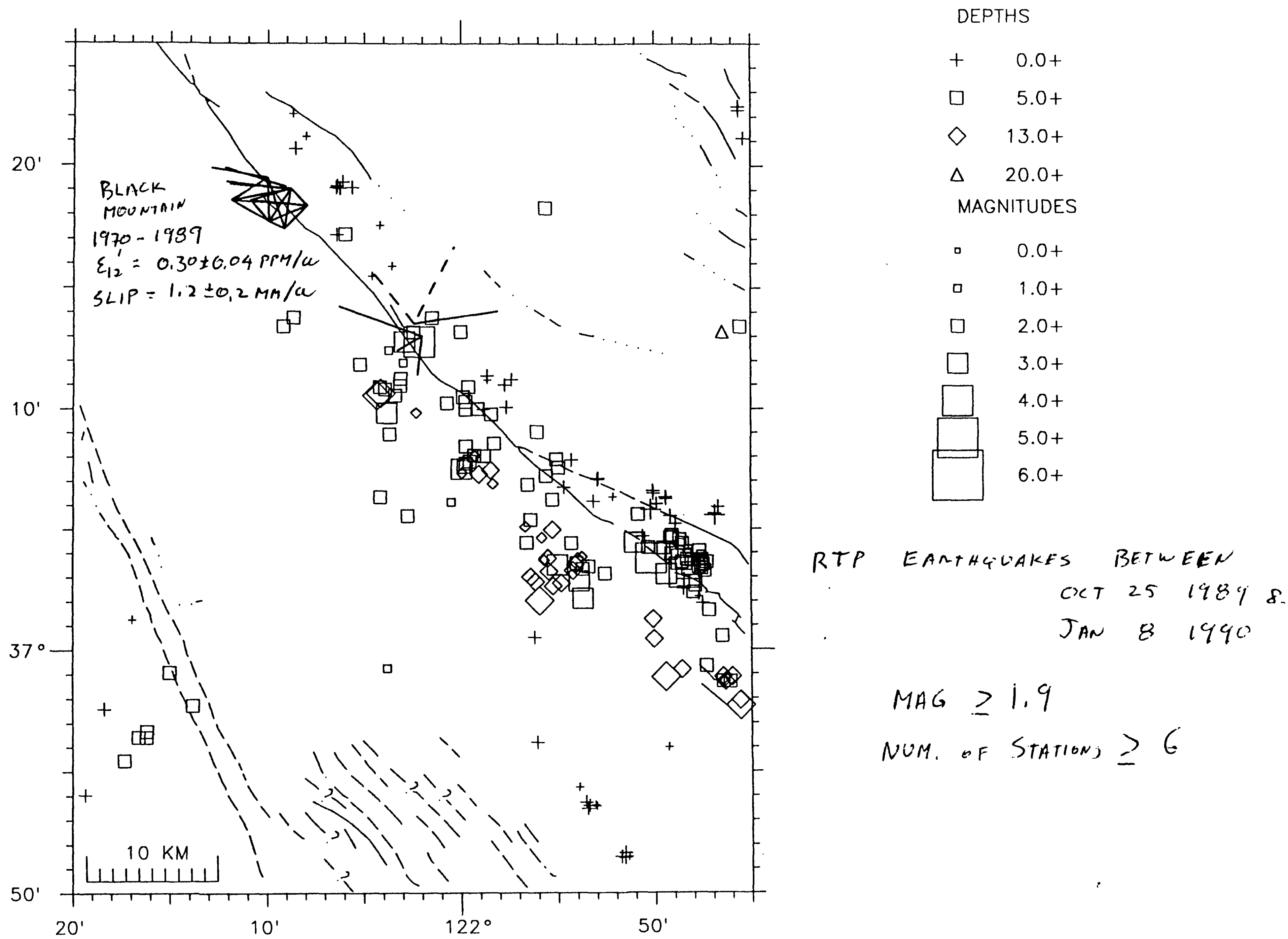

BLACK MOUNTAIN
1970 - 1989
ε'12 = 0.30±0.04 PPM/a
SLIP = 1.2 ±0.2 MM/a
20'
10'
37°
50'
20'
10'
122°
50'
10 KM
DEPTHS
+ 0.0+
5.0+
13.0+
20.0+
MAGNITUDES
0.0+
1.0+
2.0+
3.0+
4.0+
5.0+
6.0+
RTP EARTHQUAKES BETWEEN
OCT 25 1989 &
JAN 8 1990
MAG ≥ 1.9
NUM. of STATIONS ≥ 6

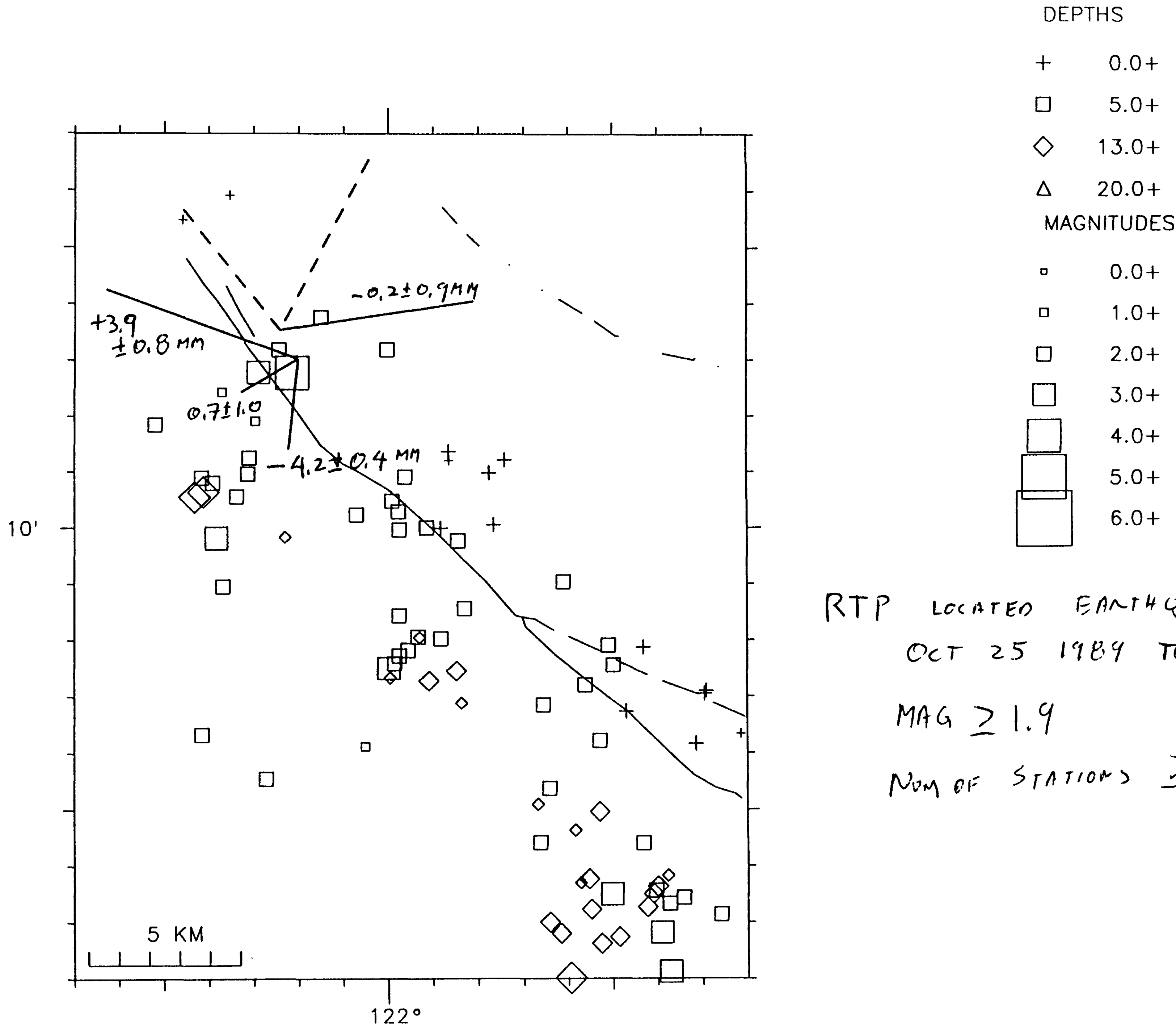

RTP LOCATED EARTHQUAKES
OCT 25 1989 TO JAN 8, 1990
MAG ≥ 1.9
NUM OF STATIONS ≥ 6

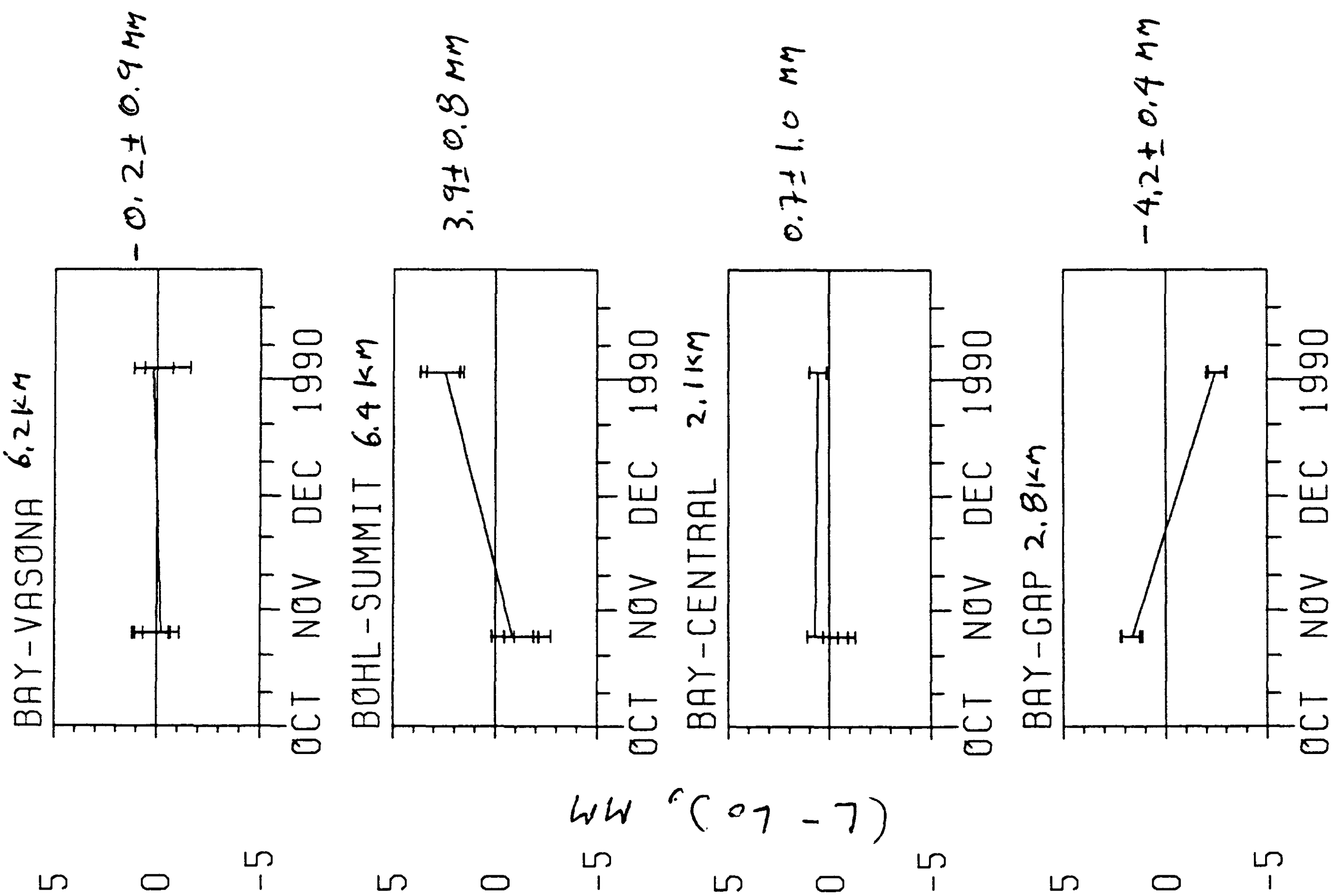
BAY-VASONA 6.2KM
-0.2± 0.9 MM
BOHL-SUMMIT 6.4 KM
3.9± 0.8 MM
BAY-CENTRAL 2.1KM
0.7± 1.0 MM
BAY-GAP 2.8KM
-4.2± 0.4 MM
OCT NOV DEC 1990
(L - Lo), MM
5
0
-5

Appendix E

Viewgraphs used by J.Dieterich to accompany presentation to NEPEC, January 11, 1990.

WORKING GROUP ON PROBABILITIES OF EARTHQUAKES IN THE SAN FRANCISCO BAY REGION

Clarence Allen	California Institute of Technology
Lloyd Cluff	Pacific Gas and Electric Co.
Allin Cornell	Stanford University
Jim Dieterich	U. S. Geological Survey
Bill Ellsworth	U. S. Geological Survey
Lane Johnson	University of California, Berkeley
Allan Lindh	U. S. Geological Survey
Stu Nishenko	U. S. Geological Survey
Chris Scholz	Lamont-Doherty Geol. Observ., Columbia
David Schwartz	U. S. Geological Survey
Wayne Thatcher	U. S. Geological Survey
Patrick Williams	University of California, Berkeley, LBL

Working Group on Probabilities of Earthquakes in the San Francisco Bay Region

Purpose:	Review and revise probabilities from Open File Report 88-398
Considerations:	Revised interpretations of data resulting from the Loma Prieta earthquake
	Physical changes resulting from the Loma Prieta earthquake
	Seismicity patterns of the 1800's
	New data on faults of the San Francisco Bay region
	Consider possible improvements in method

PRELIMINARY CONCLUSIONS

The probability of a M~7 earthquake along the San Francisco Peninsula segment of the San Andreas fault has not decreased as a consequence of the 1989 Loma Prieta earthquake. The 30-year probability is at least 0.2 (Open File Report 88-398).

New interpretations and new data increase the the 30-probability of M~7 earthquakes along both segments of the Hayward fault from 0.2 (Open File Report 88-398) to 0.3 for each segment.

New data for the Rodgers Creek fault yield a 30-probability of 0.2 for a M~7 earthquake.

The estimated probability of one or more M~7 earthquakes in the San Francisco Bay region is 0.7 for the coming 30 years. This is not a final result.

There is an acute need for intensive studies of all major faults in the San Francisco Bay region.

Significant earthquake hazard also exists in southern California. The total 30-year probability is 0.6 for one or more M=7½-8 earthquakes along the southern San Andreas fault and the total 30-year probability is 0.5 for one or more M=6½-7 earthquakes along the San Jacinto fault (Open File Report 88-398).

Probabilities of Earthquakes ($M \geq 7$) in the San Francisco Bay Region

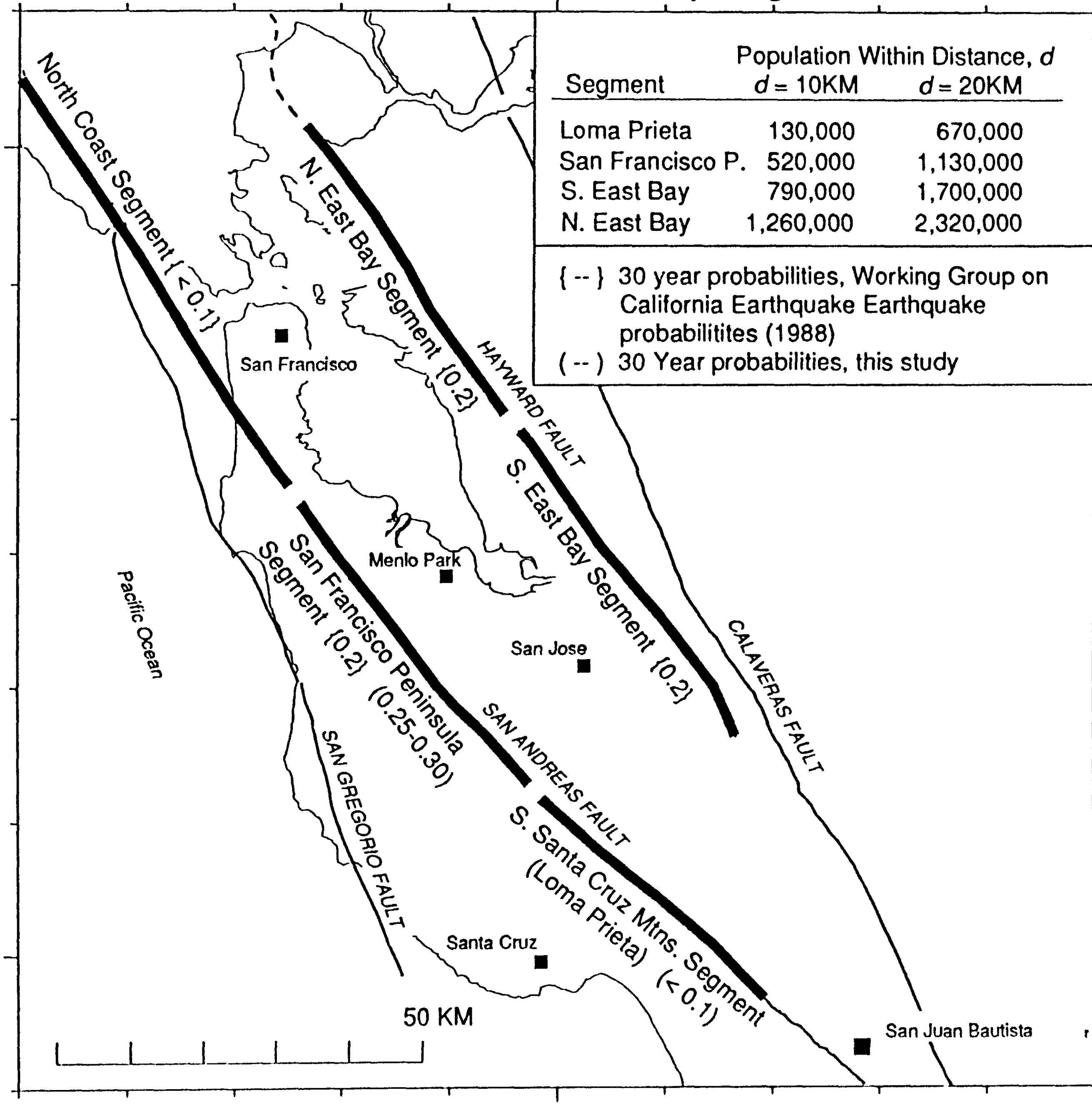

Segment	Population Within Distance, d $d = 10$KM	$d = 20$KM
Loma Prieta	130,000	670,000
San Francisco P.	520,000	1,130,000
S. East Bay	790,000	1,700,000
N. East Bay	1,260,000	2,320,000

{ -- } 30 year probabilities, Working Group on California Earthquake Earthquake probabilitites (1988)
(--) 30 Year probabilities, this study

Recurrence Times and Conditional Probabilities of Earthquakes in San Francisco Bay Region

Fault Segment	Date of Most Recent Event	Magnitude	Open File 88-398 T_{exp} (yrs)	Open File 88-398 Probability 1988–2018	1990 Revisions Preliminary Report T_{exp} (yrs)	1990 Revisions Preliminary Report Probability 1990–2020	Level of Reliability
North Coast (SA)	1906	8	281	<0.1	281*	<0.1*	B*
San Francisco Pen. (SA)	1906	7	156	0.2	156*	0.2*	C*
S. Santa Cruz Mtns. (SA)	1989	6½	125	0.3	-	-	-
Northern East Bay (H)	1836	7	187	0.2	156	0.3	D*
Southern East Bay (H)	1868	7	187	0.2	156	0.3	C*
Rodgers Creek (H)	1808?	7	-	-	222	0.2	-

SA = San Andreas Fault
H = Hayward Fault

* *Data from Open File Report 88-398*

Probability of One or More Large Earthquakes
San Francisco Bay Region

	Expected Magnitude	Total Probability*			
		5 yr	10 yr	20 yr	30 yr
Open-File 88-398 *Segments: San Francisco Peninsula, N. East Bay, S. East Bay*	7	0.1	0.2	0.3	0.5
Preliminary Results (1990) *Segments: San Francisco Peninsula, N. East Bay, S. East Bay, Rodgers Creek*	7	0.1	0.3	0.5	0.7

* Total probability of one or more earthquakes in a region of interest is obtained by aggregating the probabilities of individual segments:

$$P = 1 - (1 - P_a)(1 - P_b)(1 - P_c) \ldots$$

P_a, P_b, P_c = Probability of an earthquake on segments a, b, c

Appendix F

Viewgraphs used by A.Cornell to accompany presentation to NEPEC, January 11, 1990.

WORKING GROUP METHODOLOGY

PROBABILISTIC MODEL(S)

STATISTICAL (PARAMETRIC) UNCERTAINTY

1. An Elementary Model of Recurrence

- "Segment" or "Point on Segment":

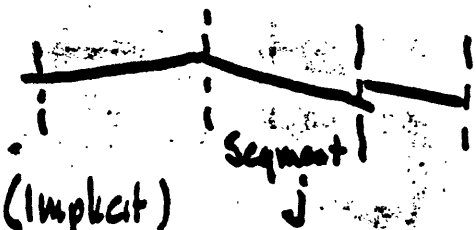

- Characteristic Magnitude Events (Implicit)
- Time Series: Marked Point Process

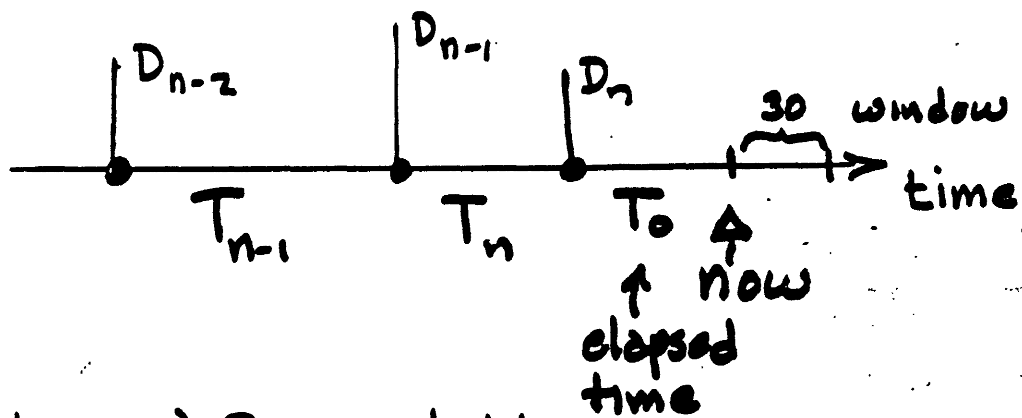

(Markovian) Renewal Model:

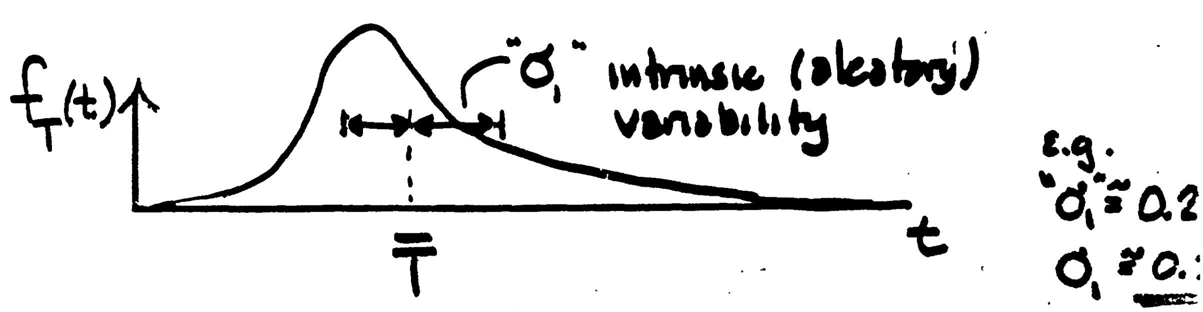

Shape: Lognormal, Weibull, Gamma ....

Prediction:

$$P_{30} = \text{Prob}[\text{event in next 30 years} \mid \underline{T_0, D_n, \cdots}\,;\, \underline{\bar{T}, \sigma}]$$

past → $T_0, D_n, \cdots$; parameters → $\bar{T}, \sigma$

Simple Renewal:

$$P_{30_{T_0}} = \text{Prob}[\text{event in next 30} \mid T_0 \,;\, \bar{T}, \sigma]$$

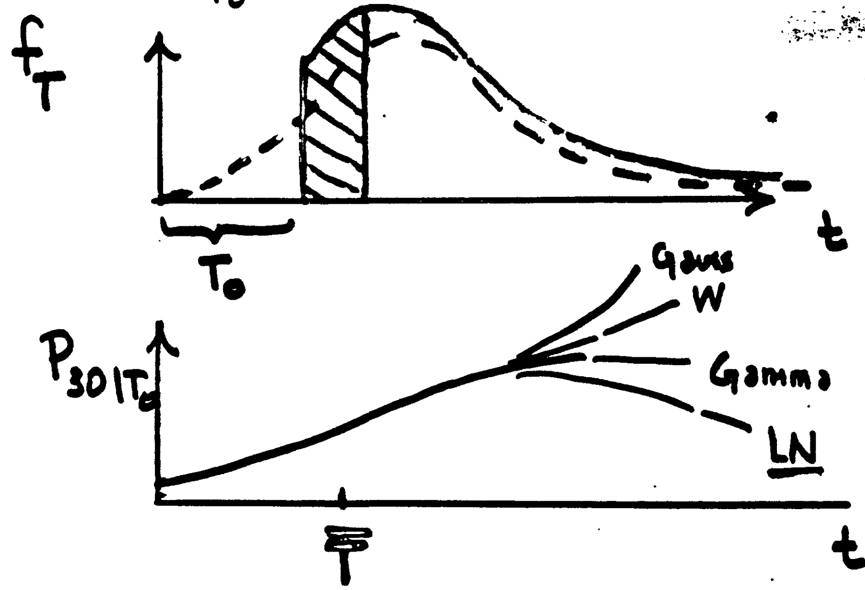

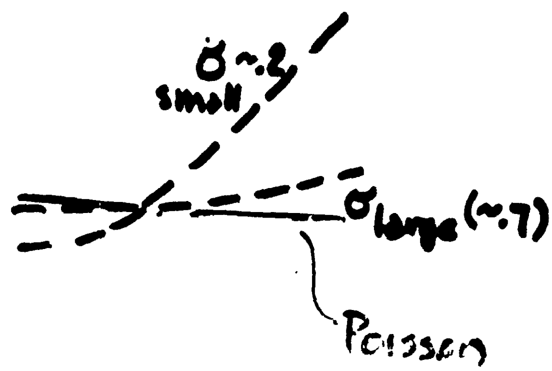
σ small (~.3)
σ large (~.7)
Poisson

Parametric Uncertainty, $\bar{T} = ? \pm ?$

(WG: $\sigma_1 = .21$ ala Nishenko/Buland)

Estimators of $\bar{T}$: (Marginal Mean)

(a) $\hat{\bar{T}} = \sum_{i=1}^{n} T_i / n$

$\sigma_{\hat{\bar{T}}} = \sigma_1 / \sqrt{n}$ ($\leq .21$ if $n \geq 1$)

$\sigma_{TOTAL} = \sqrt{\sigma_1^2 + \sigma_{\hat{\bar{T}}}^2} = \sigma_1 \sqrt{1 + 1/\sqrt{n}}$ ($\leq \sqrt{2}\sigma_1$

(b) $n = 0$?

from $\dot{u} = \frac{D_{TOT}}{T_{TOT}} = \frac{\bar{D}}{\bar{T}}$

use

$\bar{T} = \bar{D} / \dot{u}$

$\hat{\bar{T}} = \hat{\bar{D}} / \hat{\dot{u}}$

$\sigma_{\hat{T}} \cong \sqrt{\sigma_{\hat{D}}^2 + \sigma_{\hat{u}}^2}$ (these are "relative sigmas": C. of V.'s)

WG. experience ~ .3 – .4

note: for only one past event

$\sigma_{\hat{\bar{D}}} = \sigma_{\hat{D}_n}$ ← n^{th} event (last)

Prediction with Parameter Uncertainty

in general:

$$\hat{P}_{30} = \int P_{30|\bar{T}} \; f_{\hat{\bar{T}}}(\bar{T})\, d\bar{T}$$

in common special cases — e.g., LN

Predict as above with increased uncertainty

$$\sigma_{TOT} \doteq \sqrt{\sigma_1^{\,2} + \sigma_{\hat{\bar{T}}}^{\,2}}$$

(LN: ~COV's or $\sigma^2_{\text{mean of logs}} + \sigma^2_{\log T}$

WG experience:

$$\sim\sqrt{(.2)^2 + (.3 - .4)^2}$$

$$\doteq .3 - .4 \; (+)$$

parametric uncertainty dominates.

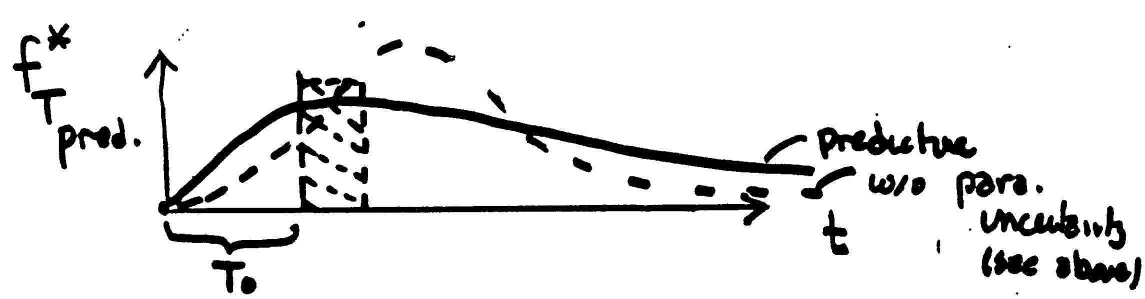

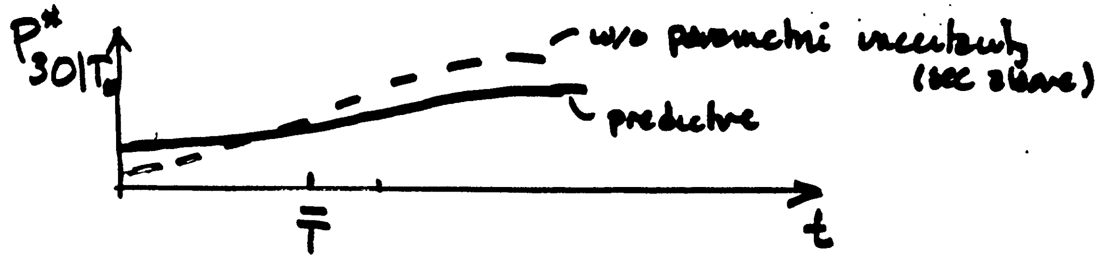

2. A "Stronger" Model (than simple renewal)

TIME PREDICTABLE

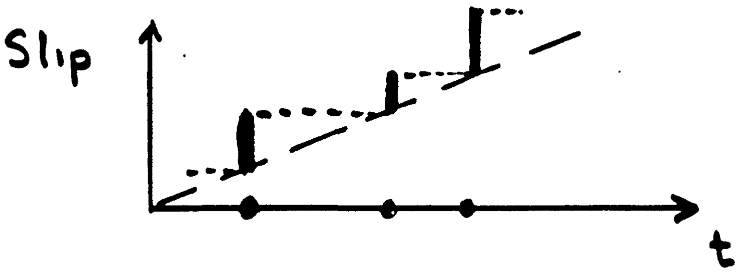

random {slips or stress drops

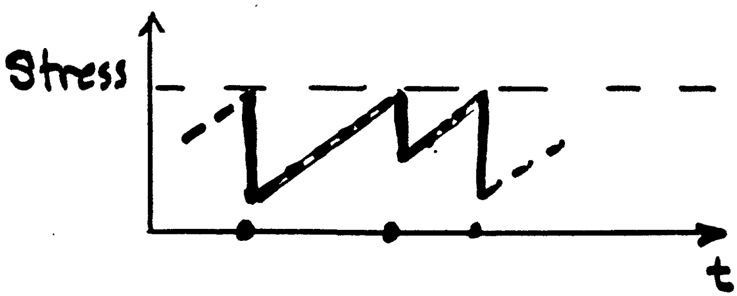

$T_{n+1} = D_n / \dot{u}$

- perfect time predictability

$\sigma_{T|D} = 0$

: (More Realistic)

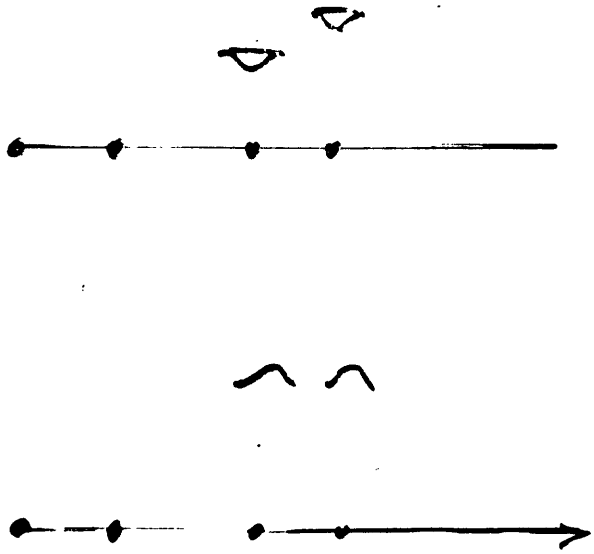

$$\sigma_{T|D} \to 0$$

$$E[T_{n+1} | D_n] = D_n/\mu$$

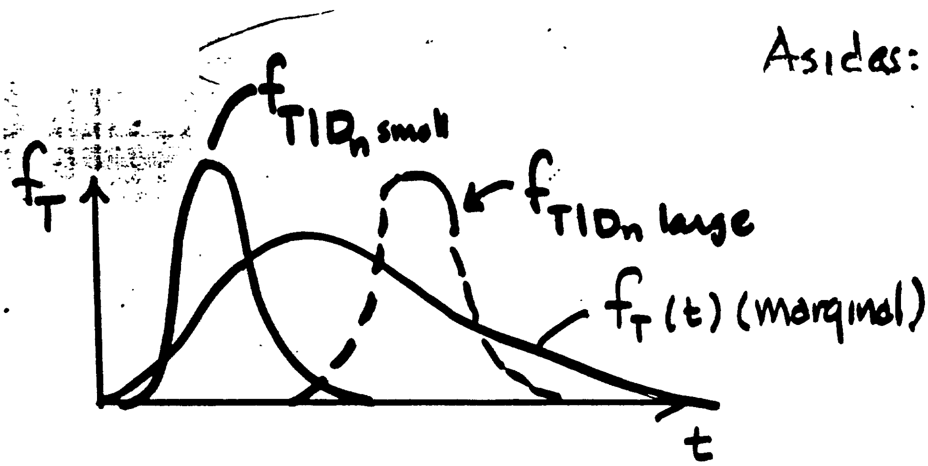

Asides: Can be shown:

(1) $\sigma_{T|D} = \sqrt{1-\rho^2_{T,D}}\,\sigma_T$

$\leq \sigma_T$

(2) $\rho = \dfrac{V_D}{V_T}$ ← rel. var. (c. of v.)

$\Rightarrow V_D \leq V_T$ (~

char. mag. implicit ! if V_T is small

6 Time - Predictable:

Advantage —

"sharper" predictions

- if ρ is large ; i.e., $\sigma_{T|D} \ll \sigma_T$
- if you know the parameters

Parametric Uncertainty:

Given last event (only).

$$\hat{E}[T_{n+1} | "D_n"] = \hat{D}_n / \hat{u}$$

$$\sigma_{\hat{E}_{T|D}} = \sqrt{\sigma^2_{\hat{D}} + \sigma^2_{\hat{u}}}$$

rel. variab. (c. of v.)

WG experience ~.3-.4

Prediction:

$$\hat{E}[T_{n+1} | "D_n"] = \hat{D}_n / \hat{u}$$

$$\sigma_{TOTAL} = \sqrt{\sigma^2_{T_{n+1}|D_n} + \sigma^2_{\hat{E}_{T|D}}}$$

WG: $\leq(.2)^2 + (.3-.4)^2$

$C_{TOT} = (.3-.4)^+$

Compare with Simple Renewal Above.

≈ SAME

Some Limitations

Models:

segments interact:

overlap

trigger

load or release stress

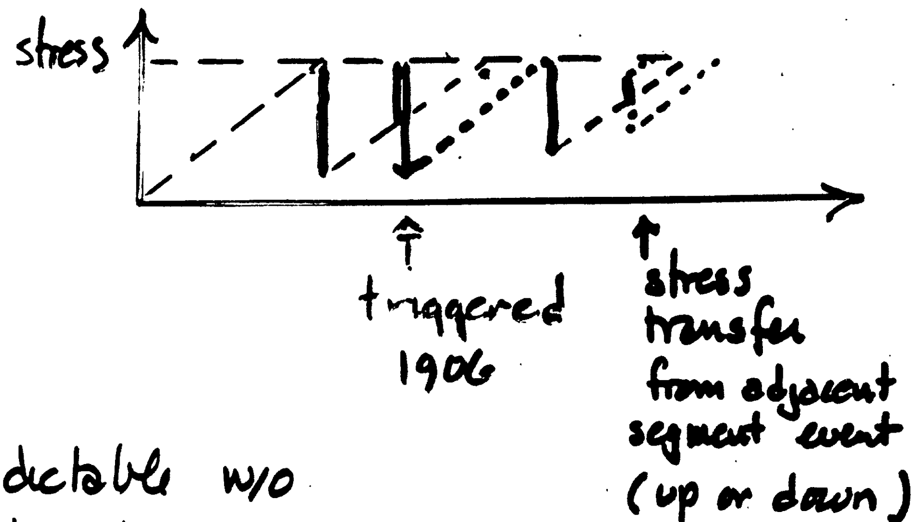

Time predictable w/o interaction fails to capture these effects

Simpler model may (with large enough sample!)

Some (Documented) Criticisms of WG 88:

- Davis, Jackson, Kagan (BSSA, Oct, 1989)
  - include "open" interval (T_0 value) in estimator of $\bar{T}$
    - yes, but not a factor in Bay Area.
  - σ known? (common)
  - Nishenko / Buland data collection process?

- Savage (manuscript drafts, 1990)
  - display uncertainty in P_{30} induced by $\sigma_{\bar{T}}$:

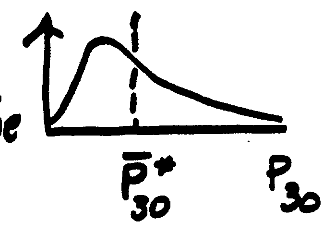

OK, but is it effective communication broadly?

  - Loma Prieta was "too soon" ⇒ Model error
    - WG 90* is responding to L.P.
    - slip rates will be larger (?)

Some Improvements in next Months:

1. Careful statement of models, assumptions, procedures for parametric uncertainty, etc
2. "Logic Trees"
3. Parametric Uncertainty: Improvement in Procedures
4. Interaction

A Logic Tree Illustration:

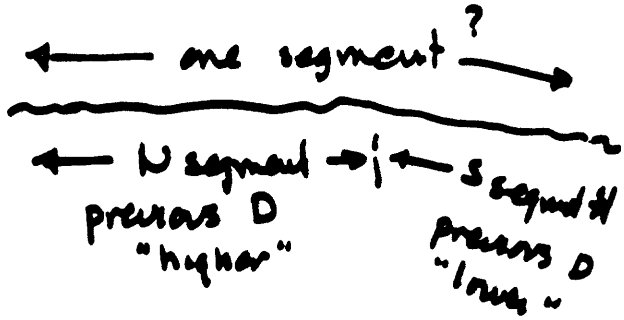

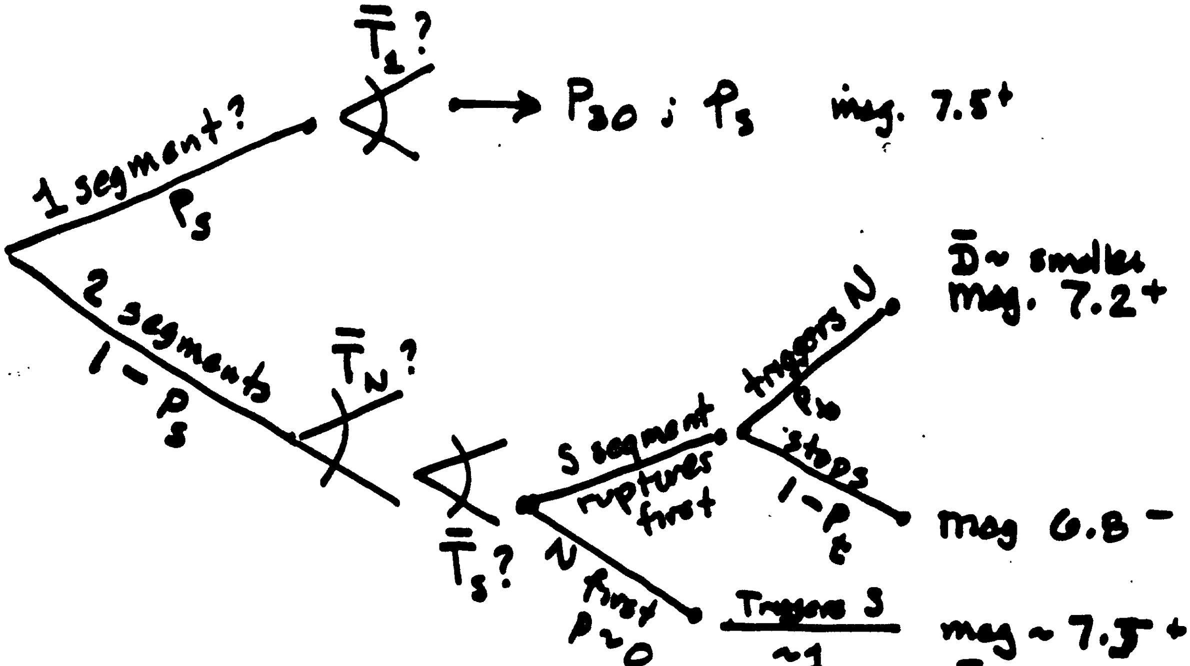

Committee Consensus on

P_s, P_t and $\bar{T}_1$, σ_T, etc.

rather than on which segmentation hypothesis is correct.

Appendix G

Handouts provided by P.Reasenberg to accompany presentation to NEPEC, January 12, 1990.

OUTLINE FOR JANUARY, 1990 NEPEC MEETING

0. Request was to summarize the method and update NEPEC on new developments.

1. Formulation of the model -- described in Science report (1989)
   a. Gutenberg-Richter magnitude distribution
   b. Modified Omori Law time distribution
   c. California data: 62 M>5 sequences, a priori distributions
   d. Probabilities for generic sequence (Table 1)
   e. Addition of ongoing sequence data

2. Numerical Uncertainties in the model probabilities --
   Science Comment I Response (1990)
   a. Large standard errors for generic model at t=0
   b. Acceptably small uncertainties after about 1 day

3. Applications to date

3.1 Brawley (M4.7) -- Science Comment II (1990)

3.2 Lake Ellsman (M5.2) 1989 -- Probabilities for a larger follow-on earthquake were calculated, faxed to OES, and released to the media. OES issued an advisory. SJ Mercury News printed a front-page color graph showing probabilities for an M>5 earthquake.

3.3 Loma Prieta (M7.1) -- Science Comment II (1990)
Some Additional Points:

a. Smootheness of the model results in time.
   1. (artificial) a numerical function was evaluated piecewise in time in a computer code, instead of continuously.
   2. (real) change in mainshock magnitude from 6.9 to 7.1
   3. (real) delayed surge of M>4 events

b. We could reduce the jumpiness by increasing the variance of the sample estimates accordingly.

c. Appearance of jumpiness:
   Reports were for 1-day intervals for first 4 days
   Then, 1-day and 2-month intervals for next 15 days
   Then, 1-week and 2-month intervals for next 25 days.
   -->In future, recommend consistent (1-week and 2- or 3-month) intervals for all forecasts.

4. Types Uses of the Model -

4.1 Use after a moderate earthquake, to estimate the short-term probabilities of a larger follow-on earthquake.
(e.g., The Brawley and Lake Ellsman sequences)

4.2 Use after a strong earthquake, to estimate the probabilites of hazardous aftershocks (smaller than the mainshock) (e.g., Loma Prieta sequence)

4.3 Use after a strong earthquake, to estimate the probabilites of an even stronger follow-on earthquake (e.g., memo to the NEPEC Working group on Post-Loma Prieta Probabilities)

4.4 Use fter a strong earthquake, to estimate probabilites of aftershocks for planning seismological field studies (e.g., U.S.G.S. response to Loma Prieta) (not of direct concern to NEPEC)

4.5 The generic model can contribute to the development of an earthquake prediction scenario and response plan. In a region for which the contemporary seismic and paleoseismic data are lacking or insufficient, so that the Agnew-Jones foreshock methodology cannot be used, the Generic aftershock model could provide intermediate- and long-term probabilites representative, in some sense, of an average for California. -->However, where the seismological data support it, the Agnew-Jones model would be prefered.

5. The USGS should consider policies concerning:

a. IN WHAT SITUATIONS should short-term probability estimates be released, and to whom. The decision is clearly sensitive to location, because the hazard associated with a given earthquake depends strongly on its location. Some pre-defined criteria are needed to guide this application. Possibly these criteria might imply certain alert levels that could suggest appropriate responses.

b. HOW to issue forecast information (i.e., timing, wording and frequency of information releases to OES and the press)

c. HOW to issue them consistently and with sufficient explanation that they be understood. Background information, comparisons with other earthquakes, and interpretations of probabilities should be provided to insure that the forecast is fully understood.

c. When to STOP issuing them. After Loma Prieta we tapered the frequency of forecasts, and terminated after 6 weeks.

United States
Department of the Interior
Geological Survey, Western Region
Menlo Park, California 94025

Public Affairs Office (415) 329-4000

WEDNESDAY, OCTOBER 25, 5:00 PM PDT

THE LOMA PRIETA, CALIFORNIA, EARTHQUAKE OF OCTOBER 17, 1989

AFTERSHOCK SEQUENCE OBSERVATIONS AND FORECAST

As of 5:00 PM PDT Wednesday, October 25, eight days after last Tuesday's earthquake, 79 aftershocks of magnitude 3.0 and larger were recorded by the U.S. Geological Survey in Menlo Park. The largest aftershock, magnitude 5.2, occurred 37 minutes after the mainshock. The second largest aftershock, magnitude 5.0, occurred Thursday at 3:14 AM PDT. In addition, a total of 20 aftershocks of magnitude 4.0 and larger have occurred so far. Fifty-one magnitude 3.0–3.9 aftershocks occurred during the first 24-hour period after the mainshock, and 16 occurred during the second 24-hour period. During the third day of the sequence, four aftershocks with magnitude 3.0 and larger occurred. The most recent widely felt aftershocks were two magnitude 3.7 events today at 6:01 AM and 3:02 PM, PDT.

The magnitude of the earthquake was revised to 7.1 by the National Earthquake Information Service in Golden, Colorado, at 11:00 AM Tuesday, October 24. This revision is the result of additional data received from 18 seismographic stations around the world, and represents an average of the observations made at these stations. Such revisions in magnitude are normal and reflect the increasing number of observations coming in from seismographs around the world.

Seismologists advise that additional aftershocks are expected in the next few weeks to months, some possibly strong enough to cause additional damage, especially to structures weakened in last Tuesday's quake. Because of this continuing hazard, scientists urge that earthquake preparedness measures continue to be taken, and that extreme caution be exercised in and around damaged structures.

24-HOUR FORECAST:

The probability for aftershocks decreases with time most rapidly during the first week after the mainshock; then, the probability for aftershocks decreases more slowly in the later weeks and months of the earthquake sequence. To assess the chances for additional damaging aftershocks, scientists rely on the average behavior of past California sequences, and on observations of the current earthquake sequence. The aftershocks recorded so far generally follow the behavior of a typical California sequence. From these observations, a statistical model has provided a forecast of future strong aftershocks. As of Wednesday, October 25, at 5:00 PM PDT, there is less than a one percent chance of a magnitude 6.0 or larger aftershock in the next 24 hours. In the same 24-hour period, the probability of a magnitude 5.0 or larger aftershock is four percent.

LONG TERM FORECAST:

The long term outlook underscores the enduring nature of aftershock sequences. It is not uncommon for a strong aftershock to occur several weeks or months after a mainshock. Over the next two months the probability of a magnitude 6.0 or larger aftershock is approximately 9 percent, while the probability of a magnitude 5.0 or larger event in the same two-month period is about 43 percent. Also, in the next two months, approximately three additional magnitude 4.0 or larger aftershocks are expected.

Most probably, additional earthquakes in the next few days will be smaller than last Tuesday's $M = 7.1$ earthquake. As for the possibility of an earthquake comparable to or larger than Tuesday's quake, scientists characterize the chances for that as "very small, but not zero". In a small fraction of the cases observed in California, a large earthquake has triggered a comparable or larger earthquake on an adjacent segment of the same fault, or on a neighboring fault. In particular, scientists are focusing attention on the Peninsula segment of the San Andreas fault, from Los Gatos to Daly City. This segment of the San Andreas was previously identified as being capable of producing a magnitude 7 earthquake, and was given a 20 percent chance of doing so in the next 30 years. There is concern among scientists that last Tuesday's earthquake may have increased the stress on the southern end of that fault segment, thus increasing the chances for a strong earthquake on the San Francisco Peninsula over the next few years. Such triggering, however, is considered unlikely. For example, no such triggering occurred after the magnitude 6.5 earthquake believed to have occurred on the same Santa Cruz segment of the San Andreas fault in 1865.

Seismologists will continue to monitor the aftershock sequence, as well as any unusual earthquake activity elsewhere in the San Francisco Bay area, and update the forecast for future aftershocks as the sequence progresses.

San Jose Mercury News

1989 Lake Ellsman Earthquake

Figuring the odds for another jolt

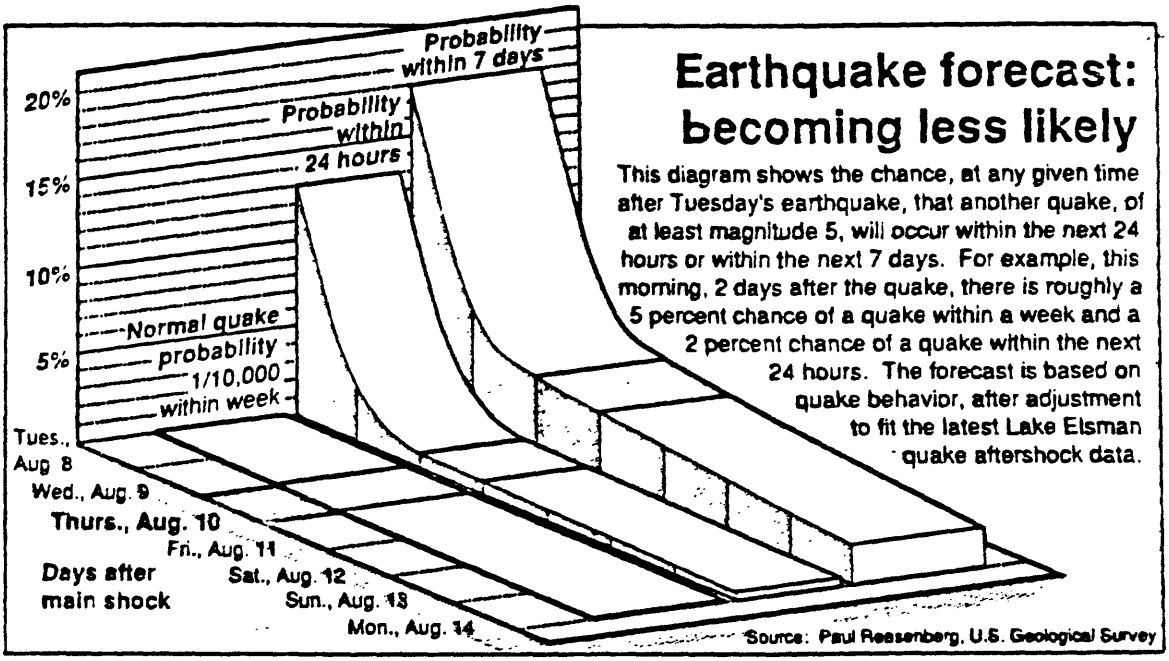

Ron Coddington — Mercury News

Warnings that Tuesday's earthquake indicated a higher probability of a strong temblor made people wonder what that meant. Probability drops with each quakeless day after the main shock. The colored band shows probabilities for another quake to strike today.

Loma Prieta Earthquake

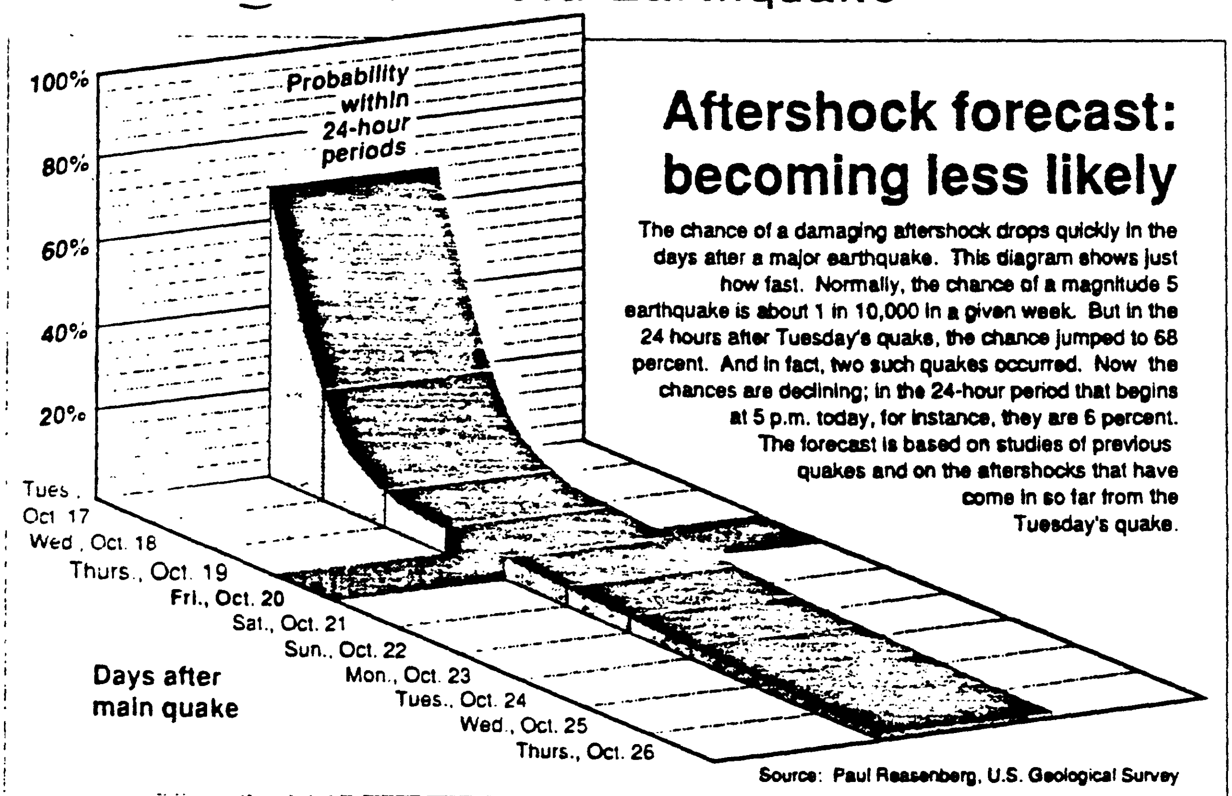

Ron Coddington - Mercury News

Appendix H

Handout provided by L.Jones to accompany presentation to NEPEC, January 12, 1990.

Appendix A
Prediction Probabilities from Foreshocks

Duncan Carr Agnew and Lucile M. Jones

1. Introduction

Many damaging earthquakes have been preceded by immediate foreshocks, smaller earthquakes that occur within a few days and a few kilometers of the mainshock (e.g., Jones and Molnar, 1979). If those foreshocks could be recognized as such before the mainshock occurs, they would be a very effective tool for short term earthquake prediction, but so far no characteristic of foreshocks has been recognized that would allow them to be distinguished from other earthquakes. However, when any earthquake occurs, the possibility that it might be a foreshock increases the probability that a larger earthquake will occur at the same site within the next few days. Jones (1985) showed that in southern California this increased probability is 6% that an earthquake larger than the first will occur within five days. Indeed, on this basis, the U. S. Geological Survey has issued four short term earthquake advisories after moderate earthquakes had occurred (Goltz, 1985). The probability of another earthquake occurring is significantly lower for a much greater earthquake; the probability of an earthquake two units of magnitude larger than the first is only 0.2%.

The results of Jones (1985) are from an emperical study of foreshocks previously recorded in southern California. It is intuitively obvious that the probability of a very large earthquake should be higher if the candidate foreshock were to occur on or near a fault known to be capable of producing that very large mainshock, especially if the fault is towards the end of its seismic cycle. This increased probability cannot be accounted for by the generic, emperical results of Jones (1985).

An expression for this probability can be analytically derived from some of the basic tenets of probability theory. We find that using this approach allows us to express the probability of a major earthquake characteristic to a particular fault, given the occurrence of a potential foreshock near to that fault as a function of several quantities that can be determined from other sources of data. The derivation of this probability is presented below. We show that it depends on the long term probability of the characteristic mainshock, the rate of background seismicity along the fault and some assumed characteristics of foreshocks. This derivation is then applied to the southern segment of the San Andreas fault—the one fault segment in California considered most likely to produce a major earthquake within the next few decades (Agnew *et al.*, 1988).

2. Models for Probabilities from Foreshocks

Because of the nature of the seismicity along the southern segment of the San Andreas fault, we have been led to address certain fundamental issues about the relationship between foreshocks and large events. This area illustrates in an extreme form the "maximum-magnitude" model introduced by Wesnousky *et al.* (1983), in which the frequency of the largest earthquakes on a fault zone is much higher than would be predicted by the extrapolation of the frequency-magnitude distribution for background events. For the southern segment as for many other parts of the San Andreas fault, this is a straightforward consequence of the low level of present-day seismicity. Extrapolating the present level of seismicity to higher magnitudes predicts that a magnitude 7.5 earthquake would occur every 2900 years, whereas the recurrence rate estimated from slip-rate data is 200–300 years.

The implication of this is that the large characterteristic earthquakes on a fault zone are somehow "different" from the background seismicity along it. This in turn suggests that the foreshocks to such events might share in this difference, and so should be regarded as a separate class of earthquakes from the background events. Making this conceptual distinction does not of course imply that we can distinguish foreshocks from background events from the records we have of them; rather, they can only be identified statistically, and after the fact. This is, of course, exactly the case for another class of earthquakes, namely aftershocks.

2.1 Zero-Dimensional Model

From the assumption that foreshocks are a separate class of event from background earthquakes, we can set out a formal probabilistic scheme for finding the probability of a large event, given the occurrence of a possible foreshock. To keep matters simple, we begin with a "zero-dimensional" model, ignoring spatial variations, magnitude dependence, and other complications. We thus define events (in the probability-theory meaning of the term):

B: A background earthquake has occurred.

F: A foreshock has occurred.

C: A large (characteristic) earthquake will occur.

We assume that B is independent from C and that F and B are disjoint (we have a foreshock or a background event, but not both).

The probability that we seek is the conditional one of C, given either F or B (because we do not know which type we have). This is, by the definition of conditional probability,

$$P(C|F \cup B) = \frac{P(C \cap (F \cup B))}{P(F \cup B)} \tag{1}$$

Because F and B are disjoint, the probability of their union is the sum of the individual probabilities. Thus, the numerator of (1) can be written as

$$P((C \cap F) \cup (C \cap B)) = P(C \cap F) + P(C \cap B) = P(C \cap F) + P(C)P(B)$$

and the denominator can be written as

$$P(F \cup B) = P(F) + P(B)$$

By the definition of a foreshock, $P(F|\overline{C}) = 0$ (we cannot have a foreshock with no mainshock), and then

$$P(F) = P(F|C)P(C) \tag{2}$$

where $P(F|C)$ is the probability that a mainshock is preceded by a foreshock. Using the definition of conditional probability once more to get $P(C \cap F)$, we find that

$$P(C|F \cup B) = \frac{P(F|C)P(C) + P(C)P(B)}{P(F|C)P(C) + P(B)} \tag{3}$$

Equation (3) has a number of desirable properties. If $P(F|C)$ is zero (no foreshocks), we find that $P(C|F \cup B) = P(C)$, the background rate; if, however, we had $P(B) = 0$, the expression becomes one (any candidate event must be a foreshock).

This expression is a function of three quantities, which in practice we obtain from very different sources. $P(B)$, the probability of a background earthquake, would be found from long-term recordings of the seismicity of the fault zone. $P(C)$, the probability of a characteristic earthquake, would be found from calculations of the type presented by Agnew *et al.* (1988). If we had a record of the seismicity before many such characteristic earthquakes, we could evaluate $P(F|C)$ (which we shall hereafter call R_{FC}) from it. (For this simple model, R_{FC} is just the fraction of large earthquakes preceded by foreshocks.) Of couse, we do not have such a record, and so are forced to make a kind of reverse ergodic assumption, namely that the time average of R_{FC} over many events on one fault is equal to the spatial average over many faults. This may not be true, but it is for now the best we can do.

2.2 A One-Dimensional Model

As a simple extension of the previous discussion, suppose that we have N "regions," and that C_i, B_i, and F_i denote the occurrence of an event in the i-th regions, with C (for example) now being the occurrence of a large earthquake in any possible region. These regions can be sections of the fault, or (as we will see below), areas in a multidimensional space of all relevant variables. The quantity of interest is now $P(C|F_i \cup B_i)$: we have a candidate foreshock in one region, and want the probability of a large earthquake starting in any region. Assuming that the C_i's are disjoint (the epicenter can only be in one place), we then have that

$$P(C) = \sum_{i=1}^{N} P(C_i)$$

and so

$$P(C|F_i \cup B_i) = \sum_{j=1}^{N} P(C_j|F_i \cup B_i)$$

and by similar manipulations to those of the last section we find that

$$P(C|F_i \cup B_i) = \sum_{j=1}^{N} \frac{P(C_j)R_{FC}(i,j) + P(B_i)}{P(B_i) + \sum_{l=1}^{N} P(C_l)R_{FC}(i,l)} \tag{4}$$

where $R_{FC}(i,j) = P(F_i|C_j)$. We may regard R_{FC} as a kind of "transition probability" between a large earthquake in region j and a foreshock in region i; we call it the reverse transition probability because it operates in reverse time. In this simple case we might suppose (for example) that $R_{FC}(i,j) = \alpha\delta_{ij}$, which would imply that large events are preceded by foreshocks only in the same region, and even then only a fraction α of them have foreshocks at all.

If we extend equation (2) to the one-dimensional case we get

$$P(F_i) = \sum_{j=1}^{N} R_{FC}(i,j)P(C_j) \tag{5}$$

in which case equation (4) reduces to

$$P(C|F_i \cup B_i) = \frac{P(F_i) + P(C)P(B_i)}{P(F_i) + P(B_i)} \tag{6}$$

Equations (5) and (6) are the basic ones we shall use in the more general case. Equation (5) shows us how to compute the probability of a foreshock happening in the location of our candidate event, by summing over all possible mainshocks. The use of the reverse transition probability R_{FC} is the key to this approach; we can (and in the next section shall) design it to embody our knowledge and assumptions about the relation between foreshocks and the earthquakes they precede. Having found the foreshock probability, we then use equation (6) to find the conditional probability of a large event.

An important consequence of equation (5) is that we may sum over all possible foreshocks (again assuming disjointness) to get

$$P(F) = \sum_{i=1}^{N}\sum_{j=1}^{N} R_{FC}(i,j)P(C_j) \tag{7}$$

giving us the overall probability of a foreshock somewhere in the total region. This must satisfy $P(F) = \alpha P(C)$, where α is the fraction of mainshocks with foreshocks; these two equations supply a constraint on R_{FC}, which must be so normalized as to make them hold.

3. Multidimensional Model and Application to Foreshocks

We now proceed to develop an expanded version of equation (5), which contains all the relevant variables. To begin with, we must define our events more thoroughly; they now are:

- B: A background earthquake has occurred at (Cartesian) coordinates $(x_0 \pm e_0, y_0 \pm e_0)$, during the time period $[t, t+\delta_0]$, with magnitude $M \pm \mu$. (All of the quantities e_0, δ_0, μ are small and are included because we will be dealing with probability density functions; as will be seen below, they cancel from the final expression).
- F: A foreshock has occurred, with the same parameters as in event B.
- C: A major earthquake will occur somewhere in the region of concern, which we denote by A_C (also using this variable for the area of this region). This earthquake will happen during the time period $[t+\Delta, t+\Delta+\delta_1]$, with magnitude between M_C and $M_C + \mu_C$.

Once again, we assume that we are computing the probability at some time in the interval $(t+\delta_o, t+\Delta)$; the possible foreshock has happened, but the predicted mainshock is yet to come.

3.1 Rate Densities of Earthquake Occurrence

We begin by defining a rate of occurrence for the background seismicity (in the literature on point processes this would be called an intensity, a term we avoid because of existing seismological usage). This rate (or strictly speaking rate density) is $\Lambda(x, y, M)$, such that the probability of B is:

$$P(B) = \int_{t}^{t+\delta_0} dt \int_{x_0-e_0}^{x_0+e_0} dx \int_{y_0-e_0}^{y_0+e_0} dy \int_{M-\mu}^{M+\mu} dM\, \Lambda(x, y, M) \tag{8}$$

by not making Λ dependent on the time t we make the occurrence of background events into a Poisson process, with $P(B) \propto \delta_0$. If we assume that at any location the Gutenberg-Richter magnitude-frequency relation holds, we may write

$$\Lambda(x, y, M) \equiv \Lambda_s(x, y) e^{-\beta(x,y)M} \tag{9}$$

where β is 2.3 times the usual b-value. If β is constant over a region of area A, and during a time interval T the cumulative number of earthquakes of magnitude M or less is given by the usual formula

$$N(M) = 10^{a-bM} \tag{10}$$

then, since

$$N(M) = \int_{0}^{T} dt \int_{M}^{\infty} dM \iint_{A} dx\, dy\, \Lambda_s(x, y)\, e^{-\beta M} \tag{11}$$

we have that $\Lambda_s = (10^a\beta)/(AT)$ for Λ_s constant within the region.

Similarly, we can define a rate density for the occurrence of large events,

$$\Omega(x,y,M,t) \equiv \Omega_s(x,y,t)e^{-\beta'(x,y)M} \tag{12}$$

In this case, we introduce a dependence on time t because the occurrence of large earthquakes is often formulated (e.g., by Nishenko and Buland (1986)) as a renewal process, with time in practice being measured relative to the last event. The probability of C is then

$$P(C) = \int_{t+\Delta}^{t+\Delta+\delta_1} dt \int\int_{A_C} dx\,dy \int_{M_C}^{M_C+\mu_C} dM\,\Omega(x,y,M,t) \tag{13}$$

where A_C is the area of concern; in this case, the Coachella segment of the San Andreas. In most cases Ω changes very slowly with time, so that the time integral in the above expression can be replaced by a simple proportionality to δ_1.

For lack of better information, we would usually take Ω_s to be a constant, but we could choose to make it spatially varying. Such variation could include increases near fault jogs and terminations if we think that rupture nucleation is more likely there, or a proportionality to Λ_s if we suspect that background events are (on the average) the likely triggers of large ones. For Ω_s constant, we have that

$$\Omega_s = \frac{P(C)\beta'}{A_C\delta_1 e^{-\beta M_C}(1 - e^{-\beta'\mu_C})} \tag{14}$$

Note that while we have regarded both A and A_C as two dimensional regions (and hence also as the areas of such regions) we may in fact make them three-dimensional or one-dimensional if we so choose, making sure that we adjust the numbers of the integrals in equations (8) and (13) accordingly. The one-dimensional model is easiest to develop analytical expressions for, and may be an adequate approximation for the case of a long fault zone. In this case, of course, we need to project the background seismicity (out to some distance away) onto the fault zone.

3.2 Computation of the Foreshock Probability

We are now in a position to write the formal expression for the foreshock probability, $P(F)$, in the same way as was done in equation (5) for the discrete one-dimensional case. In this case, R_{FC} becomes a density function over all the variables involved, its value indicating with what relative frequency foreshocks with different parameters occur before mainshocks with particular ones. Instead of a single sum, as there, we have a multiple integral:

$$P(F) = \int_{t}^{t+\delta_0} dt \int_{x_0-e_0}^{x_0+e_0} dx \int_{y_0-e_0}^{y_0+e_0} dy \int_{M-\mu}^{M+\mu} dM \int_{t+\Delta}^{t+\Delta+\delta_1} dt' \int\int_{A_C} dx'\, dy' \int_{M_C}^{M_C+\mu_C} dM'$$
$$\cdot R_{FC}(t,t',x,y,x',y',M,M')\,\Omega_s(x',y',t')e^{-\beta'(x',y')M'} \tag{15}$$

Of these eight integrals, the last four are the integration of the reverse transition density times the density of mainshock occurrence over the space of possible mainshocks; these multiple integrals are the equivalent of the sum in equation (5). But this gives only the rate density for foreshocks, which must in turn be integrated over the space of the candidate event (the first four integrals) to produce the actual probability, $P(F)$.

Equation (15) is clearly quite intractable as it stands. To render it less so, we assume that we can separate the behaviors in time, magnitude, and location. This implies the following assuptions:

1. The frequency-magnitude dependence for the mainshock described by β' does not in fact depend on x' or y'.
2. Over the range of integration, Ω_s does not depend on t'.
3. The dependences of the reverse transition density on time, space and magnitude are not interdependent, so that we can write it as

$$R_{FC} = R_s(x,y,x',y')R_t(t,t')R_m(M,M')$$

Of these assumptions, only the third seems controversial, as the dependence on distance and the dependence on time might both seem likely to be correlated with magnitude. In this particular case, the most likely correlation (with mainshock magnitude) does not matter very much, since our range of integration of this variable is small.

Once we make these assumptions, we can divide the integral in equation (15) into a product of three integrals (in space, time, and magnitude), so that

$$P(F) = \int_{t}^{t+\delta_0} dt \int_{t+\Delta}^{t+\Delta+\delta_1} dt' R_t(t,t') \cdot \int_{M-\mu}^{M+\mu} dM \int_{M_C}^{M_C+\mu_C} dM'\, R_m(M,M')\, e^{-\beta' M'}.$$
$$\int_{x_0-e_0}^{x_0+e_0} dx \int_{y_0-e_0}^{y_0+e_0} dy \int\int_{A_C} dx'\, dy' R_s(x,y,x',y')\,\Omega_s(x',y') \tag{16}$$

3.3 Functional Forms for the Foreshock Density

These three reverse transition densities, R_t, R_s, and R_m, can be used to incorporate our knowledge and assumptions about foreshocks. In the following sections, we detail what is known about the temporal, spatial and magnitude dependences of foreshock occurrence. From these data, we determine a functional form for the relevant R; this form must include both the actual dependence on the variables and a normalization. The nature of the normalization can be seen if we imagine extending the range of the first four integrals in equation (15) to cover all possible foreshocks (however we chose to define them) the resulting $P(F)$ must then be equal to $\alpha P(C)$, where α is, as for the one-dimensional model, the fraction of mainshocks preceded by foreshocks.

3.3.1 Time

Foreshocks occur very close in time to their mainshock. An increase in mainshock occurrence above the background rate has only been seen for a few days (Jones, 1984; 1985; Reasenberg 1985) to a week (Jones and Molnar, 1979) after the occurrence of potential foreshocks. Mainshocks are most likely to occur within 1 hour of the foreshock (26% of Californian mainshocks) and the rate of mainshock occurrence after foreshocks decays rapidly with a $1/t$ type behavior (Jones, 1985; Jones and Molnar, 1979) as shown in Figure 1. The change in rate is well fit by a dependence of the same kind as represented by Omori's law for aftershocks; we use the form found by Reasenberg and Jones (1989) for California aftershock sequences, and write

$$R_t(t,t') = \frac{N_t}{t' - t + c} \tag{17}$$

where, as before, t is the foreshock time and t' that of the mainshock; c is a constant, found by Reasenberg and Jones (1989) to be 200 seconds for aftershocks. The integral can then be written as

$$\int_{t}^{t+\delta_1} dt \int_{t+\Delta}^{t+\Delta+\delta_1} dt'\, R_t(t,t') = \delta_0 N_t \ln[1 + \delta_1/(\Delta + c)] \tag{18}$$

where we have assumed that δ_0 (the uncertainty of the time of the candidate event) is small. The normalization is determined by the requirement that

$$\int_{t+\delta_0}^{t+\delta_0+t_W} dt'\, R_t(t,t') = 1 \tag{19}$$

where t_w is the total time window within which we admit preceding events to be foreshocks. This then gives

$$\int_{t}^{t+\delta_1} dt \int_{t+\delta_0}^{t+\delta_0+t_w} dt'\, R_t(t,t') = \delta_0 \frac{\ln[1+\delta_1/(\Delta+c)]}{\ln[1+t_W/(\delta_0+c)]} \equiv \delta_0 I_t(\Delta,\delta_1) \qquad (20)$$

where, with an eye to future simplifications, we have separated out the δ_0 term. Note that equation (17) predicts a finite rate for all times, whereas the assumption of a limited time window automatically forces the rate to fall to zero beyond some time; we can easily modify R_t to allow for this.

3.3.2 Location

Foreshocks not only occur close in time to the mainshock, but are also nearby in space. Epicenters of mainshocks ($M \geq 7$) and their foreshocks in the NEIC catalog were found to be almost all within 30 km (approximately the location error for the NEIC catalog) of each other (Jones and Molnar, 1979). With more accurate locations, epicenters of mainshocks ($M \geq 3$) and their foreshocks in the Caltech catalog were found to be almost all within 10 km of each other (Jones, 1985). Relative relocations of the foreshocks to $M \geq 5$ mainshocks within the San Andreas system (Jones, 1984) also showed the epicenters of foreshocks all within 10 km of their mainshocks. Even the largest foreshocks ($M \geq 6$ at Mammoth Lakes and Superstition Hills), have had epicenters within 10 km of the epicenters of their mainshocks.

To examine the dependence of the distance between foreshocks and mainshocks on the magnitudes of the earthquakes, a data set of sequences with high quality locations has been put together. This data set includes all foreshock-mainshock pairs with $M_{foreshock} \geq 2.5$ and $M_{mainshock} \geq 3.0$ recorded in southern California since 1977 (the start of digital seismic recording). In addition, sequences relocated in a special study with relative location accuracy of at least 1 km were included. The distance between foreshock and mainshock is plotted versus magnitude of the mainshock (a) and magnitude of the foreshock (b) for this high quality data set in Figure 2.

The epicentral distance between foreshock and mainshock does not correlate strongly with the magnitude of either the foreshock or the mainshock (Figure 2). The data could be described as falling into two classes, foreshocks that are essentially at the same site as their mainshock (< 3 km) and foreshocks that are clearly spatially separate from their mainshocks. Only foreshocks to larger mainshocks ($M_m \geq 5.0$) occur at greater epicentral distances (5-10 km). Of these spatially separate foreshocks, some, *but not all*, had rupture zones that closely approach the epicenter of the mainshock as shown by the hatched zones in Figure 2. The greatest reported distance between foreshock rupture zone and mainshock epicenter is 6.5 km.

Another spatial question is whether foreshocks are preferentially located in some sections of major faults. Several authors have suggested that foreshocks (Jones, 1984) and the epicenters of mainshocks (Nabelek and King, 1985; Bakun *et al.*, 1986) are more common at points of complication of the faults. This could well be true but the complexities are small enough that differentiating between the many possible complex sites and the "smooth" parts of the fault would requiring gridding at the kilometer scale. We do not feel that our knowledge and data are sufficient to justify this level of differentiation.

One further choice we might wish to consider is whether to make R_s dependent on the local rate of background activity Λ_s. This would assert that most mainshocks with foreshocks occur in areas with high background seismicity. This could be true if,

1. Mainshocks preferentially occur on faults with high seismicity, or
2. The epicenters of mainshocks are preferentially located at points of relatively high seismicity for that fault, or
3. Foreshocks are more likely to precede mainshocks that occur at points of high seismicity.

The first premise was proven false with the installation of the first local seismic networks. The greatest earthquakes occur in general on the faults with the lowest levels of background activity. Recent results have also refuted the second premise. Studies of the Calaveras and San Andreas faults have shown that the slip in the largest earthquakes occurs on the areas of the fault that do not have background seismicity or aftershocks (Oppenheimer *et al.*, 1989; Mendoza and Hartzell, 1988). In addition, one of the two great, historic San Andreas earthquakes, the 1857 event, appears to have nucleated near Parkfield where the seismicity is the highest for that rupture zone (Sieh, 1978) while the other great earthquake, the 1906 event, nucleated in San Franciso bay (Boore, 1977) where the rate of background activity is particularly low. The rate of foreshock activity preceding moderate earthquakes in California (Jones, 1984) does not support the third premise. The percentage of moderate earthquakes preceded by foreshocks does vary by region but does not appear to be related to background seismicity. This is exemplified by the complete lack of foreshocks on the Calaveras fault of central California which has a relatively high rate of background activity.

These data clearly show that foreshocks and mainshocks occur close together in space, within 10 km of each other in all resolvable cases. No other dependence of foreshock rate on spatial variables can be recognized. We therefore have made R_s depend only on ρ, the distance between candidate event and possible mainshock ($\rho = [(x-x')^2 + (y-y')^2]^{1/2}$). The condition for R_s to be properly normalized is

$$\int\int_{A_C} dx\,dy \int\int_{A_C} dx'dy'\, R_s(x,y,x',y')\Omega_s(x',y') = \int\int_{A_C} dx'dy'\,\Omega_s(x',y') \qquad (21)$$

which in general can be done only numerically, even for Ω_s constant and R_s having a simple dependence on ρ. If, however, we make the simplification, mentioned in Section 3.1, of making our spatial integrals one-dimensional (with A_C then being the length of the fault), assume Ω_s constant, and make R_s constant for $\rho \le \rho_w$ and zero for larger ρ, we can determine that

$$R_s = \begin{cases} \frac{1}{\rho_w(1-\rho_w^2/4A_C)} & \text{if } \rho \le \rho_w \\ 0 & \text{if } \rho > \rho_w \end{cases} \qquad (22)$$

We use $\rho_w = 10$ km to agree with the data presented above. Then, provided that the location x_0 of the candidate event is more than a distance ρ_w from an end of the fault zone, and that $\Omega_s(x')$ is constant over a distance $2\rho_w$, the integral needed in (16) is

$$\int_{x_0-e_0}^{x_0+e_0} dx \int_{A_C} dx' R_s(x,x')\,\Omega_s(x) = 2e_0 \frac{\Omega_s(x_0)}{1-\rho_w^2/4A_C} \equiv 2e_0 I_s(x_0) \tag{23}$$

where we have defined I_s in a parallel way to I_t; the dependence on x_0 comes through the dependence on the value of Ω_s near the candidate event.

3.3.3 Magnitude

The functional form for $R_m(M,M')$ is probably the least certain part of R_{FC}. Plots of the difference in foreshock and mainshock magnitudes with a uniform magnitude threshold for foreshocks and mainshocks (e.g., Jones, 1985) have shown a negative exponential distribution to the magnitude difference curve. However, to consider all possible foreshocks to a given mainshock, the completeness threshold for the foreshocks should be much lower than for the mainshocks. A bivariate plot of foreshock and mainshock magnitudes for all recorded foreshocks in southern California (Figure 3) suggests that for any given narrow range of mainshock magnitude, all foreshock magnitudes are equally likely.

If all foreshock magnitudes are equally likely, this implies that R_m is constant, and thus may be set equal to the normalizing factor N_m. The value of this quantity is given by the formula

$$\int_{M_D}^{\infty}\int_{M_D}^{M'} R_m(M,M')\,dM\,dM' = \alpha \int_{M_B}^{\infty} e^{-\beta' M'}\,dM' \tag{24}$$

Equation (24) says that if we look before all mainshocks with magnitudes greater than M_B, for foreshocks above a cutoff magnitude of M_D, we find that a fraction α of the mainshocks have foreshocks. Above, we have normalized R_t and R_s to be equal to one, so that R_m must contain the information about the likelihood of a foreshock preceding the mainshock.

Equation (24) also implies that the percentage of mainshocks preceded by foreshocks should increase monotonically as the magnitude threshold for foreshocks decreases. This is consistent with reported foreshock activity. The data suggest that foreshocks are relatively common before major strike-slip earthquakes. Jones and Molnar (1979) found that 30% of the $M \geq 7.0$ earthquakes occurring outside of subduction zones were preceded by foreshocks in the NEIC catalogue ($M \geq 4.5$–5.0) and almost 50% had foreshocks $M \geq 2$ reported in the written literature. Jones (1984) showed that half of the $M \geq 5.0$ strike-slip earthquakes in California were preceded by $M \geq 2.0$ foreshocks. (Foreshocks were less common on thrust faults).

For R_m constant, equation (24) implies that

$$N_m = \frac{\alpha\beta'}{1+\beta'(M_B - M_D)} \tag{25}$$

The data presented by Jones (1984), with M_B 5.0 and M_D 2.0, gave α equal to 0.5 for strike-slip events. Adopting this value, with a β' of 2.3, gives $N_m = 0.15$. A consequence of taking R_m constant is then that all earthquakes should have foreshocks within 6.5 units of magnitude of the mainshocks; clearly the form of R_m cannot be constant for all M, but for the problem at hand this does not present any difficulties.

The integral needed for equation (16) is then

$$\int_{M-\mu}^{M+\mu} dM \int_{M_C}^{M_C+\mu_C} dM' R_m(M, M') e^{-\beta' M'} = 2\mu N_m e^{-\beta' M_C} \frac{1 - e^{-\beta'\mu_C}}{\beta'}$$

$$\equiv 2\mu I_m(M_C, \mu_C) \tag{26}$$

where we have assumed μ small, and again separated it out from the rest of the expression.

3.4. Estimate of Mainshock Probability

We now can combine the integrals in equations (18), (23), and (26) into equation (16) to get the foreshock probability,

$$P(F) = 4\delta_0 \mu e_0 I_t I_s I_m$$

Solving the integral in equation (8) for the background event gives

$$P(B) = 4\delta_0 \mu e_0 \Lambda_s(x_0) e^{-\beta M}$$

We substitute these values of the background and foreshock probabilities into (6) to obtain:

$$P(C|F \cup B) = \frac{I_s I_t I_m + P(C)\Lambda_s(x_0)e^{-\beta M}}{I_s I_t I_m + \Lambda_s(x_0)e^{-\beta M}} \tag{27}$$

The candidate event errors δ_0, e_0, and μ have canceled out.

For making preliminary calculations, it is also useful to set I_t equal to one (solve for the probability in a fixed time interval), and (for the case of a linear fault) take I_s in (23) to be equal to $\Omega_s(x_0)$. If we take Ω_s to be constant, and combine (14) and (26), we find that the dependence on M_C and μ_c cancels out, and we are left with

$$P(C|F \cup B) = \frac{(N_m P(C)/A_C\delta_1) + P(C)\Lambda_s(x_0)e^{-\beta M}}{(N_m P(C)/A_C\delta_1) + \Lambda_s(x_0)e^{-\beta M}} \tag{28}$$

4. Application to the Southern San Andreas Fault

We have now an expression for the conditional probability of a characteristic earthquake, given the occurrence of a candidate event that is either a background event or a foreshock, applicable to any fault. We now further refine the procedure by applying it to the southern segment of the San Andreas fault. We can estimate the probability for any time period. We use a time period, δ_1, of 3 days to match the recent usage of the U. S. Geological Survey and the California's Governor's Office of Emergency Services in issuing earthquake advisories.

Because we do not have a long history of foreshocks to southern San Andreas mainshocks on which to base R_{FC}, we have, as discussed above, used the average properties of Californian foreshocks for R_{FC}. $P(C)$ and $P(B)$, however, can be specified for the southern San Andreas fault.

The long-term probability of a characteristic mainshock of 7.5 to 8.0 ($M_C = 7.5$, $\mu_c = 0.5$) on the southern San Andreas fault was estimated by Agnew *et al.* (1988) to be 0.4 over 30 years. With δ_1 equal to 3 days ($1.09 \cdot 10^5$ seconds), the 3-day probability, $P(C)$, is $1.09 \cdot 10^{-4}$. We assume β' equal to 2.3. This is equivalent to a b-value for the mainshocks of 1.0. This is used only to solve for N_m from α. We use a length, A_C, for the southern San Andreas fault of 222 km, from the Salton Sea to Cajon Pass.

The one remaining quantity to put into the equation (28) is the rate density for the background seismicity. This is determined from the earthquakes recorded between 1977 and 1987 by the Caltech/USGS Southern California Seismic Network (Given *et al.*, 1988). Background seismicity can be defined in many ways; it is important in this application that it be defined in the same way as the foreshocks will be. Because foreshocks can be up to 10 km from their mainshock (Figure 2), background seismicity up to 10 km from the surface trace of the San Andreas fault are included in the background rate.

It is well known that earthquakes exhibit short term temporal clustering such as aftershock sequences and earthquake swarms. If an earthquake of, say, $M = 6$ were to occur on the southern San Andreas fault with an aftershock sequence, we will evaluate the probability that the $M = 6$ earthquake is a foreshock; we will not individually determine the probability that the $M = 6$ and each of its aftershocks is a foreshock and then sum the probabilities. We therefore define the background seismicity to be from a declustered catalogue. In a declustered catalogue, sequences are recognized by some algorithm and replaced in the catalogue with one earthquake at the time of the largest event in the sequence with a magnitude equivalent to the summed moment of all the events in the sequence. We use the declustering algorithm of Reasenberg (1985).

The rate of background seismicity is not constant along the length of the southern San Andreas fault. This section of the fault includes the most seismically active part of the whole fault north of Banning and one of the quietest sections in the Coachella Valley (Figure 4). To account for this variation, we have divided the southern segment into 4 subsegments based on the rate of background seismicity—San Bernardino, San Gorgonio, Indio and Mecca Hills. San Bernardino is the moderately active section from Cajon Pass to the intersection with the Crafton Hills fault where normal faulting predominates (Jones, 1988). San Gorgonio is the most active section of the fault and runs from the Crafton Hills fault to the eastern end of the 1986 North Palm Springs aftershock zone (Jones *et al.*, 1986). All types of earthquake faulting occur within this region, with reverse faulting quite common (Jones, 1988). At the eastern end of the 1986 aftershock zone, the rate of seismicity drops significantly, almost all of the background activity jumps to the east of the surface trace of the fault and the type of faulting changes to mixed strike-slip and normal faulting (Jones, 1988). This region is the Indio subsegment which extends south to the city of Indio. At this point, the rate of seismicity again drops significantly, so that the largest earthquake recorded between Indio and the Salton Sea in the last 55 years was $M = 3.6$. This subsegment, Mecca Hills, extends south to the end of the San Andreas fault and the intersection of the Brawley Seismic Zone.

The rates of background seismicity within each of these regions has been determined from the earthquakes recorded between 1977 and 1987. The lengths of the segments and the parameters of the backgorund seismicity are given in Table 1.

TABLE 1. Parameters for the Microseismic Regions of the Southern San Andreas Fault

Segment	A(km)	a	b	β	Λ_s(events/km-s)
San Bernardino	65	4.32	1.00	2.30	$2.13 \cdot 10^{-6}$
San Gorgonio	70	4.62	0.97	2.23	$3.83 \cdot 10^{-6}$
Indio	40	3.78	0.95	2.18	$9.48 \cdot 10^{-7}$
Mecca Hills	47	3.64	0.95	2.18	$5.85 \cdot 10^{-7}$

We now have the data to use equation (28) to solve for the conditional probability of a characteristic earthquake given the location and magnitude of a candidate foreshock. In practice, alert levels will be defined to correspond to certain probabilities and the magnitudes of earthquakes needed to trigger those alert levels are the desired quantities. For the southern San Adreas fault, we have used alert levels A, B, and C corresponding to probabilities of 10%, 1%, and 0.1%. Using equation (28) to find the magnitudes corresponding to these alarm levels, we obtain:

TABLE 2. Magnitudes of Potential Foreshocks for the Southern San Andreas Fault

Segment	Probability		Level
	≥10.0%	1.0%–10.0%	0.1%–1.0%
San Bernardino	5.9	4.9	3.8
San Gorgonio	6.4	5.3	4.2
Indio	5.9	4.8	3.7
Mecca Hills	5.7	4.6	3.4

The false alarm rate along any section is given by $[1 - P(C)|F \cup B)]P(B)$, and the total false alarm rate by the sum of this over all segments. If we express this in terms of expected return period, we find that we expect a probability 0.1 alert every 63 years, a 0.01 alert every 5 years, and a 0.001 alert every 5 months (note that this last is only 5 times the background probability).

5. Discussion and Conclusions

The derivation of this conditional probability is not specific to foreshocks and could also be used for any potential earthquake precursor. Equation (6) makes clear the data that are needed to assess the probability. These are (1) the long term probability of the mainshock, (2) the rate at which the precursor precedes mainshocks (is it seen before all earthquakes, 50%, 10%?), and (3) the rate at which that phenomena is recorded without being followed by earthquakes (background). At present, these data are not available for any precursor but foreshocks. For instance, the background rate of creep events can be determined for some sections of the San Andreas fault system but how often they precede large earthquakes is not known.

This derivation is very general and for foreshocks could be expanded to include factors well beyond those used in the application to the southern San Andreas fault. Several of these factors have been mentioned in the above analysis; for instance, we have not used in the final application a dependence on time, information about the most likely epicenters for the mainshock (such as fault jogs or terminations) or number of aftershocks to the candidate foreshock. In addition, however, the same scheme could be used to integrate over other variables than the four used here. For instance, evidence suggests that most foreshocks have focal mechanisms similar to that of their mainshock (Jones and Lindh, 1987). If that relationship were parameterized, integration could be performed over variables expressing the difference in focal mechanisms so that normal or reverse faulting earthquakes would be given a lower probability of being a foreshock to a San Andreas mainshock. If any characteristics are recognized as being more common in foreshocks than other earthquakes, this formulation allows that information to be included in our assessment of the conditional probabilities.

References

Agnew, D. C., C. R. Allen, L. S. Cluff, J. H. Dieterich, W. L. Ellsworth, R. L. Keeney, A. G. Lindh, S. P. Nishenko, D. P. Schwartz, K. E. Sieh, W. Thatcher, and R. L. Wesson, 1988, Probabilities of large earthquakes occurring in California on the San Andreas fault, *U.S. Geol. Surv. Open-file Rep. 88–398*, 62 pp.

Bakun, W. H., G. C. P. King, and R. S. Cockerham, 1986, Seismic slip, aseismic slip, and the mechanics of repeating earthquakes on the Calaveras fault, California, in *Earthquake Source Mechanics*, S. Das and C. Scholz, editors, Geophysical Monograph 37, American Geophysical Union, Washington D. C., 195–207.

Given, D. D., L. K. Hutton, L. Stach and L. M. Jones, 1988, The Southern California Network Bulletin, January - June, 1987, *U.S. Geol. Surv. Open-file Rep. 88-408.*

Goltz, J., 1985, The Parkfield and San Diego earthquake predicitons: a chronology. Special Report by the Southern California Earthquake Preparedness Project, Los Angeles, CA, 23pp..

Jones, L. M., 1984, Foreshocks (1966–1980) in the San Andreas System, California, *Bull. Seismol. Soc. Amer.*, **74**, 1361–1380.

Jones, L. M., 1985, Foreshocks and time-dependent earthquake hazard assessment in southern California, *Bull. Seismol. Soc. Amer.*, **75**, 1669–1680.

Jones, L. M., 1988, Focal mechanisms and the state of stress on the San Andreas fault in southern California, *J. Geophys. Res.*, **93**, 8869–8891.

Jones, L. M., and P. Molnar, 1979, Some characteristics of foreshocks and their possible relationship to earthquake prediction and premonitory slip on faults, *J. Geophys. Res.*, **84**, 3596–3608.

Jones, L. M., L. K. Hutton, D. D. Given, C. R. Allen, 1986, The North Palm Springs, California, earthquake sequence of July 1986 *Bull. Seismol. Soc. Amer.*, **76**, 1830-1837.

Jones, L. M., and A. G. Lindh, 1987, Foreshocks and time-dependent conditional probabilities of damaging earthquakes on major faults in California, *Seismol. Res. Letters*, **58**, p. 21.

Mendoza, C., and S. H. Hartzell, 1988, Inversion for slip distribution using teleseismic P waveforms: North Palm Springs, Borah Peak and Michoacan earthquakes, *Bull. Seismol. Soc. Amer.*, **78**, 1092–1111.

King, G. C. P., and J. Nábělek, 1985, Role of fault bends in the initiation and termination of rupture, *Science*, **228**, 984–987.

Nishenko, S. P., and R. Buland, 1987, A generic recurrence interval distribution for earthquake forecasting, *Bull. Seismol. Soc. Amer.*, **77**, 1382–1399.

Oppenheimer, D. H., W. H. Bakun, and A. G. Lindh, 1989, On the site of future moderate earthquakes on the southern Calaveras fault, California, *Bull. Seismol. Soc. Amer.*, in press.

Reasenberg, P., 1985, Second-Order Moment of Central California Seismicity, 1969–1982, *J. Geophys. Res.* **90** 5479–5496.

Reasenberg, P. A., and L. M. Jones, 1989, Earthquake hazard after a mainshock in California, *Science*, **243**, 1173–1176.

Sieh, K. E., 1978, Central Californian foreshocks of the great 1857 earthquake, *Bull. Seismol. Soc. Amer.*, **68**, 1731–1749.

Wesnousky S. G., C. H. Scholz, K. Shimazaki and T. Matsuda, 1983, Earthquake frequency distribution and faulting mechanics, *J. Geophys. Res.*, **88**, 9331–9340.

Figure Captions

Figure 1. The number of foreshock-mainshock pairs recorded in southern California versus the time between foreshock and mainshock in hours for foreshocks $M \geq 2.0$ and mainshocks $M \geq 3.0$ recorded between 1932 and 1987.

Figure 2. Distance between foreshock and mainshock epicenters versus the (a) magnitude of the mainshock and (b) magnitude of the foreshock for foreshock-mainshock sequences (foreshocks $M \geq 2.5$ and mainshocks $M \geq 3.0$) recorded in the Caltech catalog between 1977 and 1987. Sequences that have been relocated in special studies are also plotted and include 1966 Parkfield, 1968 Borrego Mountain, 1970 Lytle Creek, 1972 Bear Valley, 1975 Haicheng ($M = 7.3$), 1975 Galway Lakes ($M = 5.2$), 1979 Homestead, 1980 Livermore, 1981 Westmoreland, 1985 Kettleman Hills, 1986 Chalfant Valley, and 1987 Superstition Hills.

Figure 3. The number of foreshock-mainshock pairs in half unit of magnitude bins for the magnitudes of foreshock and mainshock. Data included all $M \geq 2.0$ foreshocks and $M \geq 3.0$ mainshocks recorded between 1932 and 1987 in southern California.

Figure 4. A map of $M \geq 2.0$ earthquakes located within 10 km of the Coachella Valley segment of the southern San Andreas fault recorded in the Caltech catalog between 1977 and 1987.

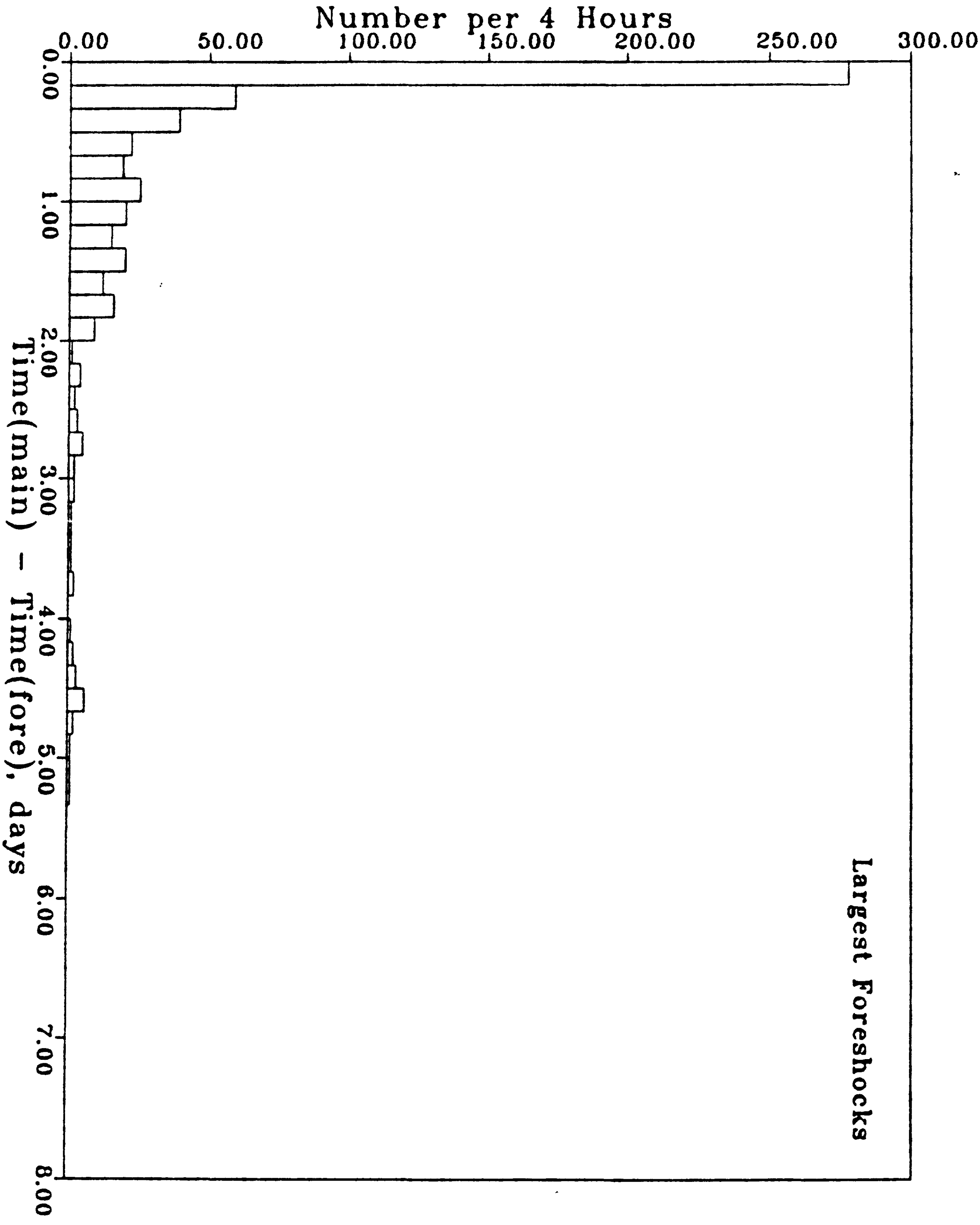
Number per 4 Hours
0.00
50.00
100.00
150.00
200.00
250.00
300.00
Time(main) - Time(fore), days
1.00
2.00
3.00
4.00
5.00
6.00
7.00
8.00
Largest Foreshocks

Figure 1

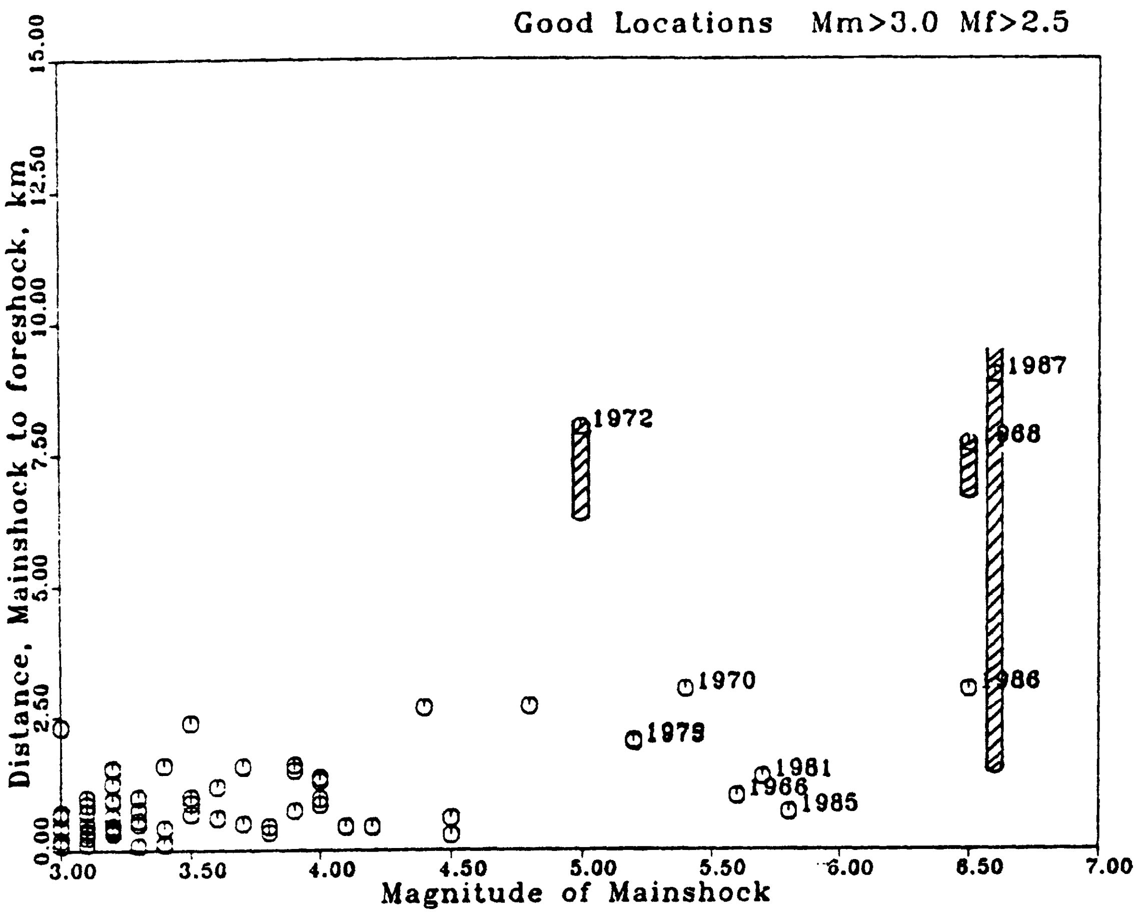
Good Locations Mm>3.0 Mf>2.5
Distance, Mainshock to foreshock, km
0.00
2.50
5.00
7.50
10.00
12.50
15.00
3.00
3.50
4.00
4.50
5.00
5.50
6.00
6.50
7.00
Magnitude of Mainshock
1987
1972
1968
1970
1986
1979
1981
1966
1985

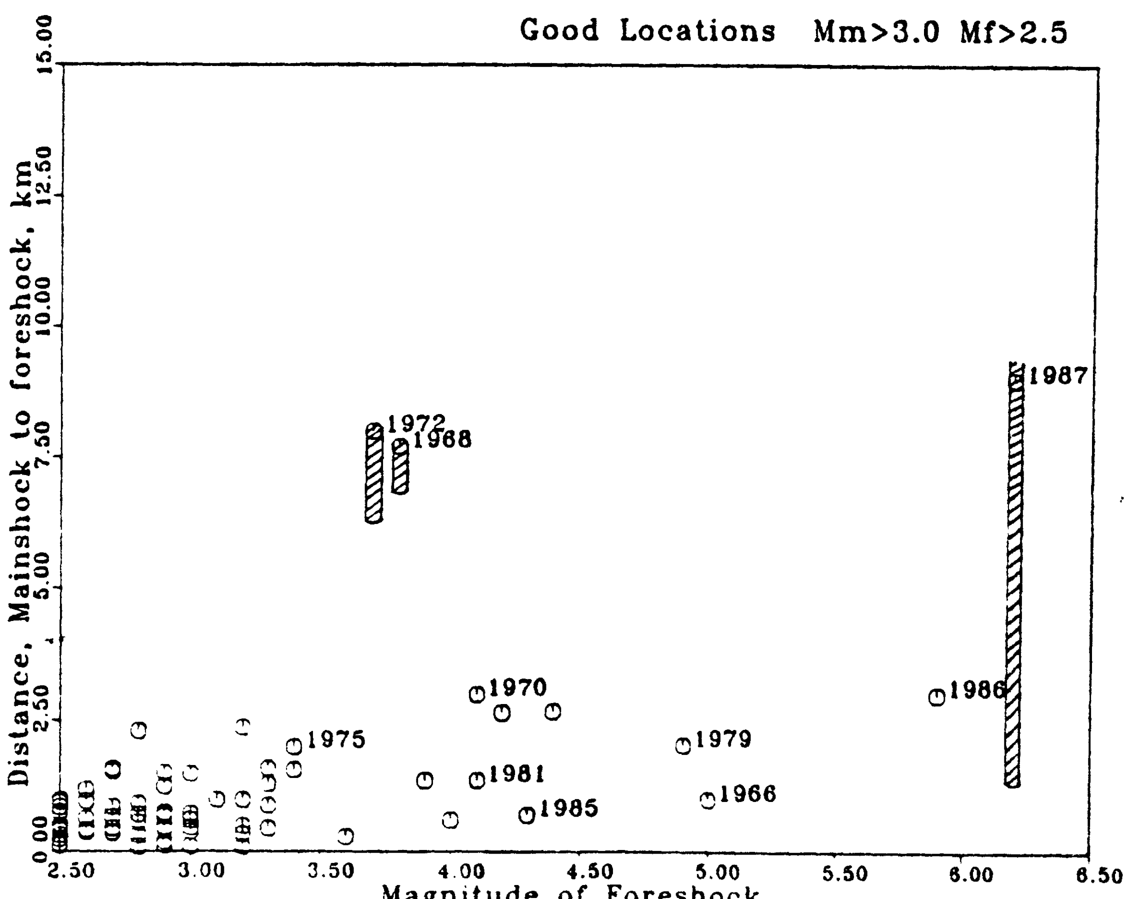
Good Locations Mm>3.0 Mf>2.5
Distance, Mainshock to foreshock, km
0.00
2.50
5.00
7.50
10.00
12.50
15.00
2.50
3.00
3.50
4.00
4.50
5.00
5.50
6.00
6.50
Magnitude of Foreshock
1987
1972
1968
1970
1986
1975
1979
1981
1966
1985

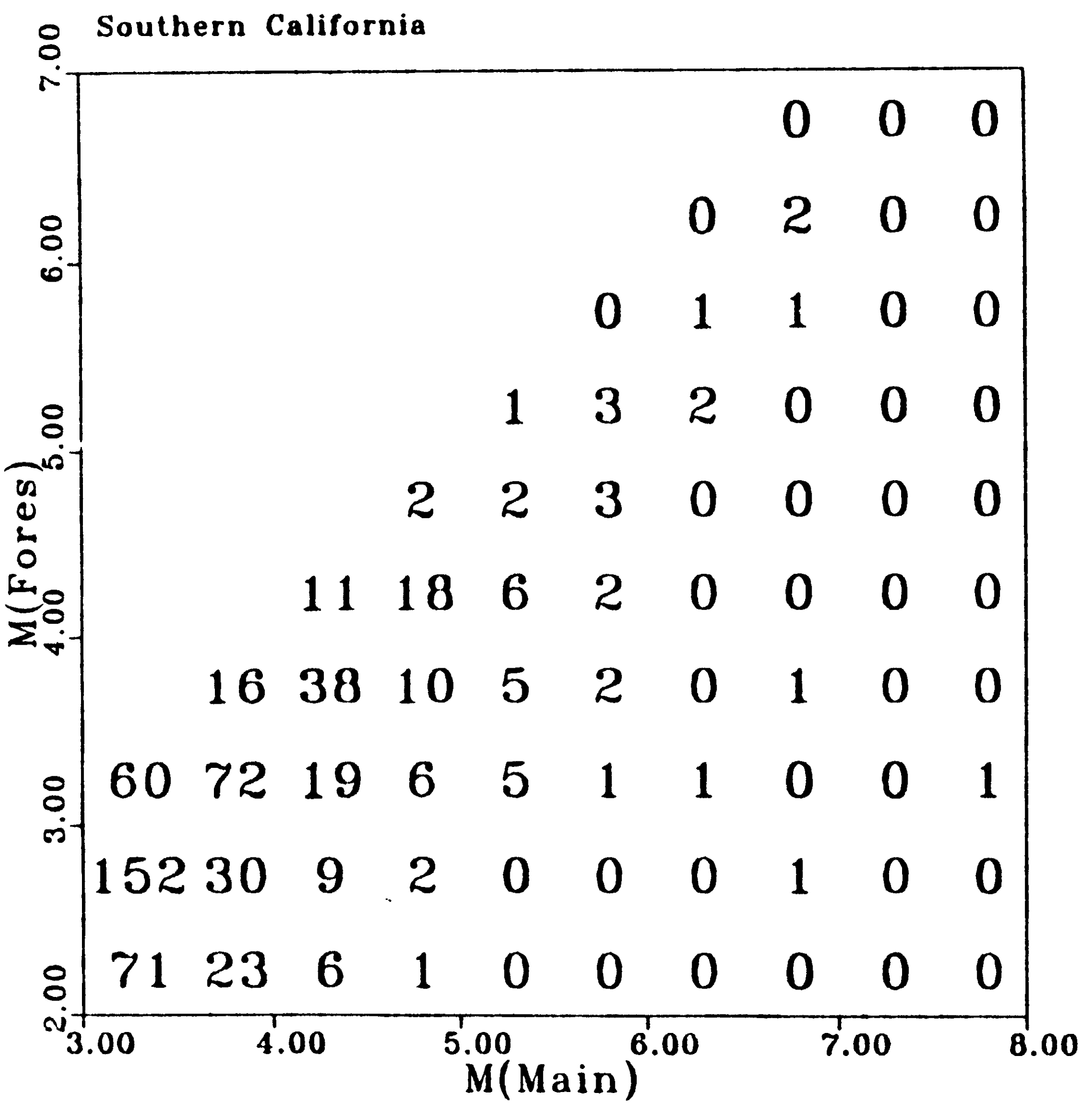
Southern California
M(Fores)
M(Main)
7.00
6.00
5.00
4.00
3.00
2.00
3.00 4.00 5.00 6.00 7.00 8.00
0 0 0
0 2 0 0
0 1 1 0 0
1 3 2 0 0 0
2 2 3 0 0 0 0
11 18 6 2 0 0 0 0
16 38 10 5 2 0 1 0 0
60 72 19 6 5 1 1 0 0 1
152 30 9 2 0 0 0 1 0 0
71 23 6 1 0 0 0 0 0 0

Figure 3

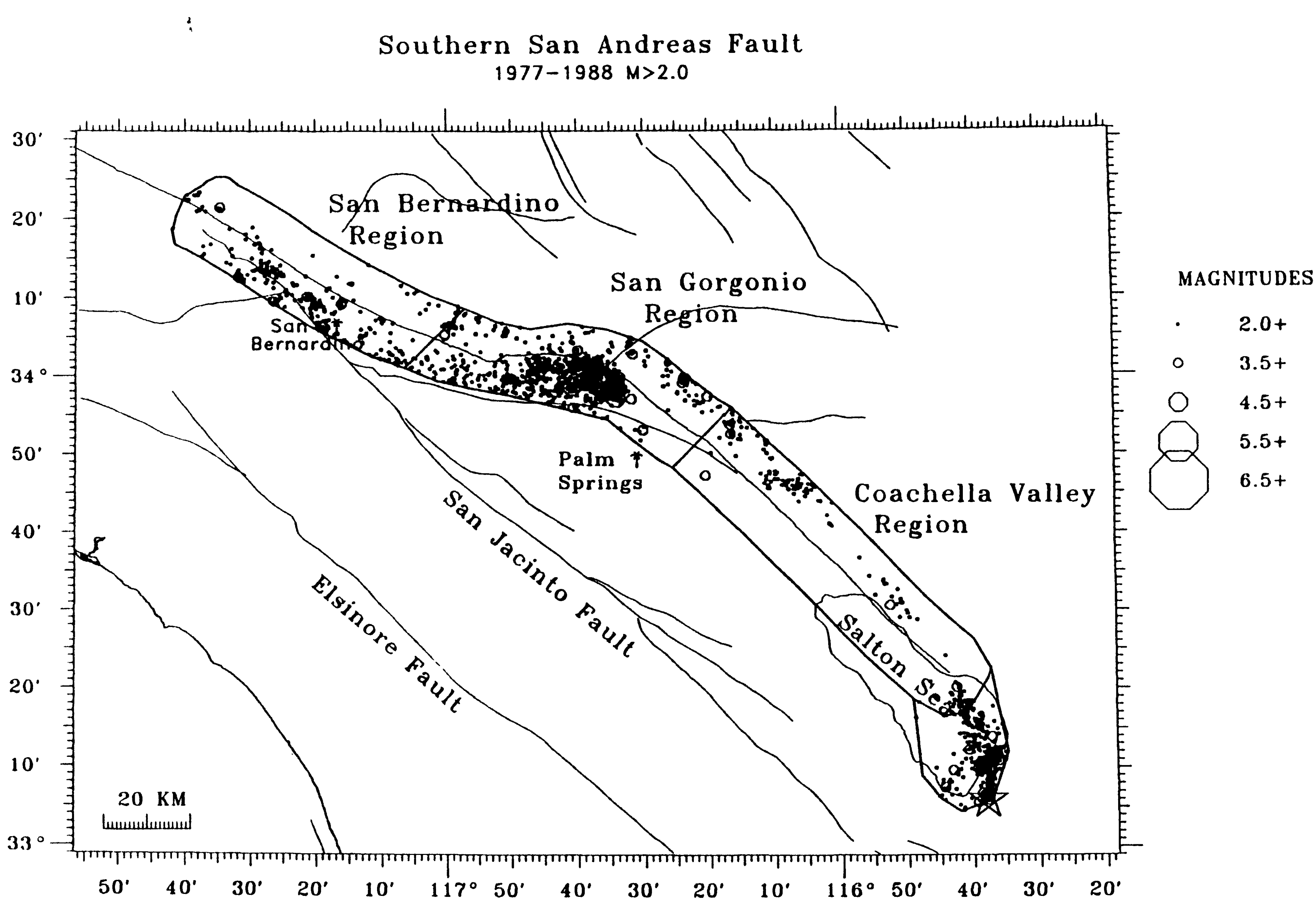
Southern San Andreas Fault
1977–1988 M>2.0
San Bernardino Region
San Gorgonio Region
Coachella Valley Region
San Bernardino
Palm Springs
San Jacinto Fault
Elsinore Fault
Salton Sea
20 KM
MAGNITUDES
2.0+
3.5+
4.5+
5.5+
6.5+
30'
20'
10'
34°
50'
40'
30'
20'
10'
33°
50'
40'
30'
20'
10'
117°
50'
40'
30'
20'
10'
116°
50'
40'
30'
20'

Figure 4

Appendix I

Handout provided by L.Jones summarizing activity on the San Jacinto fault zone for December 1989 to January 3, 1990.

Earthquake Activity along the San Jacinto Fault, December 1989 - January 8, 1990

Lucile Jones, U.S. Geological Survey, Pasadena, CA
Egill Hauksson, Caltech, Pasadena
Kate Hutton, Caltech, Pasadena

4:30 pm, January 3, 1990

Disclaimer: This is a preliminary report for informational use only, and should not be construed as an earthquake prediction, warning or advisory.

Introduction

From 2 December 1989 to 3 January 1990 two earthquakes of $M > 4$ (M4.2 and M4.3) and six earthquakes of $3 < M < 4$ have been recorded along the San Jacinto fault (Figure 1). This level of activity is relatively high even for the very active San Jacinto fault.

This increase in earthquake activity is of some concern because the San Jacinto fault has an average geological slip rate of 11 mm/yr (Agnew et al., 1988), which is about one third of the slip rate of the southern San Andreas Fault. The San Jacinto fault has also had several large earthquakes of M=6–7 during the last century (1899 July, 1899 December, 1918, 1923, 1942, 1954, 1968, and 1987). Furthermore, the San Jacinto fault has a 50 km long seismic gap (called the Anza segment) which has a 30% probability (with a level of reliability rating of D) of having a large earthquake in the next 30 years or before 2018 (Agnew et al. (1988). Two other segments, the San Bernardino Valley and San Jacinto Valley segments located to the north, have 20% and 10% probability, respectively, of having large earthquakes (M7) in the next 30 years (Agnew et al., 1988).

Earthquakes December 1989 – January 1990

The current episode of activity consists of five sequences so far. The first sequence started on December 2 with a M4.3 earthquake near the northern end of the Anza segment (Figure 2). The mainshock that showed right-lateral strike-slip movement was preceded by a M2.8 foreshock and followed by several aftershocks. The second sequence occurred on December 6 and consisted of a M3.4 thrust faulting mainshock followed by several aftershocks. The third sequence occurred on December 22 and was located 3 km to the southeast of the first sequence of December 2 or near the north end of the Anza segment. The fourth sequence was a foreshock-mainshock-aftershock sequence that occurred on December 27–28, 7 miles north-northwest of the city of San Bernardino. These events are associated with a north striking normal fault, located between the

San Jacinto and San Andreas faults. The fifth sequence occurred on December 31 and included a M2.9 foreshock preceding a normal faulting M3.2 mainshock and followed by several aftershocks. This sequence is located in the middle of the Anza segment, between the San Jacinto and Buck Ridge faults. One event of M3.5 and several smaller events that occurred on January 2nd were located close to the epicenter of the December 2nd mainshock.

Our impression is that these sequences represent an unusual but not unprecedented level of activity. Because these sequences do not show a simple unilateral migration of activity along the fault, it is difficult to interpret them as being caused by a "strain event" migrating at depth along the fault. They have occurred within three distinct segments of the San Jacinto fault, the San Bernardino Valley segment, the San Jacinto Valley segment and the Anza segment. Thus these sequences do not point out one of these segments as being more active than the other.

Earthquakes 1984–1990

The San Jacinto fault has caused more large earthquakes during this century than any other fault in southern California (Agnew et al. 1988). It has also shown a very high level of background seismicity since the advent of modern seismic networks. The seismicity from 1984–1990 January 3rd is shown in Figure 3. The fault trace coincides with the epicentral distribution indicating that the fault is almost vertical or has a steep dip. The depth cross section along the fault shows a significant change in the maximum depth of earthquakes along the fault (Figure 3). In addition within the San Jacinto Valley segment, which has been assigned the low probability of 10% of a large earthquake occurring within the next 30 years, there is almost no activity located in the depth range of 0–13 km but a high level is observed in the depth range of 13–18 km. This unusual depth distribution of background seismicity is similar to the distribution of seismicity recorded along the San Andreas fault in the southern Santa Cruz Mountains, where the M7.1 1989 Loma Prieata earthquake occurred.

In Figure 4 the time distance distribution of the seismicity along the San Jacinto fault is shown. The most noticable sequence within this plot is the November 1987 Superstion Hill sequence. The star symbols represent earthquakes of magnitude 4 or larger. Excluding the 1989 events there has been only one other $M > 4$ event north of the Anza Gap since 1983. The most noticeable aspect of the recent activity is the increase at the southern end of the San Jacinto Valley segment.

References

Agnew, D. C., C. R. Allen, L. S. Cluff, J. H. Dieterich, W. L. Ellsworth, R. L. Keeney, A. G. Lindh, S. P. Nishenko, D. P. Schwartz, K. E. Sieh, W. Thatcher, and R. L. Wesson, 1988, Probabilities of large earthquakes occurring in California on the San Andreas fault, *U.S. Geol. Surv. Open-file Rep. 88-398*, 62 pp.

EVENTS $M_L \geq 3.0$, San Jacinto Fault

Date(GMT)			Time	Latitude	Longitude	Depth	Mag	Focal Mechanism		
1989	12	01	14:30	33° 38.39	116° 45.18	12.78	2.8	160°	30°	50°
1989	12	02	23:16	33° 38.10	116° 44.98	13.69	4.2	135°	55°	20°
1989	12	06	19:15	33° 48.45	117° 2.31	14.27	3.4	245°	45°	90°
1989	12	22	3:03	33° 37.38	116° 42.03	11.25	3.4	140°	50°	20°
1989	12	27	22:10	34° 11.30	117° 23.26	11.14	3.2	310°	70°	-50°
1989	12	28	9:41	34° 11.54	117° 23.22	11.13	4.3	70°	40°	-150°
1989	12	28	10:00	34° 11.16	117° 23.19	10.43	3.3	155°	70°	20°
1989	12	30	10:17	33° 29.98	116° 27.72	10.45	2.9	110°	80°	20°
1989	12	31	12:55	33° 28.95	116° 27.45	11.28	3.1	235°	55°	-110°
1990	01	02	9:52	33° 38.71	116° 46.60	12.74	3.5	220°	80°	171°

San Jacinto Fault

December 1, 1989 – January 3, 1990

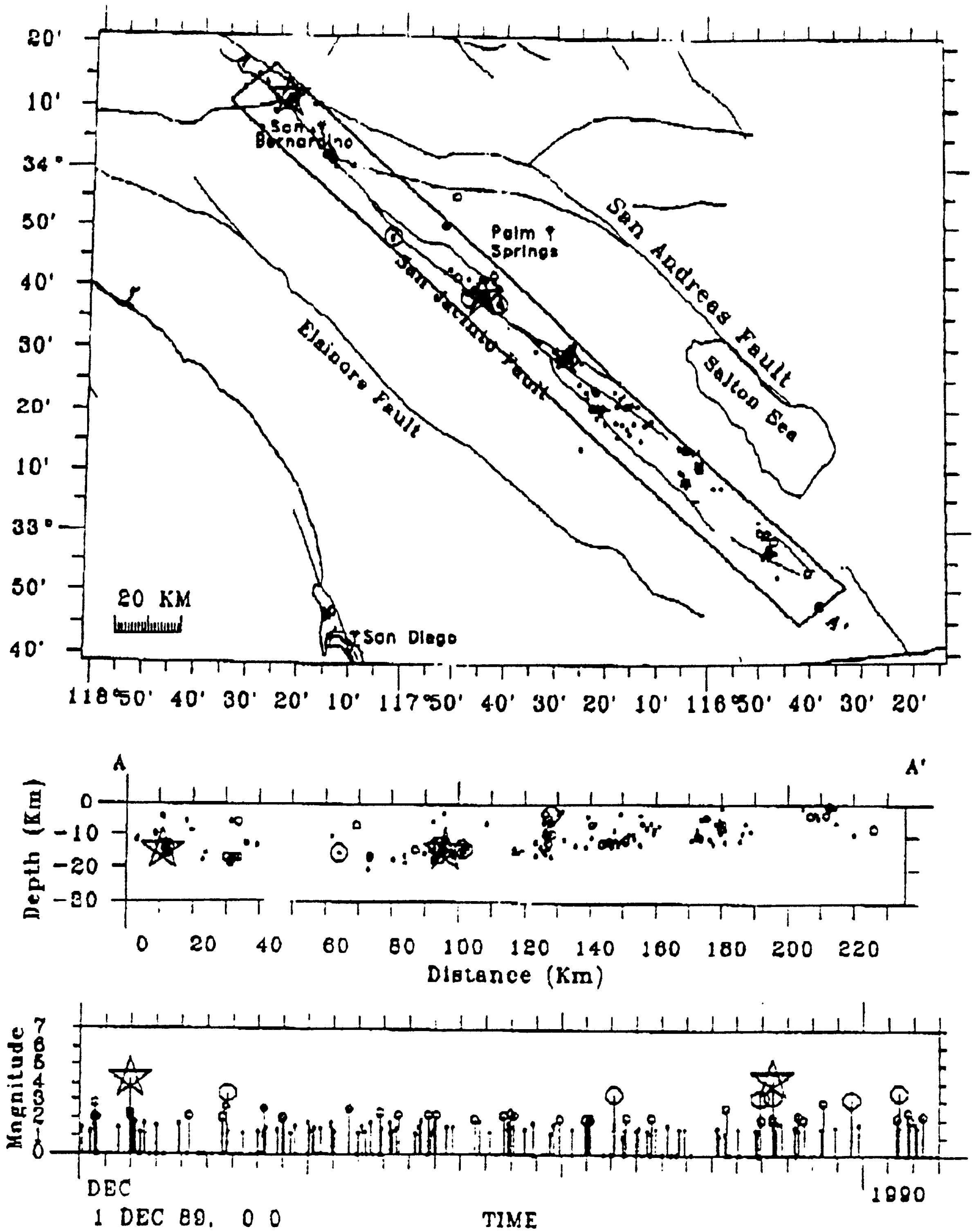

San Jacinto Fault 12/1/89–1/3/90 M>2.8

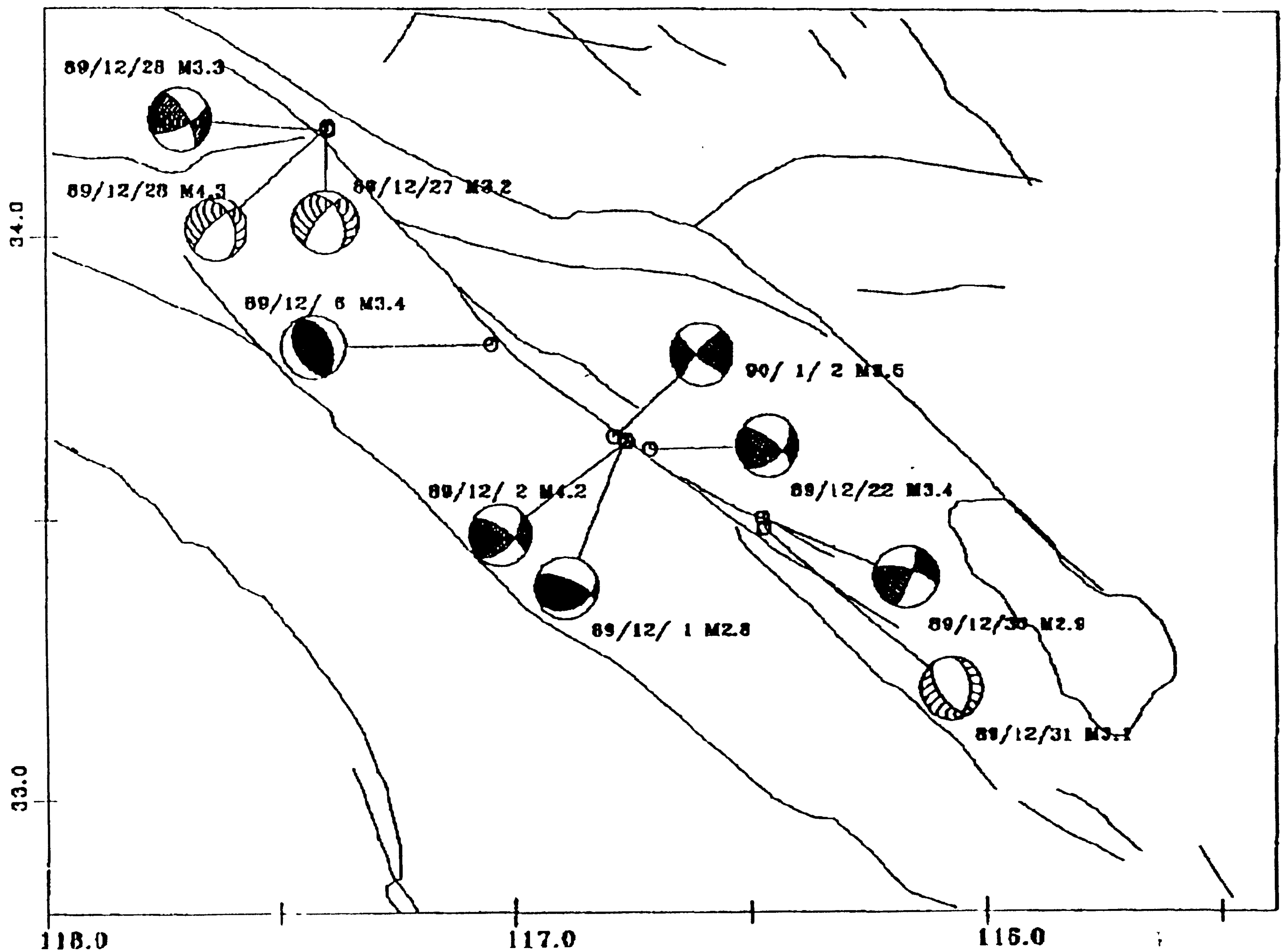

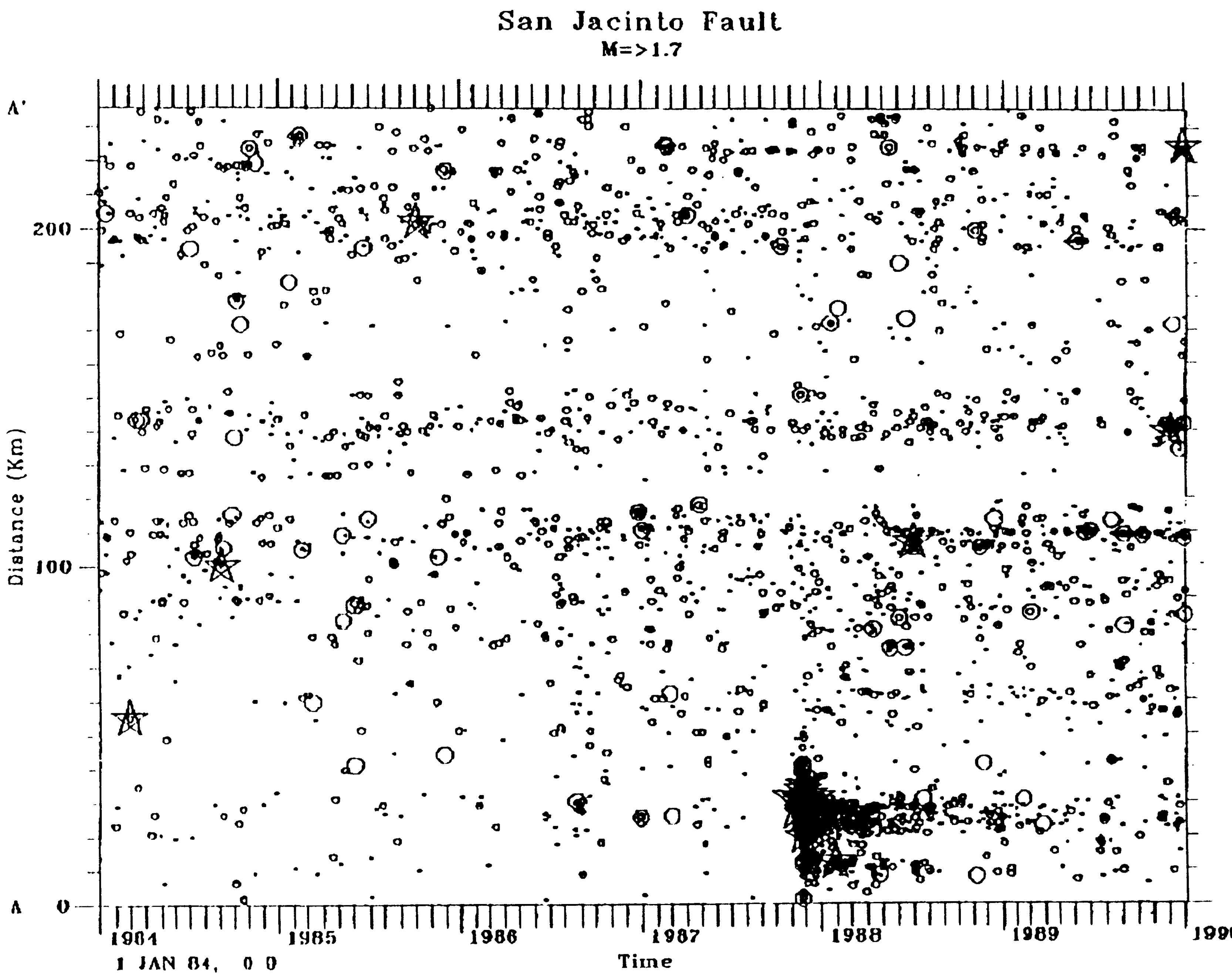

San Jacinto Fault
M=>1.7
A'
200
100
0
A
Distance (Km)
1984
1985
1986
1987
1988
1989
1990
1 JAN 84, 0 0
Time

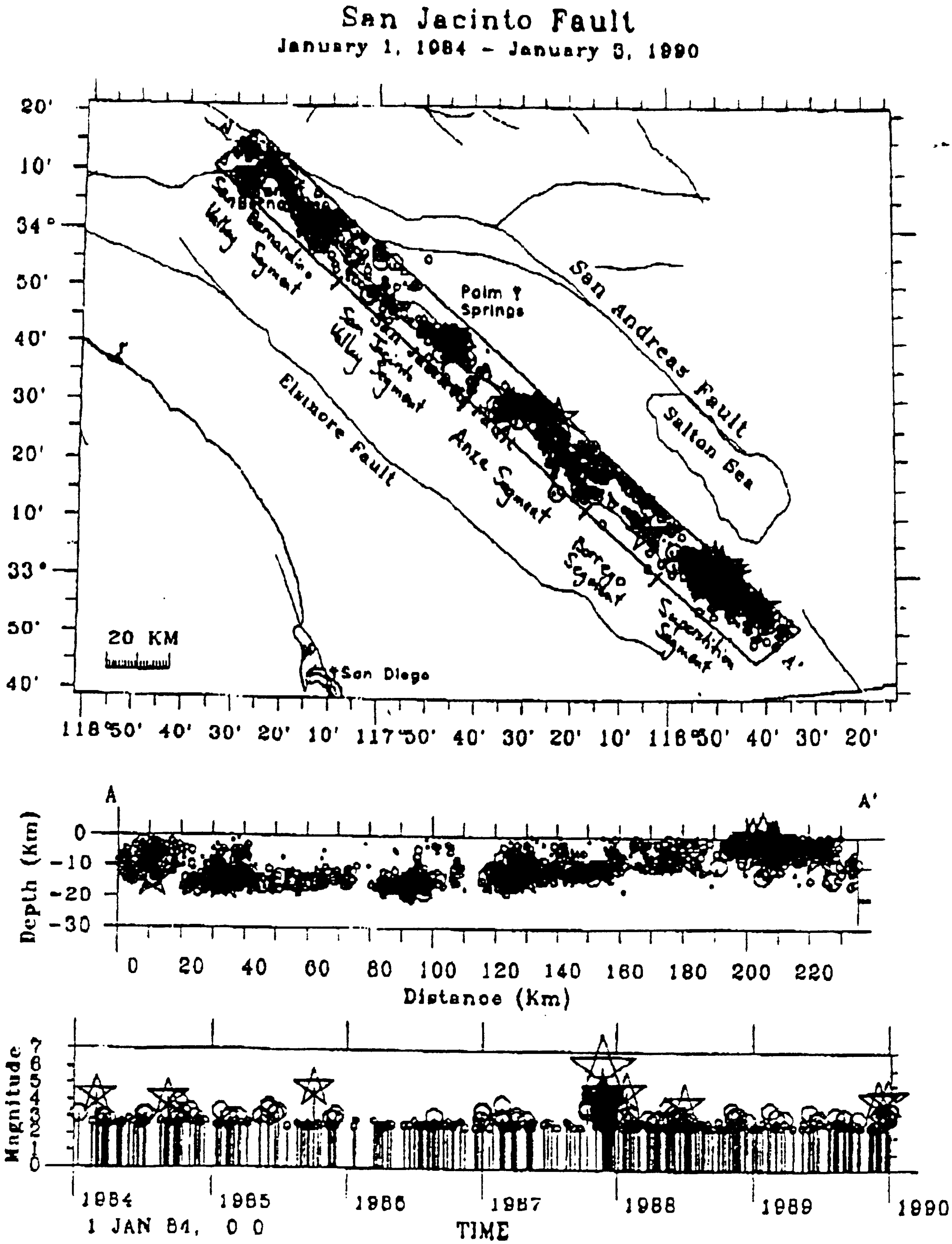
San Jacinto Fault
January 1, 1984 - January 3, 1990
San Andreas Fault
Palm Springs
Salton Sea
Elsinore Fault
San Diego
20 KM
Anza Segment
Depth (Km)
Distance (Km)
Magnitude
TIME
1 JAN 84, 0 0

Appendix J

Handouts provided by D.Hill to accompany presentation to NEPEC, January 12, 1990.

LONG VALLEY MONITORING REPORT
JULY, AUGUST, SEPTEMBER, 1989

MAMMOTH MOUNTAIN SWARM

Seismicity

The swarm of small earthquakes that began under Mammoth Mountain on May 4 (see the April-June report) has continued through September (Figures S1-S3), although the rate of activity began to slow somewhat in mid August (Figure S5). The swarm has included two more $M = 3$ events; one on July 12 (11:15 PDT) and the other on August 1 (02:17 PDT). A third $M = 3$ event occurred 3 km southeast of the swarm volume in the Mammoth Lakes basin (Figure S3) on September 21 (11:09 PDT). The cumulative seismic moment of all swarm earthquakes from early May through the end of September approaches 3×10^{22} dyne-cm, or the equivalent of one $M = 4$ earthquake. We continue to record spasmodic bursts (rapid-fire bursts of earthquakes with over-lapping coda) through September, although their occurrence rate also began to decline in mid-August.

Figure S7 shows the distribution of swarm earthquakes in map view and cross section for the period May through August. The initial swarm activity began on May 4 at depths between 5 and 6 km beneath the southwest flank of the mountain at the junction in the dense, Y-shaped cluster of epicenters (Figure S7a). Five days later it deepened to define the slab-like body at depths between 6 to 9 km (Figure S7b,c). Activity continued within this initial, limited volume through the rest of May. In early June it began expanding at a fairly uniform rate both northward and to shallower depths such that by the end of August, the entire volume illustrated in Figure S7 had become active with $M \geq 0.5$ events. During this interval, minimum depths of $M \geq 0.5$ events became progressively shallower at a rate of roughly 2 km per month with the mean depth following at about 1 km per month. This shallowing tendency for $M \geq 0.5$ events culminating in the flurry of $M < 2.5$ events on August 29 at depths less than 3 km beneath the southwest flank of the mountain. Smaller events had been occurring at these shallow depths since at least mid June, however, as revealed by numerous $M < 0.5$ earthquakes with S-P times less than 0.5 sec recorded on the MMP station just south of the mountain. Although these events were too small for multi-station locations, their short S-P times require that they be located somewhere within the upper 3 km of the crust beneath the southwest flank of the mountain.

Fault plane solutions determined for all swarm earthquakes that occurred during the period May 11 through September 16 with at least 15 P-wave first-motion observations show a mix of normal and strike-slip mechanisms with T-axes dominantly oriented in a northwest-southeast direction (Figure S7d). The T-axes for events occurring within the dense, Y-shaped seismicity distribution tend to be perpendicular to the arms and tail of the Y. Note in particular that the T-axes tend to be perpendicular to the deep dike-like structure that forms the tail of the Y.

The caldera itself has remained relatively quiet through the duration of this Mammoth Mountain swarm. The only noteworthy activity from June through September involved a flurry of small ($M < 1.5$) earthquakes along the eastern margin of the resurgent dome on July 6-8 and a $M = 2.6$ event in the south moat at 11:15 AM (PDT) on August 11 (Figures S1 and S2).

Deformation

Borehole dilatometer at Devils Postpile (POPA) has shown a steady extensional trend from July through mid-September after which it begins to flatten. The total extensional change during this period amounts to just over one microstrain (Figure D2-3). The only other time the dilatometer has shown sustained extensional strain was for the two months following the July 21, 1986, Chalfant Valley earthquake (Figure D2). Although we cannot uniquely determine whether the current extensional trend is related to the Mammoth Mountain swarm, it is consistent with results from the newly established two-color geodimeter network spanning the southeast flank Mammoth Mountain from an instrument site

INFORMAL COMMUNICATION
NOT TO BE CITED FOR PUBLICATION

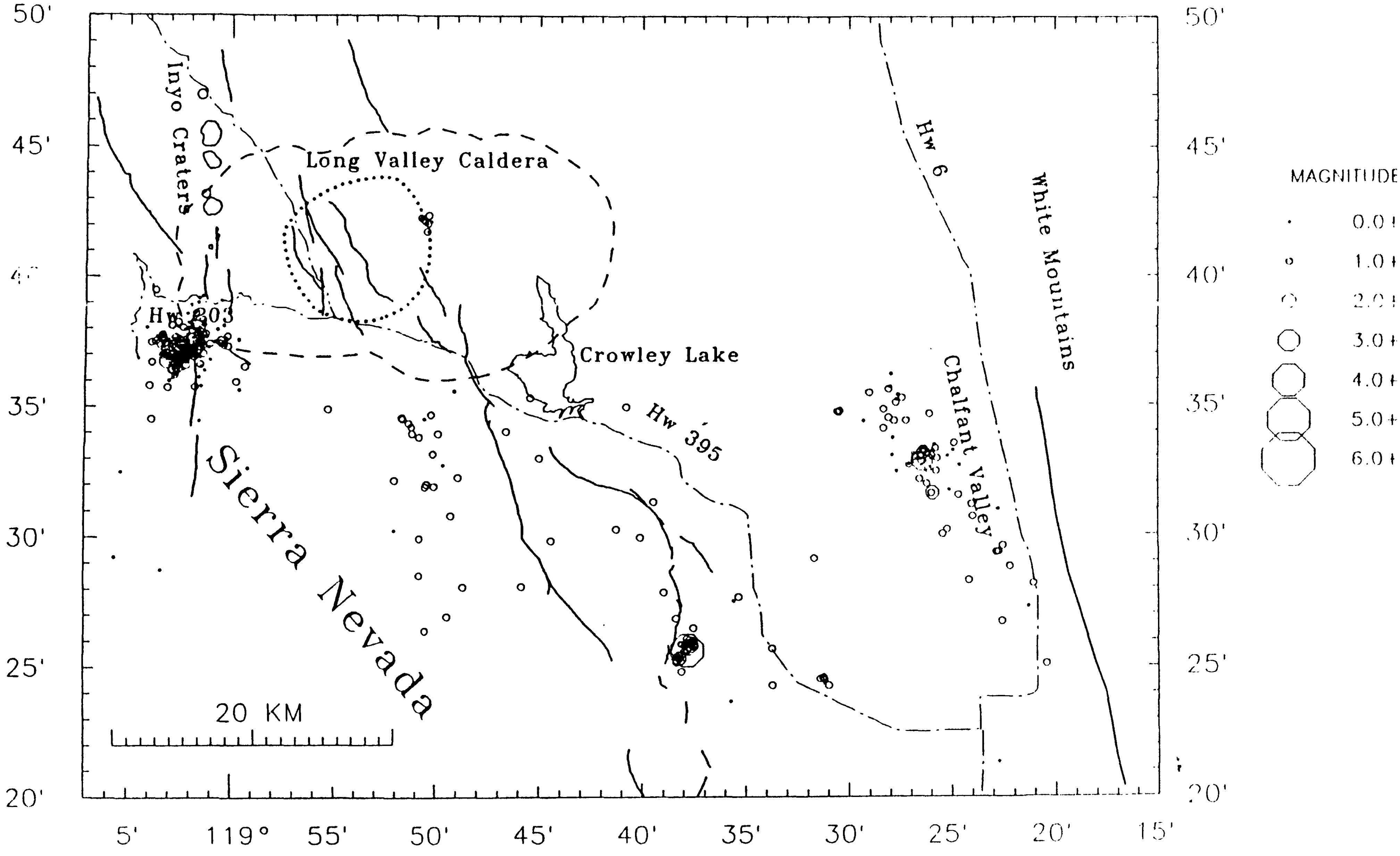

Figure S1: Earthquake epicenters in the Long Valley region for July 1989

INFORMAL COMMUNICATION
NOT TO BE CITED FOR PUBLICATION

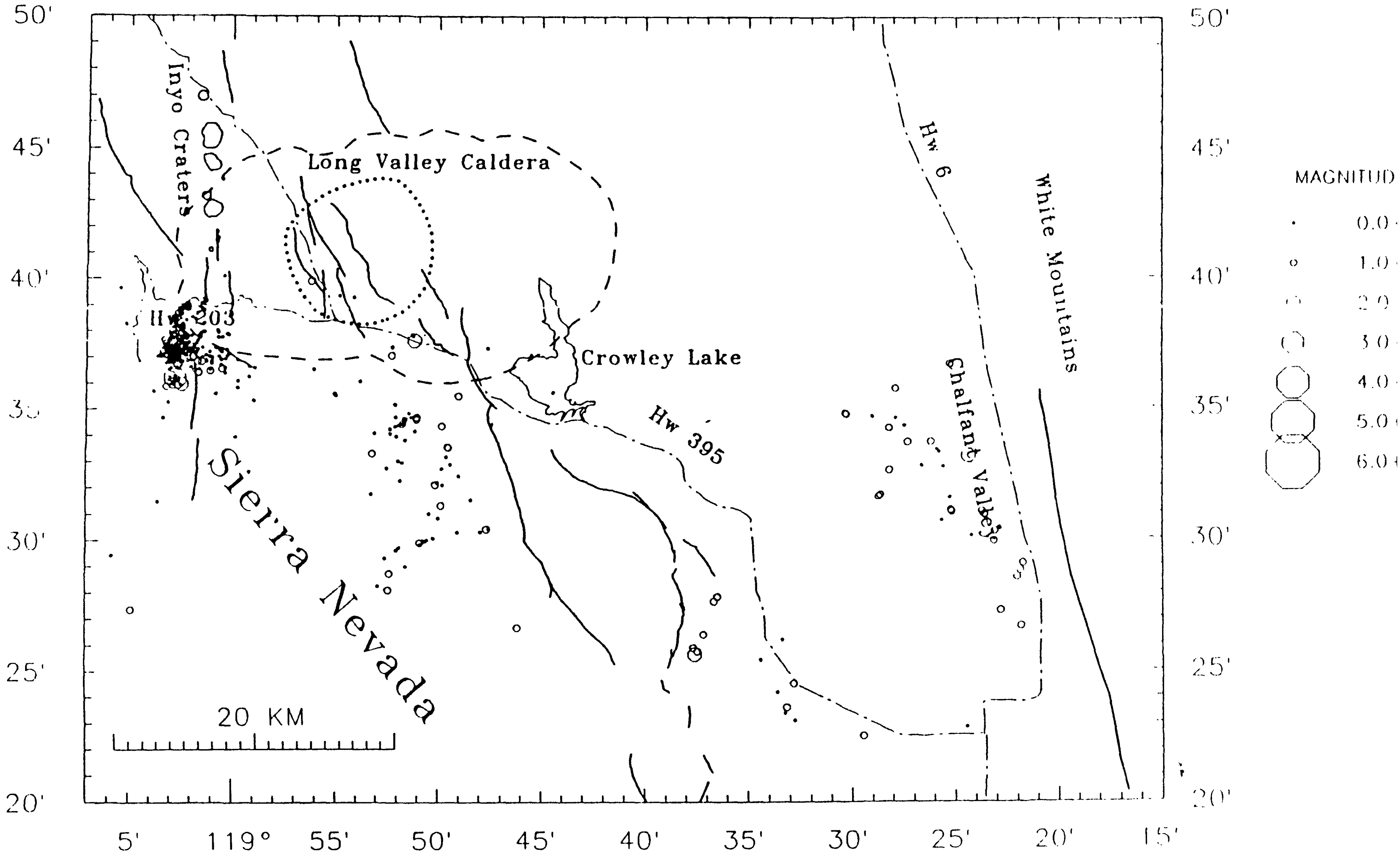

Figure S2: Earthquake epicenters in the Long Valley region for August 1989

INFORMAL COMMUNICATION
NOT TO BE CITED FOR PUBLICATION

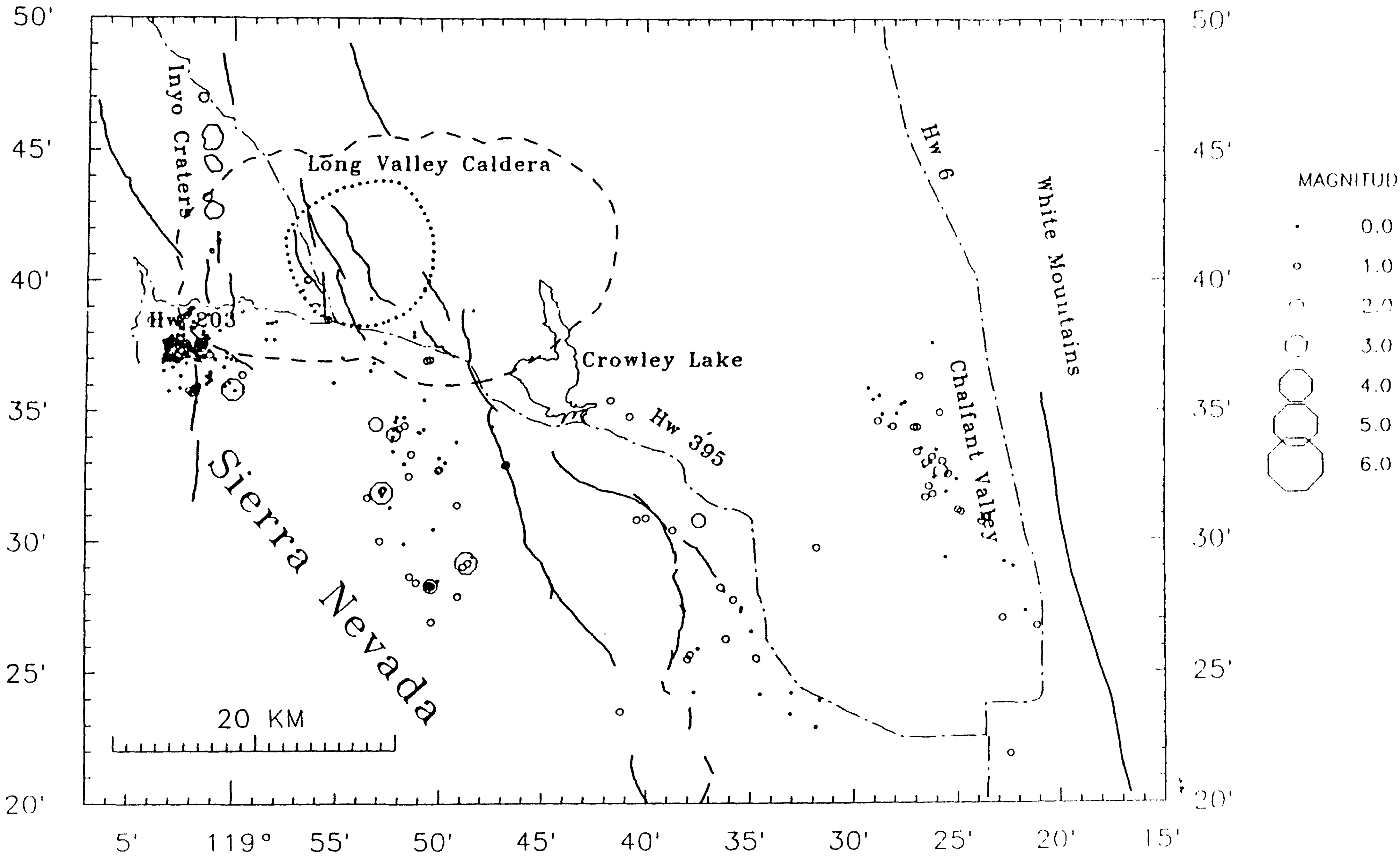

Figure S3: Earthquake epicenters in the Long Valley region for September 1989

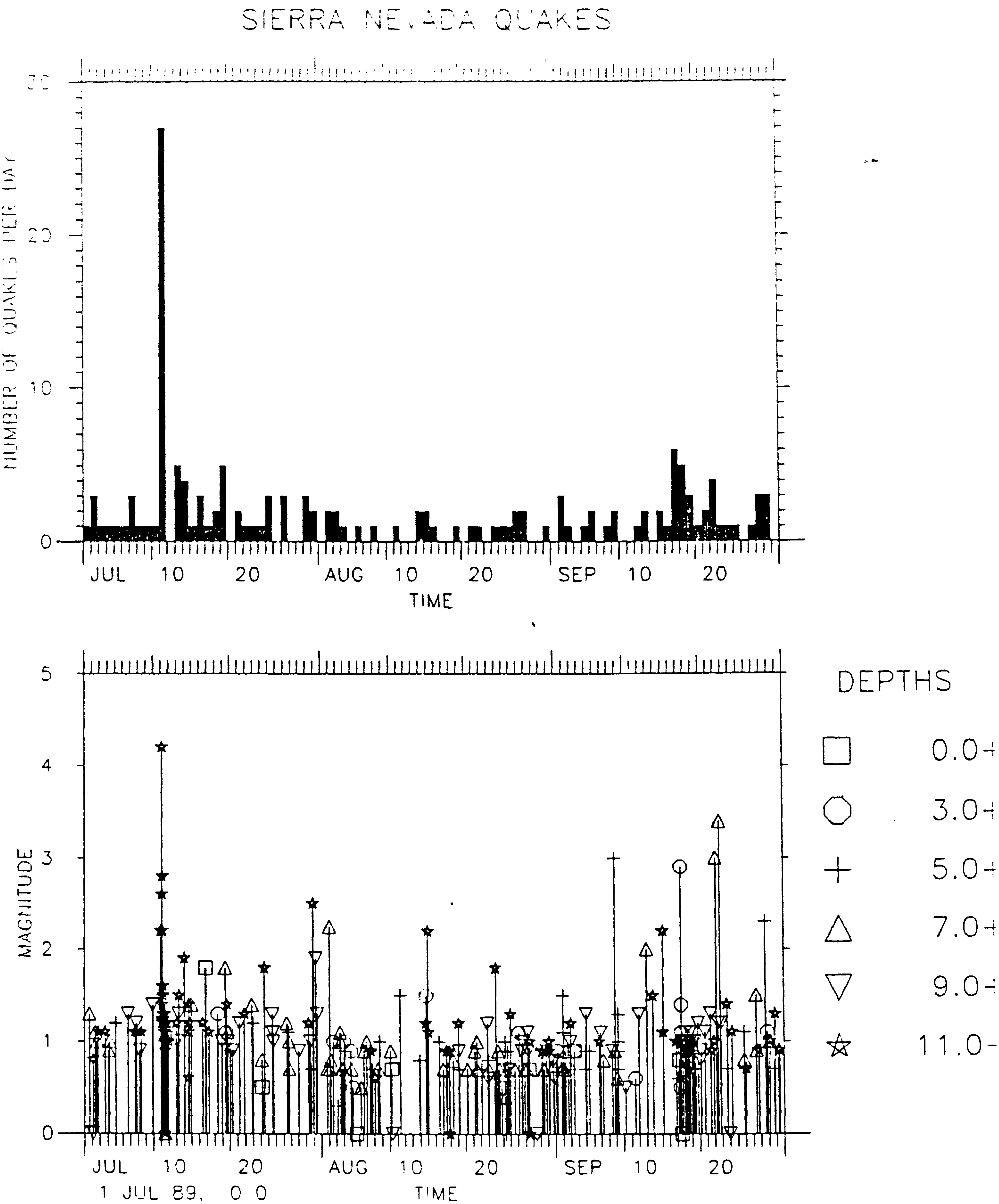

Figure S4: Temporal occurrence of earthquakes in geographic subregions of the area shown on figures S1, S2, and S3. Top: number of ≥ ·1 events per day. Bottom: event magnitudes proportional to line length with ·cal depth indicated by symbol at top of line.

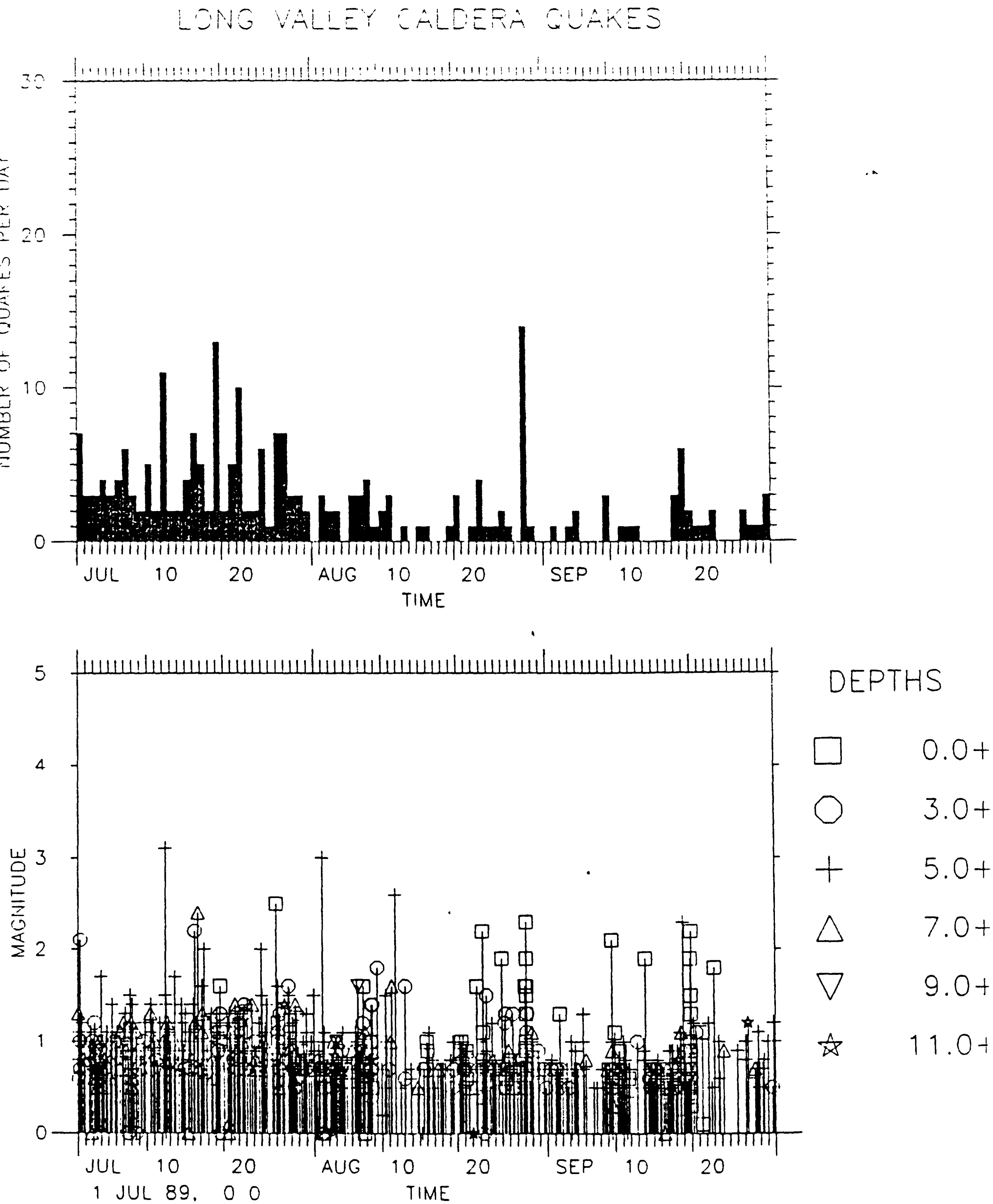

Figure S5: Temporal occurrence of earthquakes in geographic subregions of the area shown on figures S1, S2, and S3. Top: number of >M1 events per day. Bottom: event magnitudes proportional to line length with focal depth indicated by symbol at top of line.

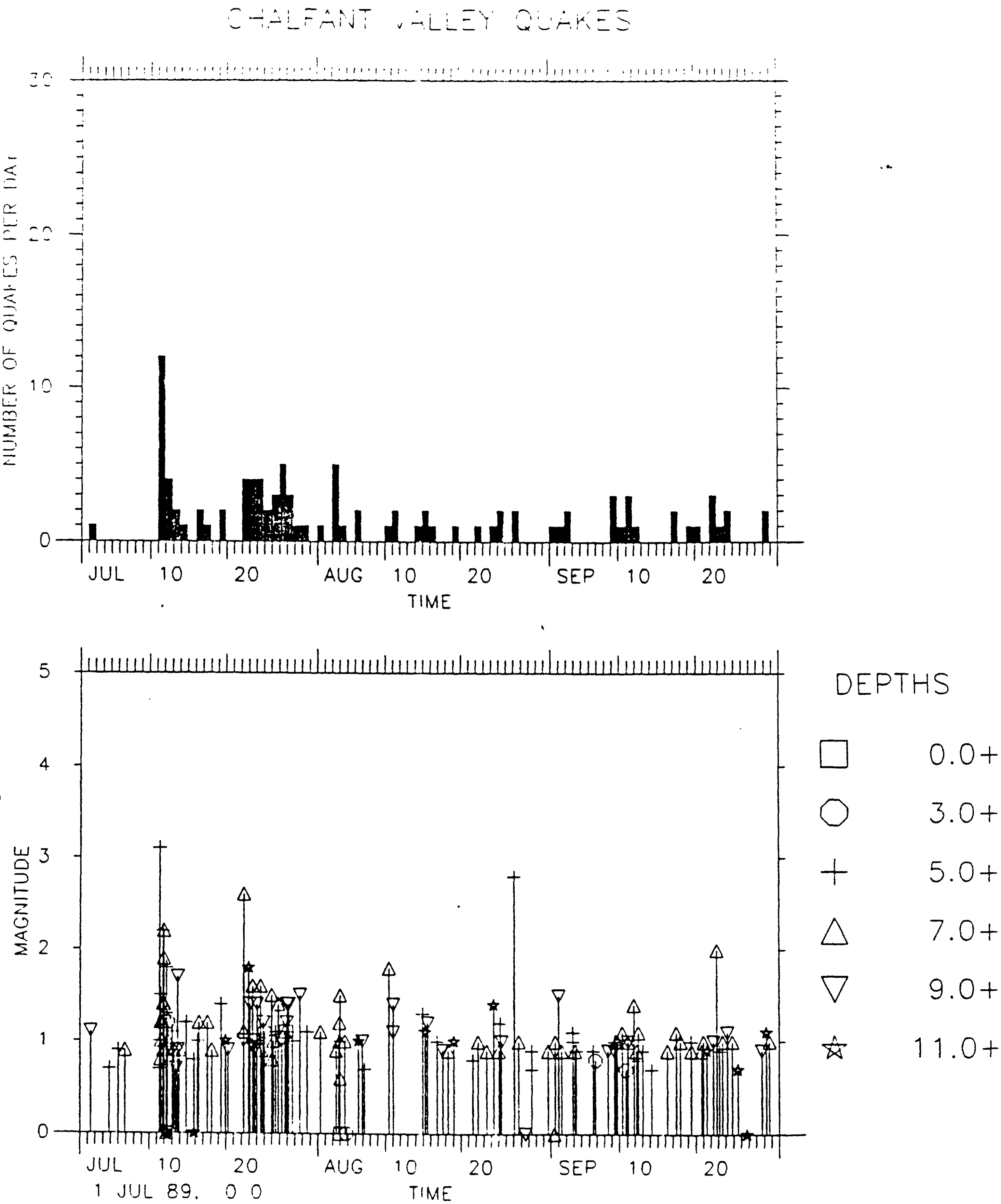

INFORMAL COMMUNICATION
NOT TO BE CITED FOR PUBLICATION

Figure S6: Temporal occurrence of earthquakes in geographic subregions of the area shown on figures S1, S2, and S3. Top: number of >M1 events per day. Bottom: event magnitudes proportional to line length with focal depth indicated by symbol at top of line.

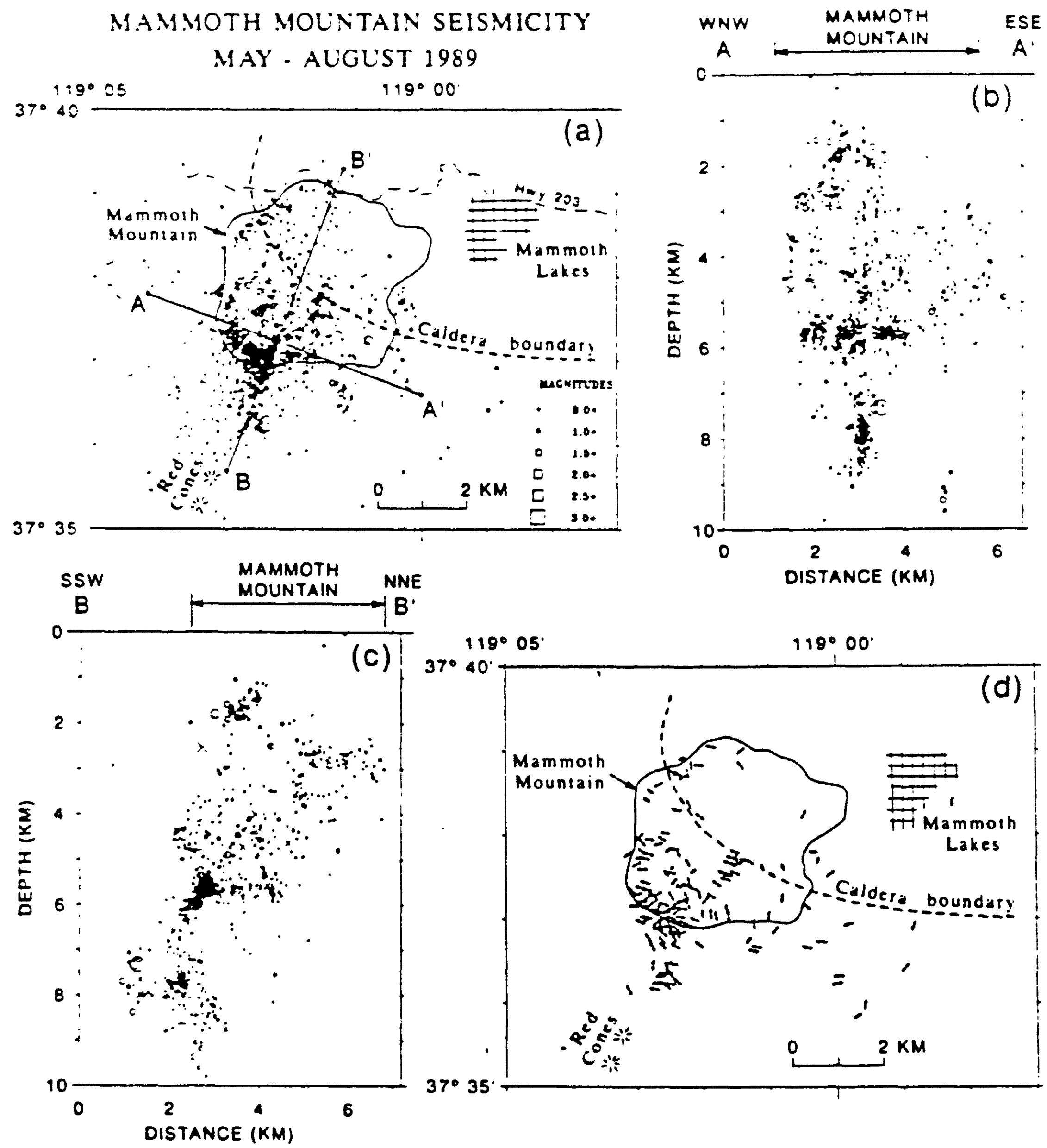

FIGURE S7. Seismicity map and cross sections for the Mammoth Mountain earthquake swarm from May through August, 1989: a) epicenter map; +, events in May and June; x, events in July; o, events in August; b) depth section with hypocenters in (a) projected onto the A-A' plane; c) depth section with hypocenters in (a) projected onto the B-B' plane; d) T-axis orientations of 303 focal mechanisms determined for well-recorded swarm earthquakes.

INFORMAL COMMUNICATION
NOT TO BE CITED FOR PUBLICATION

INFORMAL COMMUNICATION
NOT TO BE CITED FOR PUBLICATION

LONG VALLEY NETWORK

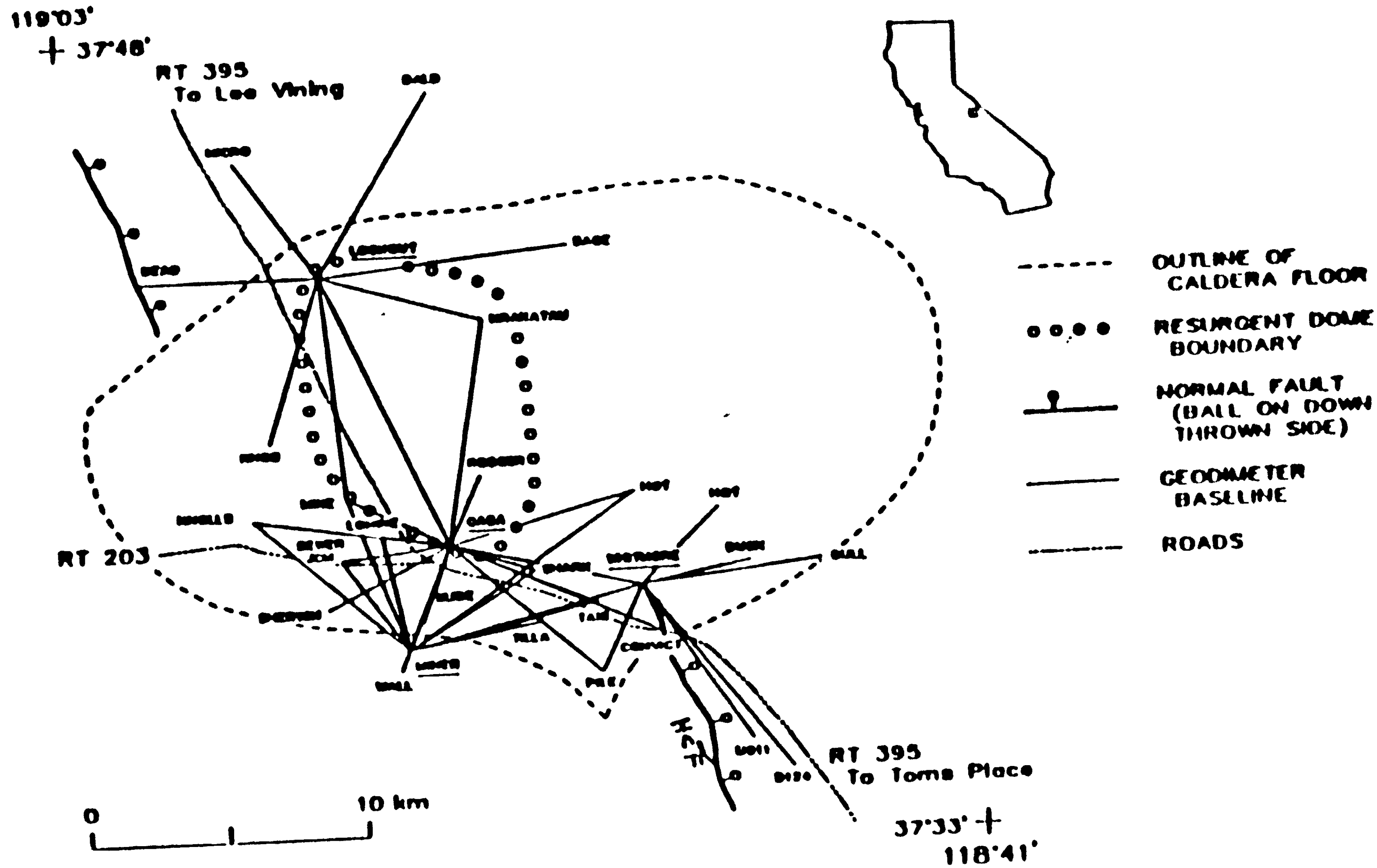

FIGURE TC1. Map showing two-color geodimeter lines.

INFORMAL COMMUNICATION
NOT TO BE CITED FOR PUBLICATION

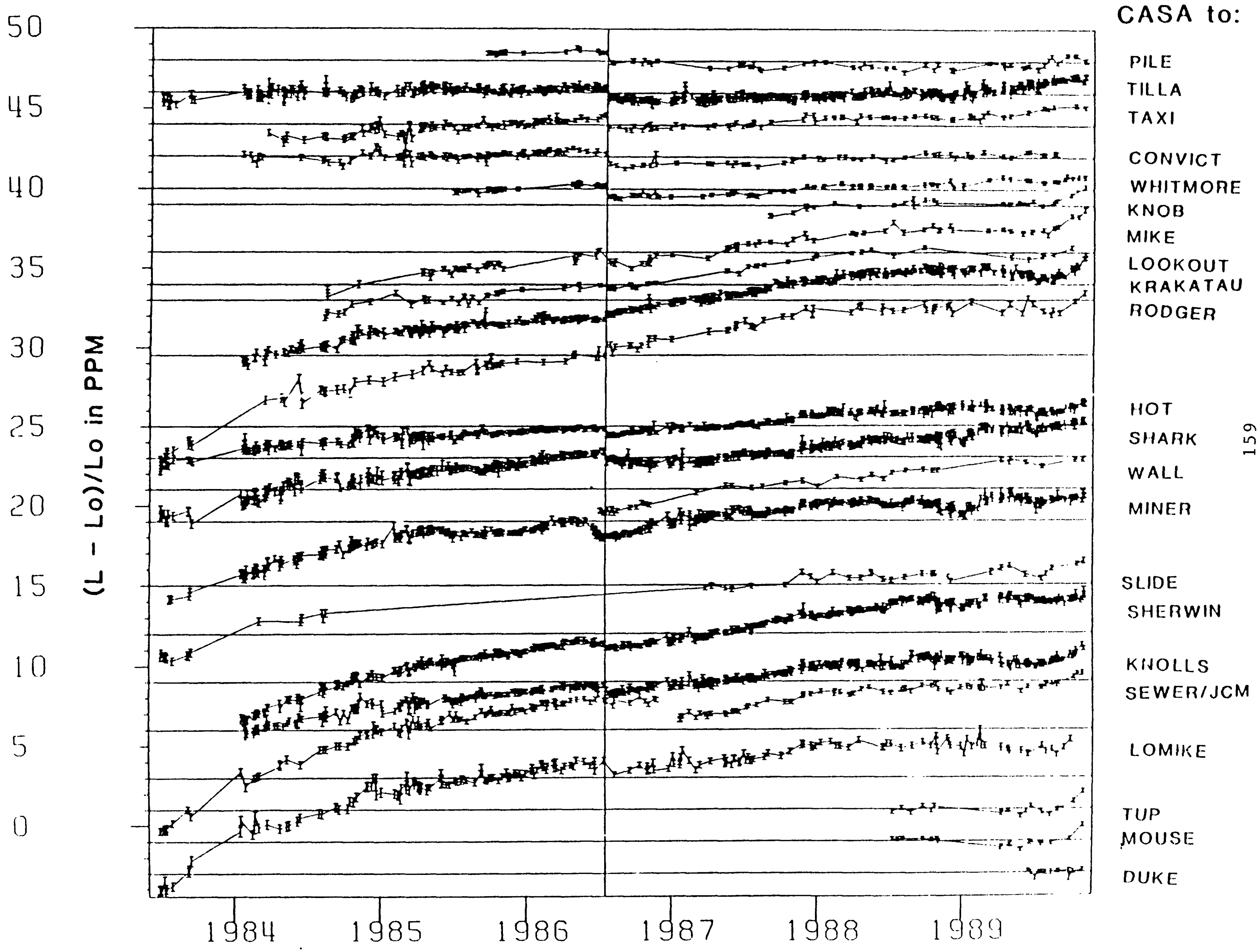

Geodolite Survey

J. C. Savage and W.K. Gross

The Geodolite network (Figure G1) was resurveyed in September, 1989. The measured line length L (less a constant nominal length L_0) is plotted as a function of time in Figures G2, G3, and G4 for each of the forty lines observed. The times of the Round Valley (Nov. 23, 1984) and Chalfant (July 31, 1986) earthquakes are shown in those figures by arrows. In general, deformation is not correlated with the earthquakes. The rate of deformation appears to be decreasing uniformly with time.

A principal component analysis of the Geodolite data indicates that the deformation can be represented by a single mode. That is, the length of the i^{th} line at t_j, the time of the j^{th} survey, can be approximated by

$$L_{ij} = a_i \, C(t_j) + L_{io}$$

where a_i and L_{io} are constants for each line and C(t) is shown in Figure G5. This fit to the data is shown by the continuous line in Figures G2, G3, and G4. Only seven measurements deviate from the fit by more than two standard deviations: the 1985 measurement of Bald-Crowley, the 1985 measurement of Banner-Glass, the 1986 and 1989 measurements of Casa-Laurel, the 1985 measurement of Convict-Crowley, the 1985 measurement of Laurel-Sherwin, and the 1984 measurement of Lookout-Val. One would expect 10 residuals greater than two standard deviations among the 280 observations. Thus, the fit of the single principal mode to the data is considered satisfactory.

The displacement pattern for the 1st principal mode is shown in Figure G6. The ovals at the ends of the arrows indicate the 95% confidence ellipses. The solution shown gives the minimum displacement vectors. The pattern is predominantly a radial displacement outward from the center of the resurgent dome (i.e., a point about halfway between Casa and Lookout). The displacements accumulated since the 1983 survey can be calculated by multiplying the value of C(t) read from Figure G5 for the appropriate time and the displacement vector scaled from Figure G6.

Notice that the time function C(t) (Figure G5) is closely approximated by an exponential decay with a relaxation time of 3.27 years. Although we have maintained in the past that the post-1983 data may be fit by a linear trend, the new data make it seem more likely that the source (magma injection at depth?) is dying out.

Notice that the lines into Mammoth measured in 1989 do not appear anomalous. Thus, no effect of the unusual seismic activity there since last May was detected.

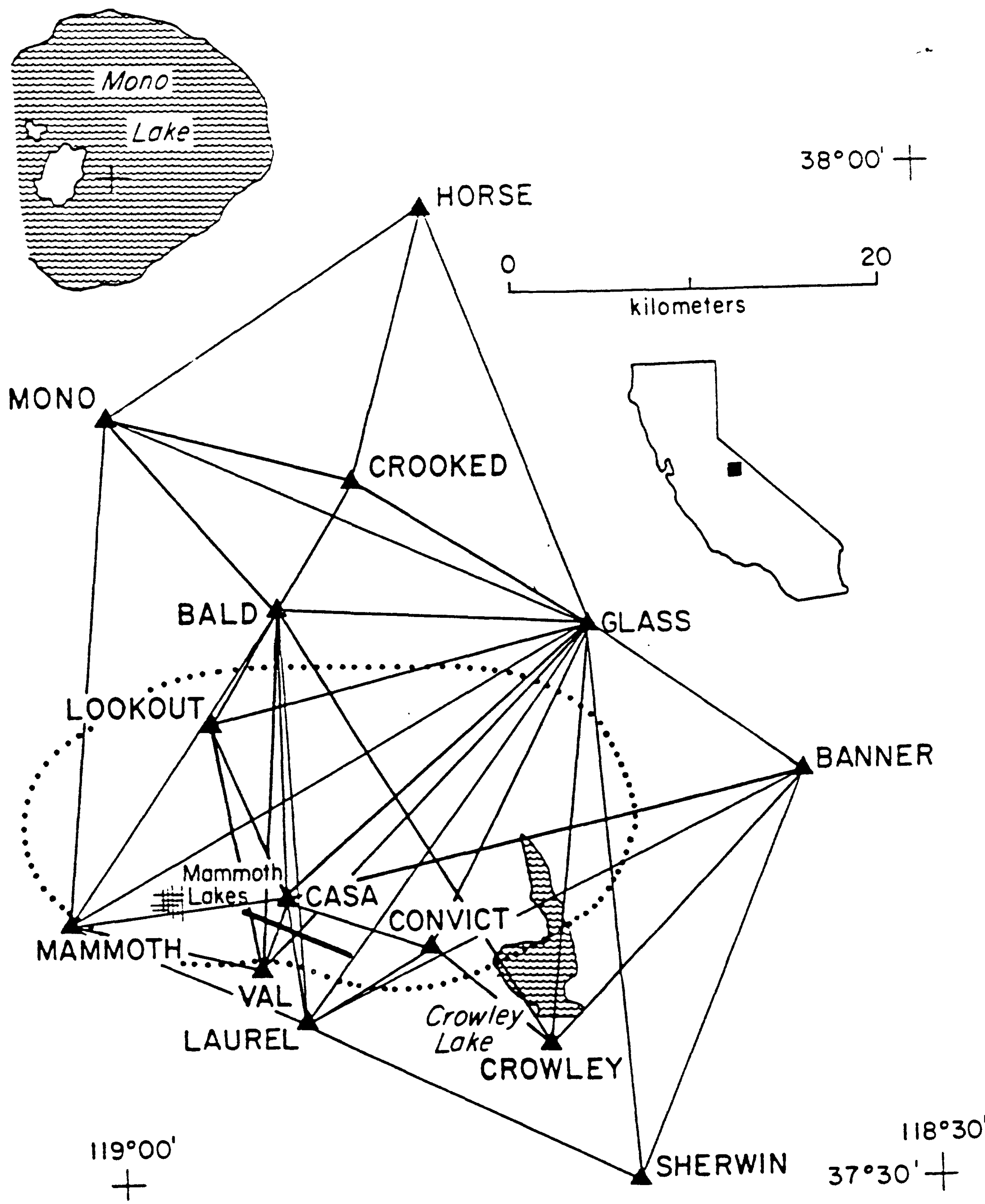

G 1

INFORMAL COMMUNICATION
NOT TO BE CITED FOR PUBLICATION

INFORMAL COMMUNICATION
NOT TO BE CITED FOR PUBLICATION

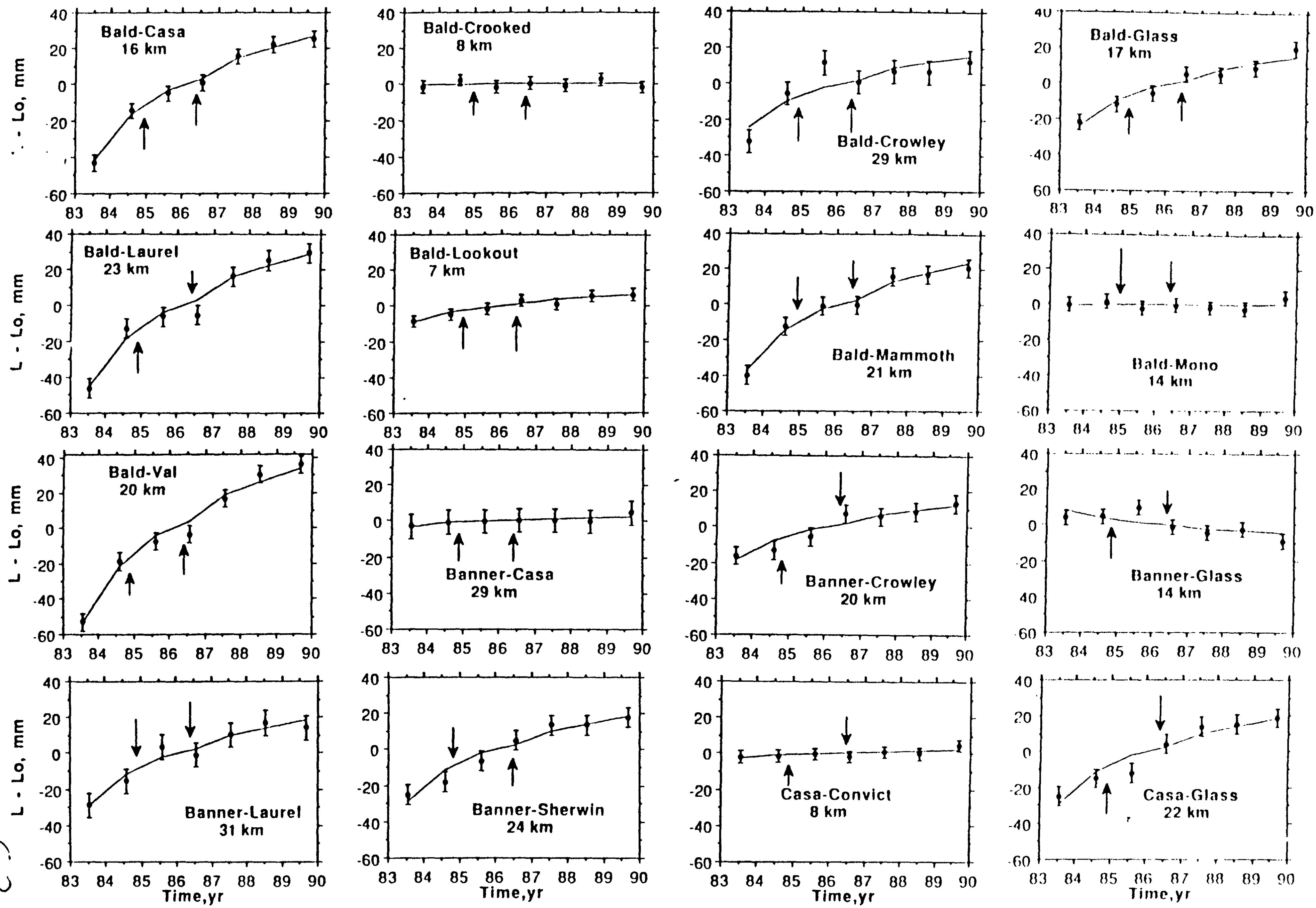

G2

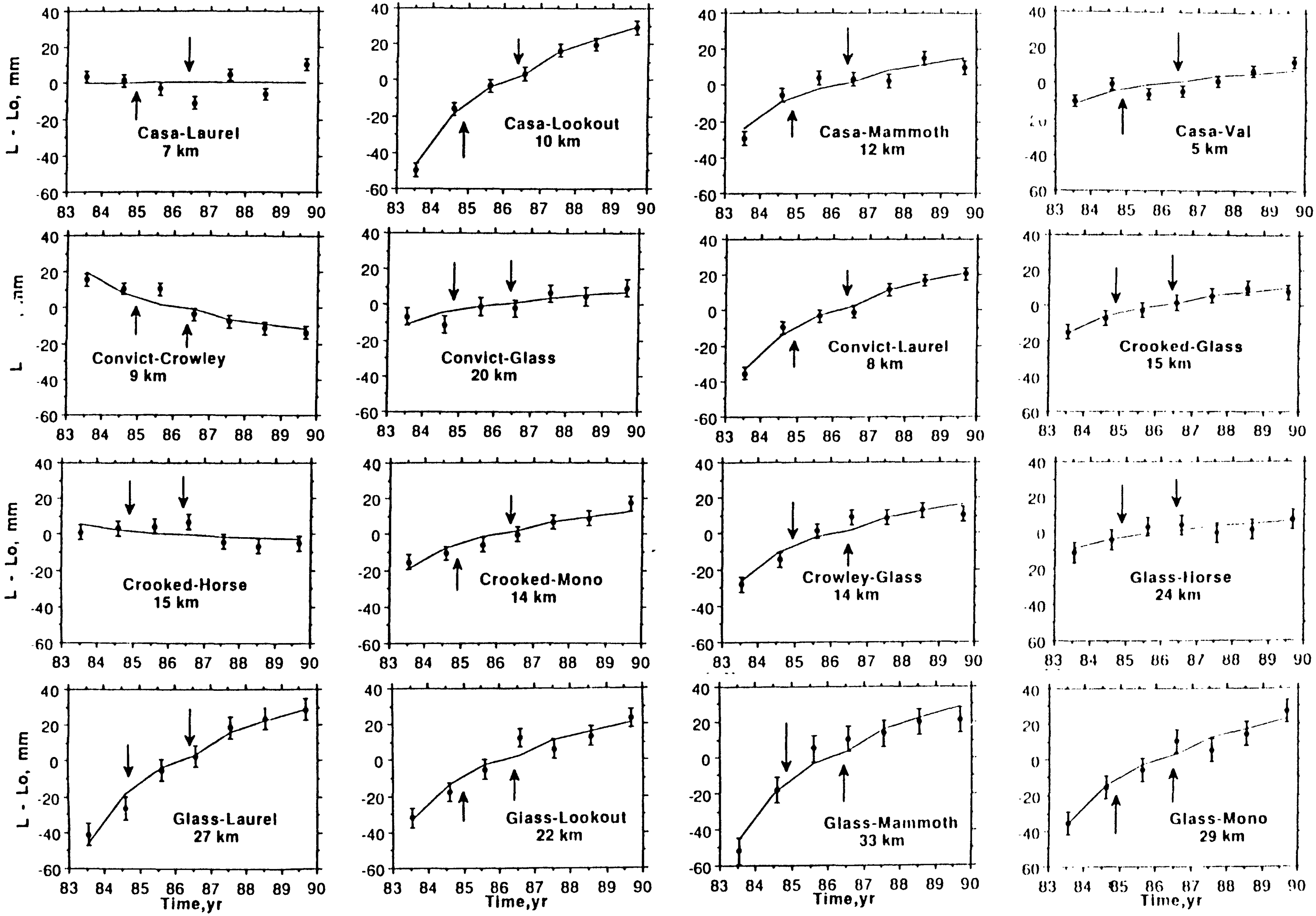

INFORMAL COMMUNICATION
NOT TO BE CITED FOR PUBLICATION

F.

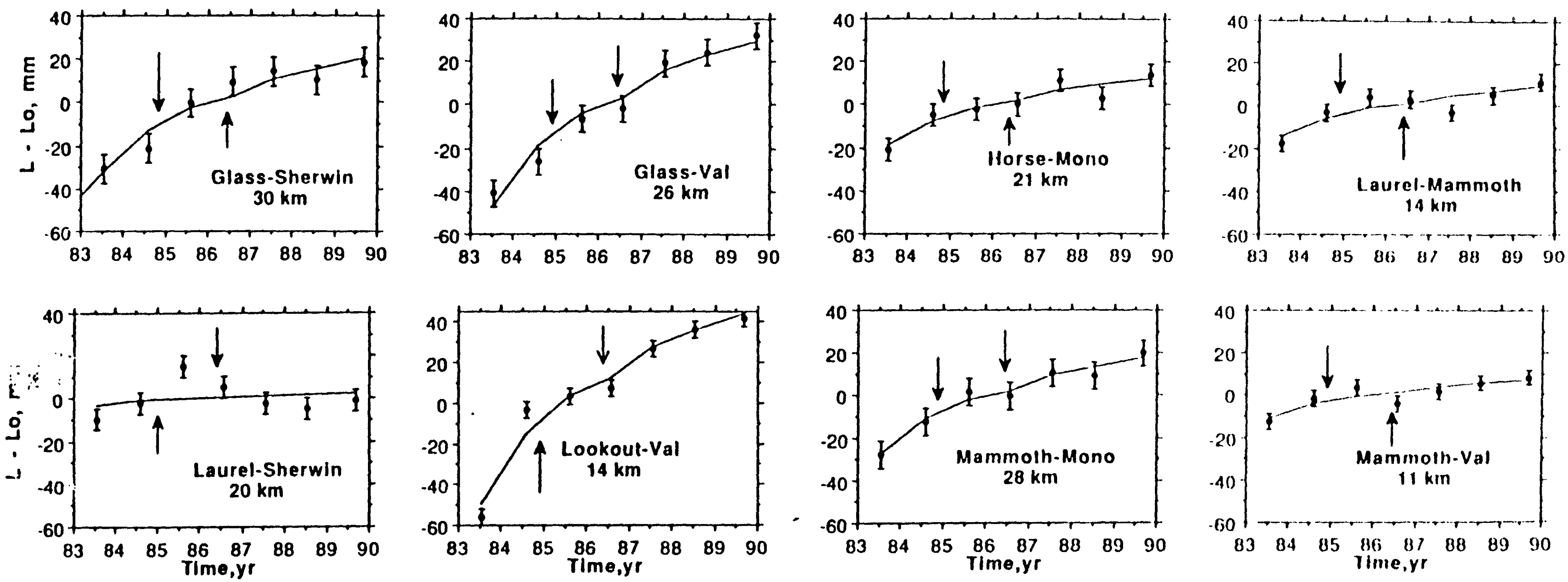

INFORMAL COMMUNICATION
NOT TO BE CITED FOR PUBLICATION

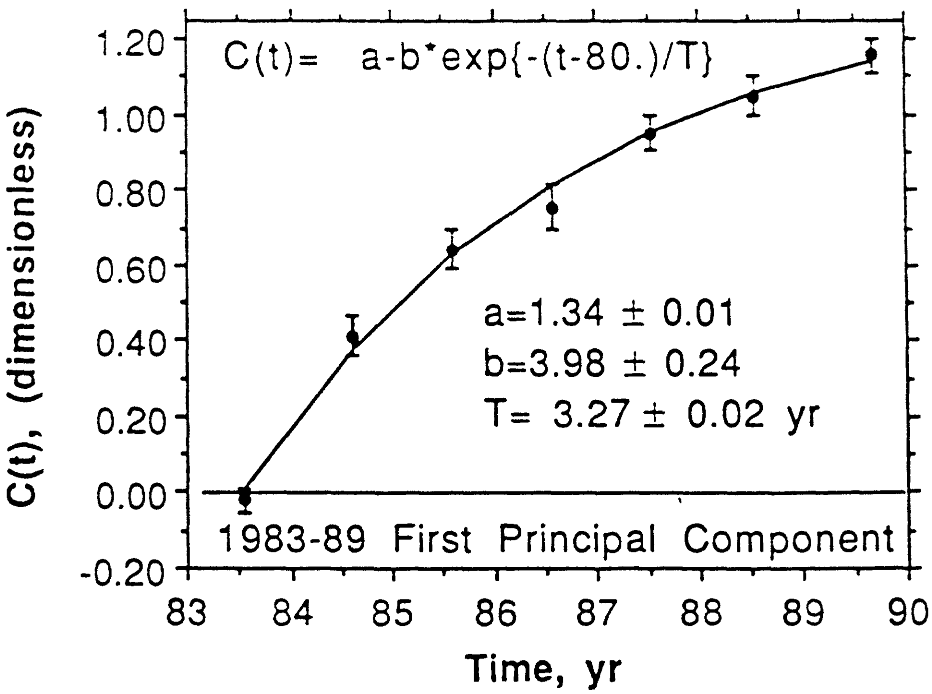
C(t)= a-b*exp{-(t-80.)/T}
a=1.34 ± 0.01
b=3.98 ± 0.24
T= 3.27 ± 0.02 yr
1983-89 First Principal Component
C(t), (dimensionless)
1.20
1.00
0.80
0.60
0.40
0.20
0.00
-0.20
83
84
85
86
87
88
89
90
Time, yr

G 5

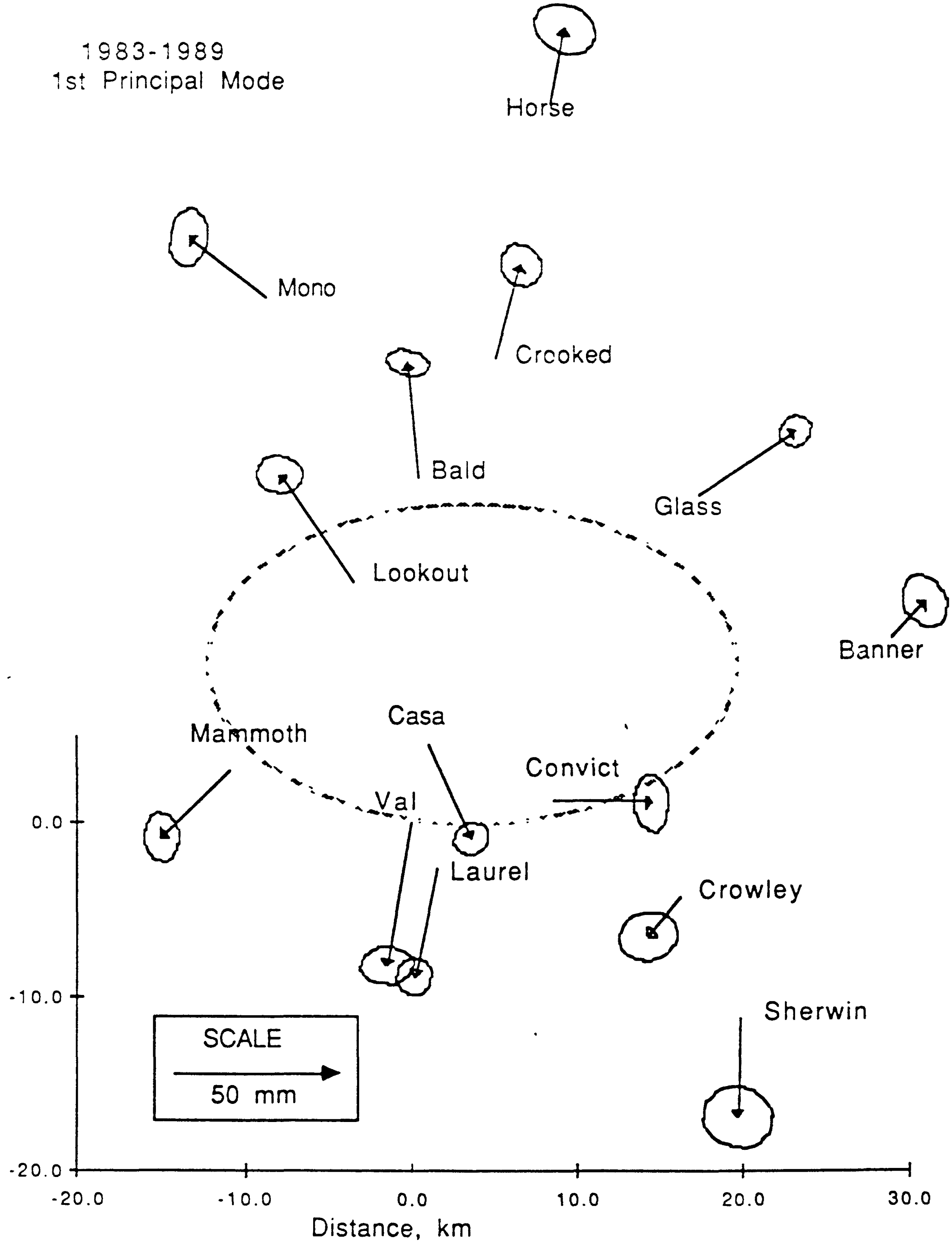

INFORMAL COMMUNICATION
NOT TO BE CITED FOR PUBLICAT'

G6

HIGHLIGHTS OF TILTMETER RESULTS FROM THE LONG VALLEY CALDERA FOR THE PERIOD 01 JULY TO 30 SEPTEMBER 1989

C.E. Mortensen, R.P. Liechti, V. Keller

1. The tiltmeter data for the period 01 July through 30 September 1989 are shown in Figures T2 through T8. The data in Figure T8 are from the long-baseline tiltmeter installed by Roger Bilham of the University of Colorado while the data in the other figures are from the USGS shallow-borehole instruments. None of the Westphal instruments, which are co-located with the USGS tiltmeters, are working, although the sensors are still in place and could be revived if necessary. Nearby consruction activity as well as geothermal production operations have resulted in a very high drift rate at the Casa Diablo site.

As with the other tiltmeters, the data from Bilham's long-baseline instrument are telemetered to Menlo Park via the GOES satellite. The data are "cleaned" using the automatic algorithm, as with the data from other tiltmeter sites, but are not reviewed for accuracy. In particular, the interferometers that sense the height of water at the ends of the instrument occasionally jump fringes. These fringe jumps may not all be removed by the automatic cleaning algorithm.

Starting in June, Univ. of Colo. personnel have been installing deep anchors at the end stations of the long baseline tiltmeter. This has affected the EW component data in particular and repairs are underway at the time of this writing. Questions concerning the particular details of the long-baseline instrument or data should be addressed to Roger Bilham at Univ. of Colorado.

2. Small signals that are coherent across the array occurred around August 8th and September 18th. These changes are quite dramatic at the Casa Diablo site, which seems to be especially sensitive to meteorological effects and to operations at the nearby geothermal field. The September fluctuations appear in the long-baseline data as well as the shallow borehole data. The fluctuations correspond approximately in time with the passing of a significant cold front through the area and may represent either instrumental or thermoelastic response to that event.

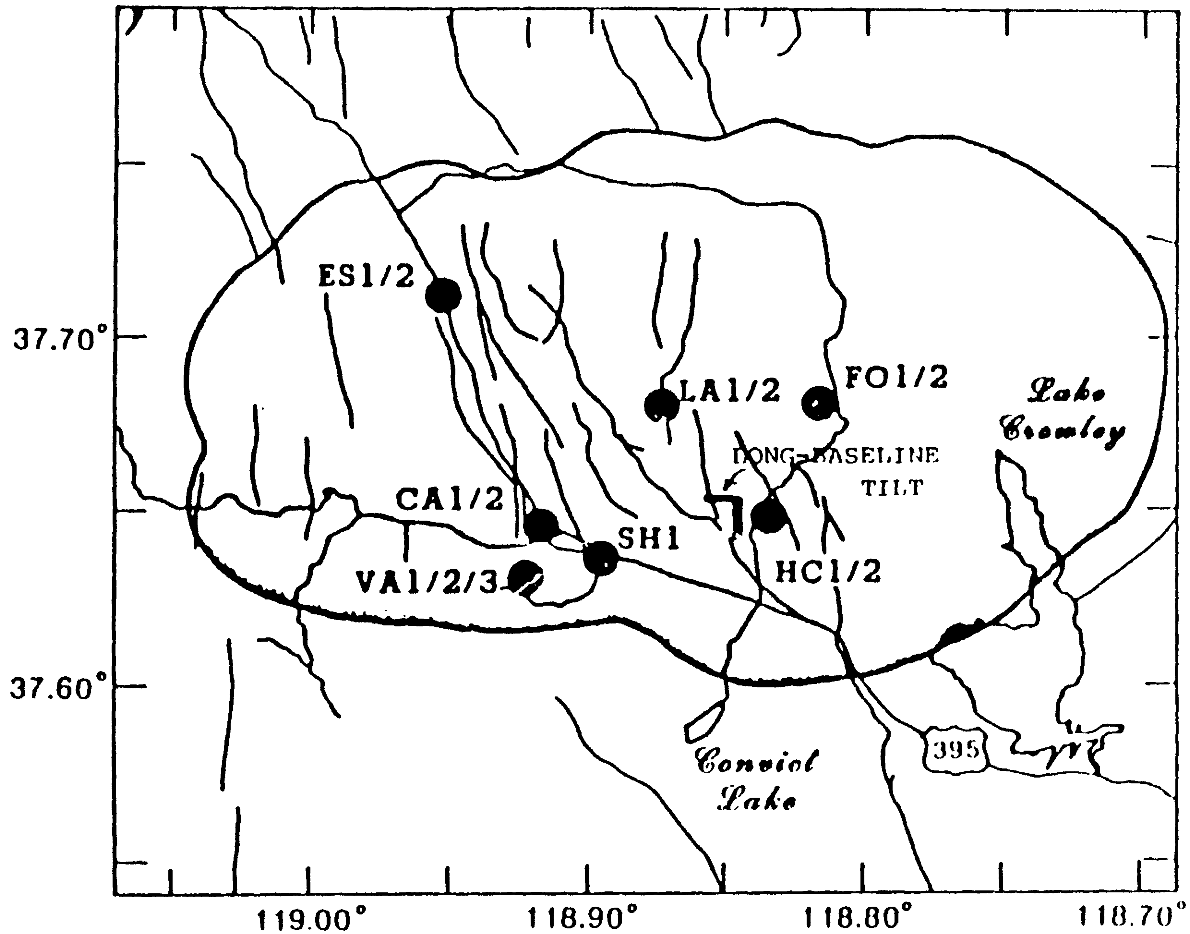

Figure T 1. Map of the Long Valley tiltmeter array

INFORMAL COMMUNICATION
NOT TO BE CITED FOR PUBLICATION

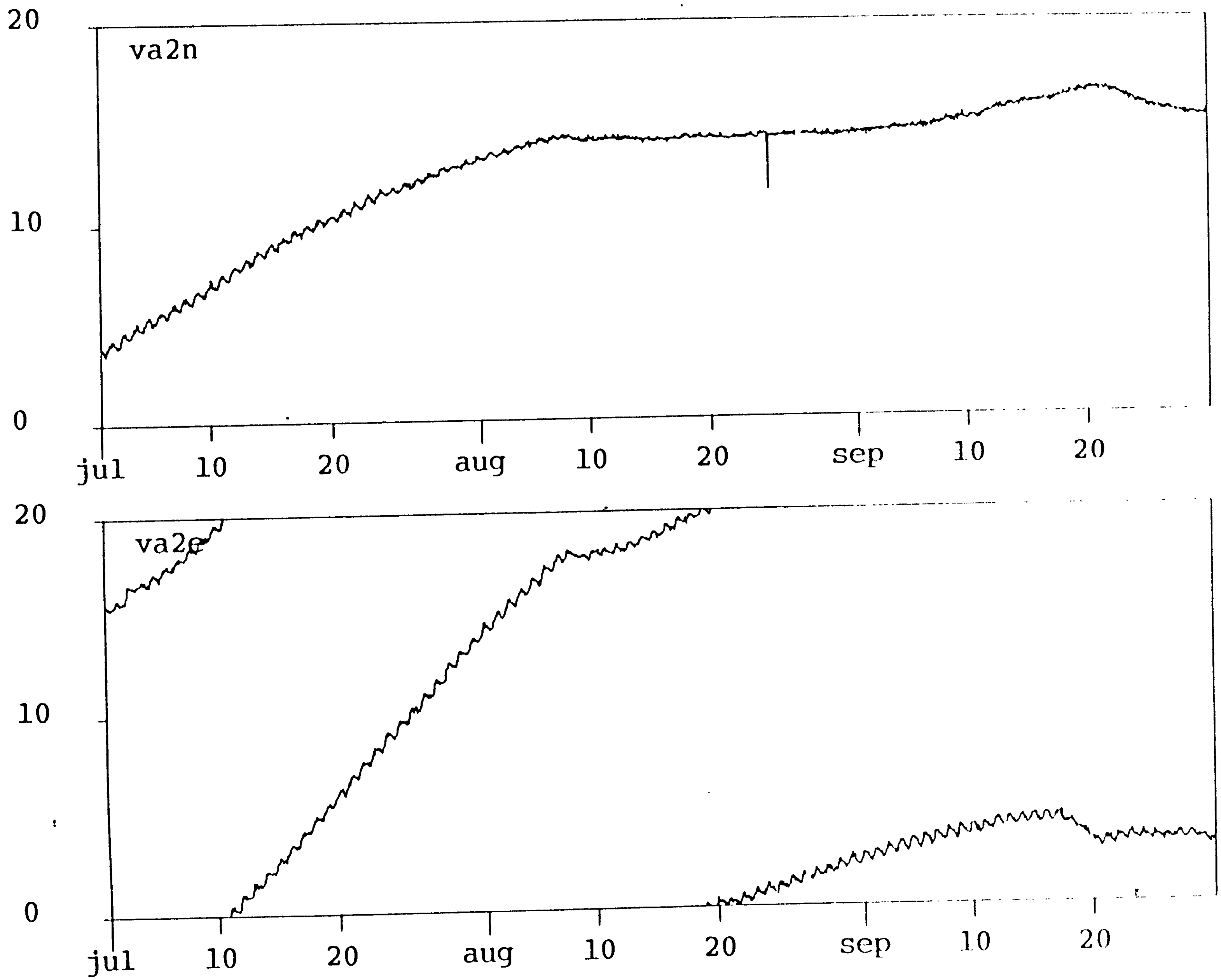

Figure T 2. Valentine raw tiltmeter data (Kinemetrics instrument) - units are microradians.

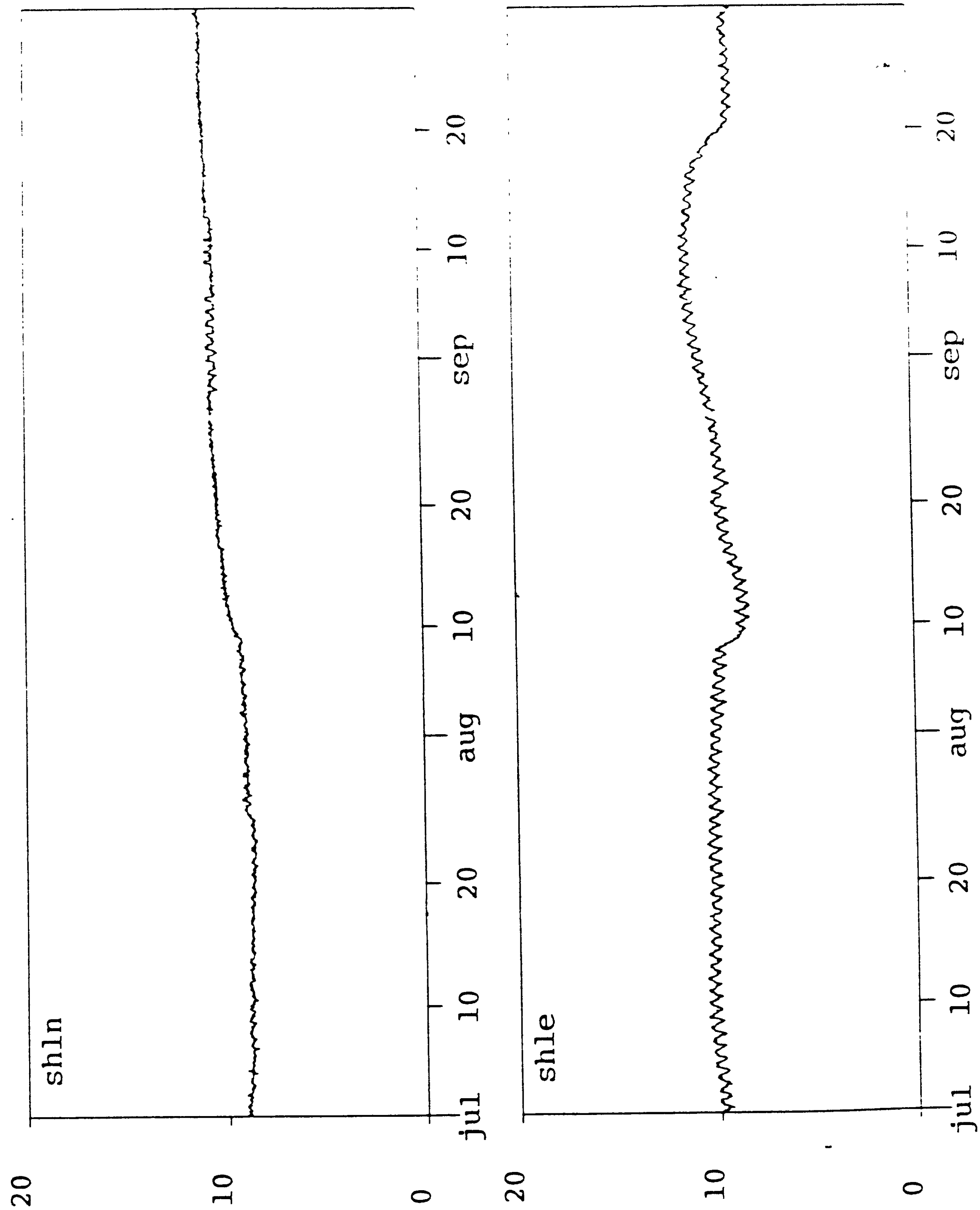

Figure T 3. Sherwin Creek tiltmeter data - units are microradians.

INFORMAL COMMUNICATION
NOT TO BE CITED FOR PUBLICATION

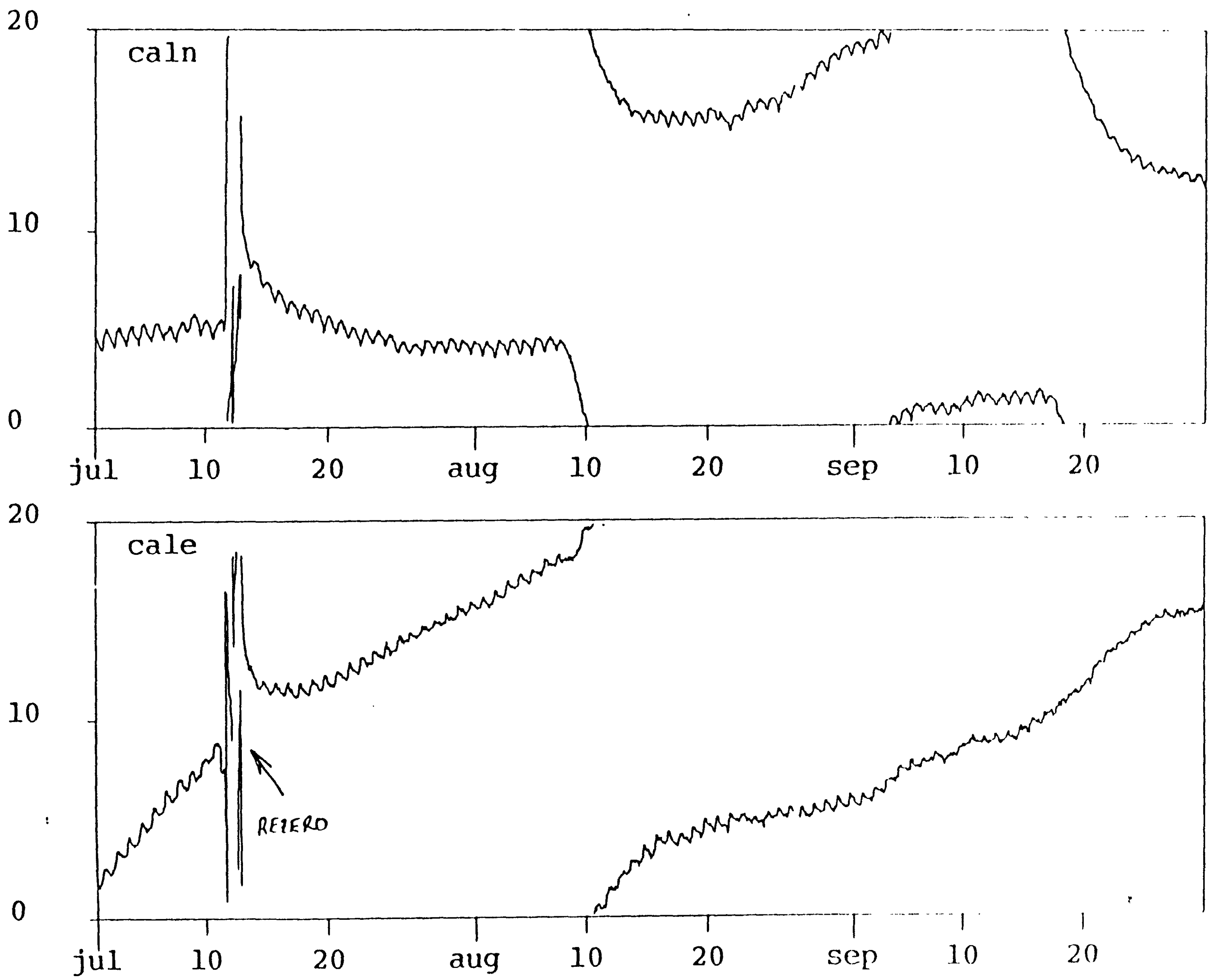

Figure T 4. Casa Diablo tiltmeter data - units are microradians.

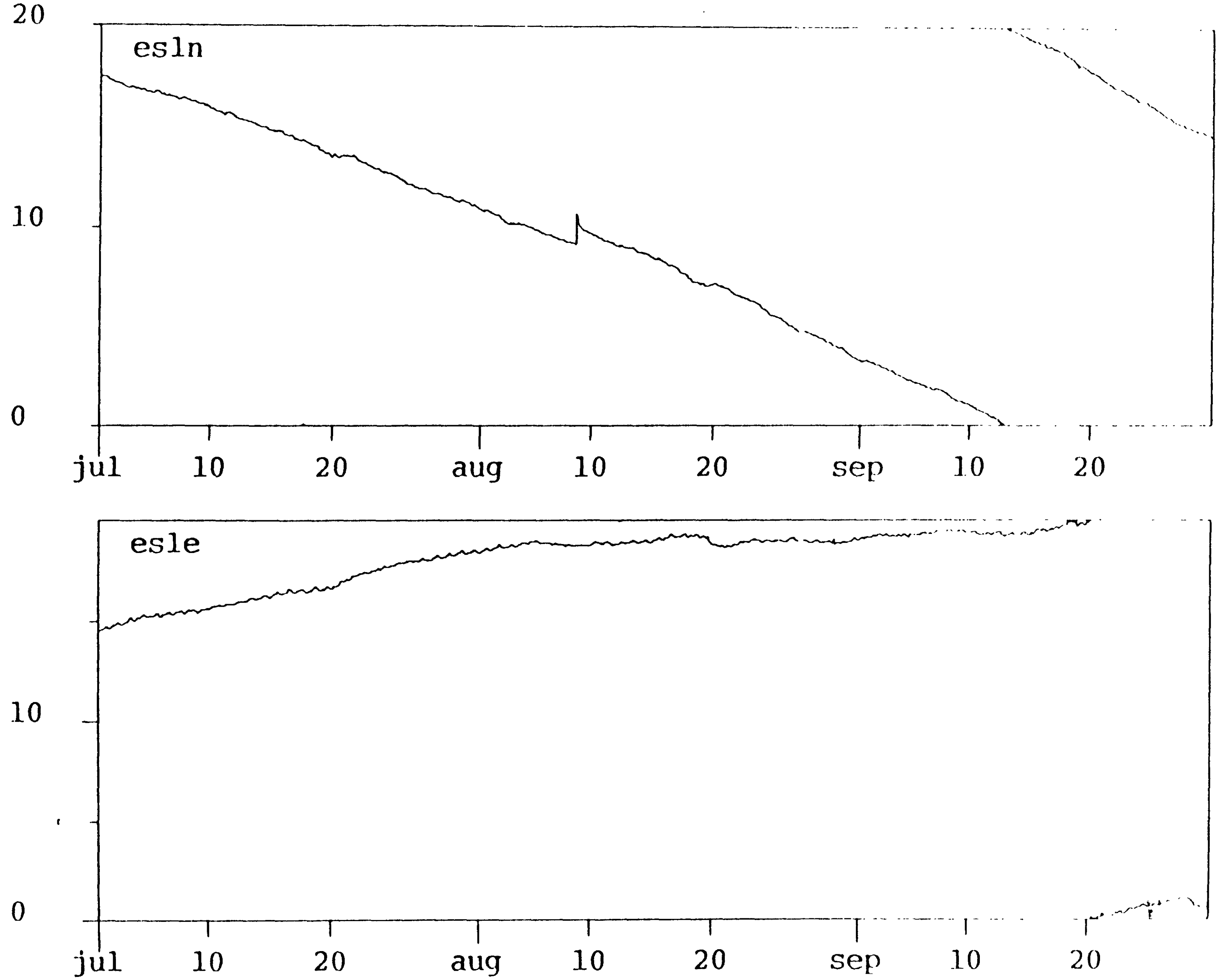

Figure T 5. Escape tiltmeter data - units are microradians.

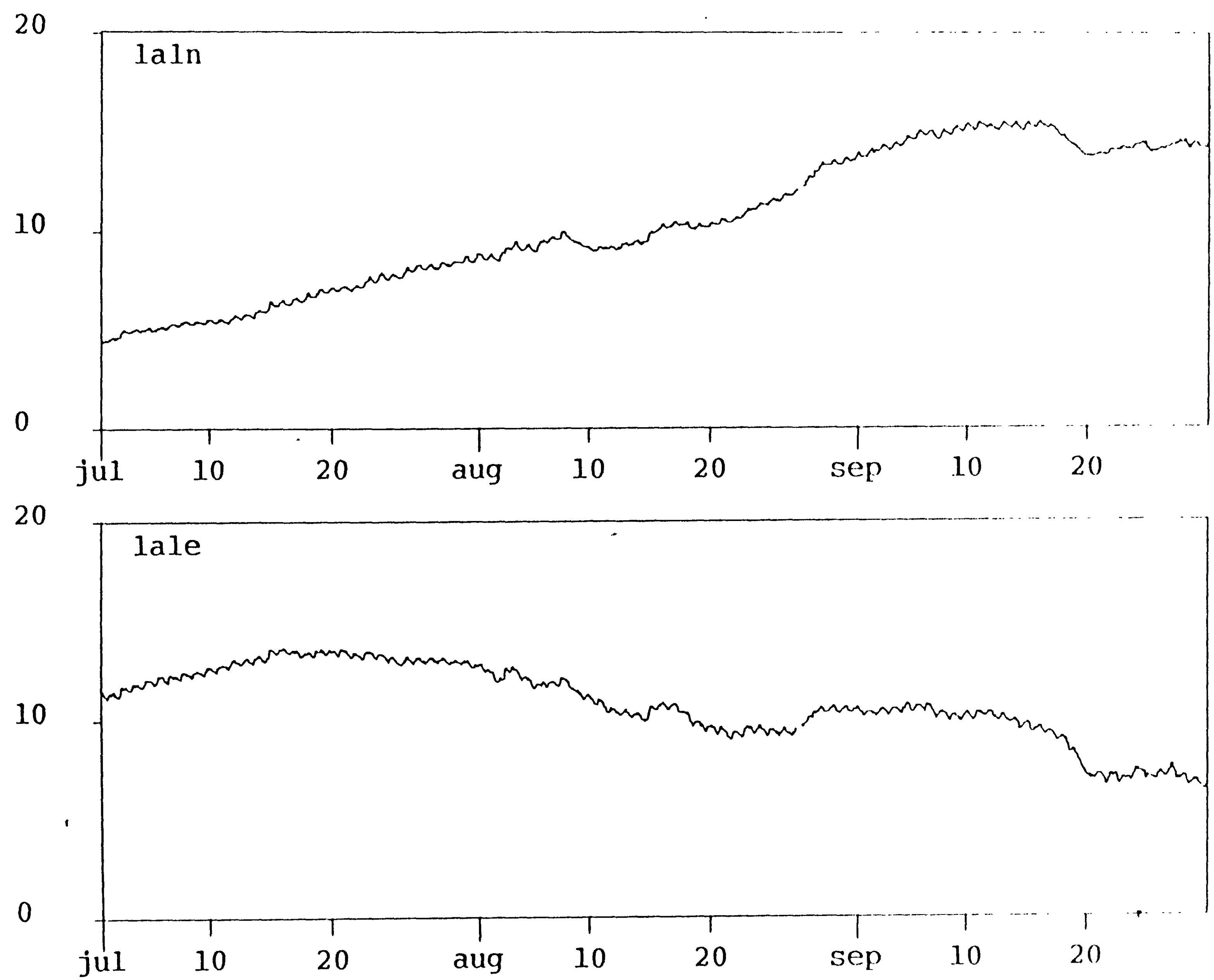

Figure T 6. Little Antelope Valley data - units are microradians.

INFORMAL COMMUNICATION
NOT TO BE CITED FOR PUBLICATION

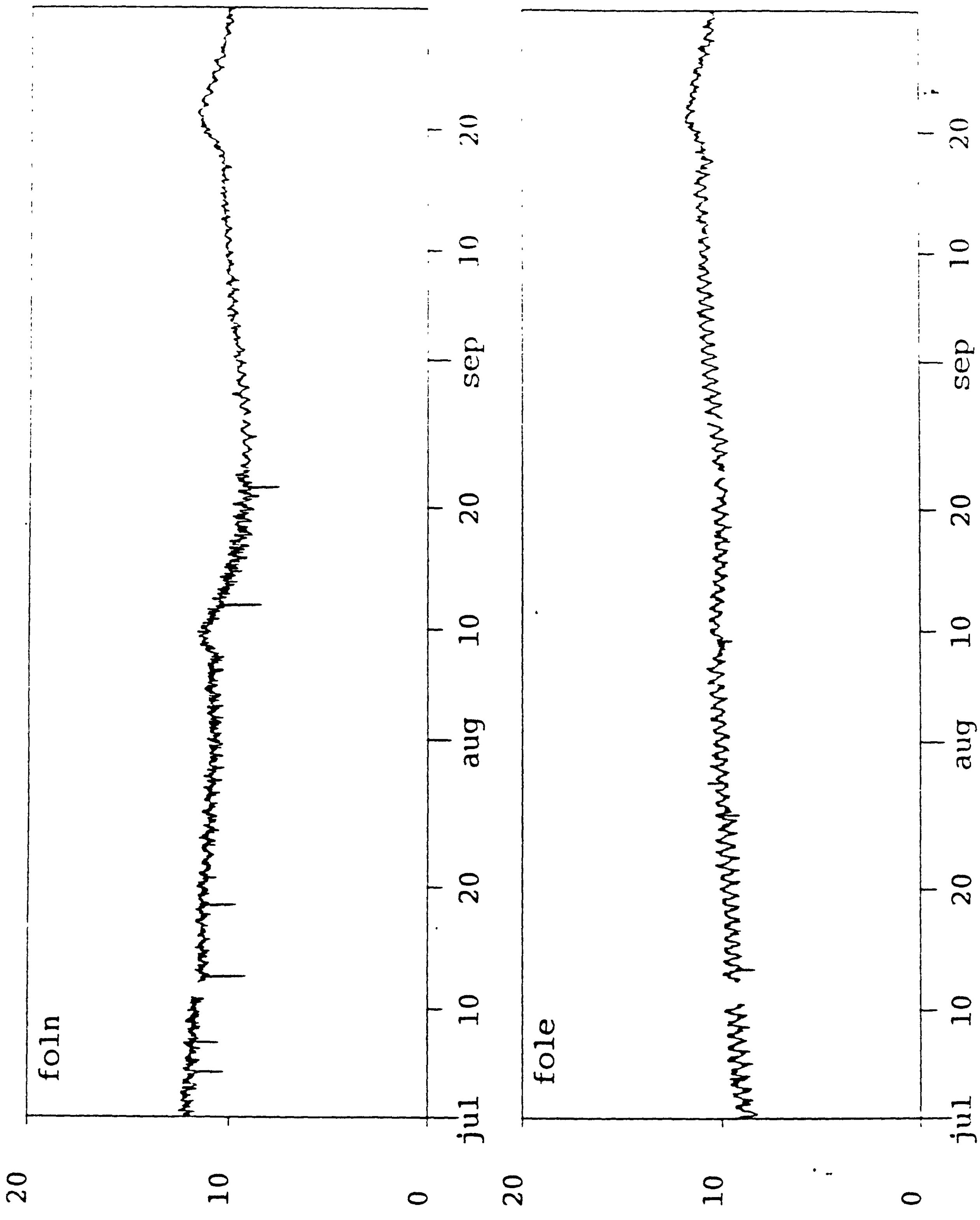

Figure T 7.   Fossil tiltmeter data - units are microradians.

INFORMAL COMMUNICATION
NOT TO BE CITED FOR PUBLICATION

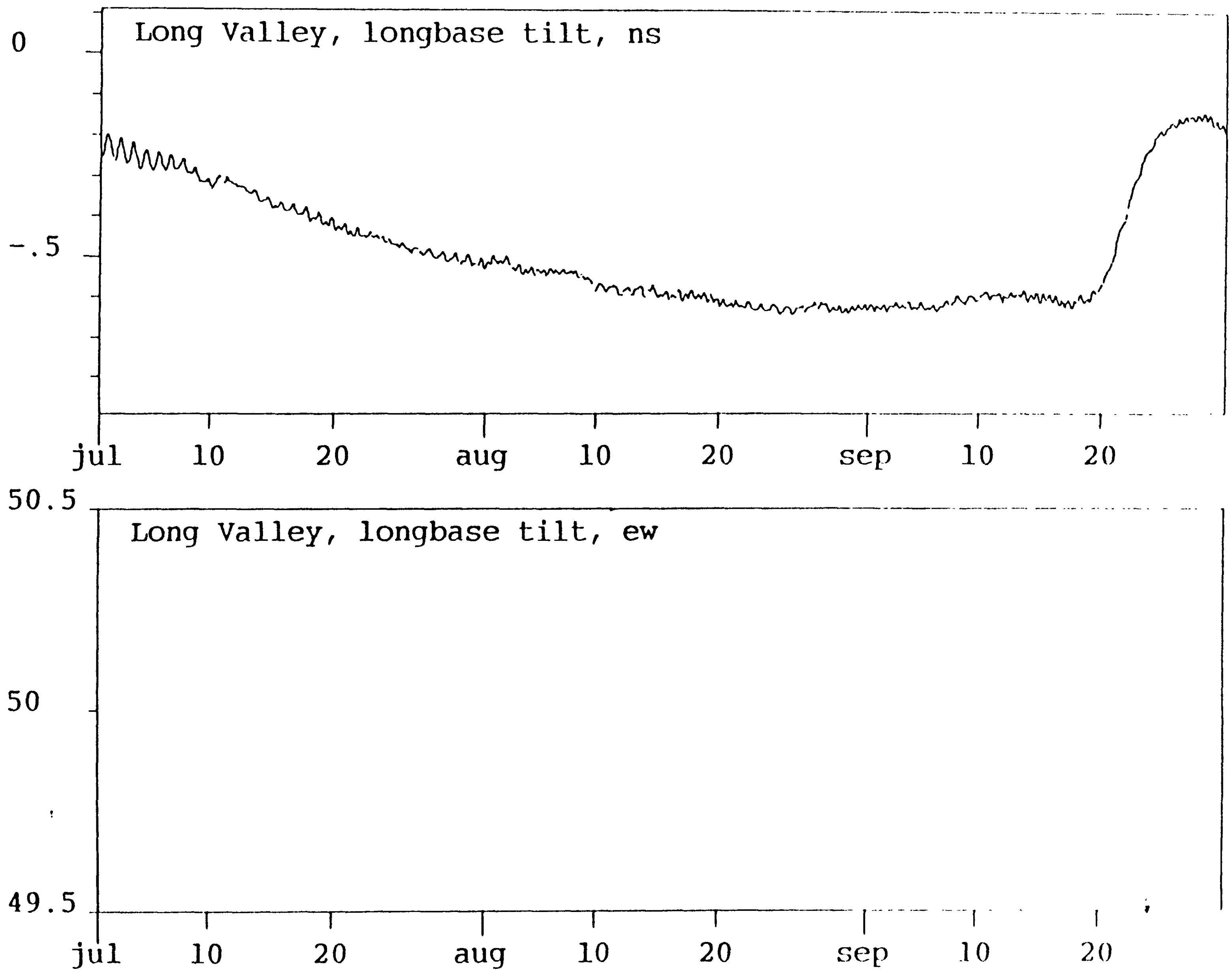

Figure T 8. Long Baseline tiltmeter data - units are microradians, tilt down to the north is positive, down to the east positive.

INFORMAL COMMUNICATION
NOT TO BE CITED FOR PUBLICATION

BOREHOLE STRAIN SITE IN LONG VALLEY

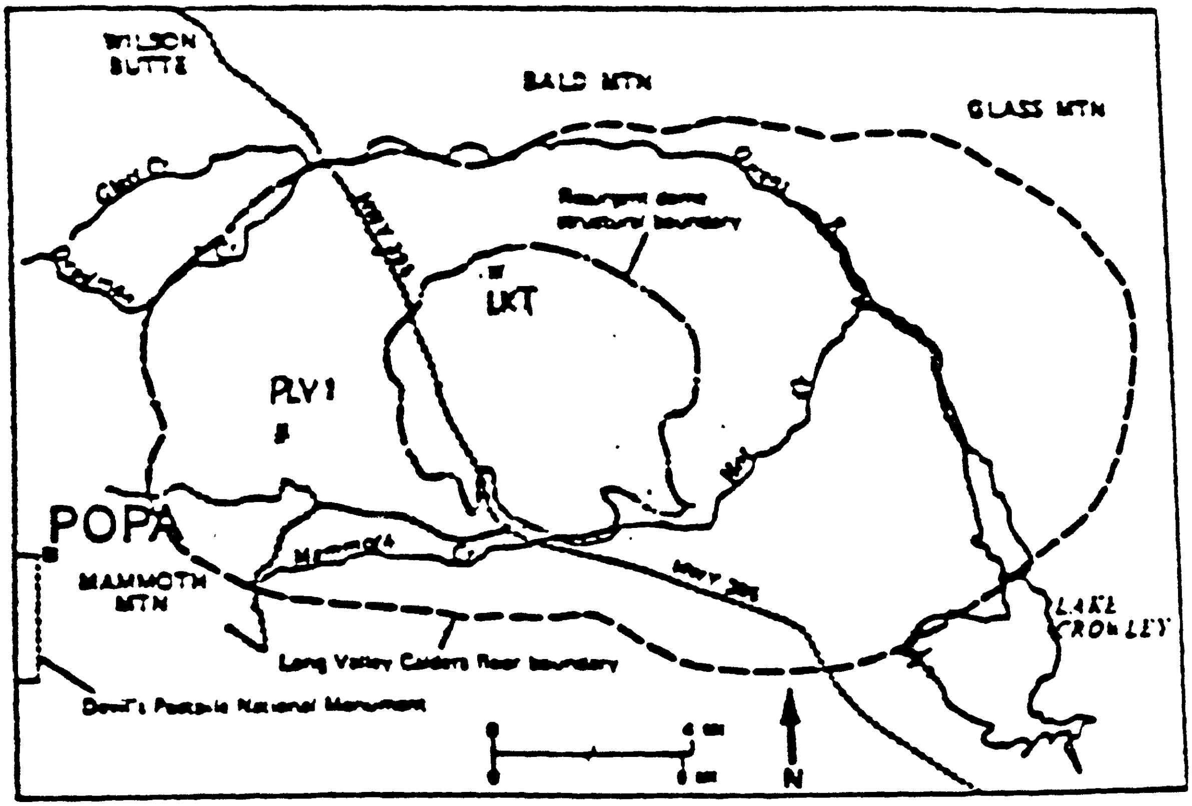

FIGURE D1. Map showing location of Devils Postpile dilatometer (POPA), the newly installed dilatometer (PLV1), and the Lookout Mountain water well (LKT).

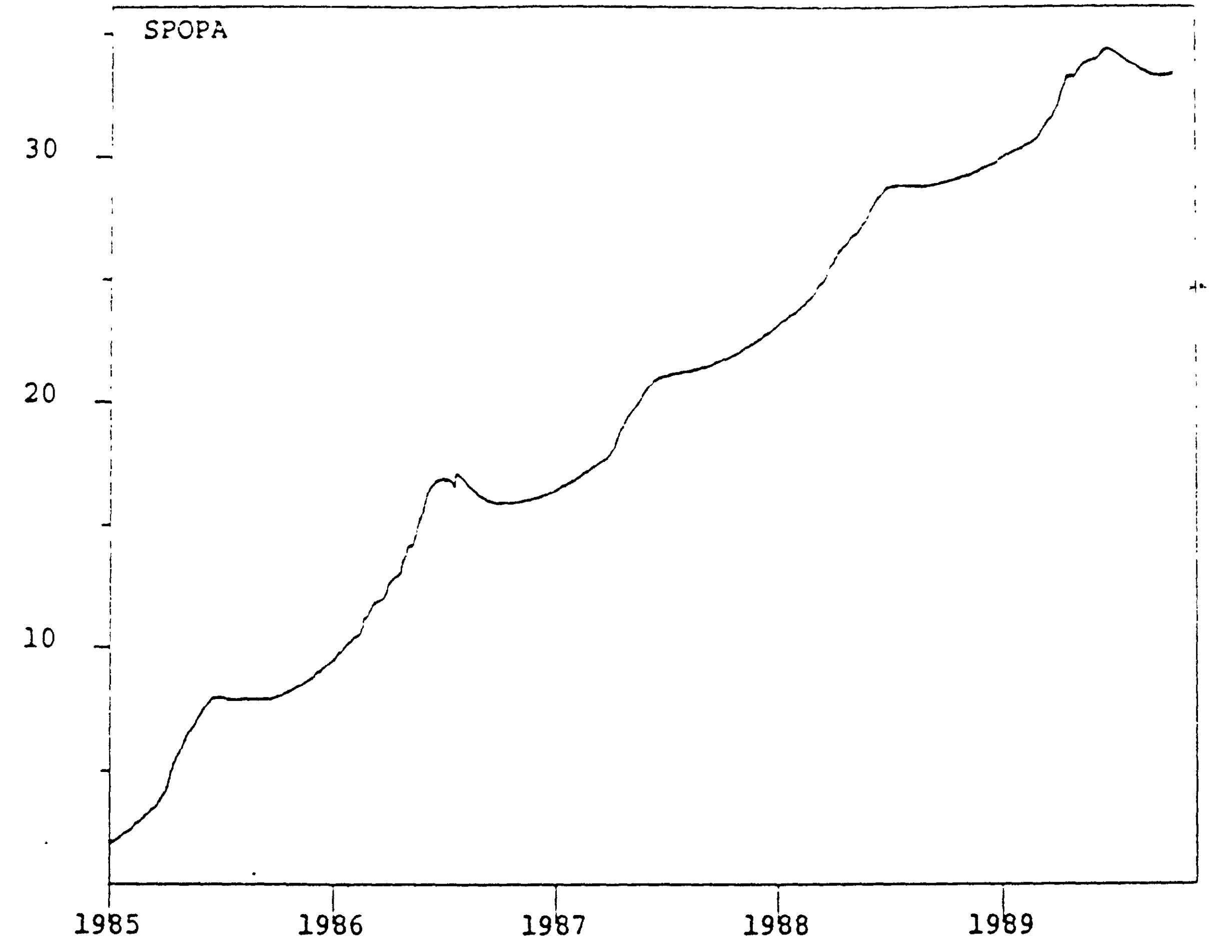

FIGURE D2. Devils Postpile dilatometer record from 1985 through September 1989.

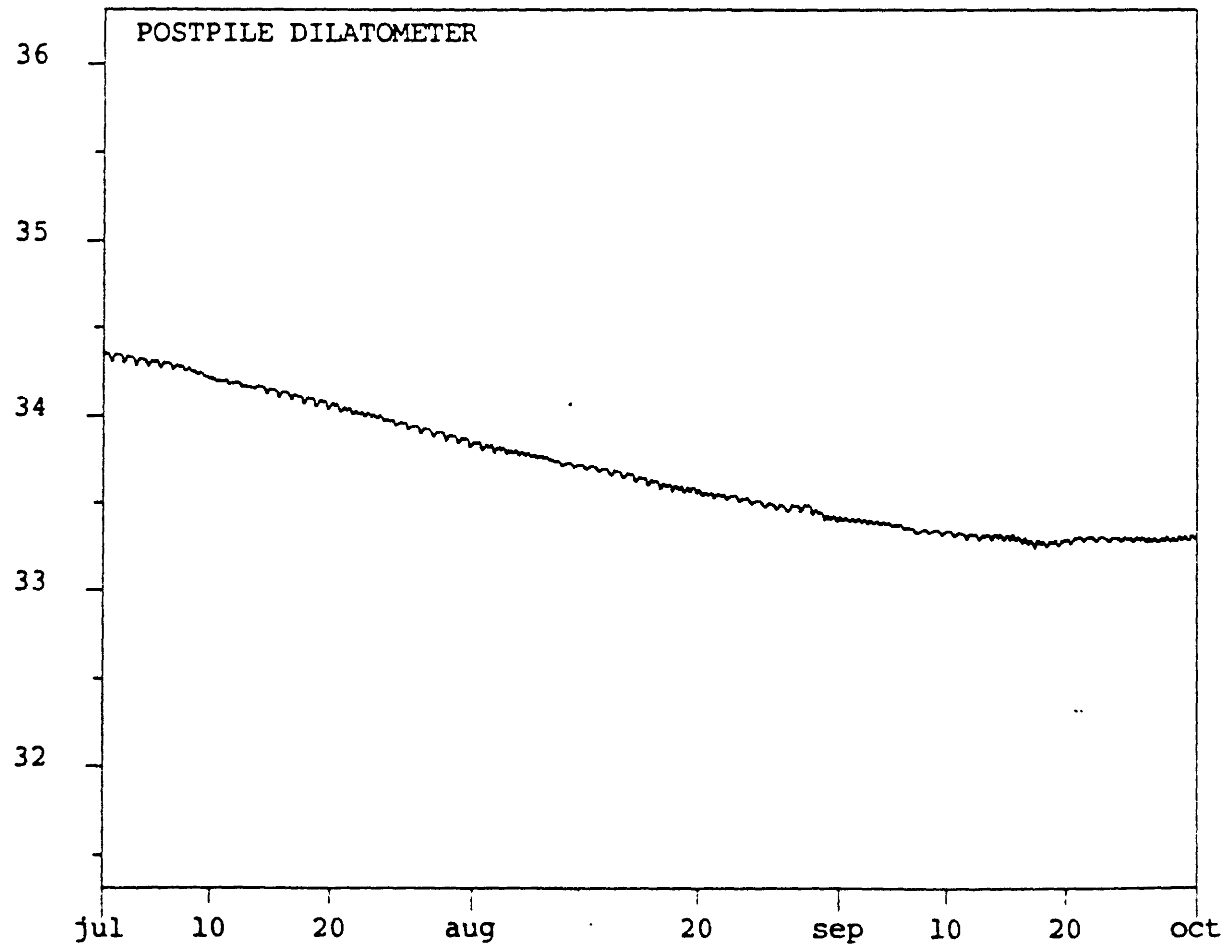

FIGURE D3. Devils Postpile dilatometer record for July-September 1989.

INFORMAL COMMUNICATION

Appendix K

Summary of activity at Parkfield Earthquake Prediction
Experiment during 1989.

Prepared by E.Roeloffs, USGS, Menlo Park, CA

The Parkfield, California, Earthquake Prediction Experiment: 1989 Summary for NEPEC

Parkfield Alerts during 1989

During 1989, there were 11 level D and 2 level C alerts in Parkfield (see attached table). Twice, it was decided not to combine simultaneous level D alerts to a level C alert, either because the combination of observations had been seen several times before, or because the instruments generating the alerts were too far apart. Neither the B nor the A alert levels have ever been reached since the beginning of the experiment in 1985.

Significant Observations in 1989

Observation of aseismic fault slip by water wells and strainmeters. Several more creep events on or south of Middle Mountain produced water level changes and strain steps on borehole volumetric strainmeters.

M 4 earthquake at Gold Hill. This was the largest seismic event at Parkfield in 1989. It was felt in San Miguel and Paso Robles, produced strain steps, and triggered strong motion arrays.

Shortage of earthquakes M 2 and greater within 5 km of anticipated nucleation point. Only one earthquake of M > 2 occurred in that volume between 1984 and 1989, compared with more than 15 between 1977 and 1982 (Aviles and Valdés, *EOS, 70*, p 1226).

Coseismic creep and strain produced by Loma Prieta earthquake. Coseismic creep was greatest at the XVA1 creepmeter south of Middle Mountain, where 2.0 mm of right lateral creep took place. Volume strain changes were recorded by borehole strainmeters and water wells.

Research in Progress

3-D velocity structure near Parkfield. Michael and Eberhardt-Phillips (*EOS, 70*, 1233) have identified a high-velocity zone along the San Andreas fault in the same location as the maximum slip during the 1966 Parkfield earthquake. This location may be an asperity with physical properties different from other parts of the fault zone.

Constraining hypocenter of foreshock to 1966 Parkfield earthquake. C. Aviles is comparing waveforms from recordings of this M 5 event with recordings at the same station of more recent, precisely located events in order to obtain a good location for the foreshock.

Possibly significant correlation of some fault creep events with earthquakes of M 2 or greater in the Middle Mountain box. The number of such earthquakes occurring within 5 days after creep events accompanied by large water level drops on Middle Mountain is greater than would be expected if the earthquakes were uniformly distributed in time. This observation is significant at the 90% confidence level.

Plans for 1990

The intriguing observation of enhanced low frequency electromagnetic signals above the epicenter of the Loma Prieta earthquake in the weeks and hours before the event have convinced many Parkfield participants that similar equipment should be brought on line in Parkfield as soon as possible.

Table. Parkfield alerts during 1989.

Date	Location	Description	Size	Level	Comments
890200	Middle Mtn	Creep	0.78 mm	D	NOT combined to C:
	Middle Mountain	Water Level	-15 cm	D	familiar combination
890315	Middle Mtn	Earthquake	M 1.6	D	NOT combined to C:
890317	Red Hills	Strain		D	instruments too
890319	Middle Mtn	Creep	0.92 mm	D	far apart
890328	Middle Mtn	Earthquake	M 1.9	D	
890409	Car Hill	Fault Slip	4 mm	D	2-color geodimeter
890423	Red Hills	Strain	0.17 ppm	D	
	Jack Canyon				
890525	N. of Gold Hill	Earthquake	M 4.0	C	
890705	Middle Ridge	Orecp	1.65 mm	D	
	XVA1	Creep	2.46 mm		
	Frohlich	Strain	3 ppb		
	Frohlich	Tensor Strain	4 ppb		
890815	Middle Mtn	Creep	0.9 mm	D	combine to C
	Middle Mtn	Water Level	1.6 cm		
	Middle Mtn	Water Level	-13 cm	D	
	Middle Ridge	Creep	1.3 mm	D	
891012	Middle Mtn	Creep	0.8 mm	D	
891025	Gold Hill	Earthquake	M 2.8	D	

Note. Right lateral creep, water level rises, and compressive strain are positive.

Appendix L

Discussion of statistical models used in the Bay Region Earthquake Probabilities report, presented to NEPEC by A.Cornell, April 30, 1990.

APPENDIX

RECURRENCE MODELS

The earthquake probability estimates in this report are based on current stochastic recurrence models of characteristic magnitudes, including explicit consideration of the uncertainty in the values of the parameters of these models. By "characteristic magnitudes" we mean the relatively narrow range of large events associated with successive "complete" ruptures of a specific segment (*e.g., Schwartz and Coppersmith*, 1989). The frequency of occurrence of such events is not necessarily predicted by extrapolation of the conventional (Gutenberg–Richter) linear (log) frequency versus magnitude relationship. Further, because characteristic magnitudes are associated with a "cycle" of major stress drop and stress recovery, it is believed that the inter–event or recurrence times of these events may follow a temporal pattern associated with a relatively narrow probability distribution. (Relative in this case to the exponential distribution associated with the reference case, a Poissonian recurrence model.) In contrast to the Gutenberg–Richter magnitude frequency distribution and the familiar Poisson recurrence model, these two general characteristics of this report's models, *i.e.,* a relatively narrow magnitude (or slip per event) range and a relatively narrow recurrence time distribution, are consistent with the notions of near–constant strain rate and a nearly–deterministic characteristic earthquake cycle. Furthermore, in this mechanical context, these two characteristics are also consistent with each other. As long as some degree of proportionality exists between actual successive earthquake slips and times, *e.g.,* that proportionality associated with a constant slip rate[1], this narrowness of one distribution will imply the narrowness of the other.

There are many probabilistic models that display these two basic characteristics. The discussion here is limited, first, to the simplest, the renewal model, because it has

[1] Note, however, that the proportionality between the mean (or median) of the slips per event and the mean (or median) of the recurrence times, is always true (by definition of the slip rate), even if, for example, the characteristic magnitudes occur in a Poisson fashion.

been widely studied, and second, to the time–predictable model favored by the Working Group. The developments for the first are easily extended to the second. In both cases the recurrence time, T, follows a probability distribution, $f_T(t)$, with (marginal) median value, $\hat{T}$, and variability or dispersion measure, σ. In this report the dispersion measure defined to be the standard deviation of the (natural) logarithm of T. In the range of our interest, this parameter is approximately equal to the coefficient of variation, *i.e.*, the standard deviation divided by the mean, of the recurrence times. Various distribution types have been used in the literature for $f_T(t)$, including normal, lognormal, Weibull and gamma. For any single segment there is insufficient data to distinguish among these distribution types; fortunately the majority of forecasts in this report are insensitive to the choice. The Working Group's general policy has been to retain the assumptions of the 1988 Working Group unless more recent evidence compels us to do otherwise. Therefore the lognormal distribution has been used again in this report. *Nishenko and Buland* (1987) supports this assumption.

Renewal Model: The renewal model for characteristic events on a segment is based on the assumption of (probabilistic) independence among the sequence of recurrence times (T_1, T_2, ...) and the sequence of slips (per event): D_1, D_2, ... Probability forecasts are based on conditional probability statements, the condition being that no event has occurred between the previous event and the day of the forecast, *i.e.*, that a time, T_e, has elapsed since the last event. For the renewal model, the forecast for the next 30 year interval is written

$$\begin{aligned} C_{30}^{T_e} &= P[T_e < T \le T_e + 30 \mid T \ge T_e] \\ &= \frac{F_T(T_e+30) - F_T(T_e)}{1 - F_T(T_e)} \end{aligned} \qquad (A-1)$$

in which the cumulative distribution function, $F_T(t)$ is related to the density function by:

$$F_T(t) = P[T \le t] = \int_0^t f_T(u)du \qquad (A-2)$$

A graphical interpretation of equation (A–1) is given in Figure A–1. equation (A–1) is equivalent to equation 2 in the main body of the report. Typical plots of the function $C_{30}^{T_e}$

versus T_e (for given parameter values, $\hat{T}$ and σ) are shown in Figure A–2. The value of σ dictates the sensitivity of the forecast to the elapsed time; for $\sigma \cong 1.0$, the probability is virtually independent of the elapsed time. (More precisely for an exponential recurrence distribution, *i.e.*, for a Poissonian recurrence model, which has a coefficient of variation of 1.0, $C_{30}^{T_e}$ is independent of T_e. In words: the Poisson process has no memory. Note that, in general, when T_e is about two–thirds of $\hat{T}$ the hazard is approximately equivalent to that of the Poisson model no matter what the value of σ. Figure A–2.)

Parametric Uncertainty. In practice it is difficult to know with precision the numerical values of parameters in this model for a specific fault. Following the 1988 Working Group (and practice in the engineering seismic hazard community), we treat the uncertain parameters in turn as random variables. The simplest model of parametric uncertainty considers only $\hat{T}$, the median, as uncertain and ignores the uncertainty in the dispersion measure. For reasons that will become clear below, this Working Group concurs with the 1988 Working Group in adopting this parametric uncertainty model and, further, in using a common value of 0.21 for the measure of variability of recurrence times. (The basis for this particular numerical value is *Nishenko and Buland* (1987), who found it to be a representative value for circum–Pacific segments.) It will be seen below that the precise value of this parameter estimate is not critical provided it is less than about 0.3. Again like the 1988 Working Group, we assume that the parametric uncertainty in the median, $\hat{T}$, can be represented by a lognormal (prior) distribution with a specified best estimate (median) value, and a specified parametric uncertainty measure, denoted σ_P, which is the standard deviation of the (natural) log of the uncertain median. In this report σ_P reflects the combined uncertainty in the slip per event and slip rate whose ratio is used to estimate the median $\hat{T}$. Typical values are about 0.4.

The simplest way to deal with parametric uncertainty is to "fold it in" with the intrinsic, obtaining what is called a "predictive distribution" on the recurrence T. For the assumptions here it can be shown (*e.g.*, *Benjamin and Cornell*, 1970, Chapter 6) that the predictive distribution of T is again lognormal with and net uncertainty parameter, σ_N:

$$\sigma_N = \sqrt{\sigma_P^2 + \sigma_I^2} \qquad (A-3)$$

in which σ_I is now used to denote the "intrinsic", random, or event-to-event recurrence time variability observed on a given segment, the parameter which was set equal to 0.21 in the discussion above. With this approach, one can again use equation (A-1) to calculate "the" conditional probability of an event in the next 30 years given an elapsed time interval of T_e years. The result is "the" value of this probability in that it has considered all possible values of $\hat{T}$ and their relative likelihoods. As we shall see below, the result can also be interpreted as a mean estimate of this conditional probability, $C_{30}^{T_e}$. Equation (A-3) explains why these estimates of $C_{30}^{T_e}$ are insensitive to the intrinsic variability σ_I: if the parametric uncertainty, σ_P, is approximately 0.4 or more, then the net uncertainty σ_N, is insensitive to σ_I, provided it is less than about 0.3.

It has been found effective when dealing with technical probability assessments to report more than simply a best estimate; we can also make explicit the degree of professional uncertainty in the estimates. Here the parametric uncertainty in the median (represented by the value of σ_P) induces uncertainty in $\hat{T}$. If we re-write equation (1) as

$$C_{30}^{T_e}(\hat{T}) = \frac{F_T(T_e + 30; \hat{T}) - F_T(T_e; \hat{T})}{1 - F_T(T_e; \hat{T})} \qquad (A-4)$$

it emphasizes the fact that it is a function of the uncertain parameter $\hat{T}$. (It is understood in this paragraph that the distribution $F_T(t; \hat{T})$ has for its dispersion level only the intrinsic value, σ_I, *i.e.*, 0.21 in these calculations.) Assuming that $C_{30}^{T_e}(\hat{T})$ is monotonically decreasing in $\hat{T}$ in the range of interest, we can find the fractile, c' of $C_{30}^{T_e}$ by calculating the probability that $\hat{T}$ exceeds the corresponding value of the median, t'. (For a given value of c', the corresponding value of t' is found by solving equation (A-4) for $\hat{T}$.) To calculate this probability we must use the distribution on the uncertain parameter $\hat{T}$. This computation is complicated somewhat by the fact that the distribution on $\hat{T}$ must be "updated" to reflect the information that this particular, current recurrence time is greater than T_e, the elapsed time since the last event (see, for example, *Davis, Jackson, and Kagan*, 1989). The updating uses Bayes theorum:

$$f''_{\hat{T}}(t \mid T > T_e) = k\, f'_{\hat{T}}(t)\, P[T > T_e \mid \hat{T} = t] \qquad (A-5)$$

In this equation $f'_{\hat{T}}(t)$ is the "prior" distribution on the uncertain median (here lognormal with and dispersion σ_P, while $f''_{\hat{T}}(t \mid T > T_e)$ is the "posterior" distribution (given the observation that $T > T_e$). Note that $f'_{\hat{T}}(t)$ is modified by the "likelihood function" (*i.e.*, the likelihood of the observation given that the true median, $\hat{T}$, has value t), which here is $P[T > T_e \mid \hat{T} = t]$. This probability is obtained from the (intrinsic; $\sigma = \sigma_I$) distribution on the recurrence time, T, but as a function of its median, $\hat{T}$. In this application $P[T > T_e \mid \hat{T} = t]$ varies from zero to one as t increases, *e.g.*, if the true median is very small, it is unlikely that one would have observed a recurrence interval as large as T_e. Therefore, such small values of $\hat{T}$ are "down-weighted". Finally, the coefficient k in equation (A-4) is a normalizing factor that "ensures" that the posterior distribution on $\hat{T}$ has unit area. In practice these computations are conducted by numerical integration (or simulation). Making the calculations at a set of values c', defines the probability distribution on the uncertain forecast $C_{30}^{T_e}$ induced by the uncertainty in the parameter $\hat{T}$. From this distribution one can read specified fractiles, *e.g.*, quantities corresponding to probabilities of 0.25, 0.5, and 0.75. Results of such calculations appear in the body of the report. In addition to fractiles, one can calculate the mean of the distribution of $C_{30}^{T_e}$; it can be shown that it is equivalent to "the" probability calculated from equation (A-1) using the predictive distribution on T, *i.e.*, using the total uncertainty σ_N (equation (A-3)). Therefore this result, which was also used by the 1988 Working Group, implicitly includes the updating of the distribution on the median due to the "open interval" information, $T > T_e$.

Time-Predictable Model. In contrast to the renewal model, the time-predictable model of characteristic earthquake recurrence is based on the assumption that there is positive correlation between the slip, D_i, in a particular event on a segment and the subsequent recurrence time, T_i, to the next event. Further, some form proportionallity is assumed between the recurrence time and the slip. In this report we adopt the probabilistic model

$$T_i = \frac{1}{V} D_i \epsilon_i \qquad (A-6)$$

in which D_i is the (random) slip in the i^{th} characteristic earthquake in a sequence, T_i is the subsequent recurrence time to the next event, V is a constant (the constant slip rate) and ϵ_i is an (independent) random deviation term (with unit median value). Then, as discussed above, the (marginal) median of T is equal to the (marginal) median of D (*i.e.*, the median slip per event) divided by the slip rate, V. Conditional on knowing that the slip D_i was say d, the conditional median of T_i is d/V. Further, noting that $\ln T_i = -\ln V + \ln D_I + \ln \epsilon_i$, we see that σ the marginal standard deviation of the log of T is

$$\sqrt{\sigma_D^2 + \sigma_\epsilon^2},$$

whereas the conditional standard deviation of $\ln T$ (given D_i) is only σ_ϵ. (We retain the somewhat unusual notation of σ for standard deviation of the log of the variable.)

We need not repeat the results (equations (A–1) through (A–5)) for the time–predictable model. All the analysis developed above for the renewal model applies equally well to the time–predictable model, provided one interprets those distributions, parameters, and probabilities as conditional on the slip in the last event. For example, $\hat{T}$ and σ in equation (A–1) are now the conditional median and (log) standard deviation given the slip. The probability distribution functions F_T and f_T in equation (A–1) and (A–2) are those of the conditional distribution of T given D, etc.

As stated, the Working Groups utilized the time–predictable model and therefore the adoption of the lognormal type of distribution and the value $\sigma_I = 0.21$ are both strictly applicable to the conditional distribution on T given the past slip. For notational and editorial simplicity in the main body of the report, the notion that all is conditional on $D = d$ is normally deleted in the presentation. It is implicit. Note, as is clear in the model above, that the conditional (log) standard deviation of T is less than (or equal to) the marginal value. Hence, using 0.21 for the conditional value is conservative, because the *Nishenko and Buland* (1987) analysis, upon which the value is based, was conducted on marginal distributions. In fact there is as yet little evidence to establish the relative values of the marginal and conditional values of these dispersion measures, or equivalently the correlation coefficient[2] between $\ln D$ and the successive $\ln T$. Preliminary investigations show negligible estimated correlation between (estimated) characteristic magnitudes and logs of the succeeding recurrence times, on a given segment, but the implied measurement noise (vis–a–vis log slips and log times) is severe.

In the current application of these models to Bay Area forecasts there is little possibility to distinguish between the renewal and time–predictable model in any case. For virtually every segment there is only one past known earthquake. Therefore the best current estimate of the median slip per event, $\hat{D}$, is simply the slip in the last event D. In this case the current estimate of the marginal median of T (*i.e.*, $\hat{D}/V$) is numerically equal to the conditional median of T given the past slip[3] (*i.e.*, D/V). The former is used in the renewal model and the latter in the time–predictable model. Provided one continues to use 0.21 for both the marginal and conditional variability measure, the two models will then produce the same forecast probability. As more information becomes available it will be possible to distinguish between the two.

[2] For the model in equation (A–6), the correlation coefficient between $\ln T$ and $\ln D$ is $\sigma_D^2/(\sigma_D^2 + \sigma_\epsilon^2)$, *i.e.*, σ_D^2/σ_T^2. The renewal model, incidently, is obtained by replacing D_i by its median $\hat{D}$ in equation (A–6)

[3] The slip in the last event, like the "constant" slip rate V, can only be estimated, of course, but that is a separate, parameter estimation problem discussed above and in the body of the report.

FIGURE CAPTIONS

Figure A–1. Graphical interpretation of $C_{30}^{T_e}$, the conditional probability of $T_e \leq T \leq T_c + 30$ given $T > T_e$.

Figure A–2. Conditional probability, $C_{30}^{T_e}$, of an earthquake in the next 30 years given an elapsed time of T_e years since the last event, for several values of σ, the degree of dispersion in the recurrence time distribution. (Assumption: $\hat{T} >> 30$)

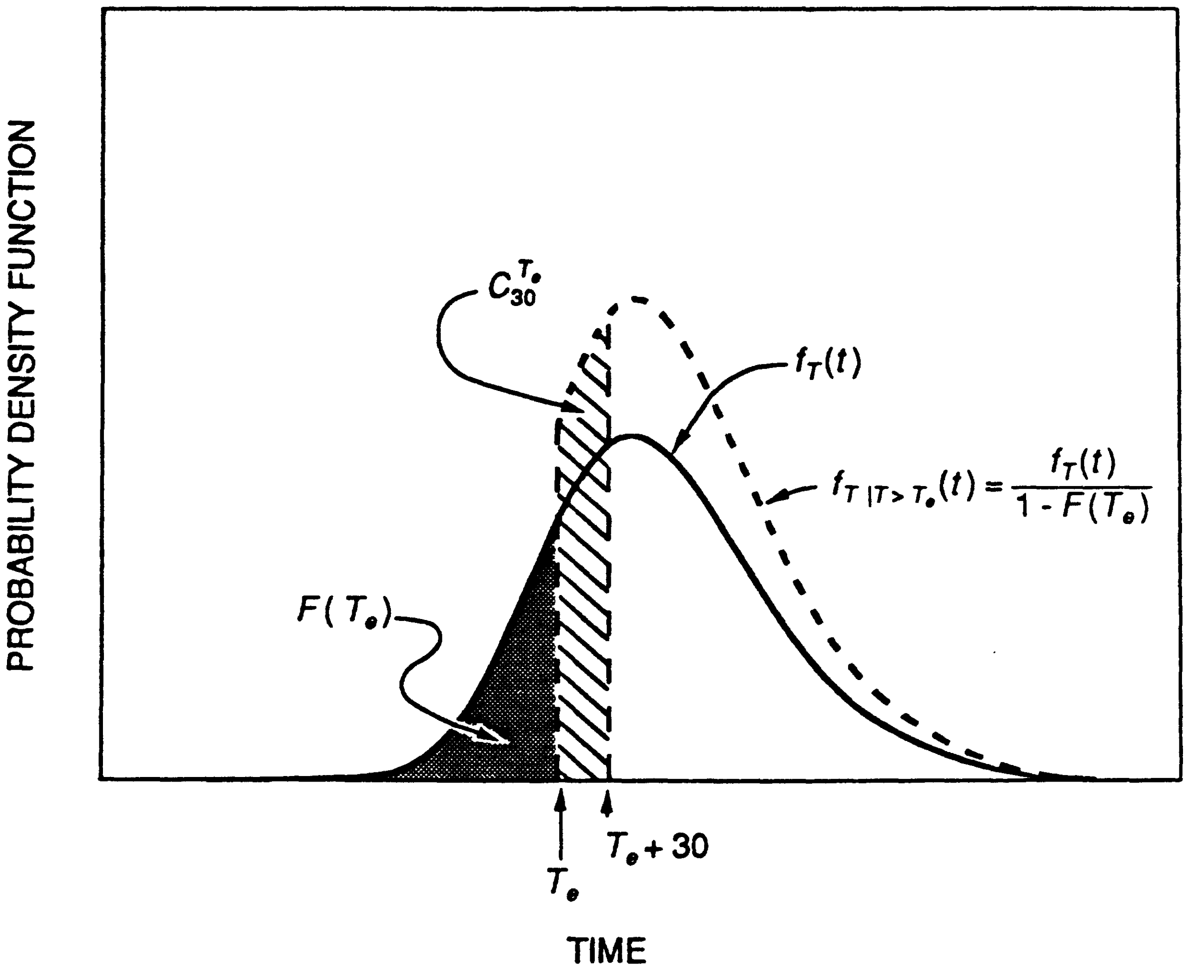
PROBABILITY DENSITY FUNCTION
$C_{30}^{T_e}$
$f_T(t)$
$f_{T|T>T_e}(t) = \frac{f_T(t)}{1 - F(T_e)}$
$F(T_e)$
T_e
$T_e + 30$
TIME

Fig. A-1

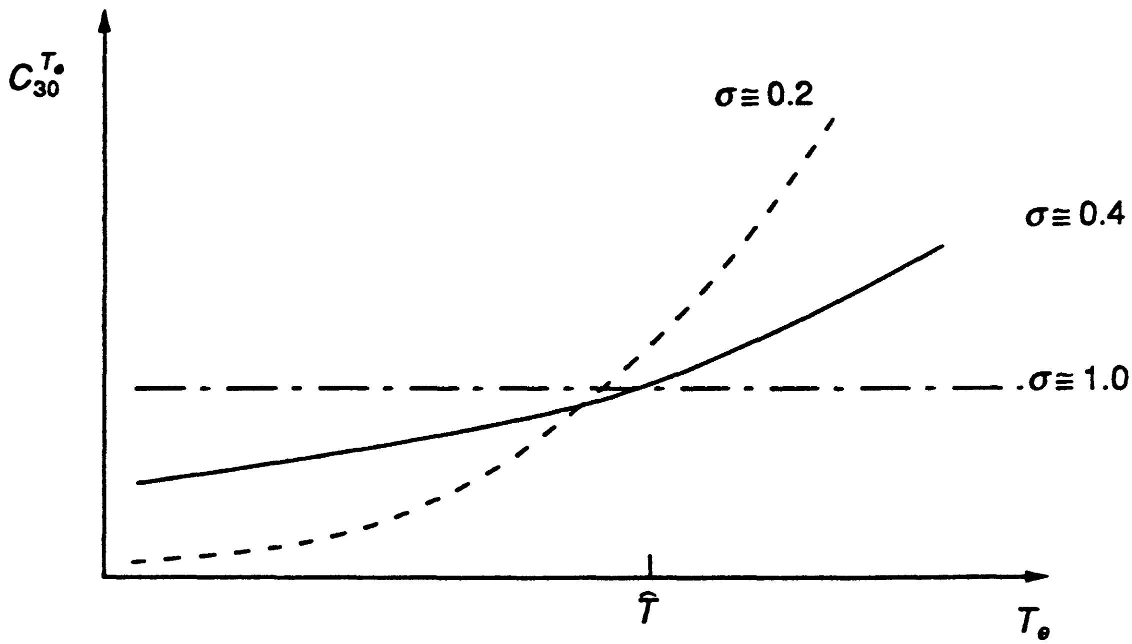

Fig. A-2

Appendix M

Discussion of the logic tree analysis, presented to NEPEC by J.Dieterich, April 30, 1990.

APPENDIX

LOGIC TREE ANALYSIS OF SAN ANDREAS FAULT PROBABILITIES

The Working Group has employed a logic tree to incorporate alternative interpretations of data and modeling of processes into the evaluation of earthquake probabilities. A logic tree analysis consists of specifying the alternatives for potential outcomes or interpretations of parameters. Relative weights or likelihoods that a specific alternative is the correct one are assigned at branch points in the analysis (nodes). The sum of the branch weights at each node totals 1.0. For this study, the weights are based on the judgments of the working group and consist of the simple average of weights polled from Working Group members.

Logic trees for earthquake probabilities on the southern Santa Cruz Mountains segment, San Francisco Peninsula segment the North Coast segment are illustrated in Figure B-1. Branch weights are indicated on the logic tree diagrams. The logic tree for the San Francisco Peninsula segment contains more branches than the others and serves as the basis for the following discussion.

Segmentation

The first node of the San Francisco peninsula segment logic tree arises from uncertainty over the segmentation of this part of the fault. The upper branch retains the single San Francisco Peninsula segment. The lower branch considers the possibility of earthquakes on two segments, the Northern Santa Cruz Mountains segment and the Mid-peninsula segment. These alternatives are discussed in the report. We have assigned a likelihood of

0.56 to the single-segment branch and a likelihood of 0.44 to the two-segment branch.

Recurrence Time

For each fault segment the next node represents the choice between models 1, 2 and 3 for estimating the median recurrence time, $\hat{T}$ and its associated parametric uncertainty, σ_P. The logic trees for the Southern Santa Cruz Mountains and North Coast segments have only this single branching point. The assigned weights for recurrence time models 1, 2 and 3 are 0.13, 0.47, and 0.40, respectively.

For models 1 and 2 the bases for the best estimate (the median) of $\hat{T}$ and its uncertainty measure, σ_P, are:

$$\hat{T} = D/V \quad , \quad \sigma_P = \sqrt{\sigma_D^2 + \sigma_V^2} \qquad \text{(B-1)}$$

Where, σ_P, σ_D , σ_V, are the standard deviations of the logs, respectively of the uncertain median, $\hat{T}$, slip in the last event, D, and slip rate, V. The value of σ_D was estimated by the coefficient of variation of D, *i.e.*, by the standard deviation of the estimate , s_D, divided by the best estimate of D. The segment displacements, D, used in the model 2 calculations were estimated using a separate logic tree described later in this Appendix.

For the case of model 3, $\hat{T}$ is based on $\hat{T}_{LP}$, the updated estimate of $\hat{T}$ for recurrence following the 1906 earthquake as given by equation (7) in the body of the report:

$$\hat{T}_{LP} = exp\left\{ \frac{\left[\frac{log132}{.31^2} + \frac{log83}{.21^2} \right]}{\left[\frac{1}{.31^2} + \frac{1}{.21^2} \right]} \right\} , \quad \sigma_P = \sqrt{\frac{1}{\frac{1}{.31^2} + \frac{1}{.21^2}}} \qquad \text{(B-2)}$$

The estimate $\hat{T}_{LP}$ is equivalent to the weighed product (*i.e.*, a geometric mean):

$$\widehat{T}_{LP} = 83^{W_1} 132^{W_2} = 83^{W_1} \left(\frac{D}{V} \right)^{W_2} \quad \text{(B-3)}$$

In which:

$$W_1 = 1 - W_2 , \quad W_2 = \left(\frac{\frac{1}{.31^2}}{\frac{1}{.31^2} + \frac{1}{.21^2}} \right) \quad \text{(B-4)}$$

Hence, from the definition of recurrence time model 3 (equation 6 in the report) the estimated recurrence time is:

$$\widehat{T} = 83^{W_1} \left(\frac{D}{V} \right)^{W_2} + \frac{\Delta D}{V} \quad \text{(B-5)}$$

Where D is the estimated 1906 slip at Loma Prieta (2.5 ± 0.6 m) and ΔD is the difference of 1906 slip on the segment of interest and the slip at Loma Prieta. The approximate squared standard deviation of $\log \widehat{T}$ can be found by first-order expansion (Benjamin and Cornell, 1970, p.180):

$$\sigma_P^2 \equiv \frac{1}{\widehat{T}^2} \left\{ \left[83^{W_1} V^{-W_2} W_2 D^{W_2 - 1} \right]^2 s_D + V^{-2} s_{\Delta D}^2 + \left[83^{W_1} (W_2 - 1) D^{W_2} 83^{W_1} - \Delta D V^{-2} \right]^2 s_V^2 \right\} \quad \text{(B-6)}$$

in which the s's are the standard deviations of the estimates of the indicated parameters.

Effect of Loma Prieta Stress Changes

The final node for the San Francisco Peninsula segment represents whether to accept or reject the calculations based on stress changes resulting from the Loma Prieta earthquake that reduce the expected recurrence time by an amount ΔT. The magnitude of ΔT is based on three-dimensional elastic dislocation calculations of the Loma Prieta earthquake slip that give the change of shear stress averaged over the entire segment of interest (Simpson and Dieterich, 1990). Details of the stress field in the zone of concentrated stresses near edge of the Loma Prieta rupture surfaceare particularly sensitive to model assumptions. Consequently, the magnitude of this effect is greatest, but possibly most uncertain for the Northern Santa Cruz Mountains segment which is relatively small and is situated adjacent to the Loma Prieta rupture. The branches for this node were independently weighted for the side of the tree having a single segment and for the side of the tree consisting of the two sub-segments. For the single San Francisco Peninsula segment, a weight of 0.84 was assigned to branches that use the stress calculation to modify the expected recurrence times and a weight of 0.16 was given to the branches that use the unmodified recurrence times. For the two-segment side of the tree, which considers the Northern Santa Cruz Mountains segment and the Mid-Peninsula segments, a weight of 0.33 was given to the branches that use the stress calculation to modify the expected recurrence times and a weight of 0.67 was given to the branches that use the recurrence times unmodified by the calculated stress.

The best estimates of the median recurrence interval from models **1** and **2** with the effect of Loma Prieta stresses included:

$$\hat{T} = \frac{D - D'}{V}\ ,\ \sigma_P = \sqrt{\sigma_{D-D'}^{2} + \sigma_{V}^{2}} \qquad \text{(B-7)}$$

Where D' is the equivalent displacement reduction resulting from the stress effect given previously in Table 4. For branches in which recurrence time is calculated using recurrence time model 3 with Loma Prieta stresses:

$$\hat{T} = 83^{W_1}\left(\frac{D}{V}\right)^{W_2} + \frac{\Delta D - D'}{V} \qquad \text{(B-8)}$$

As in the case of equation (B-6), the approximate squared standard deviation of $\log\hat{T}$ can be found by first-order expansion. The result is the same as (B-6) except that $(s^2_{\Delta D} + s^2_{D'})$ is used in place of $s^2_{\Delta D}$ and $(\Delta D - D')$ is used for ΔD.

Logic Tree for Model 2 Displacements

Recurrence times for model 2 are dependent on the displacement, D, assigned to each segment. As discussed in the report, the amount of displacement that best characterizes the behavior of each segment has been one of the most difficult parameters to constrain. This is a result of differences between the 1906 geologic and geodetic observations and the lack of slip data from the 1838 and 1865 earthquakes. To ensure that all possible interpretations were accounted for, displacement logic trees were constructed for the three possible San Andreas fault segments (San Francisco Peninsula, Northern Santa Cruz Mountains, and Mid-Peninsula). The displacements contained in each logic tree are values for which there was an observational basis or could be derived from a segment length/displacement relationship or could be based on other geologic arguments. The length/displacement relationship employed here is: $D = 2.8 \times 10^{-5} L$ (Working Group, 1988). Segment displacements and weights are given in Table B - 1.

The single San Francisco Peninsula segment contains four branches. Displacement values are: 1.8 m, from a direct calculation using a 60 km rupture length and the length/displacement relationship; 2.5 m, the maximum 1906 surface offset; an average of 1906 geologic and geodetic observations; and 3.5 m the maximum 1906 geodetic offset.

The Mid-Peninsula segment has three branches. Displacement values are: 1.1 m, the calculated value using a 40 km length and the length/displacement relationship; 2.5 m, the maximum measured 1906 surface offset; and 3.4 m, the maximum 1906 geodetic offset.

The Northern Santa Cruz Mountains segment contains five branches. Values are: 0.6 m, obtained using the rupture length of 22 km and the length/displacement relationship; 1.0 m, the maximum observed 1906 surface offset; 1.4 m, the 1906 Wright's tunnel offset, which even though located just south of this segment, had a displacement similar to 1989 and might be representative of displacements for this part of the fault; 2.6 m, the average 1906 geodetic slip; and 3.3 m, the maximum allowable 1906 geodetic offset.

Probabilities

Final consensus probability of a segment is based on the weighted probability of each tip of the logic tree for that segment. The probability of an earthquake is found using the parameters ($\hat{T}$, σ and T_e) appropriate to the branches leading to that tip. Probabilities for each segment tip are summarized in Appendix C. The final probability of a segment-rupturing earthquake is the sum of the weighted probabilities. The weighting factor for a tip is the product of the branch weights leading to that tip. For a given segment the sum of the weights equals 1.0.

For the San Francisco Peninsula segment, where two segmentation alternatives have been considered, segment probabilities are subject to additional weighting by the segmentation weights. For example, the 30-year probability of a earthquake affecting the entire San Francisco Peninsula segment is the segment probability of 0.25 multiplied by the weighting factor for that segmentation alternative (0.56) giving a probability of 0.14. Similarly, the 30-year probability of the alternate case, that of earthquakes affecting only the Northern Santa Cruz Mountains and Mid-peninsula segments are 0.44 x 0.41 = 0.18 and 0.44 x 0.20 = 0.09 respectively. The expected magnitude of an earthquake on the Northern Santa Cruz Mountains segment is about 6.5 compared to an expected magnitude of about 7.0 for both the San Francisco Peninsula and Mid-Peninsula segments.

Consequently, the total probability of an earthquake of about 7.0 originating on either the entire segment or the longer sub-segment is 0.14 + 0.09 = 0.23 .

Table B-1 Displacement Weights for Recurrence Time Model 2

Displacement (m)	Weight	Weighted Displacement
Northern Santa Cruz Mountains Segment		
0.6	0.06	0.04
1.0	0.15	0.15
1.4	0.36	0.50
2.6	0.42	1.09
3.3	0.01	0.03
		Final D = 1.80*
Mid-Peninsula Segment		
1.1	0.20	0.20
2.5	0.54	1.35
3.4	0.26	0.88
		Final D = 2.46*
Northern Santa Cruz Mountains Segment		
1.8	0.21	0.38
2.5	0.37	0.93
3.0	0.32	0.96
3.5	0.10	0.35
		Final D = 2.62

* Weighted displacements do no sum to the final displacement because of rounding error.

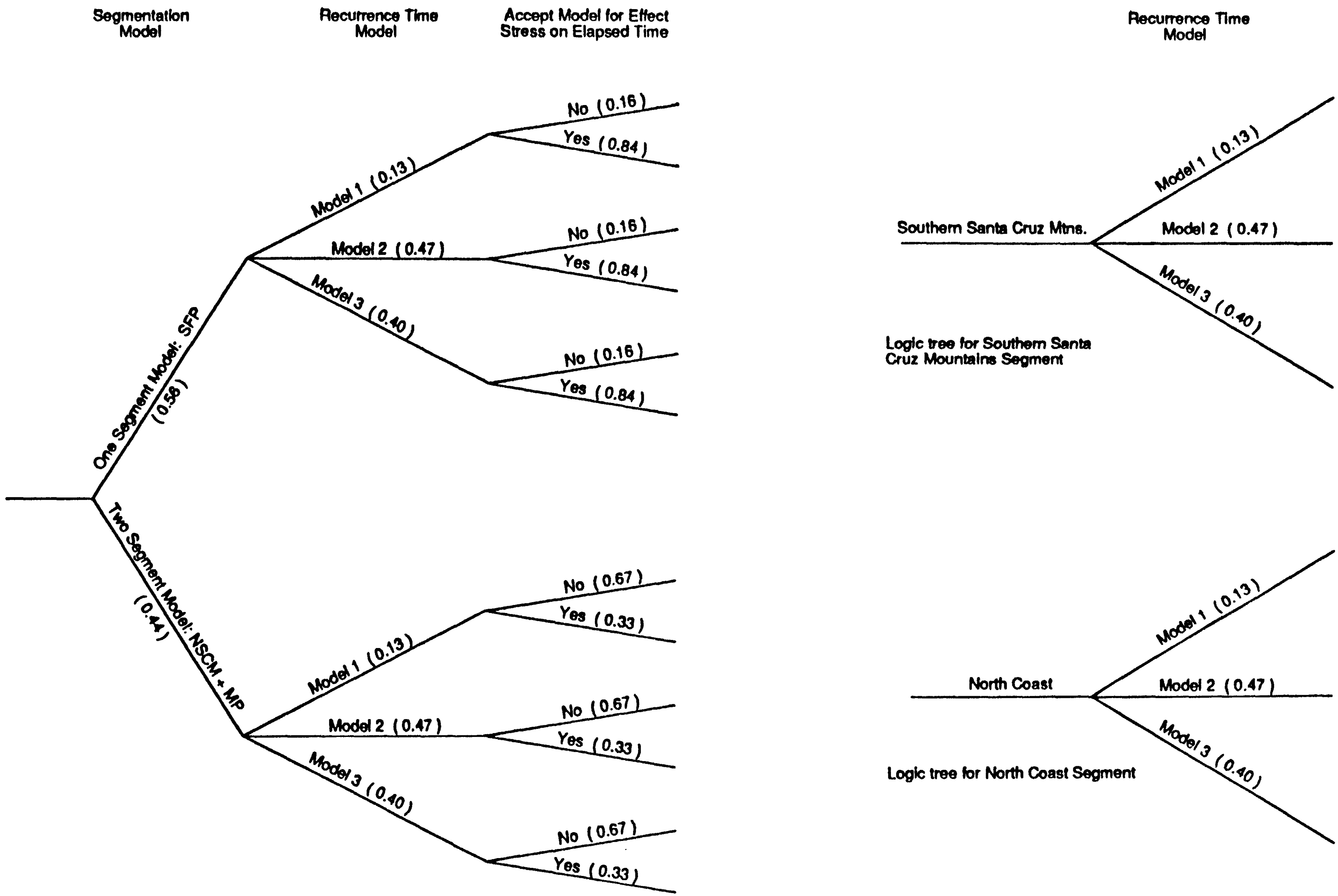

Logic tree for San Francisco Peninsula segment
( ) = assigned weight for hypothesis
SFP = San Francisco Peninsula segment
NSCM = Northern Santa Cruz Mountains segment
MP = Mid-Peninsula segment

Figure B - 1

APPENDIX

TABULATIONS OF PROBABILITIES

This appendix present tabulated results of probability calculations for intervals of 5, 10, 20 and 30 years. Although, the Working Group regards the these probabilities to be significant only to the nearest tenth, in the following, we report the probabilities to two decimal places to permit quantitative comparison of our results with other calculations.

Table C - 1 gives San Andreas fault segment probabilities for each of the logic tree branches for the described in Appendix B. The final segment probabilities are the weighted sum of the branch probabilities.

Table C - 2 lists the final segment probabilities for the San Andreas, Hayward and Rodgers Creek faults. The conditional probability obtained using the net uncertainty, σ_N and reported here corresponds to the mean of the probabilities one would obtain from a sufficiently large number of calculations using only the intrinsic uncertainty, σ_I and values of $\hat{T}$ repeatedly drawn from a lognormal distribution having the parametric uncertainty σ_P. Hence, it represents "the" probability because it has considered all possible values of $\hat{T}$ and their relative likelihoods.

In addition to the mean probabilities we report probabilities obtained using values of $\hat{T}$ at the first and third quartiles of the parametric distribution[1] and calculated with σ_I alone. These quartile probabilities provide a measure of the range of probabilities permitted by the parametric uncertainty. The probability at the first quartile, $P_{1/4}$ is the probability obtained using the value of $\hat{T}$ that is smaller than 75 percent of the recurrence times in the distribution. Hence, there is a 75 percent likelihood that the actual probability (i.e., the probability obtained if $\hat{T}$ were perfectly known) is less $P_{1/4}$ or a 25 percent likelihood that it is greater. Similarly, the probability of the third quartile, $P_{3/4}$ uses a value of $\hat{T}$ that is

---

[1]The parametric distribution on $\hat{T}$ needs to be updated to reflect the information (equation 2) that $T > T_e$. See Appendix A.

greater than 75 percent of the recurrence times in the distribution and there is a 75 percent likelihood that the actual probability is greater than $P_{3/4}$. There is a 50 percent chance that the actual probability lies between $P_{1/4}$ and $P_{3/4}$. For the San Andreas fault segments the quartiles were found by numerical integration of the weighted sum of the posterior parametric distributions (given $T > T_e$) employed in the logic tree analysis.

Table C - 1 Probabilities of Logic Tree Branch Tips

Model	Stress Effect	$\hat{T}$ (years)	σ_P	Weight	Probability for Intervals Beginning 1/1/90: 5	10	20	30
Southern Santa Cruz Mountains Segment (previous event = 1989)								
1	n. a.	100 ± 24	0.24	0.13	0.00	0.00	0.00	0.00
2	n. a.	84 ± 24	0.28	0.47	0.00	0.00	0.00	0.00
3	n. a.	96 ± 16	0.17	0.40	0.00	0.00	0.00	0.00
Northern Santa Cruz Mountains Segment (previous event = 1906)								
1	no	156 ± 45	0.28	0.09	0.02	0.04	0.09	0.15
1	yes	127 ± 45	0.34	0.04	0.04	0.09	0.19	0.29
2	no	95 ± 44	0.44	0.31	0.08	0.15	0.29	0.41
2	yes	70 ± 43	0.56	0.16	0.10	0.18	0.33	0.45
3	no	96 ± 36	0.37	0.27	0.09	0.17	0.32	0.45
3	yes	71 ± 43	0.56	0.13	0.10	0.18	0.33	0.45
Mid-Peninsula Segment (previous event = 1906)								
1	no	213 ± 60	0.27	0.09	0.00	0.01	0.02	0.03
1	yes	210 ± 60	0.27	0.04	0.00	0.01	0.02	0.04
2	no	129 ± 49	0.37	0.31	0.04	0.09	0.18	0.27
2	yes	127 ± 49	0.38	0.16	0.04	0.09	0.18	0.28
3	no	149 ± 31	0.21	0.27	0.02	0.03	0.09	0.16
3	yes	147 ± 30	0.20	0.13	0.02	0.04	0.09	0.17
San Francisco Peninsula Segment (previous event = 1906)								
1	no	188 ± 54	0.28	0.02	0.01	0.01	0.04	0.07
1	yes	176 ± 53	0.29	0.11	0.01	0.02	0.05	0.10
2	no	138 ± 40	0.28	0.08	0.03	0.06	0.14	0.23
2	yes	128 ± 38	0.29	0.39	0.04	0.09	0.18	0.29
3	no	138 ± 29	0.21	0.06	0.02	0.05	0.13	0.22
3	yes	129 ± 28	0.21	0.34	0.03	0.07	0.17	0.29
San Francisco Peninsula Segment (previous event = 1906)								
1	n. a.	281 ± 76	0.27	0.13	0.00	0.00	0.00	0.00
2	n. a.	237 ± 73	0.30	0.47	0.00	0.00	0.01	0.02
3	n. a.	201 ± 49	0.24	0.40	0.00	0.00	0.02	0.03

Table C - 2 Final Probabilities

Segment	Interval Beginning 1/1/90 (years)	Conditional Probability (Mean)	Quartile Probabilities $P_{1/4}$	$P_{3/4}$
S. Santa Cruz Mtns.	5	0.00	0.00	0.00
	10	0.00	0.00	0.00
	20	0.00	0.00	0.00
	30	0.00	0.00	0.00
N. Santa Cruz Mtns.[1]	5	0.03	0.05	0.00
	10	0.07	0.11	0.00
	20	0.13	0.22	0.02
	30	0.18	0.31	0.04
San Francisco Peninsula[2]	5	0.03	0.03	0.00
	10	0.06	0.08	0.00
	20	0.14	0.21	0.01
	30	0.23	0.38	0.02
North Coast	5	0.00	0.00	0.00
	10	0.00	0.00	0.00
	20	0.01	0.00	0.00
	30	0.02	0.01	0.00
S. East Bay	5	0.04	0.05	0.00
	10	0.08	0.12	0.00
	20	0.16	0.25	0.01
	30	0.23	0.40	0.02
N. East Bay	5	0.05	0.08	0.01
	10	0.10	0.16	0.01
	20	0.19	0.32	0.03
	30	0.28	0.46	0.06
Rodgers Creek	5	0.04	0.05	0.00
	10	0.07	0.11	0.01
	20	0.14	0.23	0.02
	30	0.22	0.35	0.04

1 Subsegment of the San Francisco Peninsula segment. Probability includes segmentation weight.

2 Weighted average of San Francisco Peninsula segment and the Mid-Peninsula sub-segment probabilities.

Appendix N

Criticism of some forecasts of NEPEC as presented by J.Savage, April 30, 1990.

Savage 4/90

CRITICISM OF SOME FORECASTS OF THE NATIONAL EARTHQUAKE PREDICTION EVALUATION COUNCIL

J.C. Savage

U.S. Geological Survey

345 Middlefield Road, MS/977

Menlo Park, California 94025

ABSTRACT

The Working Group on California Earthquake Probabilities has assigned probabiliies for rupture in the interval 1988–2018 to various segments of the San Andreas fault on the basis of the lognormal distribution of recurrence times of characteristic earthquakes postulated by Nishenko and Buland (1987). I question the validity of those probabilities on the basis of three separate arguments: 1) The distributions of recurrence times of the four, best-observed, characteristic–earthquake sequences are each only marginally consistent with the Nishenko-Buland lognormal distribution. 2) The range of possible 30–year conditional probabilities for many of the fault segments is so great due to uncertainty in the average recurrence time for that segment that the assigned probability is virtually meaningless. 3) The 1988 forecasts not subject to the foregoing objection are those in which there is a low probability of an earthquake in the near future (*e.g.,* only a 5% chance of rupture of the North Coast segment before the year 2049 and of the Carrizo segment before the year 2018). However, the same reasoning would assign only a 5% chance of rupture before mid–1993 to the south Santa Cruz Mountains segment, the segment that failed in October 1989.

Finally, the forecast of the next Parkfield earthquake (95% probability before 1993.0) by Bakun and Lindh (1985) depends upon an *ad hoc* explanation of the out–of–sequence 1934 earthquake. A less–contrived forecast would have assigned a conditional probability of about 60 ± 20% to the 1985.0–1993.0 interval and 30 ± 15% to the 1990.0–1993.0 interval.

INTRODUCTION

This paper is concerned with the assessments of the probability of future rupture of identified segments of the San Andreas fault as formulated by the Working Group on California Earthquake Probabilities (WGCEP) (Agnew *et al.*, 1988). The segments considered and the probabilities of rupture in the interval of 1988–2018 assigned to those segments are shown in Figure 1. The forecasts serve a valuable function in defining rupture segments and the expected earthquake magnitude on each. What I question here are the probability assessments.

The probability estimates of the WGCEP are based upon the hypothesis that the recurrence intervals T between characteristic earthquakes on a given fault segment are governed by the lognormal probability density distribution

$$p(T,\hat{T},\sigma) = [(2\pi)^{1/2}T\sigma]^{-1}exp\{-[lnT/\hat{T}]^2/2\sigma^2\} \tag{1}$$

where $\hat{T}$ is the median recurrence time and σ is the shape factor (Nishenko and Buland, 1987, p. 1387; the factor μ in that paper has been set equal to $-\sigma^2/2$ here to conform to the usual lognormal rotation). The average interval between earthquakes is then (Hastings and Peacock, 1974, p 84)

$$T_{av} = \hat{T}\exp(\sigma^2/2) \tag{2}$$

and the probability that rupture occur within the interval of duration T following the preceding rupture is

$$P(T,\hat{T},\sigma) = \int_0^T p(\tau,\hat{T},\sigma)d\tau \tag{3}$$

Nishenko and Buland (1987) suggested that the shape factor σ is 0.21 for all characteristic earthquake sequences, a supposition which I refer to as the Nishenko–Buland hypothesis. The Nishenko–Buland hypothesis greatly simplifies the use of (1) because then only one parameter $\hat{T}$ needs to be determined.

Rupture forecasts based upon (3) can be improved by including the information that the segment has not yet ruptured at the time at which the forecast is made. (See Davis *et al.*, 1989, for a more sophisticated utilization of this information.) Measure time from the instant after the preceding rupture of the segment, and let time T_1 be the time at which the forecast is formulated. Given that rupture has not yet occurred by time T_1, the conditional probability that rupture occur before time T is (Nishenko and Buland, 1987, p. 1392)

$$P_c(T,T_1,\hat{T},\sigma) = [P(T,\overline{T},\sigma) - P(T_1,\hat{T},\sigma)]/[1 - P(T_1,T,\sigma)] \tag{4}$$

Thus, given $T, T_1, \hat{T},$ and σ, evaluation of the conditional probability involves only simple integration. Indeed, because the lognormal distribution of T is equivalent to the normal distribution of $\ln T$ (mean $\ln \bar{T}$ and standard deviation σ; Hastings and Peacock, 1974, p. 88), integration is seldom required: Tables or computer programs for the evaluation of the normal distribution provide the necessary solutions.

Of the four parameters ($T, T_1, \bar{T}$, *and* σ) necessary to evaluate (4) only $\bar{T}$ is adjustable. T is chosen by the forecaster, T_1 is the time at which the forecast is formulated, and $\sigma = 0.21$ is given by the Nishenko–Buland hypothesis. Thus, for a given $\bar{T}$ there is a unique conditional probability $P_c(T, T_1, \bar{T}, 0.21)$. However, for any characteristic earthquake sequence $\bar{T}$ must be estimated, and such estimation inevitably involves uncertainty. Therefore, in practice, $\bar{T}$ must be replaced by $\bar{\mathbf{T}}_e$, a distribution of estimates reflecting the uncertainty in the estimation process.

Given a long historic record, sufficient recurrence intervals may have been observed to permit an estimate of $\bar{T}$. If n recurrence intervals T_i have been observed, the best estimates of $\ln \bar{T}$ and its standard error $\bar{\sigma}$ are (Nishenko and Buland, 1987, p. 1389–1390)

$$\ln \bar{T}_o = n^{-1} \sum_{i=1}^{N} \ln T_i \tag{5}$$

$$\bar{\sigma} = \sigma / n^{1/2} \tag{6}$$

Because $\ln T_i$ is normally distributed, so also is the estimate of $\ln \bar{T}$. It follows that $\bar{\mathbf{T}}_e$, the distribution of the estimates, is lognormal with median $\bar{T}_o$ and shape factor $\bar{\sigma}$.

In the absence of an adequate historical record, $\bar{T}$ may be estimated by the so-called direct method (Agnew *et al.*, 1988, p. 14). In the direct method the coseismic slip $u \pm \sigma_u$ measured after the preceding rupture is taken to represent an average event, and estimates of the secular slip rate $r \pm \sigma_r$ from geologic or geodetic data are assumed to be available. The average recurrence time is then $T_{av} = u/r$ with standard deviation $\sigma_{av} = T_{av}[(\sigma_u/u)^2 + (\sigma_r/r)^2]^{1/2}$. Estimates of u, σ_u, r, and σ_r for the various fault segments are given by Agnew *et al.*(1988, Table 1). The mean $\bar{T}_o$ and the standard deviation σ_m of $\bar{\mathbf{T}}_e$, the distribution of the estimates of $\bar{T}$, follows from (2).

Because either method of estimating $\bar{T}$ results in a distribution $\bar{\mathbf{T}}_e$, each sample of which implies a different conditional probability, the resultant conditional probability must itself be represented by a distribution, the breadth of which indicates the uncertainty in the assigned conditional probability. Nishenko and Buland (1987, pp. 1392–1393) recognized this uncertainty and suggested that conditional probabilities be quoted as a range of probabilities representative of the distribution $\bar{T}_e$. For example if $\bar{T}_e$ were normally distributed, one could quote the range of conditional probabilities corresponding to the 90% confidence interval for $\tilde{T}$ (*i.e.*, $\tilde{T} = \tilde{T}_o \pm 1.65\ \sigma_m$)

TEST OF THE NISHENKO–BULAND HYPOTHESIS

Nishenko and Buland (1987) postulate that the recurrence intervals for characteristic earthquakes are lognormally distributed with a unique shape factor $\sigma = 0.21$. This is an easy proposition to test. The hypothesis implies that $\ln(T/\tilde{T})$ is normally distributed with standard deviation $\sigma = 0.21$. Given a sequence of n observed recurrence intervals T_i, form the χ^2 statistic

$$\chi^2 = \sum_{i=1}^{n} (\ln T_i/\tilde{T}_o)^2/(0.21)^2 \tag{7}$$

where $\tilde{T}_o$ is determined from (5). The probability that a larger χ^2 would result from n random recurrence intervals drawn from the lognormal distribution (1) with $\sigma = 0.21$ is then given by the χ^2 distribution with $n-1$ degrees of freedom (Crow *et al.*, 1960, p. 70). Too large or too small a probability would be taken as evidence against the Nishenko–Buland hypothesis.

Nishenko and Buland (1987) have listed observed recurrence intervals for 15 different characteristic earthquake sequences where three or more consecutive ruptures have been observed. In two of these sequences recurrence intervals were determined by ^{14}C dating, which introduces uncertainty in the duration of the recurrence intervals. Of the historically dated earthquake sequences, most contain only two or three recurrence intervals, too few for a discriminating χ^2 test. The observed recurrence intervals T_i for the remaining four characteristic earthquake sequences are shown in Table 1 along with the probability that a random sample from (1) with $\sigma = 0.21$ would result in a larger χ^2.

The probabilities in Table 1 indicate that the four, best-documented recurrence sequences are not adequately described using the single shape factor $\sigma = 0.21$. Recall that too good a fit, (*e.g.*, $P > 0.95$) is as unacceptable as too poor a fit (*e.g.*, $P < 0.05$) (see

Jeffreys, 1948, pp. 281–282.) The Chilean data fit the distribution too well, suggesting that $\sigma = 0.21$ may be too large, whereas the Japanese and California data fit the distribution poorly, suggesting that the value $\sigma = 0.21$ is too small. Indeed, a standard F-test (Crow *et al.*, 1960, p. 74) shows that of the two distributions most compatible with $\sigma = 0.21$ in Table 1, the Miyagi–Oki and the Concepcion sequences, the former has a significantly (90% confidence level) larger shape factor σ than the latter. Although each of the four earthquake sequences is marginally consistent with the postulated ($\sigma = 0.21$) lognormal distribution, it is very unlikely that all four sequences should be only marginally consistent if the postulated distribution were in fact correct. Using a Monte Carlo simulation, I estimate that the probability that four sequences drawn at random would show worse agreement than that shown by the samples in Table 1 is about one in 250. If account were taken of the fact that these very samples were used to estimate the shape factor $\sigma = 0.21$ tested, the odds would be even longer. Moreover, there is evidence in Table 1 for at least two different distinct values of σ, a small value for the Chilean sequences and a larger value for the other two sequences.

DISTRIBUTION OF CONDITIONAL PROBABILITIES

In this section I reassess the WGCEP conditional probability estimates for rupture of various segments of the San Andreas fault. Although I question the validity of the Nishenko–Buland hypothesis, I constrain σ in (1), (2), (3), and (4) to the value 0.21 to be consistent with the WGCEP. Finally, I consider only fault segments for which the estimate of $\bar{T}$ has been made by the so-called direct method (Agnew *et al.*, 1988, Table 1 and p. 14) in which T_{av} is taken to be the quotient of the coseismic slip and the secular slip rate. Finally, I assume that the estimate of the parameter $\bar{T}$ is represented by a normal distribution $\bar{\mathbf{T}}_e$.

Because each sample $\bar{T}_e$ from the distribution $\bar{\mathbf{T}}_e$ yields a separate conditional probability, the distribution of estimates $\bar{T}_e$ necessarily implies a distribution of conditional probabilities. To evaluate the distribution of conditional probabilities I use a Monte Carlo technique, calculating 300 values of the conditional probability, one for each sample $\bar{T}_e$ drawn from a random number generator programmed for the normal distribution $\bar{\mathbf{T}}_e$.

Given these 300 conditional probabilities, one can plot a histogram showing how frequently each range of cumulative conditional probabilities has been observed. In this paper the histogram is plotted for deciles (0 to 10%, 10 to 20%, ..., 90 to 100%) in the conditional probabilities in most cases. The histograms shown are the average of the results of two runs of 300 random samples each. The results of the two runs in each case were reasonably consistent, and the average of the two is thought to be a fair representation of the conditional probability distribution.

In cases where the estimate of the distribution $\bar{\mathbf{T}}_e$ depends upon the direct method, one can use the information that an earthquake has not yet occurred at time T_1 (the nominal time of the forecast) to improve the estimate of the distribution $\bar{\mathbf{T}}_e$. This is a straightforward application of inverse probability (Jeffreys, 1948, p. 29). The distribution $\bar{\mathbf{T}}_e$ describes the prior probability of a given value of $\tilde{T}_e$. The likelihood that a value of $\tilde{T}_e$ is consistent with the observation that rupture has not yet occurred at time T_1 is

$$w(T_1, \tilde{T}_e) = 1 - P(T_1, \tilde{T}_e, 0.21) \quad (8)$$

Then the posterior probability of $\tilde{T}_e$ is proportional to the product of w and the prior probability of $\tilde{T}_e$.

One can easily incorporate this posterior estimate of the probability of $\tilde{T}_e$ into the Monte Carlo estimate of the conditional probability distribution. Draw a sample $\tilde{T}_e$ from the prior distribution $\bar{\mathbf{T}}_e$. Using this value of $\tilde{T}_e$, calculate both a conditional probability (4) and a weight (8) for the given values of T and T_1. Repeat this process with a new $\tilde{T}_e$ drawn from $\bar{\mathbf{T}}_e$ until an adequate sample of conditional probabilities and associated weights have been assembled. Now determine the distribution of this sample by summing the weights of the conditional probabilities in each quantile of the histogram. The frequency for each quantile is the sum of the weights of all conditional probabilities in that quantile divided by the sum of all weights. I refer to this histogram as the weighted distribution. The simple mean of the weighted distribution is the conditional probability reported by the WGCEP (see appendix).

Figure 2 shows the 30-year conditional probability distributions for the San Bernardino segment of the San Andreas fault. Because the weighting diminishes the contributions from small values of $\hat{T}_e$, which are associated with large values of conditional probability, conditional probabilities in the 70–100% range are strongly attenuated in the weighted distribution (Figure 2a) relative to the unweighted distribution (Figure 2b). Both the weighted and unweighted distributions are so broad that one hesitates to choose a single value to represent the conditional probability distribution for the segment. The WGCEP chose the mean value of the weighted distribution (arrow in Figure 2a) as representative of the distribution.

Figure 3 shows the 30–year conditional probability distributions for the Mojave segment of the San Andreas fault. The weighted distribution (Figure 3a) is deficient in the 80 to 100% probability range relative to the unweighted distribution (Figure 3b) for the same reason as given for the San Bernardino segment. The unweighted distribution is so flat that there is no single preferred probablity; the mean value is preferred only in the sense that, being at the center of the distribution, it minimizes the risk of being too far wrong. The weighted distribution (Figure 3a) is informative principally in that it virtually excludes probabilities in the 80 to 100% range. The WGCEP chose the mean value of the weighted distribution (arrow in Figure 3a) to represent the distribution.

Figure 4 shows the 30–year conditional probability distributions for the Cholame segment of the fault. Once again the weighted distribution (Figure 4a) is deficient in the 80 to 100% probability range relative to the unweighted distribution (Figure 4b). Clearly, the most likely probability in both distributions lies in the first decile. However, the distributions are sufficiently broad that one would have little confidence that this most likely choice would in fact be the correct choice. The WGCEP chose the mean value of the weighted distribution (arrow in Figure 4a) to represent the distribution.

Figure 5 shows the weighted 30–year conditional probability distributions for the San Francisco peninsula (Figure 5a) and southern Santa Cruz Mountains (Figure 5b) segments of the San Andreas fault. For these segments the estimated recurrence times (roughly 150 $\pm$ 45 yr) lie on the high side of the interval (82 to 112 yr) for which the probability of rupture is forecast. The probability of rupture before the beginning of that interval is then small, and the weights (8) are all near 1. Thus, the weighted and unweighted conditional probability distributions are very similar, and it suffices to show only the weighted distribution. For both fault segments the most likely conditional probability lies in the first decile. If the objective is to identify the decile in which the actual conditional probability lies, one would do better to choose the mode rather than the mean of the distribution. The WGCEP chose the mean values (arrows in Figure 5) to represent the distributions.

For the North Coast and Carrizo segments of the San Andreas fault the 30–year conditional probability distributions are concentrated almost wholly in the first decile. Thus, I have calculated the distribution for those segments by percentile, of which the first decile is shown in Figure 6. Because there are only minor differences between the weighted and unweighted distributions for these segments, only the weighted distributions are shown. The distributions in Figure 6 suggest that the probability of rupture of either segment before the year 2018 is small. I think both distributions are better described by the mode (less than 1%) than by the mean, but the difference is not likely to be significant. The WGCEP preferred to use the mean (arrow in Figure 6) to represent the distributions.

Because of the southern Santa Cruz Mountains segment of the San Andreas fault has ruptured recently, it is of interest to ask what odds the WGCEP would have set in 1988 on such an occurrence. Using the usual criterion that 5% is a low risk, the WGCEP might have solved for the time interval at which the cumulative conditional probability would reach 5%. As shown in Figure 7 the mean of the conditional probability distribution attains 5% in 1993.5. Only the first decile of the distribution is shown in Figure 7. An additional 12% of the distribution is found in the second decile, 3% in the third, and less than 1% in the fourth. Because the WGCEP used only the mean value of the weighted conditional probability distribution in assessing risk, they should have concluded that there was only a 5% risk of rupture of the southern Santa Cruz Mountains segment before mid–1993. Yet, the Loma Prieta earthquake did rupture that segment in 1989 (U.S. Geological Survey Staff, 1990). Thus, an event has occurred which would be regarded as unlikely on the basis of the set of hypotheses used to formulate the forecast. Such a circumstance is generally interpreted as evidence against the hypotheses. Although the forecast for the southern Santa Cruz Mountains segment was assigned the lowest level of reliability by the WGCEP, that was done on the basis of uncertainty in the segment geometry (Agnew *et al.*, 1988, p.

17), a geometry which proved to be correct. Thus, forecasts for the southern Santa Cruz Mountains segment should have been reasonably reliable by the standards of the WGCEP, and failure to anticipate imminent failure of the southern Santa Cruz Mountains segment of the San Andreas fault casts doubt upon the reliability of other WGCEP forecasts.

THE PARKFIELD SEGMENT

The occurrence of six consecutive earthquakes on the Parkfield segment during historic time furnishes a sufficient number of observed recurrence intervals to estimate both $\bar{T}$ and σ in a lognormal distribution of recurrence times for that segment. That is, sufficient data are available that one need not invoke the Nishenko–Buland hypothesis ($\sigma = 0.21$) to describe the distribution of recurrence times. The best estimate of $\bar{T}$ can be found from (5) and the best estimate of σ from (Hastings and Peacock, 1974, p. 86)

$$\sigma^2 = \sum_{i=1}^{n} [\ln T_i/\bar{T}]^2/(n-1) \qquad (9)$$

where $\bar{T}$ has been determined from (5) and n is the number of available recurrence times T_i. For the Parkfield data n (Table 1) = 5, and the best estimates of $\bar{T}$ and σ are 20.9 yr and 0.35. Because $\bar{T}$ and σ are estimated from a limited set of data, both are uncertain and should be represented by distributions. Although the distributions that govern the estimates of $\ln \bar{T}$ and σ are known (Arley and Buch, 1950, pp. 93–95), it is more convenient to generate those distributions directly by a Monte Carlo method. Suppose the distribution of recurrence times is actually given by a lognormal distribution with the parameters just calculated, median $\bar{T}_o = 20.9$ yr and shape factor $\sigma = 0.35$. Call this the parent distribution. Generate five random values of the recurrence time T from the parent distribution and calculate estimates $\bar{T}_e$ and σ_e of the median and shape factor of the parent distribution using (5) and (9). This, of course, is the same procedure used to estimate the median and shape factor of the parent distribution from the five observed Parkfield recurrence times. One can now calculate the conditional probability and its weight for any given values of T and T_1 using (4) and (8) in a lognormal distribution with the estimated parameters $\bar{T}_e$ and σ_e. By repeating the entire cycle beginning with sampling the parent distribution to obtain new estimates of $\bar{T}_e$ and σ_e one can obtain additional conditional probabilities until a sufficient sample of the conditional probabilities so generated is obtained. A histogram can then be constructed to represent the distribution of conditional probabilities that would be expected if the parent lognormal distribution were actually correct. That histogram then represents the best estimate of the conditional probability and its uncertainty.

Weighted conditional probability distributions for rupture of the Parkfield segment before 1993 as might have been constructed in 1985 and 1990 are shown in Figure 8. The forecasts differ in that the 1990 forecast (Figure 8b) includes the additional information that rupture did not occur in the 1985–1990 interval. Despite the availability of five observed recurrence intervals, the conditional probability distributions in Figure 8 are relatively broad. The problem is that two parameters $\bar{T}$ and σ must be defined by just five observed recurrence intervals. This information is adequate to define $\bar{T}$ and σ only within broad confidence limits (at the 95% confidence level $15.2 < \bar{T} < 28.8$ yr and $0.21 < \sigma < 1.01$). The situation would clearly be improved if σ could be specified by some external relation such as the Nishenko–Buland hypothesis.

Bakun and Lindh (1985) proposed a model of the Parkfield segment in which the probability of rupture before 1993.0 was stated to be 95%. The model is based upon the observation that the 1934 rupture in the Parkfield sequence (ruptures in 1857, 1881, 1901, 1922, 1934, and 1966) apparently occurred 10 years too early. That is, had the 1934 rupture occurred in 1944, the recurrence intervals would have been much more closely grouped around the mean value 21.9 yr. The 1934 earthquake did occur at about the time normal seismicity following the post-aftershock quiescence was expected to resume. Thus, it is possible that the 1934 earthquake was triggered prematurely by background seismicity which happened to occur close to the nucleation region for the Parkfield earthquakes. On this basis Bakun and Lindh extrapolated the time of occurrence of past Parkfield earthquakes, omitting the 1934 event, to predict that the next event would occur in 1988.0 ± 5.0 yr (95% confidence interval). On that basis the conditional probability in 1985.0 that the Parkfield segment would rupture before 1993 was 97%; by 1990.0 the conditional probability became 88%. Both conditional probabilities are substantially higher than the comparable mean conditional probabilities in Figure 8.

DISCUSSION

The WGCEP forecasts are based upon the hypothesis that recurrence intervals for characteristic earthquake sequences are distributed lognormally with shape factor $\sigma = 0.21$. For such a distribution 95% of the recurrence intervals should lie in the interval $0.66\ \hat{T} < T < 1.52\ \hat{T}$ where $\hat{T}$ is the median recurrence time for the particular fault segment. Thus, one could be 95% confident that the next rupture will occur in the interval $0.66\ \hat{T}$ to $1.52\ \hat{T}$ after the preceding rupture. The breadth of the confidence interval precludes precise prediction of an individual event. However, given $\hat{T}$ the distribution of recurrence times would be known, and one can then calculate a precise probability that rupture will occur in any particular time interval. Of course, $\hat{T}$ will not be known precisely, and the uncertainty in $\hat{T}$ will introduce a corresponding uncertainty into the probability estimate.

There are two separate estimates of $\hat{T}$, a prior estimate $\bar{\mathbf{T}}_e$, which is calculated by the direct method (coseismic slip/slip rate), and a conditional estimate, which is the prior estimate updated by the information that rupture had not yet occurred at time T_1 after the previous earthquake. The unweighted distribution of conditional probability is calculated from the prior estimate of $\hat{T}$, and the weighted distribution is calculated from the conditional estimate of $\hat{T}$. In general, one should prefer the conditional estimates of $\hat{T}$ and the weighted distribution of conditional probability. The likelihood used in deriving the conditional estimate from the prior distribution $\bar{\mathbf{T}}_e$ assumes that recurrence intervals are distributed as $P(T, \hat{T}_e, 0.21)$, the same assumption used in deriving the conditional probability. If that distribution is not correct, one has compounded the error by using the distribution to calculate both weights and conditional probabilities.

Figure 9 shows these two estimates of T_{av} for the southern Santa Cruz Mountains segment of the San Andreas fault as well as a third estimate made after the occurrence of the Loma Prieta earthquake. The prior estimate in Figure 9 is related to the distribution $\bar{\mathbf{T}}_e$ by (2). The conditional estimate is the prior distribution modified according to the condition that rupture had not occurred by 1988.0. The posterior distribution is the prior distribution revised in the light of the occurrence of the Loma Prieta earthquake using inverse probability (posterior probability is proportional to the product of the likelihood and prior probability; Jeffreys, 1948, p. 29). The prior estimate is a normal distribution with mean 125 yr and standard deviation 36.8 yr, and the likelihood of the Loma Prieta event for a given T_{av} is $p(T_2, \hat{T}, 0.21)$ where $\hat{T}$ is related to T_{av} by (2) and T_2 is the interval between the Loma Prieta event and the previous earthquake ($T_2 = 1989.8 - 1906.3 = 83.5$ yr). The posterior probability is then the product of the prior probability and the likelihood divided by the integral of that product over $\hat{T}_e$. The posterior probability (Figure 9) is more sharply peaked than the prior probability and the mean value is shifted toward smaller T_{av}. The posterior probability distribution is also the estimate as of 1990.0 of the time to the next rupture of the southern Santa Cruz Mountains segment of the San Andreas fault. The 95% confidence interval for time of the next rupture of the southern Santa Cruz Mountains segment is 2054 to 2126 for the posterior distribution and 2043 to 2187 for the prior distribution. The former interval is half of the latter. If one assumes that posterior distribution is the most nearly correct, it is clear from Figure 9 that the weighting involved in constructing the conditional distribution from the prior distribution has skewed the conditional distribution in the wrong direction. That is, the prior distribution is more nearly correct than the conditional distribution

Clearly, the mean values alone are not an adequate description of the weighted distributions shown in Figures 2 through 4. Some indication of the breadth of the distribution should be included. That information could be conveyed by quoting the standard deviation (square root of the variance) of the distribution. The conditional probability then could be quoted as the mean value $\pm$ the standard deviation of the distribution. For example, the weighted 30-year conditional probabilities are: San Bernardino (Figure 2), $41 \pm 20\%$; Mojave (Figure 3), $39 \pm 23\%$; and Cholame (Figure 4), $35 \pm 25\%$. The Parkfield conditional probabilities (Figure 8) are for 1985-1993, $62 \pm 18\%$ and for 1990-1993, $32 \pm 15\%$. Notice that the quoted values refer to the conditional probability and its standard deviation not to the mean value and its standard deviation.

The probability distributions in Figures 5, 6, and 7 are heavily skewed toward the low–probability end of the distribution. For those distributions the mode may be a better representation of the risk than the mean. The choice depends upon the objective of the risk analysis. The mode identifies the most likely value of the conditional probability whereas the mean minimizes the risk of being very far wrong. The difference between the mean and the mode may be appreciable (*e.g.,* 25% in Figure 5b).

Conditional probability distributions for very high and very low risks are compact, (*e.g.,* Figure 6), but the distribution for intermediate risks tend to be broad (Figure 2, 3, and 4) unless the distribution $\bar{\mathbf{T}}_e$ is sharply peaked. This tendency is shown in Figure 10 for the Cholame segment of the San Andreas fault. The risk has been increased by lengthening the interval covered by the conditional probability in 20–year increments. By making the interval short (20-year conditional probability, Figure 10a) probability is concentrated at the low end. For 40– and 60–year intervals (Figure 10b and c) the conditional probability distribution is relatively flat. Finally, for a 80–year interval (Figure 10d) the probability concentrates at the high end. This indicates that the conditional probability is not resolved beyond broad categories such as low (10% or less), intermediate (10 to 90%), and high (90% or more) risk. A more quantitative assessment is not justified.

How should one assess the probability that the Parkfield segment will rupture before 1993? Compound probability provides a framework for such an assessment. Let Q denote the validity of the Bakun–Lindh hypothesis (essentially that the probability of rupture of the Parkfield segment is normally distributed with mean 1988.0 and standard deviation 2.5 yr) and $\sim Q$ denote the contrary. Let x denote the proposition that rupture will occur on the Parkfield segment before 1993 and H denote the condition that rupture had not yet occurred by 1990. Finally, let Prob $(x \mid Q, H)$ denote the probability of x given Q and H. Then

$$\text{Prob}(x) = \text{Prob}(x \mid Q, H)\ \text{Prob}(Q \mid H) + \text{Prob}(x \mid \sim Q, H)\ \text{Prob}(\sim Q \mid H) \qquad (9)$$

The likelihoods $\text{Prob}(x \mid Q, H)$and $\text{Prob}(x_y \mid \sim Q, H)$ are taken from the previous section to be 0.88 and 0.32. The latter choice is based upon an arbitrary identification of $\sim Q$ with the model of Figure 8. Thus,

$$\text{Prob(x)} = 0.88\ \text{Prob(Q | H)} + 0.32\ \text{Prob}(\sim \text{Q | H}) \tag{10}$$

The choice of $\text{Prob}(Q \mid H)$ and $\text{Prob}(\sim Q \mid H)$ is subjective, but, of course, the two must sum to 1. In the absence of any compelling reason to prefer Q to $\sim Q$, I assign 0.5 to both probabilities. The resulting estimate of $\text{Prob}(x)$ is 0.60. Other choices are clearly possible, but the range of values is $0.32 < \text{Prob}(x) < 0.88$.

In 1993 one will have the opportunity to reassess the hypotheses Q and $\sim Q$ on the basis of whether or not rupture of the Parkfield segment has occurred. This is a simple application of inverse probability, the posterior probability being proportional to the product of the likelihood and the prior probability (Jeffreys, 1948, p. 29). Let y denote that the Parkfield segment ruptures before 1993 and $\sim y$ denote the contrary. Then

$$\text{Prob}(Q \mid y, H) = 0.88\ \text{Prob}(Q \mid H)/\text{Prob}(x)$$

$$\text{Prob}(Q \mid \sim y, H) = 0.12\ \text{Prob}(Q \mid H)/\text{Prob(x)}$$

where $\text{Prob}(x)$ is given in (10). The corresponding probabilities for $\sim Q$ are obtained by subtracting the above posterior probabilities from 1. If the prior probabilities Prob $(Q \mid H)$ and $\text{Prob}(\sim Q \mid H)$ are both 0.5 then

$$P(Q \mid y, H) = 0.73 \qquad P(\sim Q \mid y, H) = 0.27$$

$$P(Q \mid \sim y, H) = 0.15 \qquad P(\sim Q \mid \sim y, H) = 0.85$$

None of these posterior probabilities is particularly large or particularly small. Thus, the occurrence or nonoccurrence of rupture of the Parkfield segment before 1993 will not be decisive in choosing between Q and $\sim Q$.

CONCLUSIONS

There does not appear to be convincing evidence that the distribution of recurrence times for a fault segment subject to characteristic earthquakes is lognormal with shape factor 0.21. If the distribution is lognormal, the evidence suggests that different shape factors are associated with different fault segments.

The uncertainties in the estimates of median recurrence time for individual fault segments limits resolution in estimating conditional rupture probabilities. Specifically, the breadth of the distribution of conditional probabilities calculated in this paper is such that resolution beyond low (below 10%), intermediate (10 to 90%), and high (above 90%) does not seem justified. Nor is a ranking of risks in the intermediate range where risks differ only by 20 to 30% generally significant. Ranking should be based upon a comparison of probability distributions not simply a comparison of mean values of the distribution.

Finally, the very high (95%) probability for rupture of the Parkfield segment cited by Bakun and Lindh (1985) is conditional upon acceptance of a model in which the 1934 Parkfield earthquake is regarded as an exceptional event. Those authors explicitly recognized this dependence and cited a lower probability (67%) on an alternative hypothesis (Bakun and Lindh, 1985, note 29, p. 624). This distinction was not clearly conveyed by National Earthquake Prediction Evaluation Council who endorsed the Parkfield prediction citing the higher (95%) probability (Shearer, 1985a, p. 9; 1985b, p. 175).

REFERENCES

Agnew, D.C., C.R. Allen, L.S. Cluff, J.H. Dieterich, W.L. Ellsworth, R.L. Keeney, A. G. Lindh, S.P. Nishenko, D.P. Schwartz, K.E. Sieh, W. Thatcher, and R.L. Wesson (1988). Probabilities of large earthquakes occurring in California on the San Andreas fault, U.S. Geological Survey Open-File Report 88-398, Reston, Virginia.

Arley, N., and K.R. Buch (1950). Probability and Statistics, John Wiley & Sons, New York.

Bakun, W.H., and A.G. Lindh (1985). The Parkfield, California, earthquake prediction experiment, Science, 229, 619-624.

Crow, E.L., F.A. Davis, and M.W. Maxfield (1960). Statistics Manual, Dover, New York.

Davis, P.M., D.D. Jackson, and Y.Y. Kagan (1989). The longer it has been since the last earthquake, the longer the expected time till the next? Bull. Seismol. Soc. Am., 79, 1439-1456.

Hastings, N.A.J., and J. B. Peacock (1974). Statistical Distributions, Butterworths, London.

Jeffreys, H., Theory of Probability 2nd Ed. (1948). Oxford Univ. Press, London.

Shearer, C.F. (1985a). Minutes of the National Earthquake Prediction Evaluation Council, November 16-17 1984, U.S. Geological. Survey Open File Report 85-201, Reston, Virginia.

Shearer, C.F. (1985b). Minutes of the National Earthquake Prediction Evaluation Council March 29-30, 1985, U.S. Geological Survey Open File Report 85-507, Reston, Virginia.

U.S. Geological Survey Staff (1990). The Loma Prieta, California, earthquake, an anticipated event, Science, 247, 286-293.

APPENDIX

This appendix is concerned with the relation between the Monte Carlo technique used in this paper to evaluate the earthquake risk and the method employed by the WGCEP. Let $p(T,\bar{T},\sigma)$ denote the lognormal density distribution (1) and $P(T,\bar{T},\sigma)$ denote the associated cumulative distribution (3) of recurrence times T. $\bar{T}$ is the median recurrence time and σ is the shape factor. The Nishenko–Buland hypothesis requires that the recurrence times T for a characteristic earthquake sequence have the distribution $P(T,\bar{T},0.21)$ where $\bar{T}$ must be estimated for each sequence. Any estimate of $\bar{T}$ involves uncertainty so that the estimates of $\bar{T}$ are represented by a distribution $\bar{\mathbf{T}}_e$. Thus, there will be a corresponding probability distribution $P(T, \bar{\mathbf{T}}_e, 0.21)$. That is, there will not be a unique probability that the recurrence time is less than some value T but rather a distribution of such probabilities, each probability associated with a particular value of the random variable $\bar{T}_e$. Then the risk of an earthquake in the interval of duration T following the preceding rupture is given by the distribution of probabilities $P(T, \bar{\mathbf{T}}_e, 0.21)$.

The WGCEP has used another approach to evaluating the earthquake risk $P(T,\bar{T},0.21)$. They assume that $\bar{\mathbf{T}}_e$ is a lognormal distribution with median $\bar{T}_o$ and shape factor σ_m. This implies that $\ln \bar{T}_e$ is normally distributed with mean $\ln \bar{T}_o$ and standard deviation σ_m. Furthermore, Nishenko and Buland (1987) concluded that $\ln(T/\bar{T})$ is normally distributed with zero mean and standard deviation 0.21 (*i.e.,* $T/\bar{T}$ is lognormally distributed). Consider the identity

$$\ln T = \ln(T/\bar{T}_e) + \ln \bar{T}_e \qquad (A1)$$

The terms on the right are independent, normally distributed variables with means 0 and $\ln \bar{T}_o$ and standard deviations 0.21 and σ_m. Therefore, $\ln T$ is normally distributed with mean $\ln \bar{T}_o$ and standard deviation $\sigma_a = [(0.21)^2 + \sigma_m^2]^{1/2}$. This, in turn, implies that T is lognormally distributed with median $\bar{T}_o$ and shape factor σ_a. From (A1) it is clear that in this case T refers to the aggregate of estimated recurrence times generated from $p(T,\bar{T}_e,0.21)$ for all values of $\bar{T}_e$ within the lognormal distribution $p(\bar{T}_e,\bar{T}_o,\sigma_m)$. Thus, $P(T,\bar{T}_o,\sigma_a)$ is the probability that a recurrence time drawn from the aggregate of all distributions $p(T, \bar{T}_e, 0.21)$ should be less than some value T. The distribution $P(T, \bar{T}_o, \sigma_a)$ could be generated by repeating the following sampling process: First draw a value $\bar{T}_e$ from the distribution $p(\bar{T}_e, \bar{T}_o, \sigma_m)$, and then draw a recurrence time T from the distribution $p(T, \bar{T}_e, 0.21)$. The WGCEP has chosen to use $P(T, \bar{T}_o, \sigma_a)$ as its estimate of earthquake risk. Thus, a unique probability, not a distribution of probabilities, is assigned to each interval $0, T$.

It can be shown by direct integration that the WGCEP estimate of earthquake risk $P(T, \bar{T}_o, \sigma)$ is simply the average of the Monte Carlo risk distribution

$$\langle P(T, \bar{T}_e, 0.21) \rangle = \int p(\bar{T}_e, \bar{T}_o, \sigma_m)\, P(T, \bar{T}_e, 0.21)\, d\,\bar{T}_e = P(T, \bar{T}_o, \sigma_a)$$

The WGCEP computes the conditional probability from (4) using the aggregate probability distribution $P(T, \bar{T}_o, \sigma_a)(i.e., \bar{T} = \bar{T}_o and \sigma = \sigma_a$ in equation 4). This estimate of the conditional probability is not a direct consequence of the assumed $\bar{T}_e$ distribution $P(\bar{T}_e, \bar{T}_o, \sigma_m)$, but rather skews the $\bar{T}_e$ distribution in favor of the larger values of T_e. This comes about as follows: In forming the conditional probability, the WGCEP has pooled the distributions of the various $\bar{T}_e$ samples to form the aggregate distribution and then truncated the distribution by eliminating all $T < T_1$. The conditional probabilities are then calculated from the truncated distribution. The operations could have been done in the reverse order, first truncate and normalize (equation 4) the individual distributions then pool the modified distributions into an aggregate conditional distribution. The former procedure discriminates against small values of $\bar{T}_e$ because they are under represented in the truncated distribution. The latter procedure amplifies the contribution from small values of $\bar{T}_e$ in the normalization procedure before combining the distributions into an aggregate.

The conditional probability calculated by the WGCEP is a weighted average of the Monte Carlo conditional probability distribution. Recall that in the Monte Carlo distribution each individual conditional probability is associated with a sample $\bar{T}_e$ from the distribution $\bar{T}_e$. Given that rupture has not occurred in the interval T_1 following the preceding earthquake, one should assign the probability $1 - P(T_1, \bar{T}_e, 0.21)$ to the proposition that a particular value of $\tilde{T}_e$ governs the rupture process. If this probabiity is assigned as a weight to each conditional probability sample in the Monte Carlo distribution, the weighted average of the Monte Carlo distribution will equal the WGCEP conditional probability. Briefly stated, the WGCEP conditional probability is not the average of the conditional probabilities implied by the $\tilde{T}_e$ distribution $P(\tilde{T}_e, T_o, \sigma_m)$ but rather is the average implied by the $\tilde{T}_e$ distribution $P(\tilde{T}_e, T_o, \sigma_m)$ modulated by $1 - P(T_1, \tilde{T}_e, 0.21)$. That is, the $\tilde{T}_e$ distribution is skewed to favor larger values of $\tilde{T}_e$ on the grounds that small values of $\tilde{T}_e$ are judged less likely because the fault segment has already survived the interval T_1 without rupture.

FIGURE CAPTIONS

Figure 1. Conditional probabilities of major earthquakes along segments of the San Andreas fault in the interval 1988–2018 as given by the Working Group on California Earthquake Probabilities (Agnew *et al.*, 1988).

Figure 2. Weighted (a) and unweighted (b) distributions of the conditional probability that the San Bernardino segment of the San Andreas fault will rupture in the interval 1988–2018. The average recurrence time for this segment is estimated to be 167 ± 47 yr and last rupture is taken to have occurred in 1812.

Figure 3. Weighted (a) and unweighted (b) distributions of the conditional probability that the Mojave segment of the San Andreas fault will rupture in the interval 1988–2018. The average recurrence time for this segment is estimated to be 150 ± 42 yr, and the the segment last ruptured in 1857.

Figure 4. Weighted (a) and unweighted (b) distributions of the conditional probability that the Cholame segment of the San Andreas fault will rupture in the interval 1988–2018. The average recurrence time for this segment is estimated to be 140 ± 59 yr, and the segment last ruptured in 1857.

Figure 5. Weighted distributions of the conditional probability that the San Francisco peninsula (a) and southern Santa Cruz Mountains (b) segments of the San Andreas fault will rupture in the interval 1988–2018. The average recurrence times for these segments are 156 ± 45 (a) and 125 ± 37 (b) yrs, and both segments last ruptured in 1906.

Figure 6. Weighted distribution of the conditional probability that the North Coast (a) and Carrizo (b) segments of the San Andreas fault will rupture in the interval 1988–2018. The average recurrence times for these segments are 281 ± 76 (a) and 279 ± 60 (b) yr, and the segments last ruptured in 1906(a) and 1857(b). Notice only the first decile of the distributions is shown.

Figure 7. Weighted distribution of the conditional probability that the southern Santa Cruz Mountains segment of the San Andreas fault will rupture in the interval 1988–1993.5. The average recurrence time for this segment is 125 ± 37 yr, and the segment last ruptured in 1906.

Figure 8. Weighted distributions of the conditional probability that the Parkfield segment of the San Andreas fault will rupture in the interval 1985–1993 (a) and 1990–1993 (b). The median recurrence time is estimated to be 20.9 yr and the shape factor for the lognormal distribution is estimated to be 0.35.

Figure 9. Probability density distributions for the average earthquake recurrence time in the southern Santa Cruz Mountains segment. The prior probability is derived by the direct method. The conditional probability is the revision of the prior probability to account for the absence of rupture in the first 81.7 years after the preceding rupture, and the posterior probability is the prior probability revised to account for the occurrence of rupture 83.5 years after the preceding rupture.

Figure 10. Weighted distributions of the conditional probability that the Cholame segment of the San Andreas fault will rupture in the intervals (a) 1988–2008, (b) 1988–2028, (c) 1988–2048, and (d) 1988–2068. The standard deviation indicated is the square root of the variance of the conditional probability distribution. The average recurrence time for this segment is estimated to be 140 ± 59 yr, and the segment last ruptured in 1857.

Table 1. χ^2 test of the fit of the observed recurrence intervals for four characteristic earthquake sequences to the lognormal distribution (1)

Rupture Segment	T_i, yr	$\hat{T}$, yr	χ^2	$P(>\chi^2)$*
Miyagi-Oki, Japan	30	38.8	14.5	0.07
	32			
	53			
	39			
	65			
	26			
	36			
	39			
	42			
Parkfield, California	24.07	20.9	11.6	0.02
	20.08			
	21.02			
	12.25			
	32.05			
Concepcion, Chile	87	91.9	0.61	0.89
	94			
	84			
	104			
Valparaiso, Chile	83	84.4	0.28	0.96
	92			
	84			
	79			

*Probability that a larger χ^2 would be observed for an equal sample of random recurrence intervals drawn from the lognormal density (1) with $\sigma = 0.21$

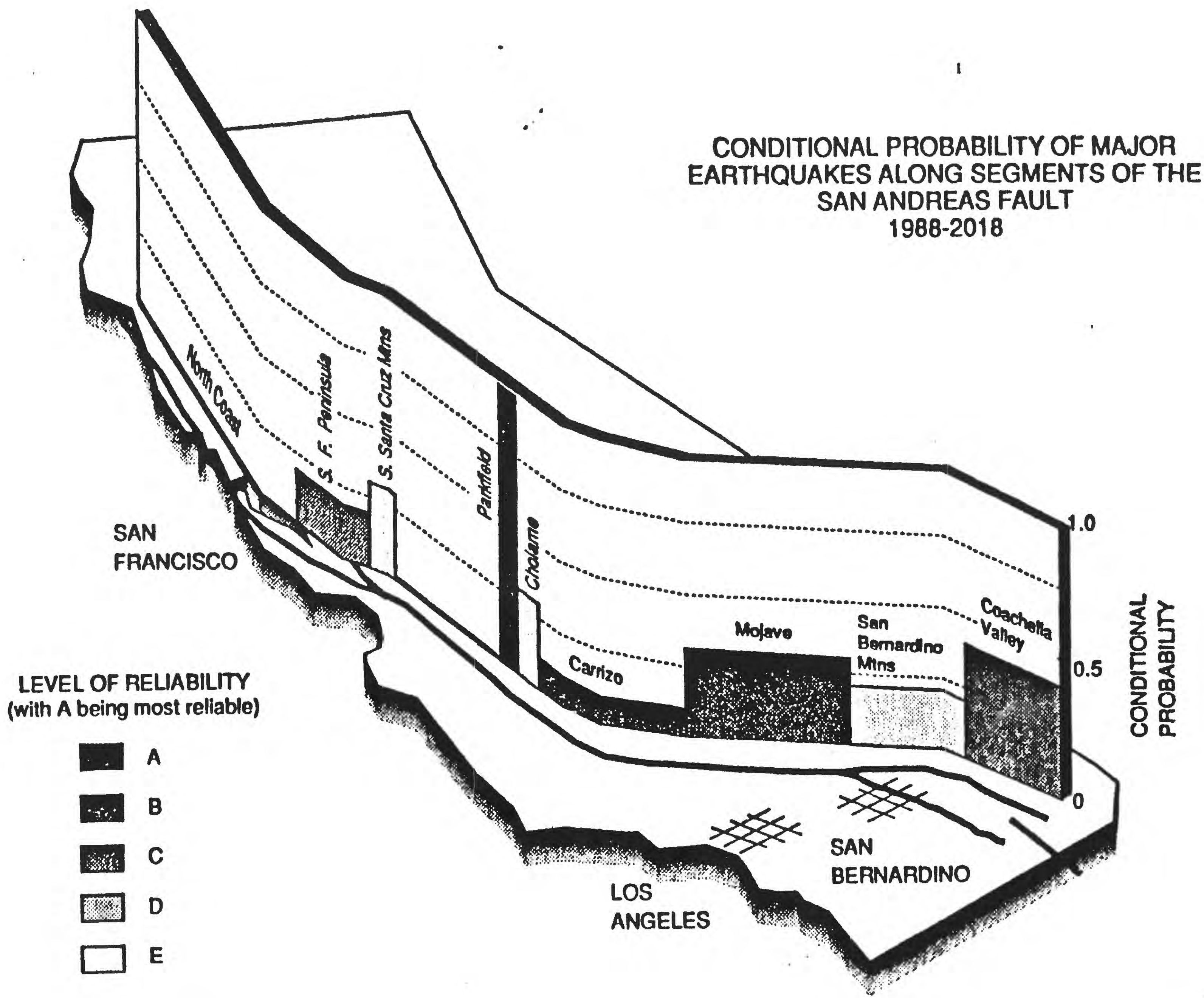
CONDITIONAL PROBABILITY OF MAJOR
EARTHQUAKES ALONG SEGMENTS OF THE
SAN ANDREAS FAULT
1988-2018
North Coast
S. F. Peninsula
S. Santa Cruz Mtns
Parkfield
Cholame
Carrizo
Mojave
San
Bernardino
Mtns
Coachella
Valley
1.0
0.5
0
CONDITIONAL
PROBABILITY
SAN
FRANCISCO
LOS
ANGELES
SAN
BERNARDINO
LEVEL OF RELIABILITY
(with A being most reliable)
A
B
C
D
E

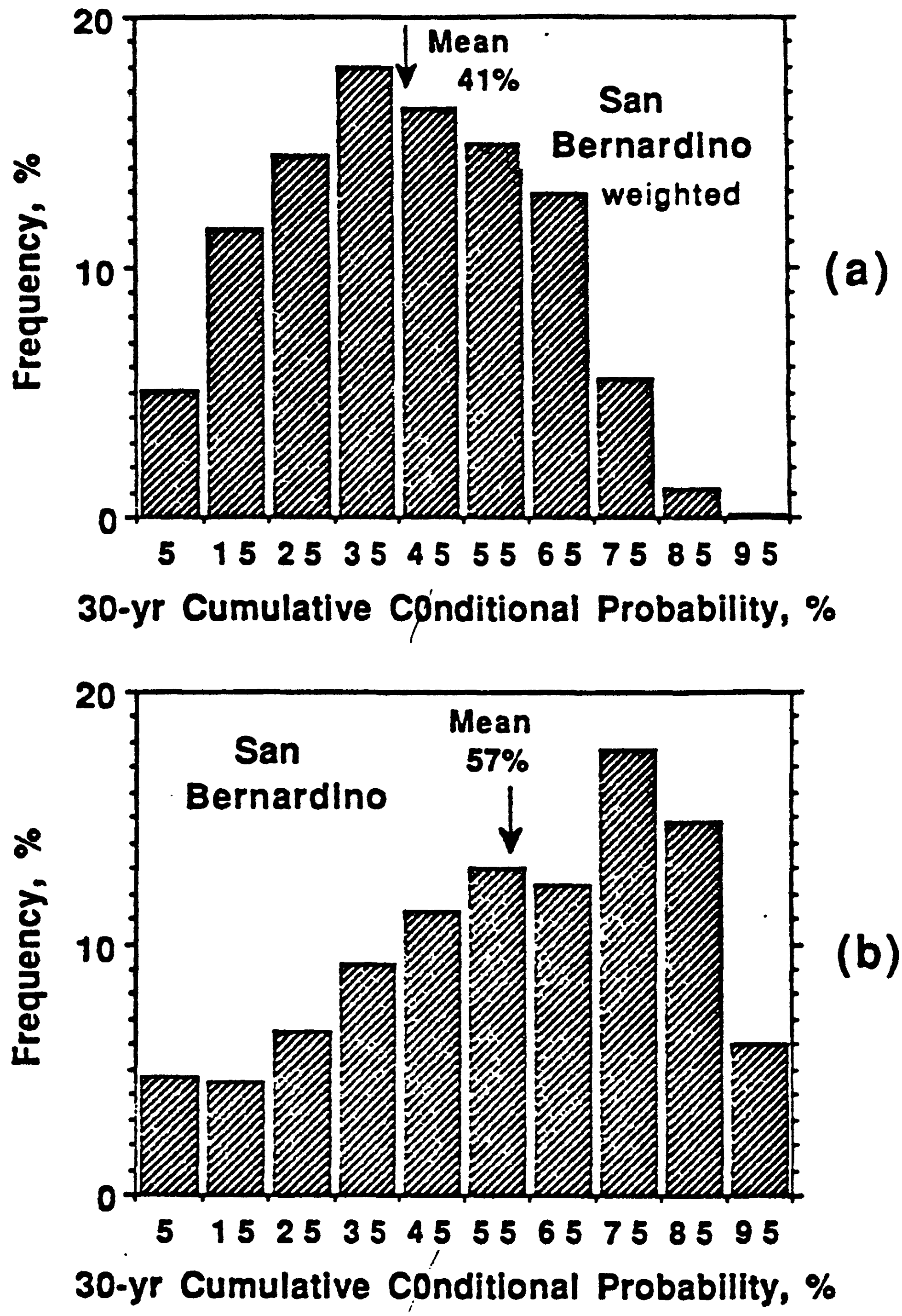
20
10
0
Frequency, %
Mean
41%
San
Bernardino
weighted
5 15 25 35 45 55 65 75 85 95
30-yr Cumulative Conditional Probability, %
(a)
20
10
0
Frequency, %
San
Bernardino
Mean
57%
5 15 25 35 45 55 65 75 85 95
30-yr Cumulative Conditional Probability, %
(b)

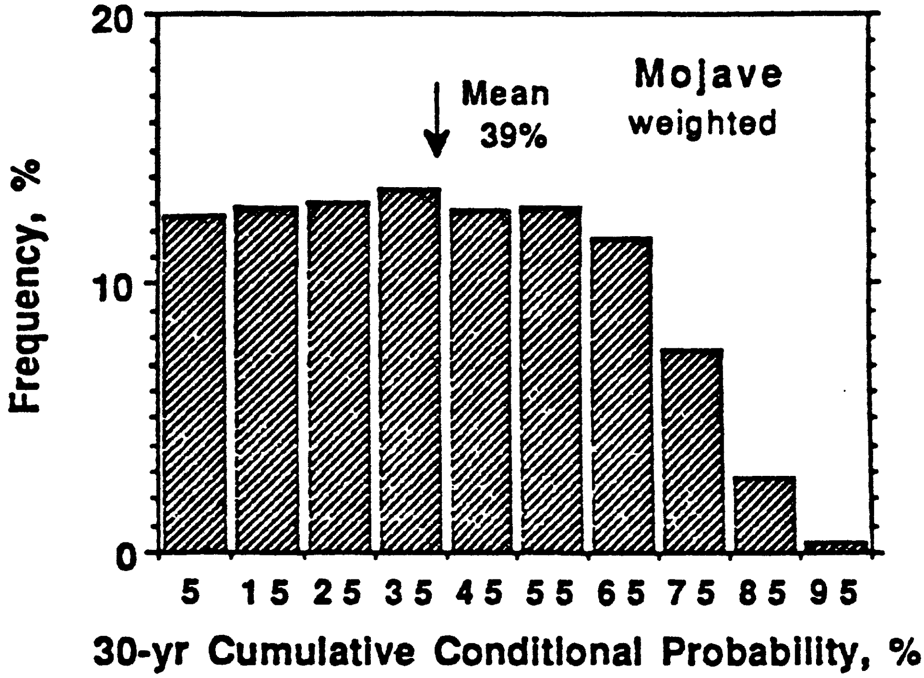

20
10
0
Frequency, %
Mean
39%
Mojave
weighted
5 15 25 35 45 55 65 75 85 95
30-yr Cumulative Conditional Probability, %

(a)

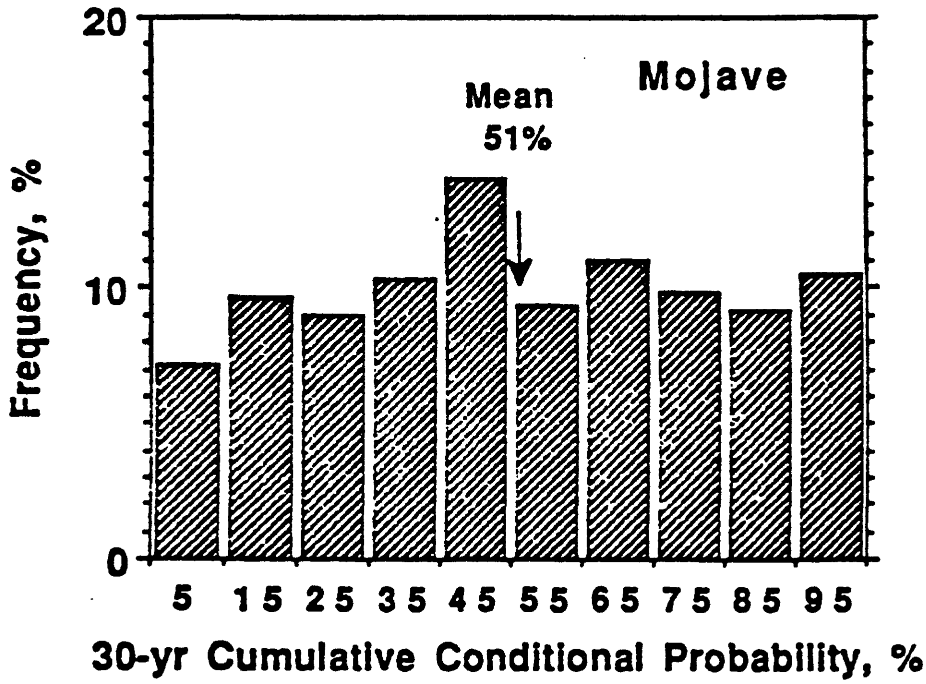

20
10
0
Frequency, %
Mean
51%
Mojave
5 15 25 35 45 55 65 75 85 95
30-yr Cumulative Conditional Probability, %

(b)

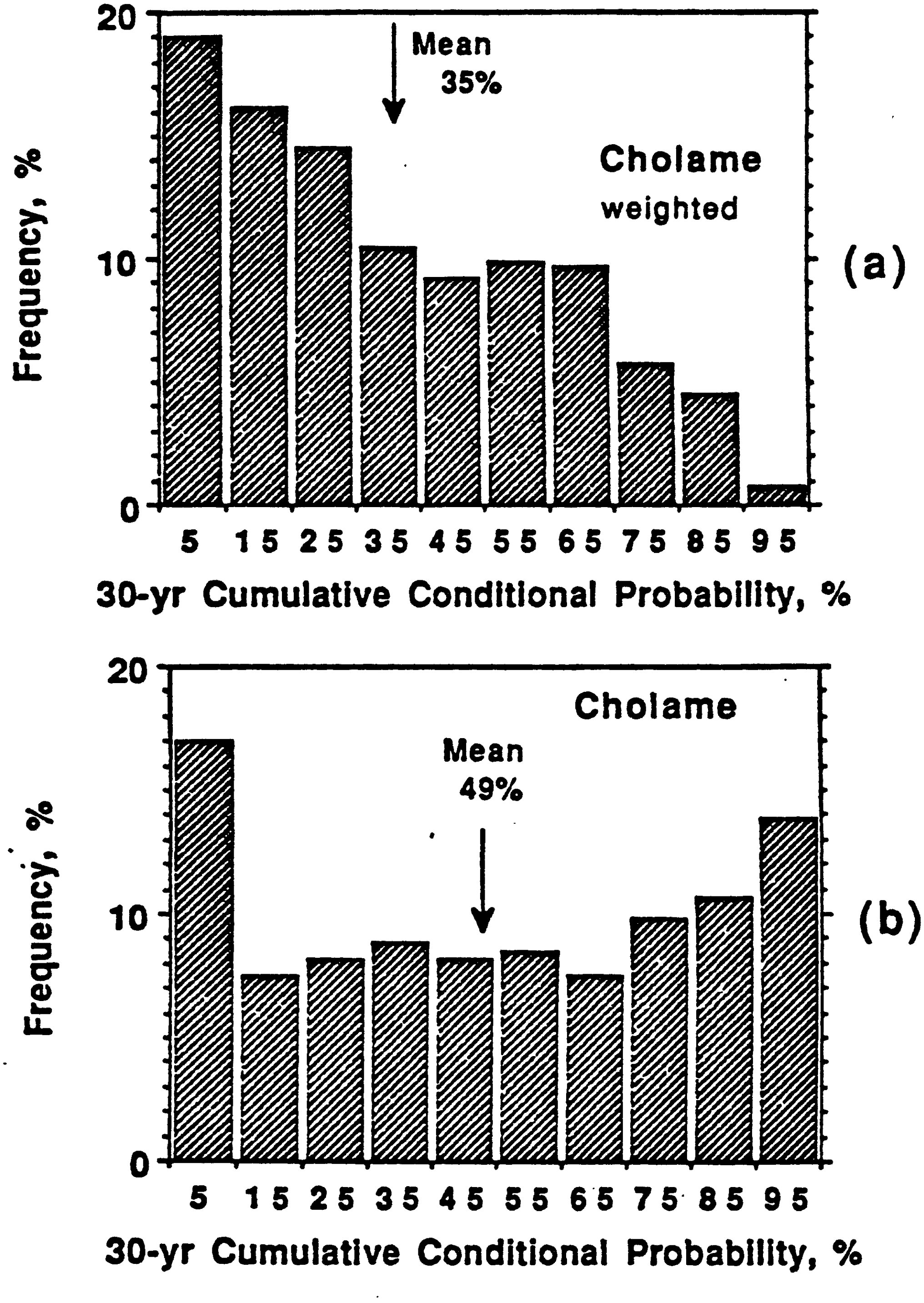

20
10
0
Mean
35%
Cholame
weighted
Frequency, %
5 15 25 35 45 55 65 75 85 95
30-yr Cumulative Conditional Probability, %
(a)
20
10
0
Cholame
Mean
49%
Frequency, %
5 15 25 35 45 55 65 75 85 95
30-yr Cumulative Conditional Probability, %
(b)

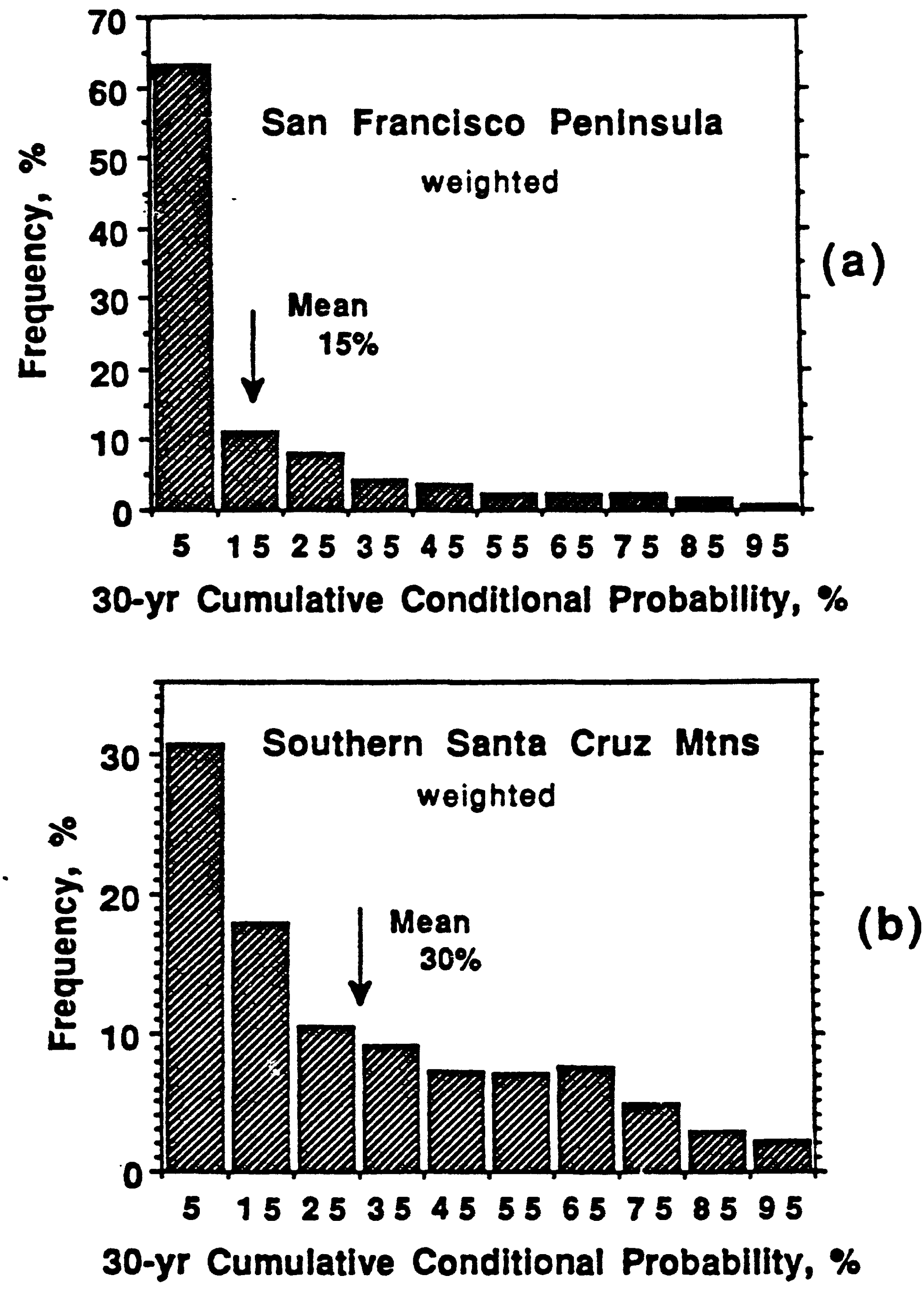

70
60
50
40
30
20
10
0
Frequency, %
San Francisco Peninsula
weighted
Mean
15%
(a)
5 15 25 35 45 55 65 75 85 95
30-yr Cumulative Conditional Probability, %
30
20
10
0
Frequency, %
Southern Santa Cruz Mtns
weighted
Mean
30%
(b)
5 15 25 35 45 55 65 75 85 95
30-yr Cumulative Conditional Probability, %

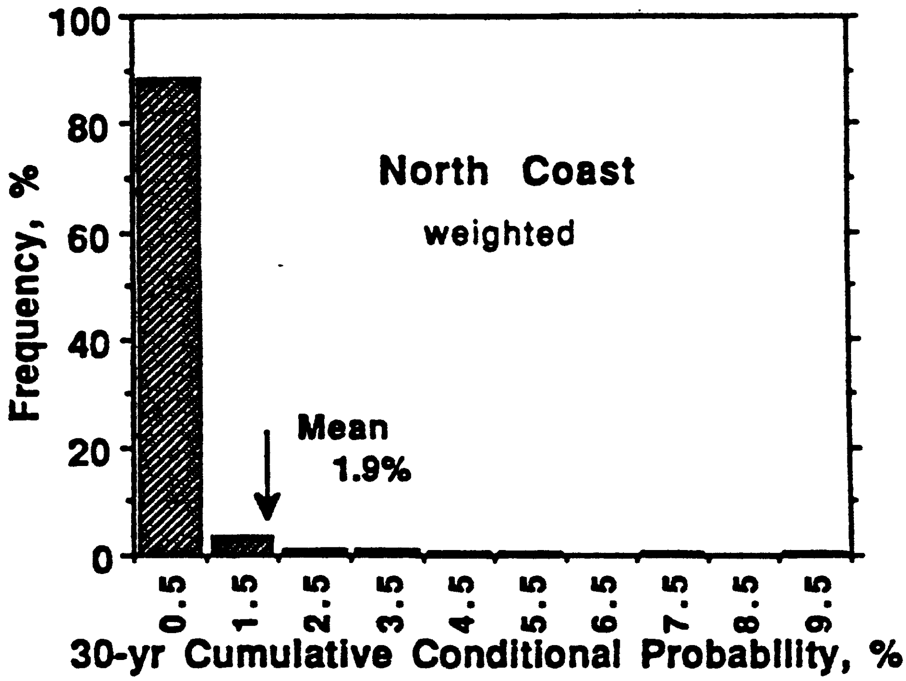

North Coast
weighted
Mean
1.9%
Frequency, %
100
80
60
40
20
0
0.5
1.5
2.5
3.5
4.5
5.5
6.5
7.5
8.5
9.5
30-yr Cumulative Conditional Probability, %

(a)

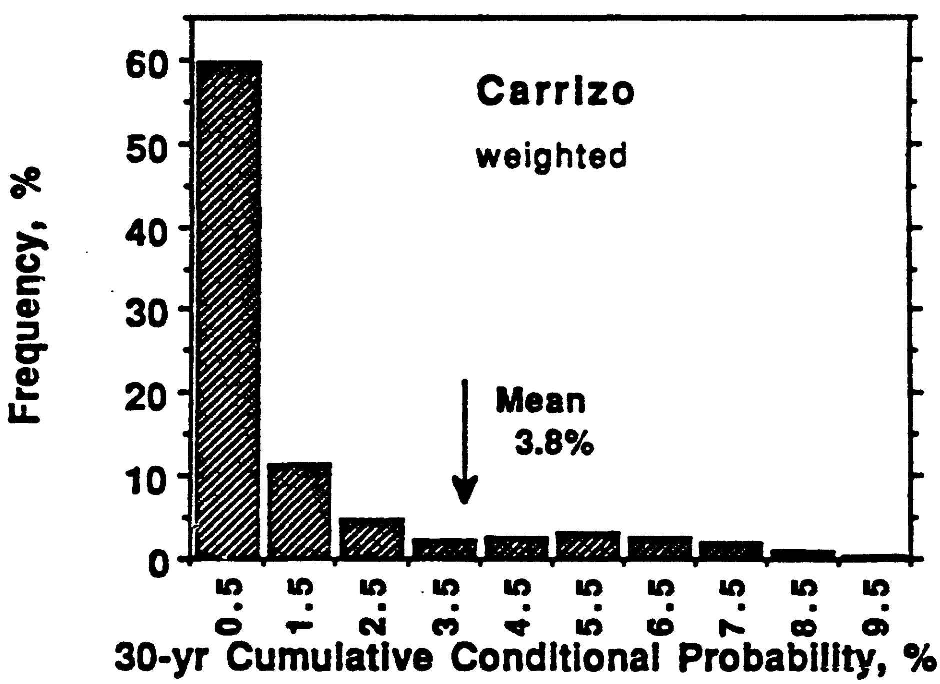

Carrizo
weighted
Mean
3.8%
Frequency, %
60
50
40
30
20
10
0
0.5
1.5
2.5
3.5
4.5
5.5
6.5
7.5
8.5
9.5
30-yr Cumulative Conditional Probability, %

(b)

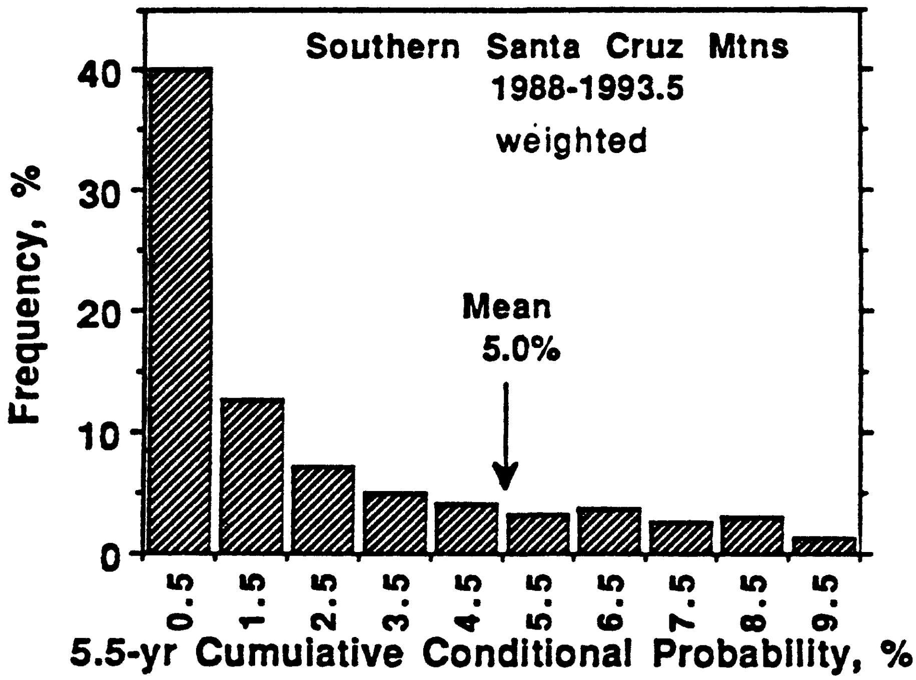

Southern Santa Cruz Mtns
1988-1993.5
weighted
Mean
5.0%
Frequency, %
40
30
20
10
0
0.5
1.5
2.5
3.5
4.5
5.5
6.5
7.5
8.5
9.5
5.5-yr Cumulative Conditional Probability, %

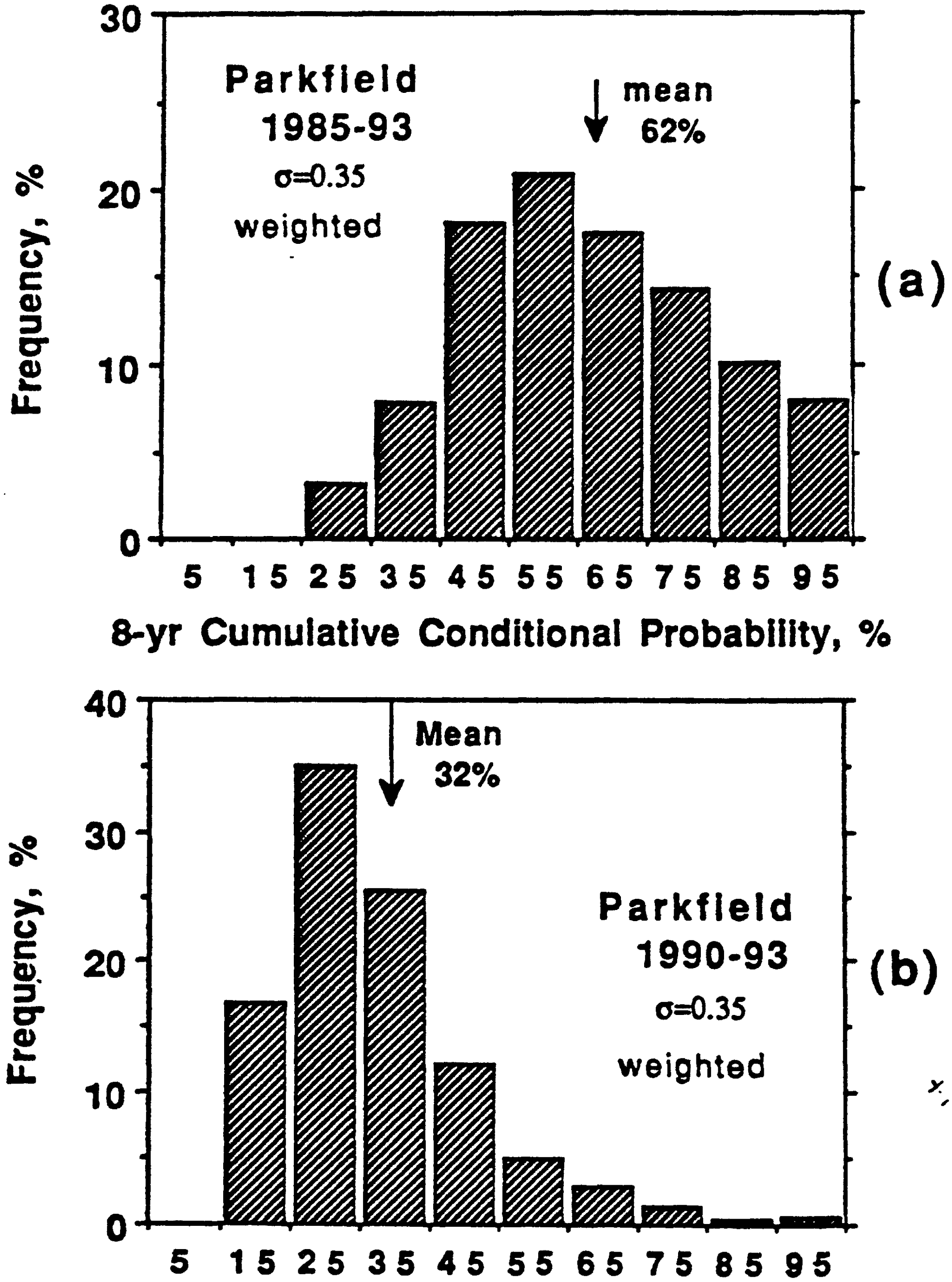
Parkfield
1985-93
σ=0.35
weighted
mean
62%
Frequency, %
30
20
10
0
5
15
25
35
45
55
65
75
85
95
8-yr Cumulative Conditional Probability, %
(a)
Mean
32%
Parkfield
1990-93
σ=0.35
weighted
Frequency, %
40
30
20
10
0
5
15
25
35
45
55
65
75
85
95
3-yr Cumulative Conditional Probability, %
(b)

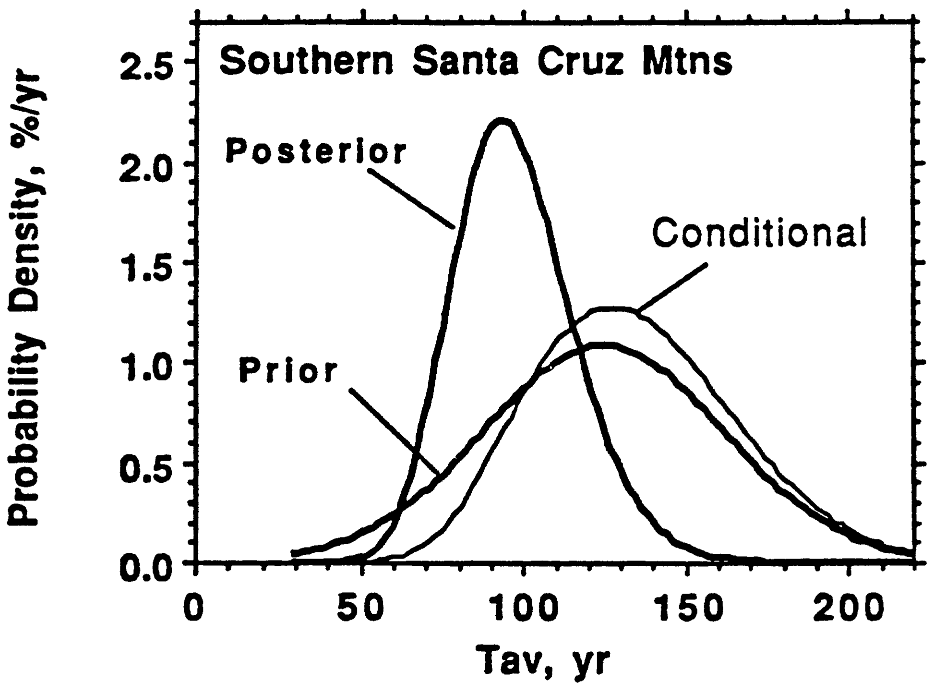
Southern Santa Cruz Mtns
Posterior
Conditional
Prior
Probability Density, %/yr
2.5
2.0
1.5
1.0
0.5
0.0
0
50
100
150
200
Tav, yr

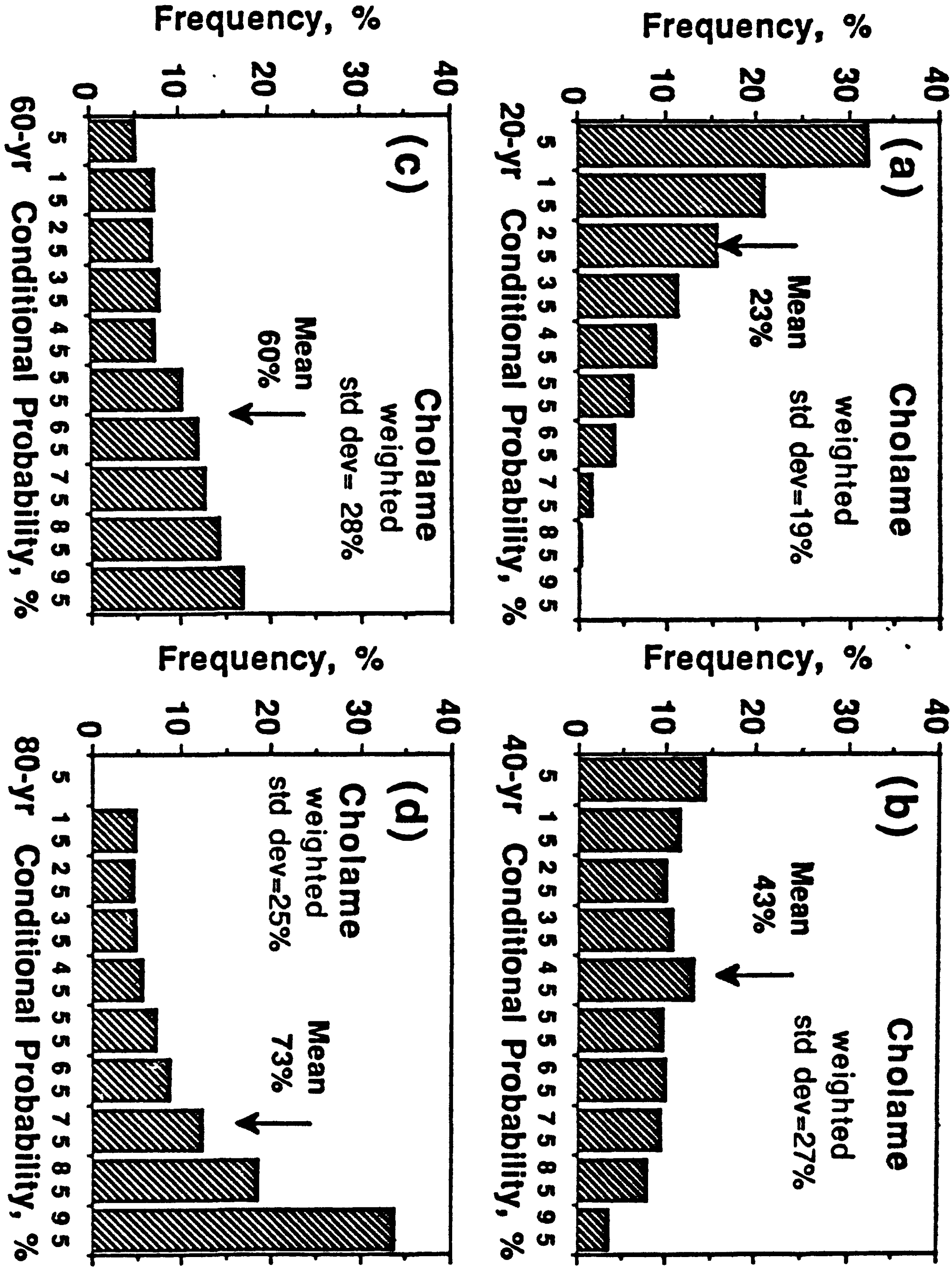

(a)
Cholame
weighted
std dev=19%
Mean
23%
Frequency, %
20-yr Conditional Probability, %
(b)
Cholame
weighted
std dev=27%
Mean
43%
Frequency, %
40-yr Conditional Probability, %
(c)
Cholame
weighted
std dev= 28%
Mean
60%
Frequency, %
60-yr Conditional Probability, %
(d)
Cholame
weighted
std dev=25%
Mean
73%
Frequency, %
80-yr Conditional Probability, %

Appendix O

Manuscript submitted to NEPEC as part of presentation by L.Jones, May 1, 1990.

4/22/90

Short-Term Earthquake Alerts for the Southern San Andreas Fault

Working Group:

Chairmen: Lucile M. Jones[1] and Kerry E. Sieh[2]

Members:
Duncan Agnew[3], Clarence Allen[2], Roger Bilham[4],
Mark Ghilarducci[5], Bradford Hager[2,6], Egill Hauksson[7,8]
Kenneth Hudnut[9,8], David Jackson[10], and Arthur Sylvester[11]

Corresponding Members:
Keiti Aki[7] and Frank Wyatt[3]

U. S. G. S. Open-file Report 90-xxx

---

[1] U. S. Geological Survey, 525 S. Wilson Avenue, Pasadena, CA 91106
[2] Division Geological and Planetary Sciences, Calif. Inst. of Tech., Pasadena, CA 91125
[3] Inst. for Geophysics and Space Physics, Univ. of California, La Jolla, CA 92092
[4] Dept. of Geological Sciences, Univ. of Colorado, Boulder, CO 80309
[5] Calif. Governor's Office Emergency Services, 2151 E. D St., Ontario, CA 91764-4452
[6] now at Dept. Earth, Atmos. and Plan. Sci., Mass. Inst. of Tech., Cambridge, MA 02139
[7] Dept. of Geological Sci., Univ. of Southern California, Los Angeles, CA 90089-0740
[8] now at Division Geol. and Planet. Sci., Calif. Inst. of Tech., Pasadena, CA 91125
[9] Lamont-Doherty Geological Observatory of Columbia Univ., Palisades, NY 10964
[10] Dept. of Earth and Space Sciences, Univ. of California, Los Angeles, CA 90024
[11] Dept. of Geological Sciences, Univ. of California, Santa Barbara, CA 93106

Table of Contents

Executive Summary

The historically dormant southernmost 200 km of the San Andreas fault (from Cajon Pass, northwest of San Bernardino, southeast to Bombay Beach on the Salton Sea) is the segment most likely to produce an earthquake of magnitude 7.5 or greater within the near future. Such an earthquake would cause widespread damage in San Bernardino, Imperial, Riverside, Orange and Los Angeles counties, which together have over 12 million inhabitants. If anomalous earthquake or other geophysical activity were to occur near the southern San Andreas fault, scientists would be expected to advise government officials on the likelihood that a major earthquake is forthcoming. This report presents a system for quantifying and communicating information about short term increases in the earthquake hazard from the southern San Andreas fault.

We use a system of four alert levels (A, B, C and D) similar to that adopted for the Parkfield earthquake prediction experiment in central California. The alert levels are defined so that the responses of the U. S. Geological Survey (USGS) will be similar to those defined for the Parkfield experiment. The probabilities that the predicted earthquake will occur within the 72 hours of the alerts are comparable to the probabilities defined for the alerts at Parkfield, but the criteria for reaching each alert level necessarily differ from those at Parkfield. The defined alert levels are:

Alert level	Response	Probability of M>7.5 earthquake in next 72 hours	Anticipated interval between alerts
D	Alert scientists involved in data collection and OES in Ontario	0.1 to 1%	5 months
C	Alert Communications Officer of OES in Sacramento, OEVE chief and response for Level-D	1 to 5%	5 years
B	Alert Director USGS, Calif. State Geologist, CDMG, start intensive monitoring and response for Level-C	5 to 25%	28 years
A	Issue Geologic Hazards Warning and response for Level-B	>25%	Not attainable at this time

The alert levels can be triggered by earthquakes, creep events (rapid aseismic surficial slip on faults) and strain events (anomalous deformation of the crust).

Our alert system is based primarily upon the observation that half of magnitude 5.0 or greater strike-slip earthquakes in California have been preceded by immediate foreshocks (defined as earthquakes within 3 days and 10 km of the mainshock). Therefore, the next major earthquake produced by the southern San Andreas could well be preceded by one or more foreshocks. This report describes a method for estimating the probability of the next major earthquake, given the occurrence of a possible foreshock. To be considered a possible foreshock, the rupture zone of the earthquake must come within 10 km of the southern San Andreas fault. The table below gives the magnitude of possible foreshock needed to reach a specified probability (or alert level) for four microseismic regions of the southern San Andreas fault.

Alert level Probability of M7.5 in 72 hr	B 5-25%	C 1-5%	D 0.1-1%
San Bernardino	5.8	5.0	3.9
San Gorgonio	6.1	5.3	4.2
Palm Springs	5.2	4.5	3.4
Mecca	4.9	4.2	3.1

Anomalous creep and strain episodes are also possible precursors to the next major earthquake along the southern 200 km of the San Andreas fault. Exact probabilities cannot be calculated for these possible strain precursors, because the data are inadequate to quantify the relationship between precursory slip or strain and large earthquakes. Therefore, only one alert level is defined for strain and aseismic slip; this is arbitrarily set equal to the lowest level (D) seismic alert. The threshold for producing such an alert is an amount of aseismic slip or strain unprecedented in the history of recording along the southern San Andreas fault.

The reliability of any short-term alert is limited by inadequacies in the data now being recorded along the southern San Andreas fault. For example, continuous measurements of ground deformation are limited to one strainmeter and four creepmeters. Because seismic stations are sparsely distributed and the automatic processing rudimentary, the depth and rupture size of most earthquake sources cannot be resolved, earthquakes above about magnitude 3.5 are not recorded on scale, and their spectral characteristics cannot be determined properly. Furthermore, the available data are not all recorded in one place. Therefore, this report recommends improvements in data management, instrumentation, and research that would increase the ability of scientists to issue a short-term warning for a great southern California earthquake. We should:

Implement centralized recording and analysis. A chief scientist for the southern San Andreas fault should be appointed and supported by the chief of the Office of Earthquakes, Volcanoes and Engineering (USGS) with the authority to issue the warnings described here. Deformation data now available from southern California should be given in real time to the Pasadena office of the USGS and Caltech to be evaluated together with the seismic data. Such evaluation will be an assigned task of the Pasadena office of the USGS and the Seismological Laboratory;

Improve seismic data. Expand the real-time earthquake analysis system to cover all the existing seismic network, add procedures for quickly estimating the magnitudes of large earthquakes, and add "high-fidelity" stations along the southern San Andreas fault.

Improve creep and strain data. An increased number of telemetered creepmeters along the southern San Andreas fault and auxiliary faults would enhance the evaluation of possible precursors. Additional deformation measurements would also be desirable, but will require careful planning. We suggest that a group of university and USGS scientists develop such a plan.

Improve our fundamental understanding of the fault. Better data would improve our ability to issue short-term warnings, as would a better understanding of the behavior of the fault. We therefore recommend that additional geodetic, paleoseismic, and broad-band seismologic research be undertaken to better understand the nature of the fault zone.

I. Introduction

The southernmost 200 km of the San Andreas fault in California, from Cajon Pass southeast to Bombay Beach on the Salton Sea (Figure 1), has not produced a major earthquake within the historic record. Both geodetic evidence of continuing strain accumulation (Savage *et al.*, 1986) and the occurrence of recent prehistoric large earthquakes (Sieh, 1986; Sieh and Williams, in press), however, document that this fault segment will eventually produce great earthquakes that pose one of the greatest hazards to southern California. An estimated 1.0-1.5 million people now live adjacent to the San Andreas fault within the projected zone of severe shaking for such an earthquake. A magnitude 7.5 to 8.0 earthquake on this segment would also cause widespread damage to San Bernardino, Imperial, Riverside, Orange, and Los Angeles counties, which together have over 12 million inhabitants. For these reasons, the Southern San Andreas Fault Working Group was formed in 1989 to recommend how the scientific community might best respond to anomalous geophysical activity along the fault, increase our understanding of regional seismotectonics, and offer timely scientific advice to state and local governments.

The southernmost 100 km of the San Andreas fault, the Coachella Valley segment from the Salton Sea to San Gorgonio Mountain, was identified by the Working Group on California Earthquake Probabilities (WGCEP, 1988) as the segment of the San Andreas fault zone most likely to produce a major earthquake of magnitude 7.5 or greater within the near future. That group estimated the conditional probability of such an event to be 0.4 within the next 30 years. The latest large earthquake on the Coachella Valley segment of the San Andreas fault occurred about 300 years ago (Sieh, 1986; Sieh and Williams, in press), and it is both realistic and prudent to assume that the next large event there will occur within our lifetimes.

The Coachella Valley segment abuts the San Bernardino segment which extends from the southern San Bernardino Mountains to Cajon Pass (Figure 1). The geologic record of earthquakes for the San Bernardino segment is more poorly understood than that of the Coachella Valley and the time of the last earthquake on that segment is not known. For this reason, the WGCEP (1988) considered the San Bernardino segment separately from the Coachella Valley and assigned it a 30-year probability of 0.2. However, it is not known, at present, how much of the southern San Andreas fault will be involved in the next great earthquake. This Working Group thought it possible or even likely that faulting in the next earthquake in the Coachella Valley will extend at least through the San Bernardino segment (over 200 km) producing a magnitude 7.5-8 earthquake and could continue to rupture through to the northwest into the Mojave segment (over 350 km) with a magnitude 8 or greater earthquake. Because of uncertainty about the final length of the next great earthquake, the section of the fault to be considered in this study was at the discretion of the Working Group. We chose to include those sections of the fault that have not slipped in the historic record; thus we excluded the Mojave segment. The region considered includes the Coachella Valley and San Bernardino segments as defined by WGCEP (1988) and extends from the Salton Sea to Cajon Pass, a distance of 210 km.

Moderate earthquakes and creep events have been recorded over the last fifty years on the southern San Andreas fault and will be again. When that happens, seismologists will be expected to advise state and local officials about the potential for further activity on the fault. In particular, they will be asked if the activity could be a precursor to the "Big One." It seems prudent to consider the most likely scenarios for such "earthquake crises" in advance, so that we can, with time available for careful evaluation, agree on appropriate answers to such questions. While experiences in public safety situations elsewhere have shown that scenario and response plan exercises often do not anticipate the details of subsequent events, they lead to more rapid and rational responses; conversely, lack of planning can be a recipe for fiasco. Thus, the primary goal of the Southern San Andreas Fault Working Group is to develop a system for quantifying and communicating information about short term increases in the earthquake hazard from the southern San Andreas fault.

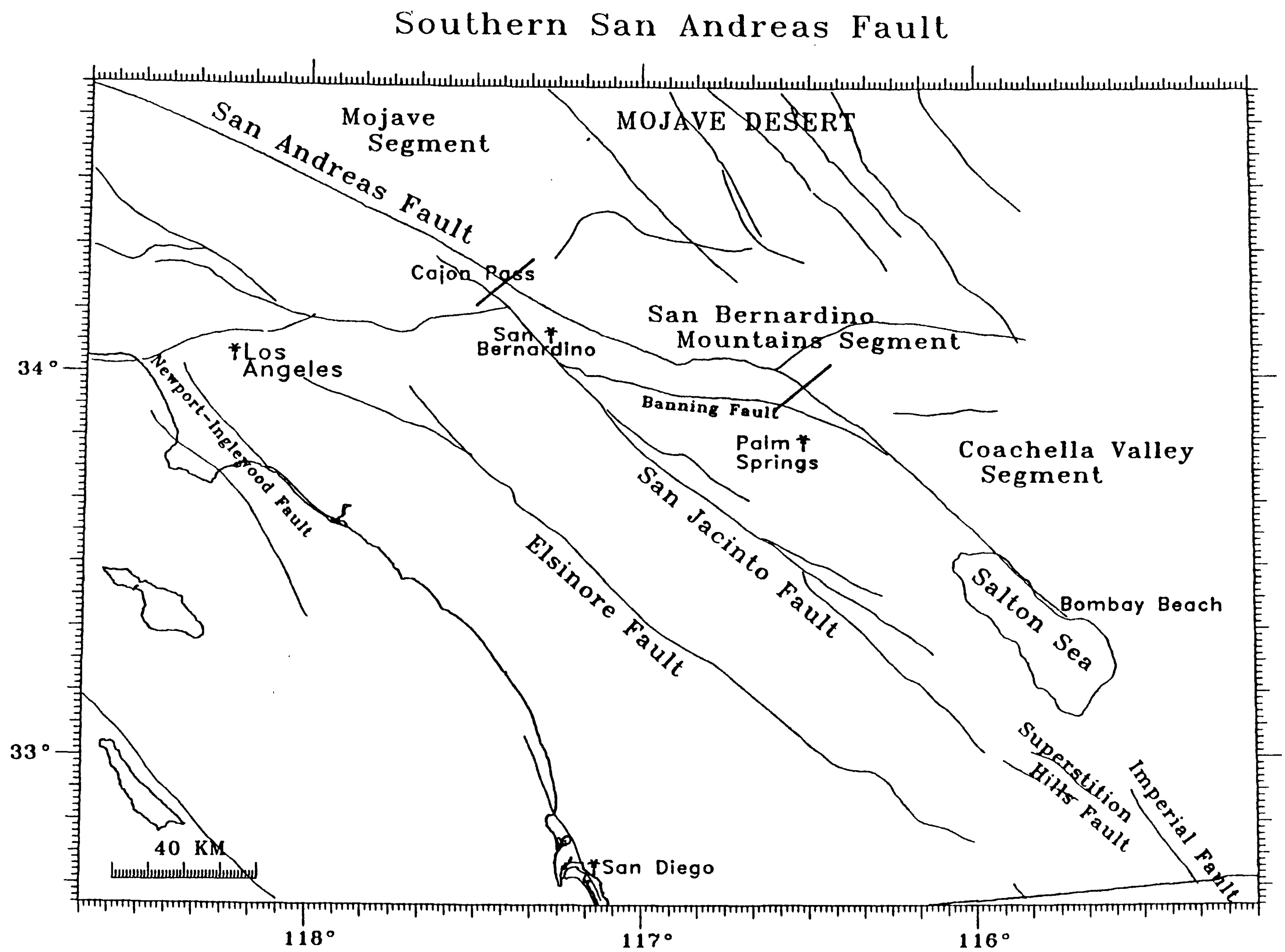

Figure 1. A map of the southernmost segment of the San Andreas fault in California, from Cajon Pass southeast to near Bombay Beach on the Salton Sea, showing locations referred to in the text. Towns are shown by palm trees. The Coachella Valley and San Bernardino Mountains segments of the San Andreas fault as defined by WGCEP (1988) are indicated. The Mecca Hills and Palm Springs microseismic regions lie within the Coachella Valley segment and the San Gorgonio and San Bernardino regions lie within the San Bernardino Mountains segment of the WGCEP.

A system for short-term warnings was developed several years ago for the Parkfield segment of the central San Andreas fault (Bakun *et al.*, 1987). At Parkfield, magnitude 6 earthquakes have recurred every 22 years on average with the last one in 1966, making that section most likely to produce a moderate earthquake within the next decade (Bakun and Lindh, 1985). Few people are at risk from that earthquake, but the greater chance of having an earthquake within a limited period of time makes Parkfield an ideal site for experiments in prediction. The U. S. Geological Survey has installed many instruments at Parkfield in an attempt to issue a short-term warning for the next Parkfield earthquake. An alert system has also been established for quantifying and communicating hazard information to the state of California (Bakun *et al.*, 1987). The Parkfield system provides a prototype for developing the alert system for the southern San Andreas fault.

In devising this system, it became clear to the Working Group that, along the southern San Andreas fault, the data now recorded are very poor, either for the immediate purpose of issuing short-term warnings or for the longer-term goal of improving our ability to do so. Members of the Working Group unanimously agreed that improved instruments and data management would increase the chance that a useful warning could be issued before the next great earthquake. The Working Group therefore decided to recommend specific improvements to the instrumentation, data management, and research effort in southern California. These improvements would significantly increase our ability to recognize changes in the physical properties of the fault that might precede a great earthquake. The improved instrumentation would also increase the scientific knowledge to be gained when the great earthquake itself occurs.

This document describes the alert system developed for the southern San Andreas fault. Section II describes the alert system and the mechanisms for entering and calling off alerts. Section III is the core of the document and describes the different precursors that could be recognized and alert criteria for them. Section IV presents the recommended response of the scientists to the alerts. Section V presents recommendations for improving geophysical recording on the southern San Andreas fault.

II. Short-term Earthquake Alerts

The Parkfield earthquake prediction experiment provides a prototype for scientific response and communication systems for short term earthquake anomalies. A system of earthquake alerts that last for 72 hours has been established to respond to short term changes in geophysical properties of the San Andreas fault near Parkfield (Bakun *et al.*, 1987). Four levels of short term alerts, labeled D, C, B and A, have been defined for increasing probabilities of the Parkfield earthquake occurring within the time of the alert. Actions on the part of various scientists in the USGS are mandated for each alert level.

We adopt a similar system for the southern San Andreas fault. Alerts are defined for 72 hour periods such that actions at each level on the part of the USGS are similar to those defined for Parkfield. The phenomena that can trigger alerts for the southern San Andreas fault differ from those at Parkfield but the probabilities that the forecasted earthquake will occur within the 72 hours are comparable. Because the social consequences of a M8 earthquake in a region with 12 million inhabitants are quite different from those for a M6 earthquake at a town with 34 inhabitants, the social response to a given alert level on the southern San Andreas fault could differ greatly from the response to the same alert at Parkfield.

Although the alerts are defined to last for 72 hours, the probability of the mainshock occurring is not evenly distributed over this time period. The hazard is highest immediately following the possible precursor and decays with time after it. However, one alarm that lasts for a fixed time is preferred by public officials who will be responding. The 72 hour period is chosen because it is long enough to include the great majority of possible mainshocks but short enough to represent a significantly increased earthquake hazard. An alert will be terminated 72 hours after it was called if no further activity commensurate with that level occurs within that time. If further activity does occur, the alerts will be extended for 72 hours from the time of the later activity.

The sole difference in response between level-B and -A alerts at Parkfield is that at level-A, a geologic hazard warning will be issued immediately and automatically by the USGS. This statement warns of approximately a 1 in 2 chance of a M6 Parkfield earthquake occurring within 72 hours and is in essence a formal earthquake prediction. We do not feel that the level of understanding of the behavior of the southern San Andreas fault allows probabilities anywhere close to 50% to be determined. As described below, we feel the highest probabilities that can be estimated for the southern San Andreas fault are on the order of 10-20%. Therefore, at the present time, a level-A alert cannot be reached for the southern San Andreas fault. We allow the definition to remain so as not to preclude the possibility of more certainty in the future as our knowledge increases.

III. Possible Earthquake Precursors

The Working Group considered three types of phenomena as possible earthquake precursors - anomalous earthquake activity, surface creep on faults, and changes in strain as recorded on strainmeters. Only earthquakes which could be foreshocks to a great earthquake are well enough recorded and understood for a formal estimate of conditional probabilities; creep and strain must be evaluated more subjectively. While other phenomena besides these three, such as ground water geochemistry or geoelectricity, might show precursory activity, they are not well enough recorded along the southern San Andreas fault nor is their relationship with large earthquakes well enough understood to be used at this time for short-term warnings.

We first summarize the equipment presently deployed to record these phenomena. Then, for each possible precursor, we discuss (1) the evidence for that phenomenon as a short-term precursor to large earthquakes, (2) its recorded history along the southern San Andreas fault and (3) appropriate levels of concern for different possibly precursory activities.

III.1 Summary of Current Instrumentation

Earthquakes in southern California are recorded by the Southern California Seismic Network, a joint project of the California Institute of Technology (Caltech) and the southern California office of the United States Geological Survey (USGS), in Pasadena (Figure 2). The average station spacing near the southern San Andreas fault is about 20 km, so that all earthquakes above magnitude 1.8 are recorded in the southern California catalog. Most of the stations consist of a single short-period vertical seismometer, so that S-wave arrival times cannot usually be determined. Two three-component, force-balance accelerometers and three high-gain three-component seismometers are located within 50 km of the southern San Andreas fault (Figure 2). Because earthquakes in the Coachella Valley tend to be shallow (above 10 km), the lack of S-wave readings and the 20 km station spacing mean that the depths of these earthquakes cannot usually be resolved within 5 km. Ten stations within 50 km of the southern San Andreas fault have an extra vertical component with a low gain setting; all other stations saturate at about magnitude 2.5-3.0.

The analog data from the seismic stations are first telemetered to Pasadena by microwave and leased telephone lines, and then digitized and recorded by a central recording computer. All of the data are processed and analyzed within one to three days. One quarter of the stations (64 for all

Southern California Seismic Network

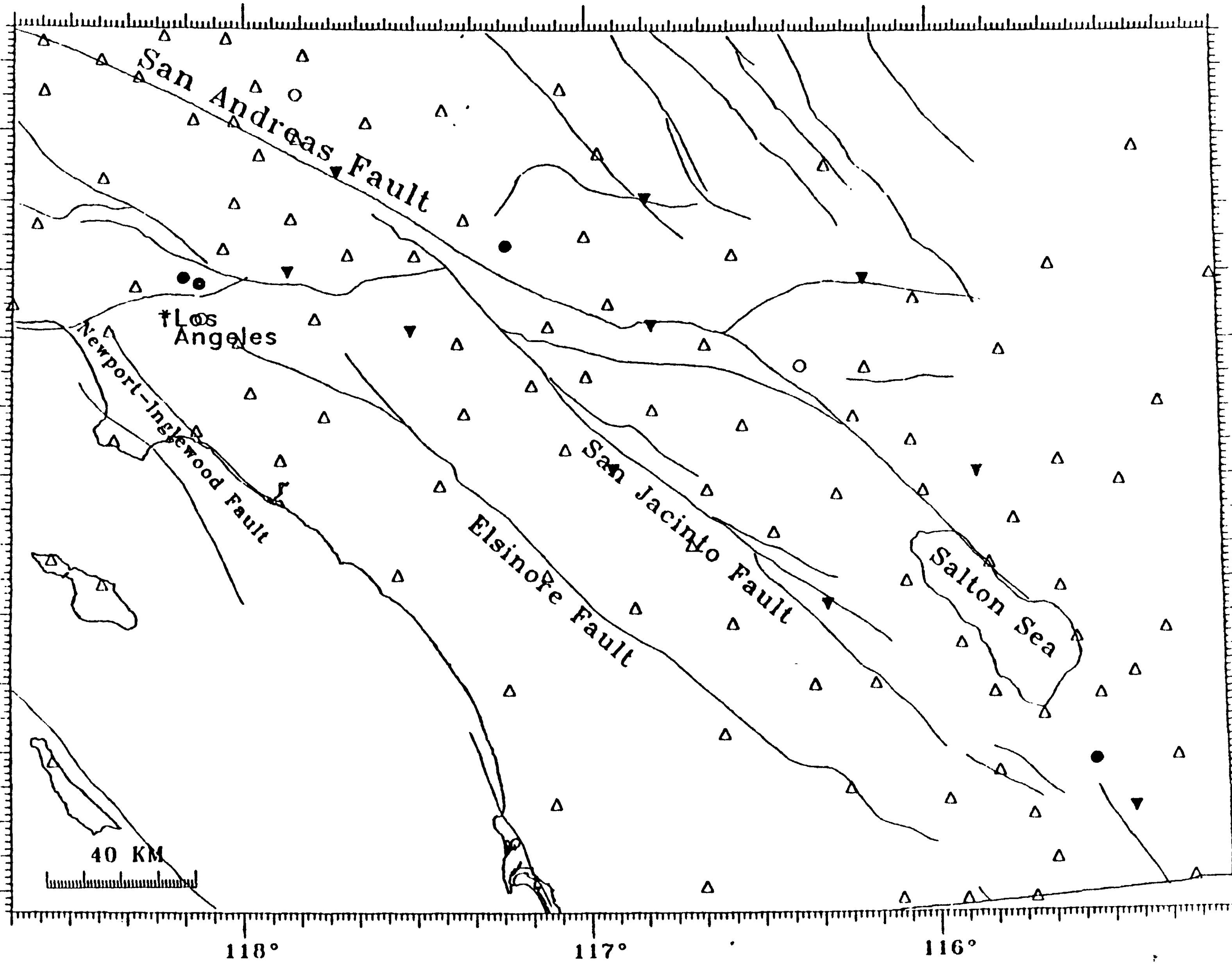

Figure 2. A map of the stations of the Southern California Seismic Network. Sites with one short-period vertical component are shown by triangles. Two-component stations (one high-gain and one low-gain vertical sensors) are shown by filled inverted triangles. Sites with two horizontal components in addition to vertical sensors are shown by circles; filled circles are sites with ultra-low-gain force-balance accelerometers.

of southern California) are analyzed by a real-time picker (RTP) (Allen, 1982). This system provides the location of any earthquake of magnitude greater than 2.2, within 5 minutes of its initiation. For earthquakes of magnitude less than 4.1, the magnitude is also determined. A new software system is being developed to provide real-time locations and magnitudes for all earthquakes with magnitudes between 1.8 and 6.5. This system is expected to be operational by 1990 or 1991.

There are relatively few measurements of ground deformation in southern California. Existing instrumentation includes alignment arrays, geodetic nets, creepmeters, several strainmeters and tiltmeters at the Pinon Flat Observatory, and a water-level tilt network in the Salton Sea (Figure 3). Alignment arrays are sets of monuments installed over a small area (typically less than 1 km^2) that are repeatedly surveyed. Alignment arrays and geodetic nets around the southern San Andreas fault are supplemented with Global Positioning Satellite (GPS) measurements. However, these arrays and networks are unlikely to provide information on short term precursors to large earthquakes, because the measurements are made too infrequently, often at yearly intervals. A permanent GPS network is being planned that could be used continuously.

Creepmeters are instruments installed to measure surface slip across the trace of a fault. Caltech operates four creepmeters, two on the San Andreas fault and two on the Imperial fault. One Imperial fault creepmeter is recorded on site; data from the others are telemetered to Pasadena. Several digital creepmeters (up to 10) will be placed along the San Andreas and San Jacinto faults over the next few years in a cooperative project between the University of Colorado and Caltech. As planned, the resulting data will be recorded on site only. Without telemetry, these instruments cannot be used for short term earthquake alerts.

The only continuous, high-precision strain measurements are made at Pinon Flat Observatory (PFO), within 40 km of most of the Coachella Valley, but 75 km away from the southernmost end at Bombay Beach (Figure 3). The instrumentation at PFO includes long-base strainmeters and tiltmeters, a borehole dilatometer, a borehole tensor strainmeter, and several borehole tiltmeters. These provide very high sensitivity recordings; however, different instruments have different time periods over which they give the best results, and different degrees of processing required to attain these results. The most easily interpreted instrument is the borehole dilatometer, because it is subject to the least environmental disturbance. The long-base instruments produce better data, but processing and interpreting these data require someone familiar with the idiosyncrasies of the instruments. Expert involvement is also desirable to interpret data from the borehole tensor strainmeter.

A closer but less sensitive record of crustal deformation is provided by the water-level recorders operated around the Salton Sea by the Lamont-Doherty Geological Observatory. The difference in water-level between stations gives a measure of tilt between them. These data also require an expert for processing and interpretation, especially because a wide range of environmental effects may cause apparent tilts. Moreover, meaningful signals cannot be resolved for periods of less than 2 days because of seiches and thermal noise, so that data from this system cannot be used for short-term analysis.

Data relevant to short-term earthquake prediction on the southern San Andreas fault are thus recorded by several different organizations. Seismic data are recorded by the cooperative Caltech/USGS southern California seismic network in Pasadena. Creepmeters on the southern San Adreas fault are recorded on site and retrieved by Caltech (2 instruments) and University of Colorado (2 instruments). Strain data from PFO are recorded on-site, along with a computer connection to the University of California at San Diego. The Salton Sea data are stored on site by a computer and accessed by modem by scientists at Lamont in New York. In addition, two dilatometers in the Mojave Desert (50-200 km from the southern San Andreas fault) have satellite telemetry to Menlo Park. A central recording and analysis facility for southern California has not been established.

Strain Instrumentation Near the
Southern San Andreas Fault

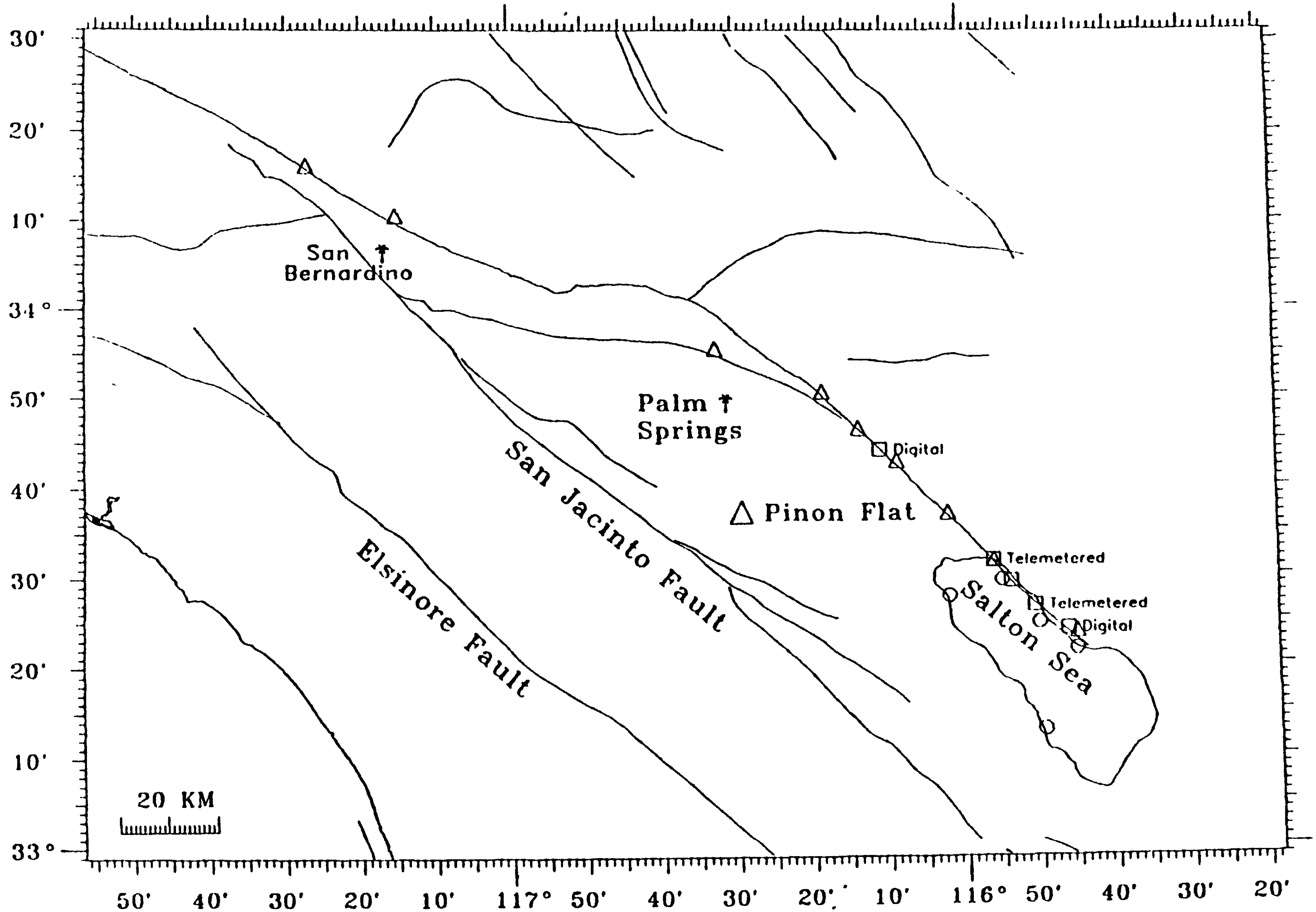

Figure 3. A map of sites at which strain, creep or tilt are measured in southern California. The Pinon Flat Strain Observatory is shown by a large triangle. Creepmeters are shown by squares and noted if they are telemetered to Pasadena or digitally recorded. Alignment arrays are shown by small triangles. The Lamont water level guage network is shown by circles.

III.2 Foreshocks

Half of the strike-slip earthquakes in California have been preceded by immediate foreshocks within 3 units of magnitude (Jones, 1984), including the 1857 magnitude 8 Fort Tejon earthquake on the southern San Andreas fault. Two of the four moderate earthquakes on the southern San Andreas fault in the last six decades have also had foreshocks.

Thus, the next southern San Andreas mainshock could well be preceded by one or more immediate foreshocks. An immediate foreshock is defined as an earthquake, smaller than the mainshock, that occurs less than 3 days before it and within 10 km of the mainshock's epicenter (Jones, 1985). Although immediate foreshocks are well-documented, they can only be defined after the later, larger earthquake occurs. So far, no characteristic has been found that distinguishes foreshocks from background earthquake activity. Therefore, when a small to moderate earthquake occurs on the southern San Andreas fault, we cannot tell if it is a foreshock, but the possibility that it is increases the probability that a major earthquake could soon occur.

This increase in the seismic hazard following moderate earthquakes has been recognized and used for a few short-term earthquake advisories (e.g., Goltz, 1985). However, these warnings have been based on a regional level of foreshock occurrence (Jones, 1985), applicable anywhere in southern California. Applying such a formula to the southern San Andreas ignores both the existence of an estimate of the long-term probability for the large event and the substantial spatial variations in background activity along this fault segment. Thus, the Working Group felt that we needed a formal method for estimating the probability of a large earthquake, given the occurrence of a possible foreshock on a major fault. A method has been developed and is described in Appendix A. In Section III.2.1 we give a relatively nontechnical discussion of the procedure used, emphasizing the reasoning behind the estimate rather than the formal mathematics (given fully in Appendix A). Section III.2.2 describes our conclusions regarding the foreshock magnitudes needed to reach particular alert levels.

III.2.1 Theory

In determining short-term probabilities, we consider foreshocks and mainshocks as separable in principle from background seismicity that occurs along the fault zone. We then suppose that some earthquake has occurred, either a background event or a foreshock, though we do not know which. If this "candidate event" is a foreshock, the mainshock will by definition soon follow. To see the reasoning used, a simple example may help. Leaving out the complications of magnitude, location, and so on, suppose that mainshocks occur on the average every 500 years, and that half of them have foreshocks (defined as being within a day of the mainshock); then we expect a foreshock every 1000 years. Suppose further that a background event occurs every year. Then, given a potential foreshock, there is very nearly one chance in 1000 that it is a foreshock. This makes the probability of a mainshock in the next day 0.1%. While this is low, it is far above the background probability, which is (assuming a Poisson process) 1 in 500 times 365, or 0.00055%.

What we have done here is to compute the probability that a mainshock will soon occur, given a foreshock *or* background earthquake; that is, a conditional probability. Appendix A gives the complete formula for this conditional probability, dependent on the same quantities we have just used: the probabilities of a background earthquake, of a mainshock, and of a foreshock if a mainshock has actually happened (which in our simple case is the fraction of mainshocks having foreshocks). In the example, all of these probabilities are assumed to have been estimated from a very long record of seismicity. In reality, we get these quantities from very different sources:

Background Seismicity. The probability of a background earthquake is derived from the magnitude-frequency relation and spatial distribution of earthquakes above magnitude 1.8

recorded over the last 11 years by the Southern California Seismic Network. The rate of background seismicity varies considerably along the southern San Andreas fault, from the highest rate for the whole San Andreas system at San Gorgonio Pass, to one of the lowest in the Mecca Hills. We have divided the southern segment into four microseismic zones to account for these variations (Figure 4). The Mecca Hills and Palm Springs microseismic regions make up the Coachella Valley segment and the San Gorgonio and San Bernardino microseismic regions make up the San Bernardino Mountains segment of WGCEP (1988)

A critical assumption in using this catalog data is that the last 11 years of earthquake activity represents the long-term rate. The magnitude-frequency distribution determined from the earthquakes above magnitude 3.0 since 1932 is comparable to that determined from the past 11 years, suggesting the 11 year interval is typical. If the rate of seismic activity along the southern segment were to change, the probabilities determined here should be modified.

Long-term Probability of Mainshocks. The long-term probability of a mainshock occurring on the Coachella Valley segment of the southern San Andreas fault is a complicated, controversial quantity that has already been the topic of another Working Group, the Working Group on California Earthquake Probabilities (WGCEP, 1988). We use here the results of WGCEP (1988), a probability of 0.4 over the next 30 years for the Coachella segment and 0.2 over 30 years for the San Bernardino Mountains segment. The committee has adopted these results because they have already been reviewed and accepted by the National and California Earthquake Prediction Evaluation Councils. Davis *et al.* (1989) have recently made a case for a much lower probability for the Coachella Valley segment: 0.09 over the next 30 years (they did not consider the San Bernardino segment). Alert probabilities have been calculated using both values to show the effect of the different assumed values for long term probability in the Coachella Valley.

We also assume that all sections of the southern San Andreas fault are equally likely to contain the epicenter of the mainshock. It has been suggested that mainshocks are more likely to occur at points of complication on the fault. However, at the gross scale at which we are analyzing the southern San Andreas fault, each region has numerous points of complication, and further refinement is not supported by our present state of knowledge. Another possibility we rejected was to assume the mainshock more likely to occur in regions with a high rate of background seismicity. One clear lesson from 50 years of seismic recording in southern California is that large earthquakes do not preferentially occur at the sites of small earthquakes.

Conditional Probability of Foreshocks. The third quantity needed is the conditional probability of a foreshock given that a mainshock has occurred. In Appendix A, we call this a "reverse transition probability" because, unlike most conditional probabilities, it goes backwards in time. We use the chance that an earlier event precedes a later one, rather than the more customary approach of discussing the chance that one type of event will be followed by another. This does not violate causality; we are simply assuming that the two types of events (foreshocks and mainshocks) are interrelated.

If we had a record of the foreshocks for many Coachella Valley mainshocks, or even many San Andreas mainshocks, we could estimate the conditional probability directly. Since we do not, we assume that the average properties and probabilities of foreshocks to moderate and large earthquakes on many southern California faults adequately approximate the temporal average over many mainshocks on the southern San Andreas fault. The simple model discussed at the start of this section presented only one type of foreshock and mainshock, so that the reverse transition probability was the fraction of mainshocks preceded by foreshocks. In actuality, both kinds of events come with additional "labels" such as location and magnitude. We must extend the conditional probability to allow for these. Again, Appendix A gives the full details, which we summarize here. Foreshocks are definable once the mainshock occurs and the average characteristics of California foreshocks are briefly described and used to define the reverse transition probability for potential San Andreas foreshocks.

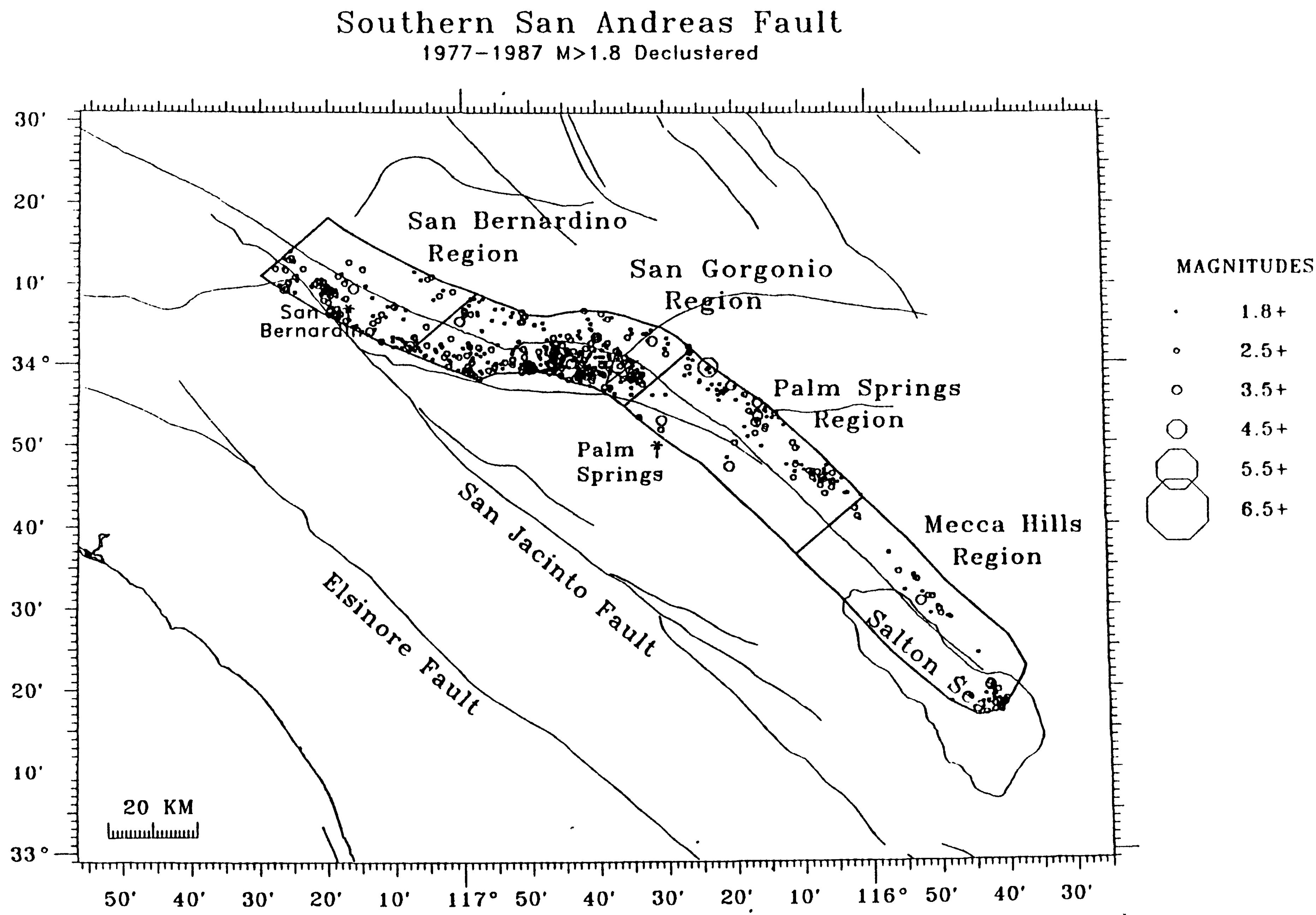

Figure 4. A map of magnitude 1.8 and greater earthquakes located within 10 km of the Coachella Valley segment of the southern San Andreas fault recorded in the Caltech catalog between 1977 and 1987.

Temporal Dependence. If a foreshock occurs, it is more likely to happen just before the mainshock than some greater time before it (Jones, 1985; Jones and Molnar, 1979). The distribution of foreshock-mainshock intervals, *t*, varies roughly as $1/t$. As a consequence, the maximum conditional probability of a mainshock occurs just after the potential foreshock, and diminishes rapidly with time. (As time elapses with no mainshock, it becomes more probable that the potential foreshock was just a background earthquake). We have not included this temporal change directly in our alert levels, but simply leave the probability unchanged for the duration of the alert. The 72 hour duration of the alert is approximately the time within which 95% of mainshocks will have occurred.

Location. Foreshocks occur close in space as well as close in time to the mainshock. All well-recorded foreshocks in southern California have had epicenters within 10 km of their mainshocks' epicenters (Figure 5; Appendix A). No dependence of this distance on magnitude of mainshock or foreshock has been seen (Figure 5). However, a significant minority of these foreshocks have occurred on a different fault from their mainshock so an earthquake need not be on the southern San Andreas fault to be considered a potential foreshock. The Working Group has chosen a somewhat more generous definition of foreshock and required only that some part of the rupture zone of the foreshock lie within 10 km of the southern San Andreas fault. Defining the distance from the fault in terms of the rupture zone of the potential foreshock allows the monitoring seismologists some flexibility in evaluating a particular earthquake sequence.

As noted above, we have assumed that the mainshock epicenter is equally likely anywhere along the southern San Andreas fault. We have also assumed that foreshocks are equally likely to occur anywhere along the fault. In particular, we discussed and rejected the hypothesis that foreshocks are preferentially located at sites of high background activity. Although data on this subject are limited, what modern data we have do not support this hypothesis (Jones, 1984). One example is the lack of foreshocks on the Calaveras fault despite a rate of background seismicity that is one of the highest in California.

Magnitude Dependence. The least certain part of the transition probability is how it depends on mainshock and foreshock magnitude. Our data on this are inevitably incomplete because a much lower magnitude threshold must be used for foreshocks than for mainshocks to consider the magnitude distribution of all possible foreshocks to a given mainshock. The southern California data suggest that for any narrow range of mainshock magnitudes all foreshock magnitudes are equally likely (except of course that foreshocks are always smaller). We have therefore assumed a flat distribution with magnitude of the foreshocks and used Jones' (1984) finding that half of the strike-slip earthquakes in California were preceded by foreshocks within 3 units of magnitude.

We have treated each of the above factors (time, location, and magnitude) separately, because the data available do not suggest any correlation between them. Likewise, we have not included any other parameters upon which the reverse transition probability might depend. For instance, while we might suspect that foreshocks would have focal mechanisms close to that of the mainshock, we lack the data to evaluate this properly. Once more data have been accumulated, differences in probability depending on focal mechanism, number of aftershocks to the potential foreshock, tectonic regime, or other criteria can be accommodated by the method described in Appendix A. But at this point, none are sufficiently well documented for inclusion.

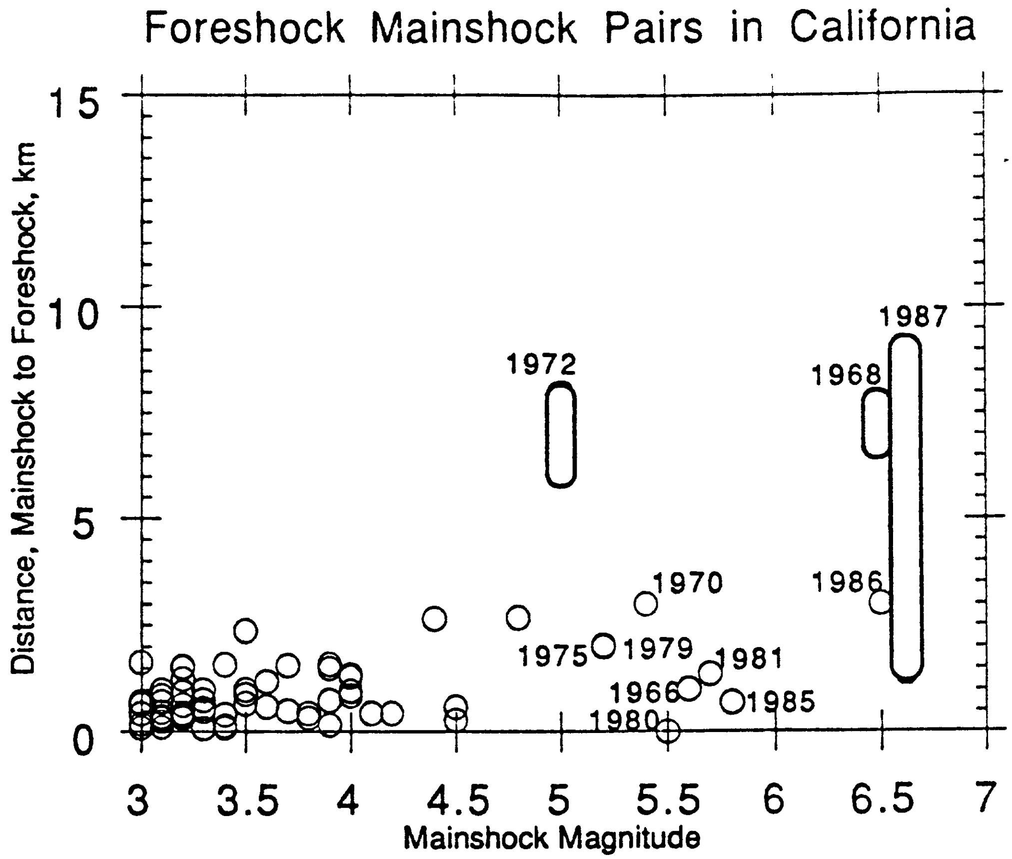

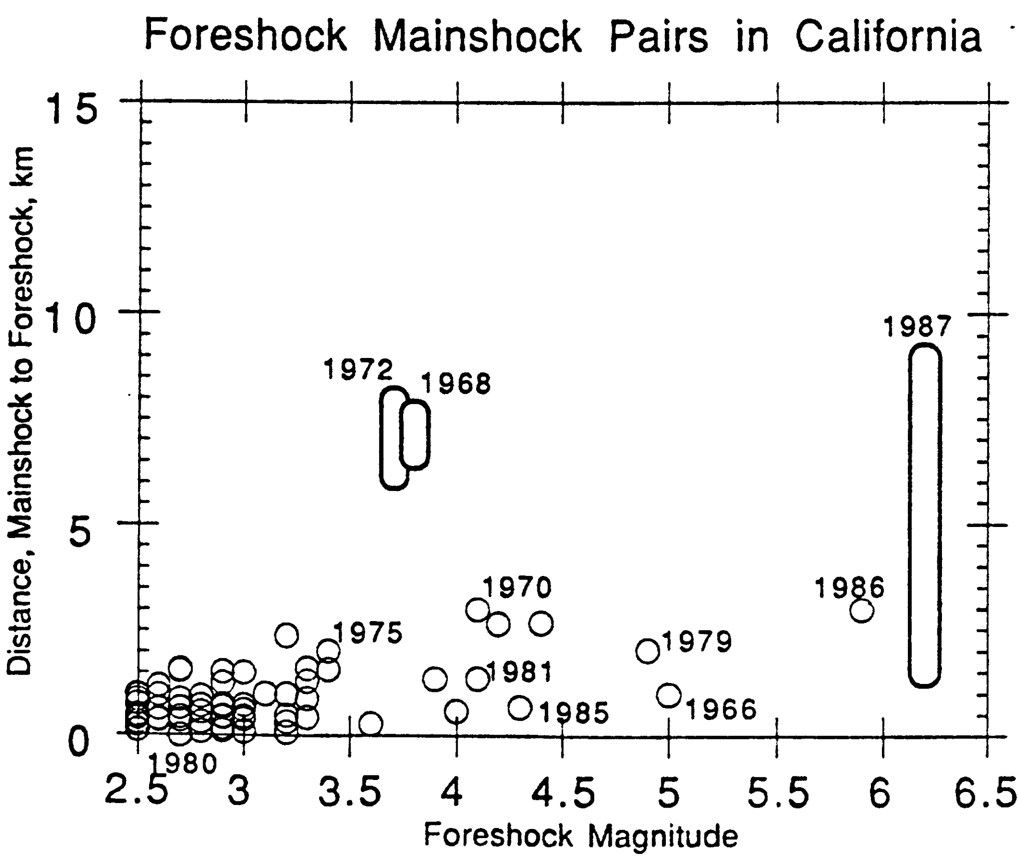

Figure 5. Distance between foreshock and mainshock epicenters versus the (a) magnitude of the mainshock and (b) magnitude of the foreshock for foreshock-mainshock sequences (foreshocks of magnitude 2.5 and greater and mainshocks of magnitude 3.0 and greater) recorded in the Caltech catalog between 1977 and 1987. Sequences that have been relocated in special studies are also plotted and include 1966 Parkfield, 1968 Borrego Mountain, 1970 Lytle Creek, 1972 Bear Valley, 1975 Galway Lakes, 1979 Homestead, 1980 Livermore, 1981 Westmoreland, 1985 Kettleman Hills, 1986 Chalfant Valley, and 1987 Superstition Hills.

III.2.2 Alert Thresholds for Foreshocks

Because we can now formally determine the probability of a large earthquake occurring after a potential foreshock, we can define minimum probabilities for each of the level-B, -C, and -D alerts. We define minimum probabilities that a mainshock will occur within the 72 hour alert interval after an earthquake along the two southern segments of the San Andreas fault of 5% for level-B, 1% for level-C, and 0.1% for level-D. We assume that if the rupture zone of the potential foreshock is within 10 km of the southern San Andreas fault, then the probability increases as outlined below. By defining the distance between the potential foreshock and the San Andreas fault in terms of the rupture zone, we require subjective judgement by the seismologists monitoring the fault. In particular, the documented tendency of earthquakes within the Brawley Seismic Zone (just south of the southern end of the San Andreas fault) to have rupture areas much larger than normally associated with earthquakes of the same magnitude (Johnson and Hill, 1982) and the presence of northeast trending faults in the same area (Hudnut et al., 1989) need to be taken into account.

Appendix A derives the conditional probability of a mainshock occurring given a potential foreshock (Equation 28). This conditional probability is a function of (a) the time window over which the probability is evaluated, (b) the long-term probability of the mainshock in that time window, (c) the length of the fault, (d) the rate density of background earthquakes (as a function of magnitude) over that length of the fault, and (e) the percentage of mainshocks preceded by foreshocks within that time period. As described in the Appendix, we have used Jones' (1984) finding that half of the strike-slip earthquakes in California were preceded by foreshocks within 3 units of magnitude and assumed a flat distribution with magnitude of the foreshocks for (e).

We have defined alert levels for two of the segments of the WGCEP (1988). They estimated the the 30-year probability of a mainshock of M = 7.5-8.0 to be 0.4 for the Coachella Valley segment and 0.2 for the San Bernardino segment (WGCEP, 1988). The corresponding long term probabilities for any 72-hour interval are 1.1×10^{-4} and 5.5×10^{-5}. The length of the two segments are 110 and 100 km, respectively. Table 1 gives the magnitudes of potential foreshocks needed to reach these conditional probabilities for characteristic mainshocks in the four microseismic zones of the southern San Andreas, given the rates of background activity as detailed in Appendix A.

TABLE 1. Magnitudes of Potential Foreshocks for the Southern San Andreas Fault

Alert level Probability of M7.5 in 72 hr	B 5-25%	C 1-5%	D 0.1-1%
San Bernardino	5.8	5.0	3.9
San Gorgonio	6.1	5.3	4.2
Palm Springs	5.2	4.5	3.4
Mecca	4.9	4.2	3.1

False alarm rates for these alert levels are calculated in Appendix A. The present rate of background seismicity will produce a level-B false alarm once every 28 years, a level-C false alarm every 5 years, and a level-D false alarm once every 5 months (note that the 0.001 probability at level-D is only 5 times greater than background). These false alarm rates are compatible with the stated probability levels. For a probability of 0.05, nineteen level-B false alarms should be issued for every successful prediction. The mean recurrence time of large earthquakes is about 250 years (WGCEP, 1988), and we assumed that half of these would be preceded by foreshocks. We should thus successfully predict once every 500 years during which time 18 false alarms would be issued (at 1 per 28 years). In the last 60 years of recorded earthquakes, one earthquake (the 1948 Desert Hot Springs local magnitude 6.5 earthquake) was large enough to trigger a level-B alert.

The magnitudes in the above table are determined using the results of WGCEP (1988) which give a 30-year probability for the Coachella Valley segment of a M=7.5-8.0 earthquake to be 0.4. Davis *et al.* (1989) have recently made a case for a much lower long-term probability of 0.09. This Working Group chose to use the 0.4 value; however, it is instructive to see the effect of this value on the total calculations. Table 2 therefore shows the same information as Table 1, but only for the Coachella Valley segment and using the lower long-term probabilities. Note that the magnitude needed to trigger each alert increases by 0.7 units for the Davis *et al.* (1989) probability.

TABLE 2. Alternate Solution Using Davis et al. (1989)
Magnitudes of Potential Foreshocks for the Coachella Valley Segment

Alert level Probability of M7.5 in 72 hr	B 5-30%	C 1-5%	D 0.1-1%
Palm Springs	5.9	5.2	4.1
Mecca Hills	5.6	4.8	3.8

The false alarm rates for these alternate values are one level-B false alarm every 126 years, one level-C false alarm every 23 years and one level-D false alarm every 2.2 years.

Tables 1 and 2 clearly demonstrate the importance of the estimated long-term probability for the short-term probabilities. The Davis *et al.* (1989) estimates require over a half unit of magnitude larger earthquake to reach each probability level. We have adopted the values in Table 1, based on WGCEP (1988), but we realize the uncertainties are large. Resolving the ambiguities in the long-term probabilities would greatly reduce these uncertainties.

III.3 Aseismic Fault Slip

Many theoretical analyses of fault rupture predict that the sudden, unstable slip of an earthquake should be preceded by some amount of stable slip on the fault (e. g., Stuart, 1986; Rudnicki, 1988; Lorenzetti and Tullis, 1989). The amount of slip depends upon the model but most models predict a measurable amount at the surface for the largest earthquakes. Fortuitous recordings from some previous earthquakes (described in Section III.3.3) also suggest that faults can start to move before the earthquake. Earthquake prediction experiments like those at Parkfield and the Tokai Gap in Japan have therefore included detailed recordings of ground deformation. However, for surface fault creep, we lack the data needed to make the formal calculation of conditional probabilities that we have for foreshocks. We have instead considered both the evidence for creep as a precursor to large earthquakes and the history of creep on the southern San Andreas fault, and from these factors developed subjective criteria for evaluating creep episodes along the southern San Andreas fault.

These criteria are restricted by the limited number of creepmeters installed along the southern San Andreas fault. At the present time, only one creepmeter is telemetered to Pasadena. If more data were available with reasonably dense spacing along the fault, then we would have required any recognized creep episode to be recorded on at least two creepmeters within 10 km. With present data, we do not have the luxury of redundancy.

III.3.1 Steady State Creep

Measurements of fault-crossing features in the Coachella Valley indicate slow aseismic surface creep. Observations of offset geological features since 1907, offset man-made features since 1950, and geodetic measurements of creep since 1970 all indicate that creep of 2-3 mm/yr has gone on for the last 80 years (Sieh and Williams, 1989). Where this aseismic creep has been monitored continuously (Figure 3), it mostly occurs in episodes lasting less than a day and having amplitudes less than 1 cm (Louie *et al.*, 1984). These episodes seem to occur randomly, but the long term rate of 2-3 mm/yr (determined on baselines of less than 20 m) appears to be steady, at least in the current century and possibly for a longer period. Geodetic data across the Coachella Valley (from baselines longer than 30 km) indicate a dextral shear rate greater than 20 mm/yr (King and Savage, 1983). A simple elastic model of the Coachella Valley suggests that the observed creep and shear strain data are consistent with an effectively frictionless fault zone in the uppermost 3-4 km of the fault, and a locked fault below that depth (Bilham and King, 1989).

III.3.2 Triggered Creep

Creep also occurs on the southern San Andreas fault at the time of, or shortly after, large local earthquakes. In 1968, 1979, and again in 1986, surface displacements of 2-20 mm occurred along segments of the fault after earthquakes with magnitude 6 or more. What causes such creep is not clear. Observed triggered creep of 22 mm at one location in the Mecca Hills in 1968 (Figure 3) may indicate that the maximum creep event amplitude may be larger than that so far observed by the few available creepmeters. The timing of the 1968 creep event, however, is not well known, and the observed displacement of 22 mm may represent several smaller creep events. The triggered creep is not necessarily coseismic; creep in 1986 occurred on Durmid Hill, 60 km from the North Palm Springs mainshock (Figure 3) and 17 hours after the mainshock (Williams *et al.*, 1989).

III.3.3 Evidence for Premonitory Creep on California Faults

There are two known cases in which creep may have occurred at the surface prior to a mainshock at depth:

> *Parkfield 1966:* En echelon cracks were observed along the fault trace in the days preceding the 1966 Parkfield earthquake, and a steel irrigation pipe across the fault broke nine hours before the mainshock (Wallace and Roth, 1967).
>
> *Superstition Hills 1987:* Six observations of developing fault creep in the hours to months following the 1987 Superstition Hills earthquake could be fit to a smooth model if 4-14 cm of creep had occurred on the northernmost 4 km of the fault before the mainshock (Sharp *et al.*, 1989).

Neither of these examples is completely satisfactory. The failed pipe at Parkfield could be a coincidence, and the surface cracks might be related to similar seasonal cracking subsequently observed in this area. The Superstition Hills evidence is better documented, but complicated by the foreshock. A large, magnitude 6.2, foreshock on the Elmore Ranch fault preceded this magnitude 6.6 earthquake by 11.4 hours. The inferred precursory creep occurred close to the intersection of the fault with the Elmore Ranch fault. When this creep occurred on the Superstition Hills fault is uncertain, and it could have been coseismic with and mechanically related to the first earthquake.

In the 1979 Imperial Valley earthquake (magnitude 6.5) on the Imperial fault, a creepmeter was in place across the fault well before the earthquake. The data from this instrument showed no fault motion until after the earthquake had begun (Cohn *et al.*, 1982). Thus precursory surface slip might occur prior to some, but certainly not all strike-slip earthquakes.

III.3.4 Alert Thresholds for Surficial Creep

We thus cannot ignore the possibility a fault slipping aseismically before a strike-slip mainshock. Even those scientists who believe that creep will not precede the next major earthquake still think that *if* a large amount of creep were seen, it should raise our expectations of a major earthquake. However, as was noted above, we lack the kind of data for creep needed to formally define the increase in mainshock probability. The Working Group therefore decided to use only one level of creep alert arbitrarily set equal to a level-D seismic alert. This would be declared whenever we observe creep greater than that so far recorded on the southern San Andreas fault, a more stringent requirement than for the seismic data (for which level-D alerts are expected annually). However, the unclear connection between creep and large earthquakes makes it appropriate to assign lower probabilities to creep alerts.

Creep alerts are defined separately for aseismic creep and creep episodes accompanying earthquakes. The three categories of creep, and the alert level for each are:

(1) Single aseismic creep events: The largest previous creep event recorded on the southern San Andreas fault was less than 1 cm (Louie *et al.*, 1984). Therefore, a single creep event exceeding 1 cm within 1 day will be considered anomalous and trigger a level-D alert.

(2) Multiple aseismic creep events: Triggered and aseismic creep combine to provide 2-3 mm/yr of creep on the southern San Andreas fault, a rate that appears constant over at least the last century. A significant increase in rate would be unusual. Therefore, if several creep events of less than 1 cm were to occur within 1 year such that the yearly rate exceeds 2 cm, the last creep event would trigger a level-D alert.

(3) Triggered creep: The documented occurrence of triggered slip following local, moderate earthquakes requires a higher slip threshold for triggered than aseismic slip. The largest previous creep event was 22 mm in the Mecca Hills following the 1968 Borrego Mountain earthquake. Triggered slip on the southern San Andreas fault will produce a level-D creep alert if it exceeds 25 mm of creep at any one site or 20 mm over at least 20 km.

Like the proposed alert levels for anomalous earthquakes, these levels should be regarded as the best educated guess until more extensive case histories permit stricter quantification.

III.4. Strain

III.4.1 Available Data

Strainmeters are not widely distributed in southern California. As described in Section III.1, only two installations measure strain within 100 km of the Coachella Valley: the Pinon Flat Observatory (PFO), 20 km south of Palm Springs, and water level monitors around the Salton Sea that can be used as a less sensitive tiltmeter (Figure 3). Short term strains on the order of one part in 10^9 can be resolved with the instruments at PFO while the Salton Sea installation can only resolve vertical deformation of one microradian per 2 days.

III.4.2 Alarm Criteria for Strain

Theory and some observations suggest that fault slip, like creep, can begin before an earthquake occurs. Thus, clear evidence of deep-seated slip on the southern San Andreas fault would be extremely anomalous and the basis for an earthquake alert. The problem is obtaining "clear evidence." Creepmeters measure surface offsets that may not be related to slip at depth where the earthquakes start. Strainmeters will respond to slip at depth but measurements of strain at one place cannot determine which fault the slip might be on. Indeed, a single record of strain change cannot show whether the strain reflects displacement along a distant fault, some kind of broad-scale deformation, or a small local displacement.

With only one set of sensitive strainmeters near the southern San Andreas fault, a strain anomaly cannot by itself indicate slip on that fault. However, strain measurements can be used to clarify data recorded by the seismic network or creepmeters. Strain measurements can limit models proposed on the basis of creep or seismicity data because over short time periods crustal response to fault slip is that of an elastic halfspace, as demonstrated by observations of coseismic strain. For example, if a large creep event were observed along a given fault, then far-field strain data may show whether it was caused by shallow or deep movement.

Declaring a strain anomaly is slightly complicated at PFO, because of the particular mix of instruments now in use there. Rather than attempting to set precise levels of anomalous behavior, we propose here to define an anomaly as a signal unprecedented in the history of the instrument, as judged by someone familiar with it. Routine monitoring would probably use the borehole instruments at PFO, because of greater simplicity in processing the data, but any anomaly seen on these should be regarded as tentative until confirmed by the PFO long-base instruments. An anomaly on the latter must be taken seriously, because these instruments have a long history of stability and are largely immune to local disturbances that might affect the borehole instruments. They are also much more accessible for testing if a problem with the instrument is suspected.

A strain anomaly would itself create only a level-D alert because of ambiguity in interpreting a strain signal from only one site. However, the location of such an anomaly could be estimated from creep or seismicity if either should occur. In the latter case, the known location and strain anomaly size would give an estimate of the source moment. To give some idea of the possible numbers, the detectable level of change in strain over 10 hours is 1-5 nanostrain depending on the instrument (if the earth tides were automatically removed). For slip along the southern part of the Coachella fault segment, this strain level at PFO corresponds to what would be seen for a magnitude 5 "slow earthquake." A smaller event farther north along the fault would give the same signal, and of course a more rapid event would be more easily detected.

III.4.3 Alert Thresholds for Strain

Borehole dilatometers used for routine monitoring of PFO strain will only be considered anomalous if confirmed by the long baseline instruments. Strain anomalies are treated differently depending on whether or not they occur together with signals from the seismic or creep networks. As for creep, large uncertainties in strain measurement and in the relation between strain and large earthquakes have led the Working Group to use only one level of strain alert, arbitrarily set equal to a level-D seismic alert.

(1) Aseismic Strain Signals: The definition of a level-D strain alert at PFO is that the signal is unprecedented in the history of the instrument as interpreted by someone familiar with it. This unsatisfying definition appears to be the best now available.

(2) Strain Accompanied by Fault Slip: Strain data from PFO can be used to delimit the type and amount of deformation when the location of the strain source can be determined, such as the

deformation associated with a magnitude 5 or greater earthquake or an aseismic creep event along the southern San Andreas fault. The level-D alert is defined to be strain signals detected by both borehole and surface instruments at PFO that indicate anomalous fault slip. "Anomalous" could mean unusually deep (greater than 8 km) or unusually large.

Because of the low sensitivity of the water level recorders at the Salton Sea, any tectonic tilt recorded at the Salton Sea should also be recorded by the more sensitive instruments at PFO. Therefore, signals from the tiltmeter network will not be used for short term alerts.

III.5 Cumulative Alert Thresholds

If more than one anomaly were recorded at one time, then the situation would be considered more threatening. For instance, as discussed in the strain section, strain anomalies accompanying a magnitude 5 earthquake that suggest abnormally large slip at greater depths (where the great earthquake is expected to begin) would be much more ominous than the magnitude 5 earthquake by itself. Indeed, many of the strain anomalies are defined as occurring with some seismic activity. Some way of combining the alert levels must be adopted.

Because the strain and creep anomalies produce only level-D alerts, the combination rules can be rather simple. We have adopted a simplified version of the Parkfield combination rules. Thus a level-D alert occurring during a preexisting level-C or -D alert will raise that alert by one level. The level-C alert would become level-B and the level-D alert would become level-C, if another level-D alert occurs within 72 hours. For instance, a magnitude 4 earthquake along the Coachella Valley segment would by itself trigger a level-D alert. If creep greater than 25 mm were to accompany or occur within 3 days of that earthquake (Creep level-D alert #3), then the combined alert level would be level-C. We feel that the relationship between possibly precursory strain and earthquakes is not well enough understood to justify raising a seismic level-B alert to level-A (a probability greater than 25%) because of a strain or creep anomaly.

IV. Response Plan for the USGS

The purpose of our alert system is to quantify and communicate information about temporary increases in the earthquake hazard. When an alert is declared, the scientists in data acquisition, both inside and outside the USGS, of course must assure the integrity of the data recording systems. But when an alert is declared, the USGS must also communicate this information to interested parties, both scientific and governmental. The response plan for the USGS detailed here is essentially the same as agreed upon for Parkfield, considering the different organizational structures of its southern and northern Californian operations. This plan involves only the scientific response to an alert level and notification of the Governor's Office of Emergency Services of the State of California (OES).

The Chief of the USGS Office of Earthquakes, Volcanoes and Engineering (OEVE) must appoint and support a chief scientist for the southern San Andreas fault. All alerts for the southern San Andreas fault will be declared by this chief scientist. Data from three different projects, the seismic network, the creepmeters and the Pinon Flat strain observatory, can trigger an alert, but only one of these projects, the seismic network, is even partially operated by the USGS. If a central data recording center is established as recommended in the next section, operations of that center will be coordinated so that the chief scientist for the southern San Andreas will be notified of anomalies in any recorded phenomena. Until such time, the seismic data are monitored by USGS scientists, but university scientists must report anomalies in the other phenomena by telephone to the chief scientist. When an alert is declared in any of the three categories, the chief scientist will ask the researchers in all three projects to check their data to (1) look for other possible anomalies and (2) assure the integrity of the data recording and analysis systems. At a minimum, this alert system should insure that data on the great earthquake not be lost because of easily fixable, but unnoticed equipment problems.

The specific scientific response by the USGS to the three levels of alerts are given below.

Level-D Alert - Awareness

A level-D alert means that the probability of a great earthquake occurring within 72 hours is in the range of 0.1-1%. The appropriate response to this level is awareness. As described above, the chief scientist will notify all groups actively monitoring the southern San Andreas and request a check on other possible anomalies and the integrity of the data recording systems. The chief scientist will notify the scientist-in-charge of the southern California office of the USGS in Pasadena, and the chiefs of the Branches of Seismology and Tectonophysics in Menlo Park. Scientists outside the USGS doing research on the southern San Andreas fault could make arrangements to receive notification by fax or electronic-mail. The chief scientist will also notify the southern California office of the OES. At these low probabilities, no further action is warranted.

Level-C Alert - Precaution

A level-C alert means that the probability of a great earthquake occurring within 72 hours is in the range of 1-5%. The appropriate response to this level is precaution. In addition to the activities undertaken for a level-D alert, the chief scientist will also notify the chief of the USGS Office of Earthquakes Volcanoes, and Engineering (OEVE) and the office of the Director of OES in Sacramento. The USGS will also request that available field geologists to go to the southern San Andreas to check for surface offsets and set baselines for measuring any future offsets.

Level-B Alert - Preparation

A level-B alert means that the probability of a great earthquake occurring within 72 hours is in the range of 5-25%. The appropriate response to this level is preparation. In addition to the activities undertaken for level-D and level-C alerts, the office chief of OEVE will also notify the Director of the USGS and the State Geologist of California. An intensive scientific monitoring effort will be undertaken, coordinated by the scientist-in-charge of the USGS' southern California office.

The extent of the intensive monitoring effort will depend on the resources available at the time of the alert. The present plan calls for notifying of the chief of the Branch of Engineering Seismology and requesting deployment around the southern San Andreas fault of several portable high dynamic range, digital seismic stations. In addition, all portable high gain and strong motion instruments available in southern California (at present 3 strong motion and 1 high gain portables) should be deployed. A geodetic resurvey of all geodetic nets on the southern San Andreas and deployment of portable GPS receivers will be requested.

V. Need for Improved Instrumentation

In preparing this report, the Working Group was struck by the inadequacy of the information available from the southern San Andreas fault. Strain is recorded at only one site and creep at only 4 sites. Seismic station spacing is so sparse that the depths of most earthquakes cannot be resolved, and the dynamic range of the telemetered stations is so limited that earthquakes above about magnitude 3.5 are not recorded on scale. Analog telemetry so limits the dynamic range and bandwidth that questions about the spectral characteristics cannot be addressed. The data are recorded at many different sites with limited coordination between the different organizations. These inadequacies reduce the chance that a useful warning about the next great southern San Andreas earthquake will be issued. The charge of the Working Group was "to recommend ways in which the scientific community might best keep abreast of the changing situation along the fault, increase its understanding of the regional seismotectonics, and offer appropriate scientific advice to local governmental agencies." To complete this task, the Working Group strongly recommends that the recording and analysis of geophysical data from the southern San Andreas fault be improved.

Earthquake precursors, especially foreshocks, can occur within a very short time, minutes to hours, before the mainshock. Thus, for information to be useful for short-term warnings, it must be immediately available to scientists; however, very few data in southern California are accessible in real time. Many of the recommendations below should improve the real-time flow of data to a central recording site.

Improving the quality of the data and not just its accessibility would also enhance our ability to issue short term warnings in southern California. Almost all instrumentation near the southern San Andreas fault was installed in the 1970's. Since that time, both the instrument quality and the scientific understanding of data from those instruments have greatly improved. As seismology has developed, we have found that information beyond the fact of earthquake occurrence could be used to assess the likelihood that an earthquake is a foreshock to a great event. Immediate questions that arise include:

1. What are the time, location, depth, magnitude and focal mechanism of the potential foreshock event(s)?
2. On which fault did the potential foreshock occur?
3. Did the potential foreshock rupture toward or away from the San Andreas fault?
4. Did surface rupture take place?
5. Is creep or slip occurring above or below the seismogenic zone?
6. What were the dynamic and static stress drops of the potential foreshock?
7. Do continuous strain data suggest significant aseismic fault slip?
8. Where and when did triggered slip occur on nearby faults?

These questions must be answered within a few minutes or at least a few tens of minutes after the potential foreshock. Unfortunately, present instrumentation near the southern San Andreas fault and current scientific understanding of the tectonics and seismicity of the fault are inadequate to answer these questions accurately. Thus, the following sections discuss short-term and long-term improvements to the existing system to provide a more detailed analysis capability for this critical section of the San Andreas fault. Within each type of operation, the recommendations easiest to implement are listed first.

V.1 Centralized Recording and Analysis

Coordination and Response. Because so many different organizations are involved in recording data in southern California, coordination and communication between the different groups has been limited. The present organization of the USGS in southern California provides no mechanism for issuing the alerts described in this report.

> **Recommendation 1:** As an organizational first step, appoint a chief scientist for the southern San Andreas fault to coordinate response. This person would monitor ongoing seismic activity and coordinate scientific investigations as has been done for Parkfield and Mammoth Lakes. This task would include developing the scientific expertise needed for short term earthquake hazard assessment using both seismic and deformation data.

Recording Center. Some instruments presently in the area record data only on site. Just the Salt Creek and North Shore creepmeters in the Coachella Valley are telemetered (intermittently via satellite) to Pasadena and the data are not routinely available for real-time analysis. Similarly, numerous strain and tilt instruments at Pinon Flat and USGS dilatometers in the Mojave Desert are recorded locally. In some cases, data are transmitted to Menlo Park via satellite, and a simple E-mail command code would permit timely transmission of these data from Menlo Park to Pasadena.

A central recording site is urgently needed where the relevant creep and strain data may be analyzed in near real-time with the seismic data. Because the seismic data are recorded in Pasadena, this is a logical site for a southern California center. In many cases, Pasadena may not have the necessary expertise to evaluate the strain data, but they should be available for display to develop such expertise, and the necessary experts can be consulted over the telephone.

> **Recommendation 2:** Install the necessary software and telemetry so that creep and strain data can be received and displayed in real-time in Pasadena. Begin with borehole strainmeter and air pressure data from Pinon Flat Observatory.

V.2 Seismological Data

Real-time Analysis. At present, only a small subset of data is easily available in real-time in Pasadena from the southern California seismic network. A 64-channel real-time processor (RTP) is now used to determine real-time earthquake locations and magnitudes. Because signals from only 64 stations can be processed in real time, and the area being monitored is all of southern California, not all available stations along the southern San Andreas fault are utilized to calculate the location and magnitude of each earthquake. With this limitation, only about 25% of the network is being used to determine the locations, so that depths cannot be determined; focal mechanisms are unreliable or indeterminate; and the location errors of the epicenters are large.

If a magnitude 5-6.5 earthquake were to occur near the southern San Andreas fault, the present system would provide an eepicentral location accurate only to about 5 km. The depth and focal mechanism of the earthquake would not be known for at least one hour, perhaps much longer. It would also be difficult to monitor the spatial development of its aftershock sequence, because epicentral locations of low quality tend to smear over a large area. If data from all currently operating seismograph stations in southern California were analyzed by a RTP, then the uncertainty in the hypocenters could be reduced from approximately 5 km to 1-2 km, and focal mechanisms could be determined with reasonable accuracy.

> **Recommendation 3:** Upgrade the real-time earthquake processing capability for southern California from 64 to all 256 seismic stations.

Magnitudes. The present RTP can determine duration magnitudes only up to about magnitude 4. This hardware limitation results from signal clipping associated with the exclusive use of high-gain seismographs.

> **Recommendation 4:** Implement available methods to determine magnitudes of large earthquakes in real time, using force-balance accelerometers and low gain seismometers already in place.

Station Density. The spacing of high-gain, short period seismic stations in southern California is about 20 km. This spacing is inadequate for obtaining high quality hypocenters and for correlating hypocenters with the mapped trace of the San Andreas fault or nearby orthogonal faults. Currently no stations are located immediately west of the fault in the Coachella Valley sediments, because borehole installations are required to avoid near-surface noise and attenuation. Data from new borehole stations would provide high quality hypocenters and source parameters, which, in turn would allow monitoring of the stress around stuck patches of the fault (e. g., Malin *et al.*, 1989). Meaningful monitoring of rupture direction and migration of hypocenters would also become possible. With digital telemetry, these stations would have sufficient band-width for many waveform studies.

> **Recommendation 5:** Upgrade the existing high-gain short period network by adding about 40 new three-component stations, some installed in boreholes for improved dynamic range. Data should be digitally transmitted for high fidelity signal recording.

V.3 Strain and Creep Data

Creep and Slip Data. Following a magnitude 5 earthquake, geologists will drive to the Coachella Valley to look for surface rupture and triggered slip. They will require 2-4 hours (presuming no major traffic delays) to reach various stretches of the Coachella Valley segment by automobile from Pasadena. Creepmeters and slip meters could provide immediate information about surface fault displacement if they were installed with 5-10 km spacing across the fault and nearby secondary faults and telemetered to the central facility.

> **Recommendation 6:** Deploy an array of at least 20 (1 every 10 km) creep and slip meters along the southern San Andreas fault and candidate complementary faults. Data from these instruments should be telemetered using channels on the planned microwave link that will also transmit the data for the seismic network to Pasadena.

Strain and Tilt Data. No borehole strainmeter is currently deployed close to the southern San Andreas fault. The utility of strain measurements in any alarm system is greatly increased if the strainmeters are deployed at more than one site. Data from at least one additional borehole strainmeter near the San Andreas fault, in conjunction with PFO strain data and Salton Sea tilt data would greatly help us in determining alert thresholds. Obviously a number of borehole or long baseline strainmeters along the San Andreas fault, although perhaps outside the actual fault zone itself, would better define possible slip models than a single borehole strainmeter. These data may be acquired in a variety of ways. However, any installation of deformation-measuring instruments will require large capital costs and a long-term commitment to operations, so the task must be well organized and coordinated.

Recommendation 7: A group of university and USGS scientists should begin the planning for the establishment of deformation measuring instrumentation to monitor strain and tilt along the southern San Andreas fault. This plan should be coordinated with new seismic equipment for a balanced expenditure of funds and an integrated field program.

V.4 Fundamental Understanding of the Southern San Andreas Fault

The above recommendations will improve the data available for issuing short-term warnings of a major earthquake, based on existing knowledge of the San Andreas fault and the behavior of past earthquakes. However, an improved understanding of the earthquakes, geologic history, and seismotectonics of the San Andreas fault as well as the earthquake process would improve our ability to use the data we had. The Working Group has found that many aspects of the southern San Andreas fault are not well understood and this impairs our ability to respond. We therefore recommend that more fundamental studies of the fault be carried out. These studies should include:

Geodetic Measurements. Because any earthquake is the result of a cycle of accumulated strain, measurements of the regional strain field and changes in that field are essential to a physical understanding of it. Measuring how the strain field close to the fault interacts with the more distant strain field (on both long and short time scales) is particularly important. At present, one large aperture and seven small aperture networks of geodetic monuments cross the southern San Andreas fault. The new satellite based measurements (GPS - Global Positioning System) are the most reliable and efficient system for regional geodetic measurements while traditional geodetic techniques are useful for smaller scale measurements.

Recommendation 8: Establish fixed networks of GPS receivers and augment the dense arrays of geodetic monuments to study strain buildup and release around the southern San Andreas fault.

Improved Probability Estimates. As Tables 1 and 2 show, the value for the long-term probability of a major earthquake is important in determining short-term probabilities after a potential foreshock. For the southern San Andreas fault, this long-term probability is extremely uncertain for two reasons. First, the geologic data applicable to this question are now limited to only one paleoseismic site. Also, there is currently disagreement (described above) on how long-term probability should be estimated from these data. These are not, however, the only factors that could be improved. We could also use information on how the frequency of foreshocks depends on both the variables we have used and on others (such as the focal mechanism) that we have not included.

Recommendation 9: Expand paleoseismic and geologic studies of the southern San Andreas fault to improve our estimates of the times and surface slip distributions of previous major earthquakes.

Recommendation 10: Continue research on the best methods for determining long-term probabilities of major earthquakes from limited data on recurrence times of previous earthquakes. Develop more complete data sets for foreshocks, and improved ways to examine their statistics.

General Seismological Studies. In addition to a dense short-period network, broad-band, high-dynamic range seismometers provide detailed information, especially about the spectrum of an earthquake, to study its physics. Studies of dynamic and static stress drops around asperities on faults, combined with high quality hypocenters from the high-gain downhole network recommended above, are promising research areas in fault zone physics.

Recommendation 11: Install several wide dynamic range, broad-band seismometers in southern California and use their data study source and path effects.

We feel that relatively inexpensive options should be implemented quickly (Recommendations 1, 2, 3, 4 and 10). If additional funding were to become available for operations along the southern San Andreas fault, a reasoned, careful approach should be undertaken to make the most cost-effective use of those funds.

References

Allen, R. V., 1982, Automatic phase pickers: Their present use and future prospects, *Bull. Seismol. Soc. Amer.*, **72**, S225-S242.

Bakun, W. H., and A. G. Lindh, 1985, The Parkfield, California, earthquake prediction experiment, *Science*, **229**, 619-624.

Bakun, W. H., K. S. Breckenridge, J. Bredehoeft, R.O. Burford, W.L. Ellsworth, M.J.S. Johnston, L. Jones, A. G. Lindh, C. Mortensen, R. J. Mueller, C. M. Poley, E. Roeloffs, S. Schulz, P. Segall, and W. Thatcher, 1987, Parkfield, California, earthquake prediction scenarios and response plans, *U.S. Geol. Surv. Open-file Rep. 86-365*, 59 pp.

Bilham, R., and G. King, 1989, The morphology of strike-slip faults: Examples from the San Andreas fault, California, *J. Geophys. Res.*, **89**, 10,204-10,216.

Cohn, S. N., C. R. Allen, R. Gilman, and N. R. Goulty, 1982, Pre-earthquake and post-earthquake creep on the Imperial fault and Brawley Seismic Zone, in **The Imperial Valley, California Earthquake of October 15, 1979**, U.S. Geol. Surv. Prof. Paper 1254, U.S. Government Printing Office, 183-191.

Davis, P. M., D. D. Jackson, and Yan Y. Kagan, 1989, The longer it has been since the last earthquake, the longer it will be to the next?, *Bull. Seismol. Soc. Amer.*, **79**, 1439-1456.

Goltz, J., 1985, The Parkfield and San Diego earthquake predictions: a chronology., Special Report by the Southern California Earthquake Preparedness Project, Los Angeles, CA, 23 pp..

Hudnut, K. W., L. Seeber, and J. Pacheco, 1989, Cross fault triggering in the November 1987 Superstition Hills Earthquake Sequence, southern California, *Geophysical Research Letters*, **16**, 199-202.

Johnson, C. E., and D. P. Hill, 1982, Seismicity of the Imperial Valley, in **The Imperial Valley, California Earthquake of October 15, 1979**, U.S. Geol. Surv. Prof. Paper 1254, U.S. Government Printing Office, 15-24.

Jones, L. M., 1984, Foreshocks (1966-1980) in the San Andreas system, California, *Bull. Seismol. Soc. Amer.*, **74**, 1361-1380.

Jones, L. M., 1985, Foreshocks and time-dependent earthquake hazard assessment in southern California, *Bull. . Seismol. Soc. Amer.*, 75, 1669-1680.

Jones, L. M., 1988, Focal mechanisms and the state of stress on the San Andreas fault in southern California, *J. Geophys. Res.*, **93**, 8869-8891.

Jones, L. M., and P. Molnar, 1979, Some characteristics of foreshocks and their possible relationship to earthquake prediction and premonitory slip on faults, *J. Geophys. Res.*, **84**, 3596-3608.

King, N. E., and J. C. Savage, 1984, Regional deformation near Palmdale, California, 1973 - 1983, *J. Geophys. Res.*, **89**, 2471-2477.

Lorenzetti, E., and T. E. Tullis, 1989, Geodetic predictions of a strike-slip model: Implications for intermediate- and short-term earthquake prediction, *J. Geophys. Res.*, **94**, 12,343 -12,361.

Louie, J. N., C. R. Allen, D. C. Johnson, P. C. Haase, and S. N. Cohn, 1985, Fault slip in southern California, *Bull. Seismol. Soc. Amer.*, **75**, 811-833.

Malin, P. E., S. N. Blakeslee, M. G. Alvarez, and A. G. Martin, 1989, Microearthquake imaging of the Parkfield asperity, *Science*, in press.

Rudnicki, J. W., 1988, Physical models of earthquake instability and precursory processes, *Pure and Appl. Geophys.*, **126**, 531-554.

Savage, J. C., W. H. Prescott, and G. H. Gu, 1986, Strain accumulation in southern California, 1973-1984, *J. Geophys. Res.*, **91**, 7455-7474.

Sharp, R. V., K. E. Budding, J. Boatwright, M. J. Ader, M. G. Bonilla, M. M. Clark, T. E. Fumal, K. K. Harms, J. J. Lienkamper, D. M. Morton, B. J. O'Neill, C. L. Ostergren, D. J. Ponti, M. J. Rymer, J. L. Saxton, and J. D. Sims, 1989, Surface faulting along the Superstition Hills fault zone and nearby faults associated with the earthquakes of 24 November 1987, *Bull. Seismol. Soc. Amer.*, **79**, 252-281.

Sieh, K. E., 1986, Slip rate across the southern San Andreas and prehistoric earthquakes at Indio, California, *Trans. Amer. Geophys. U.*, **67**, 1200.

Sieh, K. E., and P. L. Williams, 1989, Behavior of the southernmost San Andreas fault in the past 300 years, *J. Geophys. Res.*, in press.

Stuart, W. D., 1986, Forecast model for large and great earthquakes in southern California, *J. Geophys. Res.*, **91**, 13771-13786.

Wallace, R. E., and E. F. Roth, 1967, The Parkfield-Cholame California earthquakes of June-August 1966: Rates and patterns of progressive deformation, *U. S. Geol. Surv. Prof. Pap. 579.*

Williams, P. L., McGill, S. F., Sieh, K. E., Allen, C. R., and J. N. Louie, 1988, Triggered slip along the San Andreas fault after the 8 July 1986 North Palm Springs earthquake, *Bull. Seismol. Soc. Amer.*, **78**, 1112-1122.

Working Group on California Earthquake Probabilities, 1988, (D. C. Agnew, C. R. Allen, L. S. Cluff, J. H. Dieterich, W. L. Ellsworth, R. L. Keeney, A. G. Lindh, S. P. Nishenko, D. P. Schwartz, K. E. Sieh, W. Thatcher, and R. L. Wesson), Probabilities of large earthquakes occurring in California on the San Andreas fault, *U.S. Geol. Surv. Open-file Rep. 88-398*, 62 pp.

Appendix P

Memorandum and related materials prepared by P.Reasenberg to accompany presentation to NEPEC, May 1, 1990.

Draft Memorandum to NEPEC on appropriate uses of the USGS aftershock sequence model and guidelines for drafting aftershock forecasts

P. A. Reasenberg
30 April, 1990

1. Introduction

Many studies have sought patterns in earthquake occurence predictive of future strong earthquakes. Most of these studies have found that aftershock sequences – intense clusters of earthquakes in space and time associated with a mainshock – are the strongest non-random features in the seismicity. Aftershock sequences so strongly shape the seismicity that many investigators first attempt to identify and remove all aftershocks before searching for other patterns.

The fact that aftershocks occur in recognizable patterns in time, space and magnitude can be used to advantage. General laws describing the average occurence of aftershocks can be used as a basis for predicting, in a probabilistic sense, earthquakes after a mainshock. Two classes of earthquakes that may follow a mainshock are considered separately here. First are aftershocks smaller than the mainshock, which may themselves be strong enough to be hazardous. The second class are earthquakes larger than the mainshock that may follow it. (In this case, the original mainshock is retrospectively termed a foreshock.)

Probabilities of occurrence for both classes of earthquakes can be derived from the USGS aftershock model. The model is based on observations of the ongoing sequence and historic earthquake sequences. It can be applied in any seismically active region for which sufficient historic data have been compiled. At this time historic data have been compiled for California and central Japan; compilations for other regions are in progress.

It is the intention of the USGS to model earthquake sequences in real time following mainshocks in order to derive short term (days to months) probabilistic predictions of future earthquake activity. It is planned that this modeling will begin immediately after a mainshock, and may continue during the aftershock sequence. It is expected that this modeling will result in a set of reliable (statistically valid) short term estimates of the likelihood for additional damaging earthquakes – either strong aftershocks or a larger mainshock. It is the intention of the USGS that these probabilistic estimates will be expressed as concise statements, hereafter referred to as forecasts.

The first forecast, made immediatley after the mainshock, will be based on the magnitude of the mainshock and on historic patterns of aftershock sequences. In California this forecast will be communicated first to OES, which has responsibility in California to disseminate hazard warnings to the public and to county and local officials. At later times during the earthquake sequence the USGS will make forecasts utilizing additional information about the aftershocks that have already occurred.

In the following sections of this memorandum we discuss factors considered pertinent to the formulation, design, application and dissemmination of these forecasts.

2. Areas of applicability of the aftershock model.

The range of applicability of the model reflects the range over which basic assumptions of the model are valid. (See Appendix I for a description of the model and assumptions.) The basic assumptions are (1) that earthquake sequences follow the modified Omori relation in time; and (2) that earthquake sequences follow an exponential (Gutenberg-Richter) magnitude distribution. With respect to the first assumption there is generally little dispute. Some researchers prefer an exponential time distribution, but to date so little is known about the physics controlling the time behavior of the aftershock process that there is no strong reason to reject the use of a modified Omori relation for our purposes.

With respect to the assumption of an exponential magnitude distribution, however, other models of earthquake occurence may either conflict or partially conflict. First, the idea that a given region is physically incapable of producing earthquakes greater than some specified magnitude truncates the model's magnitude distribution. The arguments for such a magnitude limit may vary with region and researcher, but sometimes a concensus for one exists. In these cases, the model can be modified to accomodate this additional constraint. Therefore, when the USGS considers the idea of a maximum magnitude in a given region to be a significant factor, it should adopt a truncated magnitude model. Such a situation occurred in the 6 March, 1989, Obsidian Buttes $M4.7$ earthquake sequence (see Appendix III).

Another potential conflict with the model can arise if an aftershock sequence is located near a fault segment that is thought, for independent reasons, to be close to failure (and, accordingly, has been assigned a high intermediate-term probability for a large earthquake). In these cases the aftershock model may underestimate the actual probability for large events in the sequence, and the model probability should be considered a lower bound. For example, the model probability of a $M \geq 5.5$ earthquake occurring in the 72-hour interval after a magnitude 3.5 event on the San Andreas fault near San Ardo is less than 0.001. However, because of its proximity to the Parkfield segment (20 km northwest of Middle Mountain and within the Parkfield Alert Zone) most researchers would judge this result to be too low. For this case, the Parkfield earthquake prediction scenario estimates the probability of a characteristic Parkfield earthquake to be 0.028.

3. Design of the forecasts.

The set of earthquakes following a mainshock are known collectively as an aftershock sequence. Analogously, we refer to the set of probability forecasts that may follow a mainshock as a "forecast sequence". Obviously, one can construct many different forecast sequences – all equally correct in a numerical sense – but differing widely in frequency of issue, earthquake magnitudes and time intervals specified, wording emphasis and tone, audience targeted, method of dissemination, etc. The primary users of aftershock forecasts are officials responsible for emergency response and the media. How should the forecast sequence be designed to best address the information needs of the users?

Public officials need an immediate forecast of the short-term probability of a larger event for use in deciding whether to issue an earthquake hazard advisory. The generic model can provide such a forecast immediately after the mainshock. Public officials also need updates to this model at appropriate intervals after the mainshock. After the Loma Prieta earthquake the USGS issued updates twice a day for 8 days, then daily for the next 9 days, and then twice weekly for the next 4 weeks. This particular schedule, which evolved as the sequence progressed, reflected our day-to-day sense during the earthquake sequence of what was needed. We have not received criticism that those forecasts were either too frequent or too infrequent. Clearly, during the early stage of an earthquake sequence, relatively frequent forecasts are needed to reflect the high and rapidly decreasing hazard; later in the sequence, less frequent forecasts are needed.

The public's need for aftershock hazard forecasts is more difficult to assess. Dennis S. Mileti, Professor of Sociology and Director of the Hazards Assessment Laboratory, Colorado State University, discussed the public's hazard information needs and perceptions in his recent testimony to Congress after the Loma Prieta earthquake (Appendix IV). Mileti proposes that the individuals who receive hazard warnings go through a three-part process: hearing, perceiving (understanding, believing or personalizng) and responding. He states that all stages of this process are sensitive to many factors related to the information content and style of the warning (Appendix IV, page 4). Mileti's comments are very relevant to aftershock forecasts, and we recommend that they be used as guidelines in the design and wording of the forecasts.

One important idea Mileti brings out is that some people tend to discount the hazard of aftershocks: "Of course aftershocks occur after earthquakes; they are smaller, and if I and my house survived the mainshock, we'll survive the aftershocks." The idea that an aftershock can be damaging – possibly more damaging than the mainshock – is not always perceived.

The public needs to understand basic facts about the typical time behavior of an earthquake sequence. They should understand that the hazard will diminish with time and eventually return to a negligible level. At the same time, they need to understand that the specific times of aftershocks cannot be predicted, except in a probabilistic sense. An effective way to convey these ideas is through a sequence of regularly spaced (*e.g.*, daily) forecasts. The slowly decreasing probabilities in these forecasts make clear both the diminishing and enduring nature of the aftershock hazard.

Characterizing the hazard with probabilities. An earthquake sequence consists of very brief periods of very high hazard (earthquakes) separated by much longer intervals of no hazard. The intervals between earthquakes are, of course, random. Experiencing such a random and spiky hazard-time function is rather unusual. Other situations with a similar hazard-time function include lightening in an electric storm, incoming artillary on the battlefield and tornados during a tornado watch. These situations tend to be anxiety-raising because of the random and spiky nature of the hazard. To characterize this hazard, we use probabilities, thereby converting a spiky hazard-time function into a smooth one. But for an individual to accept these probabilities as a believable measure of the (random and spiky) aftershock hazard requires either mathematical sophistication or faith. While probabilities convey important information, they are technical and not easily interpreted and translated by individuals into hazard-mitigative actions. These ideas were alluded to in a draft Plan for Research resulting from the recent Beckman Center (January 15-16) Workshop in Irvine, California, and summarized by Thomas L. Henyey, Professor and Chairman of Geological Sciences, University of Southern California.

Describing the hazard with probabilities can be misleading because doing so leads people to focus on the probability assigned to an earthquake rather than on its potential effects. As the estimated probabilities drop with time, the public perception of the hazard decreases. However, a $M6$ aftershock that was assigned a 2% probability of occurring is just as damaging as a $M6$ earthquake that was given a 30% chance of occurring (*i. e.*, probabilities diminish, but earthquakes either happen or they don't). The appropriate response in the 2% case in many situations will be identical to that in the 30% case: prepare. To shift the focus away from probabilities and toward hazard mitigation actions we recommend that aftershock forecasts include a narrative describing the probable effects, in terms of expected additional damage, landslides, etc., expected as a result of the earthquakes that are being forecast.

Specification of the earthquake magnitude to be forecast. Obviously, forecasts should focus on earthquakes big enough to have damaging effects. This magnitude will vary depending on local geology and the degree of regional development, but a working threshhold might be $M \geq 5$. Confusion arose during the Loma Prieta earthquake sequence forecasts from the fact that probabilities were given for both $M \geq 5$ and $M \geq 6$ aftershocks. This was too much information. The facts that a hazard is present and slowly abating are effectively conveyed by consistent announcements of probabilities for one range of aftershock magnitudes. While it is true that in the Loma Prieta sequence a magnitude 6 aftershock would cause additional damage over a larger area than one of magnitude 5, this distinction may be too fine for assimilation during the chaotic times after a strong earthquake. Thus, in future situations of this kind we recommend forecasting only the probability of $M \geq 5$ aftershocks.

Specification of the time intervals in the forecast. The length of the interval over which the hazard's probability is calculated and expressed characterizes the hazard perhaps even more than the numerical value of the probability assigned to that interval. While the length of interval is formally a free parameter in the methodology, the choice of this length affects how individuals will perceive the warning, and how they will respond to it. I think it is useful to support the concepts of a short term hazard and a long term hazard. Doing so implicitely sends a message that hazard mitigation actions that take a day, a few days or even a week to accomplish are still worth doing – that the hazard has that kind of time scale associated with it. Based on our experience with the Loma Prieta sequence, I recommend using a short-term interval of 1 week and a long-term interval of 3 months for expressing earthquake probabilities.

Frequency of forecasts. At the start of the Loma Prieta sequence we calculated and announced 24-hour short term forecasts. Because the probabilities associated with this very short time window decrease rapidly in the beginning of the sequence we issued forecasts twice-daily for the first 8 days. Some members of the Irvine Workshop criticised that the forecast probabilities seemed to vary too fast or erratically the first week of the Loma Prieta sequence. This criticism was also raised by some councilmembers at the January, 1990 NEPEC meeting. I think the criticism is valid, and that at fault is the original choice of a 24-hour interval over which to estimate probabilities; it is too short. Adopting 1-week and 3-month intervals allows the frequency of forecasts to be reduced; daily forecasts in the beginning of the sequence will be adequate. Day-to-day changes in the probabilities estimated for 1-week and 3-month intervals will be relatively slow, and hopefully less confusing. For example, applying this protocol to a generic $M7$ earthquake sequence produces the following 1-week probabilities of a $M \geq 5$ aftershock calculated on each of the first 7 days after the mainshock: .97, .72, .59, .50, .44, .39, .35, .32.

The frequency of forecasts should be tapered as the sequence progresses. Perhaps a useful guideline for when to stop issuing forecasts is when the long term (3-month) probability of a $M \geq 5$ aftershock is less than 20%. (For Loma Prieta, this was November 20, 1989; in fact we issued our last forecast on November 30.)

Wording and tone of the forecasts. The language in the forecast should both reflect the hazard levels and suggest appropriate responses. Here again, many of Mileti's comments are relevant. Language that underscores the unpredictability of aftershocks should be included. Some measure of down-home, better-safe-than-sorry advice about the need for preparation would be useful. One important purpose of issuing forecasts is to personalize the risk and thus to stimulate appropriate hazard-mitigative measures by individuals. Simply stating the presence of a hazard may contribute more to raising anxiety levels than to stimulating useful preparatory responses. The widely-held perception that the period after a strong earthquake is too late for earthquake preparation must be corrected. Thus, we recommend including language in the forecast aimed at stimulating appropriate mitigative response throughout the aftershock sequence.

Caveats in the forecast. Some people are fairly sophisticated about the meaning of probabilities. We all know what "a 50% chance of rain" means, and appropriate response is obvious: close the windows, carry an umbrella. But, as discussed above, probabilities of aftershocks are not so easily interpreted. There are no 'earthquake clouds' visable to verify the forecast, and "what is one supposed to do, anyway?" The worst case of misunderstanding I can think of is one in which a person acts on the mistaken understanding that a particular aftershock forecast meant that no earthquake would occur, and as a result unnecessarilly suffers damage or loss of life when an earthquake does occur. In order to prevent misunderstandings and to help translate the information we put out into a useable form, I propose the following text for all forecasts.

> This forecast does not assure that an earthquake will or will not occur. The earthquake-related hazards remain higher than normal throughout the aftershock sequence. Because of the higher hazard, the Geological Survey recommends that earthquake preparation and response measures, such as those described in your local telephone directory, be taken now. It is not too late to take these actions, which can reduce your risk in aftershocks.

4. Dissemination of forecasts.

The USGS will disseminate aftershock forecasts at selected times during the earthquake sequence, beginning immediately after the mainshock. Transmittal will be by FAX (assuming telephone service is available). The order and timing of the FAX transmissions will reflect the priority needs of the recipients. In California, the first forecast (immediately after the mainshock) will be sent to the California Office of Emergency Services and other government agencies (FEMA, Army Corps of Engineers) responsible for emergency response. In order to give these agencies time to respond to the information they have received, we will impose a delay of one-half hour before transmitting the forecast to the media and other recipients. The distribution list USGS aftershock forecasts released during the Loma Prieta earthquake sequence is given in Appendix VI. To faciliate effective transmission of the forecasts to the non-English speaking media and public, the USGS will provide appropriate translations.

5. Recommended situations for applying the model.

1. After a large ($M6 \sim M7$) earthquake the model may be used to estimate probabilities for smaller ($M \geq 5$) aftershocks. Use of the model in these situations is expected to result in a series of public forecasts. (Example: 1989 Loma Prieta earthquake sequence.)

2. After a moderate ($M5 \sim M6$) earthquake the model may be used (following guideines in Section 2) to estimate probabilities for a larger earthquake. Use of the model in these situations is expected to result in one or more private communications to OES, and possibly also public forecasts. (Examples: 1989 Lake Elsman and Obsidian Buttes earthquake sequences.)

3. After a large ($M6 \sim M7$) earthquake the model may be used (following guideines in Section 2) to estimate probabilities for a larger event. In these cases the model results

should be used cautiously, and in conjunction with results from other models, including gap and characteristic earthquake models, and the Agnew-Jones foreshock probability model. Use of the model in these situations is expected to result in private communications to OES and/or other agencies or groups engaged in earthquake hazard assessment or response. Normally this use of the model in these situations will not result directly in public forecasts. (Example: memorandum to the NEPEC Working Group on Earthquake Probabilities, Appendix V.)

6. Example text for an aftershock forecast following a large ($M6 \sim M7$) earthquake. This example was modified from a November 1, 1989 press release issued by the Geological Survey (Menlo Park) on the Loma Prieta earthquake sequence.

> SHORT TERM (1-WEEK) FORECAST:
>
> The probability for aftershocks decreases with time most rapidly during the first week after the mainshock. Then, in the following weeks and months, the probability for aftershocks decreases more slowly. To assess the chances for additional damaging aftershocks, scientists rely on the typical behavior of past California sequences, and on the behavior thus far of the [name, if available] earthquake sequence. The [name, if available] aftershocks recorded so far generally follow the behavior of a typical California sequence. From these observations we are able to forecast the chance of future strong aftershocks. As of Wednesday, November 1, at 5:00 PM PST, there is a 10% chance in the next 7 days of an aftershock large enough to cause damage (magnitude 5.0 or larger).
>
> LONG TERM (3-MONTH) FORECAST:
>
> The long term outlook points out the lasting nature of aftershock activity. It is common for a strong aftershock to occur several weeks or months after a mainshock. Over the next three months the chance of a magnitude 5.0 or larger aftershock is about 36 percent. Also, in the next two months, the occurrence of two additional magnitude 4.0 or larger aftershocks would be typical.

7. Example text for a forecast of a larger earthquake following a moderate ($M5 \sim M6$) earthquake.

> Based on the past history of many earthquake sequences in California, the chance that today's magnitude 6 earthquake will be followed by a larger earthquake can be estimated. The chance that a similar or larger earthquake will occur in the next 7 days is about 5% The most likely area for such a follow-on event is within 10 miles of the epicenter of today's earthquake.

8. Example text for a forecast of a larger earthquake following a large ($M6 \sim M7$) earthquake.

See Appendix V.

APPENDICES

I. Original report in *Science* by P. Reasenberg and L. Jones on the aftershock model. (Not included herewith)

II. Technical comment in *Science* by P. Rydelek on the uncertainties in the model probabilities. Reply by P. Reasenberg and M. Matthews. (Not included herewith)

III. Technical comment in *Science* on applications of the model by P. Reasenberg and L. Jones. (Not included herewith)

IV. Testimony by Dennis Mileti before Congressional Field Hearing on the Loma Prieta earthquake. (Not included herewith)

V. Memorandum from P. Reasenberg to the NEPEC Working Group on Earthquake Probabilities.

VI. Distribution list for FAX transmissions of Loma Prieta aftershock forecasts.

Date: December 15, 1989

To: NEPEC Working Group on Probabilities

From: Paul Reasenberg

Subject: Long Range Forecast for Large Earthquakes after Loma Prieta

Using the Reasenberg-Jones model for aftershock probabilites to forecast the long-term probability for large earthquakes in the Bay Area after Loma Prieta requires a long leap of faith, or at least, some important assumptions. The model was developed from a learning set of mainshock-aftershock sequences. Foreshocks associated with these sequences were not considered. Thus, the model is based strictly on aftershock behavior, in which the aftershocks are, by experiment design, always smaller than the mainshock. An extension of the model has been suggested, in which the exponential distribution of magnitudes would be extended to aftershock magnitudes larger than the mainshock. While doing so is a valid modeling procedure, the following caveats should be stated.

1. The exponential distribution of magnitudes (Gutenberg-Richter law) appears to systematically underestimate the number of larger magnitude earthquakes worldwide (Utsu, 1971). While we have insufficient data to know if a similar underestimate results from our aftershock model, the possibility cannot be ruled out.

2. The R-J model is based on aftershocks smaller than the mainshock. It is an assumption that the self-similar behavior of the magnitude distribution exhibited on average by the smaller aftershocks will be followed by the larger-than-mainshock aftershocks. Even for aftershocks with magnitudes comparable to the mainshock, the seismogenic process in any particular case is obviously controlled by local physical constraints, not by laws reflecting average behavior. These constraints include the presence of neighboring Bay Area faults, the depth, topography and velocity of the ductile region, geometric and compositional barriers in the crust, and the stress footprint left in 1906.

With these caveats stated, here are the model probabilities for large aftershocks calculated using the model that best fits the Loma Prieta aftershocks to date ($a = -1.67$, $p = 1.19$, $b = 0.75$).

1-year interval: January 1, 1990 – Dec 31, 1990

$$P(M \geq 6.0) = 0.053$$
$$P(M \geq 7.0) = 0.010$$

2-year interval: January 1, 1990 – Dec 31, 1991

$$P(M \geq 6.0) = 0.067$$
$$P(M \geq 7.0) = 0.012$$

The attached graph illustrates the decay in the model probability for a $M \geq 7$ aftershock in a sliding 1-year window. The probability shown on the graph for the 1-year interval beginning 75 days after the mainshock (January 1, 1990) is slightly less than the corresponding figure (0.010) given above because the graph was prepared previously using slightly different model parameters. The baseline "blue book" probability of 0.0067 per year (20% probability in 30 years) is shown for reference.

The Loma Prieta sequence produced fewer aftershocks (and had a lower b-value) than expected for a generic $M = 7.1$ earthquake. Accordingly, the above long range forecast includes lower probabilities than would be obtained with the generic model. Furthermore, the Loma Prieta aftershock sequence characteristics may reflect conditions local to the aftershock zone, while the forecast we seek is for earthquakes outside the zone. Therefore, use of a model based on this specific sequence may not be preferable to the use of a generic model. It is arguable that the mainshock stress pulse applied to the Bay Area faults, and not the aftershock pattern, per se, is relevant to the long range Bay Area forecast. Accordingly, I give below a long-range forecast for strong aftershocks analogous to the one above, but following a "generic $M = 7.1$ earthquake" assumed to have occured on October 17, 1989.

1-year interval: January 1, 1990 – Dec 31, 1990

$$P(M \geq 6.0) = 0.113$$
$$P(M \geq 7.0) = 0.015$$

2-year interval: January 1, 1990 – Dec 31, 1991

$$P(M \geq 6.0) = 0.145$$
$$P(M \geq 7.0) = 0.019$$

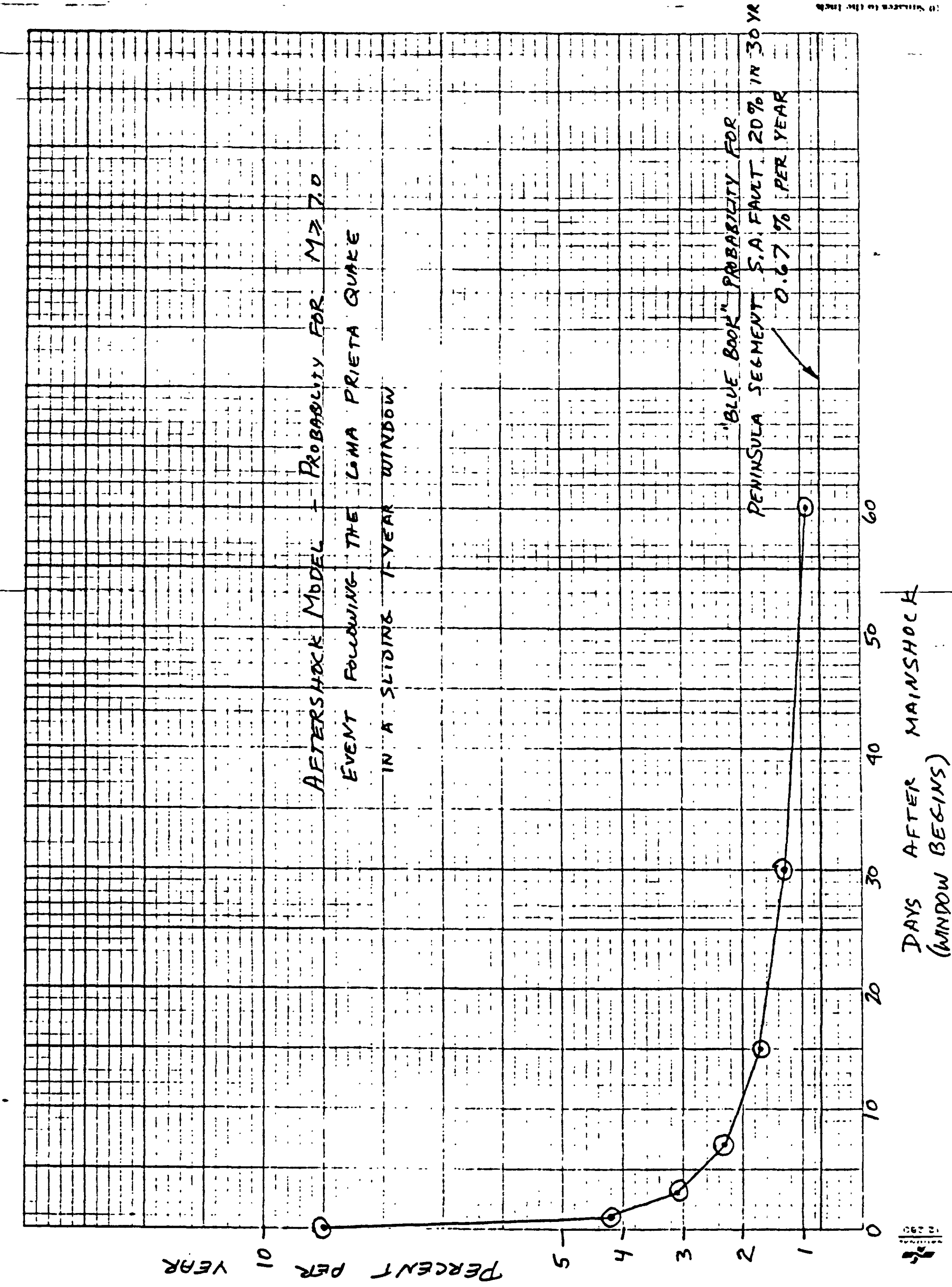
AFTERSHOCK MODEL - PROBABILITY FOR M≥7.0
EVENT FOLLOWING THE LOMA PRIETA QUAKE
IN A SLIDING 1-YEAR WINDOW
"BLUE BOOK" PROBABILITY FOR
PENINSULA SEGMENT S.A. FAULT 20% IN 30 YR
0.67% PER YEAR
DAYS AFTER MAINSHOCK
(WINDOW BEGINS)
PERCENT PER YEAR
0
10
20
30
40
50
60
1
2
3
4
5
10

APPENDIX VI
Distribution List for Loma Prieta aftershock forecasts

California Office of Emergency Services - Ontario

California Office of Emergency Services - Sacramento

FEMA - Mt. View Disaster Field Office

US Army Corps of Engineers

Navy Geotechnical Department - San Bruno

US Navy, Santa Barbara

California Division of Mines and Geology

California Division of Safety and Dams

BAREPP - Oakland

Office of Emergency Services, City of Los Angeles

California Institute of Technology

UC Santa Cruz

EERI Headquarters

USGS - OEVE, Reston

USGS - Pasadena

USGS - Seattle

USGS - Deer Creek

USGS - Geologic Risk Assessment, Denver

USGS - Global Seismology, Denver

Japan Geological Survey

Stanford Linear Accelerator Center

Associated Press - San Francisco

Bay City News

UPI - San Francisco

Approximately 20 individual newspapers, radio and television stations.

Appendix Q

Review of methodology used in Bay Region Earthquake Probabilities report, by R.Barlow, submitted June 4, 1990.

FAX 703-648-6717

June 4, 1990

Dr. Thomas V. McEvilly
Dr. Robert L. Wesson
National Earthquake Prediction Evaluation Council
Geological Survey
Mail Stop 905
Reston, VA 22092

Re: **Probabilities of Large Earthquakes in the San Francisco Bay Region**

Gentlemen:

I am replying to your request for comments relative to the draft report **Probabilities of Large Earthquakes in the San Francisco Bay Region** by the Working Group on California Earthquake Probabilities. Although I am not an expert in seismology, I do have a considerable applied probability background. The second and third pages of this letter address the 3 issues raised in your letter of May 16, 1990.

I can summarize by saying that I believe the probabilistic methodology used by the working group is internally consistent and represents recent statistical practice although it is my opinion that better methodology is on the horizon and will soon be available. My main criticism concerns the modeling issue which I also address in the attachment.

With Best Wishes,

Richard E. Barlow

Professor of Operations
Research and Statistics

COMMENTS

My interpretations of your questions followed by my answers are:

(1) Are the presentations by the Working Group in their 1990 report and the calculations of J. C. Savage consistent with each other and correct?

Answer: Yes (with qualifications)

I refer to Savages' appendix in his "Criticism of Some Forecasts...". Mathematically you can calculate the distribution of recurrence times conditional on the time since last occurrence by integrating with respect to the lognormal prior for $\overline{T}$ or by Monte Carlo sampling from the prior and then averaging over outcomes. The Monte Carlo method is only an approximation and unnecessary in this case.

J. C. Savage is arguing from the point of view that regards probability as a limiting frequency. This is completely inappropriate in predicting the time to the next large magnitude earthquake occurrence. There will only be one **next** recurrence time for a particular segment of a fault and after it occurs it will be completely known.

Confidence intervals for the probability distribution of the recurrence time have no value for decision making. For example. last Thursday the weather forecaster said there was a 30% chance of rain. He was expressing his uncertainty for this event by 30%. A confidence interval for 30% would have been meaningless. For him to give me his uncertainty for his uncertainty would have been of no use to me. This is true in general. A confidence interval has no value for decision making. For decision making, it is enough to assess the probability distribution for recurrence times. This together with your loss function for various alternative decisions (such as buying or not buying earthquake insurance) and possible earthquake recurrence times is the "rational" way to make decisions.

(2) Is the decision of the Working Group to report the mean probability justified or is some alternate central measure more appropriate?

Answer: The Working Group reported their probability unconditional on their uncertainty regarding unknown parameters. This is precisely what they should do.

(3) Given that confidence intervals are to be presented, does the reviewer have comments on percentile levels:

Answer: Confidence intervals will satisfy no one but statisticians who believe that probability is not a judgement of uncertainty but somehow exists independent of their judgement. This view is logically untenable and there is a vast literature by the very best minds in the field supporting the view that confidence intervals have no relevance for decision making. If decisions are not to be made based on this analysis, what is it good for?

COMMENTS ON THE LOGNORMAL MODEL

To quote from the Working Group's Report on page 5. "The approach used in this study assumed the probability of an earthquake along a fault segment is initially low following a large segment-rupturing earthquake and increases with time as stress on the segment recovers the stress drop of the prior earthquake." It seems to me that this is a fairly reasonable judgement and I stress that it is a judgement. Probability distributions for recurrence time with this property have **increasing occurrence rate** or failure rate. The lognormal model used to predict recurrence times does **not** have this property. The occurrence rate initially increases but then decreases and asymptotically goes to 0! I suspect some members of the working group, in particular Allin Cornell, are aware of this fact. However it is never mentioned. The truth is that the lognormal model is used for mathematical convenience and has no rational justification for this particular problem.

I have been pursuing research since December with Dr. Max Mendel on the problem of justifying models with the increasing occurrence rate property. Our approach is unique in that we first think about finite populations (the only kind that exist) and using an indifference principle derive the possible models satisfying the condition. One result of our research that only the family of distributions we have called the generalized gamma family make sense relative to this property. The lognormal cannot be justified in this way.

In Reply Refer To:
Mail Stop 905

May 16, 1990

Dr. Richard E. Barlow
Department of Industrial Engineering
and Operations Research
University of California
4177 Etcheverry Hall
Berkeley, California 94720

Dear Dr. Barlow:

We appreciate your agreeing to provide some advice on expressing the results of an analysis of the probability of future earthquakes.

The National Earthquake Prediction Evaluation Council (NEPEC) is an advisory committee established to advise the Director of the U.S. Geological Survey (USGS) on earthquake predictions. In 1987, at the request of the Director, NEPEC established a Working Group on California Earthquake Probabilities to develop consensus estimates of the probabilities of large earthquakes in California. The report of that Working Group, "Probabilities of Large Earthquakes in California on the San Andreas Fault," was endorsed by NEPEC and released by the USGS in 1988. The report acknowledged significant uncertainties about data and the applicability of models, but reported estimates for earthquakes along several segments of the San Andreas and related faults. One of the segments accorded a high probability gave rise to the Loma Prieta earthquake of October 17, 1989.

Subsequent to the Loma Prieta earthquake, NEPEC established a new working group to reassess, in the light of new data, new interpretations, and any perceived physical changes, the probabilities of earthquakes in the San Francisco Bay area. A draft of the new report and a copy of the 1988 report are enclosed. NEPEC has begun its review of the new report. The methodology used by the new Working Group is essentially that used by the previous group, with what the current group perceives to be incremental improvements.

In the meantime, James Savage, a senior scientist at the USGS, has raised questions about the appropriateness of the approach used by both the previous and current working groups to express their results. (A comment from Savage and a rebuttal prepared by the Chairman of the Working Group are enclosed.)

In brief, we are dealing with what is effectively a renewal model with uncertain mean interarrival time, but known coefficient of variation. We have subjective prior distribution on this uncertain median, and we want to state something about the probability of an event in the next 30 years given an elapsed time. The Working Group and Savage agree on the proper way to analyze the model (including updating of the distribution on the median in light of elapsed time). Questions raised by Savage revolve around expressing the results of this analysis. Approaches range from stating the probability (i.e. posterior expectation of conditional probability) to displaying distributions on the conditional probability.

A peculiar aspect of this problem is that the breadth of this latter distribution depends strongly on the ratio of the parametric variability (i.e. prior standard deviation on uncertain median) to the known "intrinsic" variability (i.e. the standard deviation of interarrival times). Because the intrinsic variability appears to be poorly known, this characteristic confuses conventional intuitive interpretation.

While comments on any aspect of this subject would be appreciated, NEPEC especially seeks your comments on the following points:

(1) Confirm that the two presentations of the analysis are consistent with each other and are correct.

(2) Provide comments on the Working Group presentation and interpretation of results. In the context of public policy and as input to economic decisions is the decision of the Working Group to report the mean probability justified or is some alternate central measure, such as the mode or even the whole distribution (as suggested by Savage) more appropriate?

(3) The Working Group has preferred to report results to the public as a single measure, and in the interest of completeness to report to a subset of the audience "confidence bands" as quartiles in Appendix C. Savage prefers that the conditional probability be reported by 90 or 95 percent confidence intervals. Given that such intervals are to be presented, does the reviewer have comments on percentile levels?

We would greatly appreciate any comments you might have that would help us resolve this matter. NEPEC will be meeting again in early June, thus your comments would be most helpful if we were to receive them before the end of May.

Thank you very much.

Sincerely yours,

Signed

Thomas V. McEvilly
Chairman, National Earthquake
Prediction Evaluation Council

Signed

Robert L. Wesson
Vice-Chairman, National Earthquake
Prediction Evaluation Council

Enclosures

cc: Chron
File
Wesson
T. McEvilly

RLWesson:jac

Appendix R

Review of methodology used in Bay Region Earthquake Probabilities report, by R.McGuire, submitted June 1, 1990.

Risk Engineering, Inc
5255 Pine Ridge Road
Golden, Colorado 80403
Telephone 303-278-9800

June 1, 1990

Thomas V. McEvilly, Chairman
National Earthquake Prediction Evaluation Council
Office of Earthquake Studies
U.S. Geological Survey
12201 Sunrise Valley Drive
Mail Stop 905
Reston, VA 22092

Dear Tom:

We have given some thought to the questions you raised in your letter dated May 16, 1990. Our thoughts are based on a first reading of the Draft Working Group report (undated), Savage's paper (undated), Dieterich's memo to Wesson (dated 5/9/90) and Savage's memo to NEPEC (dated 5/7/90).

We are really impressed and encouraged by the details of the discussion being conducted. The participants are raising the right issue, that is, the best way to represent estimates of earthquake occurrence probabilities in the context of probabilistic models when both direct observations and scientific deduction must be used. One can always think of more sophisticated models that might be devised, for example, to account for coupling between fault ruptures from one segment to another. We hope that future discussions will pursue these more detailed models; none of the methods we have today should be perceived as the ultimate tool.

Given the time available to us, we will not offer a detailed review of the issues. Some perspectives on probabilistic modeling and on the use of probability results may be useful to you, however.

1. The usual evolution of probabilistic models is to treat unexplained variations as randomness ("inherent uncertainty") and to later recognize and treat part of that randomness as uncertainty ("parametric uncertainty"). The evolution of ground motion attenuation equations is a good example: in the early 1970's we used only magnitude and distance in these equations, and the resulting σ (of ln[ground motion]) was 0.7 to 0.8. Now we use soil conditions, faulting type, instrument location and other factors in the equations, and the σ is 0.4 to 0.5. We could do further conditioning, for example, on the direction of propagation, but if we can't predict that for the next earthquake we can logically treat the effects as random. It seems that, in the papers we have seen, this process may have been short-circuited by using too low a value for inherent uncertainty, thereby requiring a

large value of parametric uncertainty to express the total σ. It may be that the earthquake sequences used to obtain the variability of inter-arrival times may be biased toward regular intervals because those sequences stick out as "regular," while irregular sequences seem to be incomplete and therefore are discounted. Ultimately, this or another Working Group must address the variability question, but to the extent that inherent uncertainty is underestimated, the effects cited by Savage are overstated.

2. Updating the "direct" estimate of occurrence probability by the time since the last event, as done by the Working Group in their appendix and by Savage, is certainly appropriate, as it incorporates information about the time since the last event. This, however, is not the ultimate model that one might devise. We say this in the context of our introductory remark that more sophisticated models can always be developed and we are encouraged that researchers are doing so. This statement doesn't invalidate the Working Group's method or results; there is no single "correct" model.

3. On the issue of uncertainty in the estimated probability, and whether it should be divulged, we encourage the Working Group to express the mean probability, with a qualitative statement that the reported results are uncertain and may change in the near future with additional data or better models. Uncertainty statements can be presented in an appendix, and we have no scientific preference on what fractiles ought to be reported. Certainly, classical decision theory tells us that we should treat "inherent" and "parametric" uncertainty equally, integrating over both to obtain a probability for decision-making. The simplest analogy is in flipping a coin to determine who pays for lunch: we shouldn't care whether we are flipping a fair coin (inherent uncertainty) or choosing a coin out of a bag composed of trick coins, 50% of which have 2 heads and 50% of which have 2 tails ("parametric uncertainty"). Indeed, we shouldn't even care if we have pulled the latter coin out of the bag and have not yet examined it: the choice of whether to play the game treats inherent and parametric uncertainty equally. In the earthquake context, decision-makers don't care if the probability of occurrence is 40% because of unknown physical processes, or if it is 40% because 40% of the earth scientists' data indicate an imminent event, and 60% of the data indicate quiescence. The important thing is that the best estimate is 40%, not 4% or 80%.

   As a simpler analogy, should an airline disclose a tip from a source of unknown reliability that a certain flight is to be sabotaged? The relevant decision-makers (the passengers) can make a strong case that they deserve that information: waiting for highly reliable information will likely increase the costs to all concerned, as long as the reliability of the source is better than a purely random guess.

We recognize that issues of earthquake forecasts and their uses do not fall into the area of classical decision theory. in that decisions are not made at one point in time and the results then affected solely by the outcome of the experiment. Indeed the process of earthquake preparedness must be a continuing effort. but we can only make progress if the best information is made available on a continuing basis. We encourage the Working Group to publish the central numbers, and to continue efforts to understand and refine the uncertainty statements in the future.

Sincerely yours,

Robin K. McGuire
President

Gabriel R. Toro
Senior Engineer

In Reply Refer To:
Mail Stop 905

May 16, 1990

Dr. Robin McGuire
President, Risk Engineering Inc.
5255 Pine Ridge Road
Golden, Colorado 80403

Dear Robin:

We appreciate your agreeing to provide some advice on expressing the results of an analysis of the probability of future earthquakes.

The National Earthquake Prediction Evaluation Council (NEPEC) is an advisory committee established to advise the Director of the U.S. Geological Survey (USGS) on earthquake predictions. In 1987, at the request of the Director, NEPEC established a Working Group on California Earthquake Probabilities to develop consensus estimates of the probabilities of large earthquakes in California. The report of that Working Group, "Probabilities of Large Earthquakes in California on the San Andreas Fault," was endorsed by NEPEC and released by the USGS in 1988. The report acknowledged significant uncertainties about data and the applicability of models, but reported estimates for earthquakes along several segments of the San Andreas and related faults. One of the segments accorded a high probability gave rise to the Loma Prieta earthquake of October 17, 1989.

Subsequent to the Loma Prieta earthquake, NEPEC established a new working group to reassess, in the light of new data, new interpretations, and any perceived physical changes, the probabilities of earthquakes in the San Francisco Bay area. A draft of the new report and a copy of the 1988 report are enclosed. NEPEC has begun its review of the new report. The methodology used by the new Working Group is essentially that used by the previous group, with what the current group perceives to be incremental improvements.

In the meantime, James Savage, a senior scientist at the USGS, has raised questions about the appropriateness of the approach used by both the previous and current working groups to express their results. (A comment from Savage and a rebuttal prepared by the Chairman of the Working Group are enclosed.)

In brief, we are dealing with what is effectively a renewal model with uncertain mean interarrival time, but known coefficient of variation. We have subjective prior distribution on this uncertain median, and we want to state something about the probability of an event in the next 30 years given an elapsed time. The Working Group and Savage agree on the proper way to analyze the model (including updating of the distribution on the median in light of elapsed time). Questions raised by Savage revolve around expressing the results of this analysis. Approaches range from stating the probability (i.e. posterior expectation of conditional probability) to displaying distributions on the conditional probability.

A peculiar aspect of this problem is that the breadth of this latter distribution depends strongly on the ratio of the parametric variability (i.e. prior standard deviation on uncertain median) to the known "intrinsic" variability (i.e. the standard deviation of interarrival times). Because the intrinsic variability appears to be poorly known, this characteristic confuses conventional intuitive interpretation.

While comments on any aspect of this subject would be appreciated, NEPEC especially seeks your comments on the following points:

(1) Confirm that the two presentations of the analysis are consistent with each other and are correct.

(2) Provide comments on the Working Group presentation and interpretation of results. In the context of public policy and as input to economic decisions is the decision of the Working Group to report the mean probability justified or is some alternate central measure, such as the mode or even the whole distribution (as suggested by Savage) more appropriate?

(3) The Working Group has preferred to report results to the public as a single measure, and in the interest of completeness to report to a subset of the audience "confidence bands" as quartiles in Appendix C. Savage prefers that the conditional probability be reported by 90 or 95 percent confidence intervals. Given that such intervals are to be presented, does the reviewer have comments on percentile levels?

We would greatly appreciate any comments you might have that would help us resolve this matter. NEPEC will be meeting again in early June, thus your comments would be most helpful if we were to receive them before the end of May.

Thank you very much.

Sincerely yours,

Thomas V. McEvilly
Chairman, National Earthquake
Prediction Evaluation Council

Robert L. Wesson
Vice-Chairman, National Earthquake
Prediction Evaluation Council

Enclosures

cc: Chron
File
Wesson
T. McEvilly

RLWesson:jac

Appendix S

Review of methodology used in Bay Region Earthquake Probabilities report, by R.Bernknopf, submitted May 31, 1990.

United States Department of the Interior

GEOLOGICAL SURVEY
RESTON, VA 22092

In reply refer to:
WGS-Mail Stop 922

May 31, 1990

Memorandum

To: Thomas V. McEvilly
Chairman, National Earthquake
Prediction Evaluation Council

Robert L. Wesson
Vice-Chairman, National Earthquake
Prediction Evaluation Council

From: Richard Bernknopf

Subject: Review of the Working Group on California Earthquake Probabilities report and critique on, "Probabilities of large earthquakes in the San Francisco Bay Region"

In response to your request, I have reviewed the Working Group on California Earthquake Probabilities report, "Probabilities of large earthquakes in the San Francisco Bay Region," and J. C. Savage's critique of the report, "Criticism of some forecasts of the national earthquake prediction evaluation council." Although I am currently considering some broader aspects of probabilistic assessment of earthquake hazards, I have limited my review comments to specific points in the subject report. In general, I agree that it is important that earthquake forecasts should be disseminated to the private and public sectors because they are a means to indicate the level of temporal risk for personal, financial, and institutional decisions.

As your letter pointed out, one of the differences between the Working Group's report and Savage's critique is the method of reporting the results of the exercise. I agree with Savage that the NEPEC report should include a measure of central tendency, such as the mean or the median, and a measure of dispersion, such as the standard deviation or variance as relevant information for public dissemination. Both the first and second moments of the probability distribution are necessary for objective financial decisionmaking. "Expected value" is used in economic analyses to determine an investment payoff with an uncertain future. An "expected value" that represents risk neutrality is a criterion that is used extensively in public decisionmaking (Arrow and Kurz, 1970, and Arrow and Lind, 1970). Estimating the variability of the return on an investment requires some measure of dispersion. Variance is used in determining risk preferences and risk premiums in financial decisions and asset portfolio management (Sharpe, 1970, Sinn, 1983, and Varian, 1984). In practice, very few individuals or firms are risk neutral; instead they have risk preferences. For example, individuals who purchase insurance show some level of risk aversion, which is reflected in their willingness to pay a premium to avoid a financial loss (Goovaerts and others, 1984). On the other hand, individuals who knowingly purchase a home in a Special Study Zone because it is a bargain (Brookshire and others, 1985) can be described as risk loving. Thus reporting the variance provides an objective basis for economic choices by individuals and institutions that apply different levels of risk aversion to their selections. Therefore, I believe NEPEC should report both statistics to maximize the utility of the report.

I am concerned about the statistical procedures used in the report. I agree with both the Working Group (models 2 and 3) and Savage (prior and posterior probability estimates) that a Bayesian model is appropriate for estimating earthquake probabilities. The basis for the Working Group model is a stationary point process model developed by Nishenko and Buland (1987). Several assumptions about statistical independence are required to use this model properly. A critical assumption in the Nishenko and Buland model is the independence of fault segments. However, the Working Group has updated stress measurements on San Andreas fault segments by adding or subtracting stress to these segments as a result of the Loma Prieta event (p.20-21). By inserting a conditional relationship between adjacent fault segments, the Working Group appears to violate the statistical independence required in adapting the Nishenko and Buland approach (see Cox and Lewis, 1966). I hope a dialogue can begin concerning the development of nonstationary probability models for earthquake forecasts over the next several months.

Overall I support the release of the report. On the other hand I believe the release should include both a mean and a variance. If you have any further questions about my review or want to continue discussion about the points raised, I would be glad to discuss them with you at your convenience.

REFERENCES

Arrow, Kenneth J., and Kurz, Mordecai, 1970, Public investment, the rate of return,and optimal policy, Johns Hopkins University Press, 218p.

Arrow, K. J., and Lind, R. C., 1970, Uncertainty and the evaluation of public investments, American Economic Review, 60, p.364-378.

Brookshire, David S., Thayer, Mark A., Tschirhart, John, and Schulze, William D., 1985, A test of the expected utility model: evidence from earthquake risks, Journal of Political Economy, 93, p.369-389.

Cox, D. R., and Lewis, P. A. W., 1966, The statistical analysis of series of events, Metheun & Co., LTD, 285p.

Goovaerts, M. J., deVylder, F., and Haezendonck, J., 1984, Insurance premiums: theory and applications, North-Holland, 406p.

Nishenko, S. P., and Buland, R., 1987, A generic recurrence interval distribution for earthquake forecasting, Bulletin of the Seismological Society of America, 77, p.1382-1399.

Sharpe, William F., 1970, Portfolio theory and capital markets, McGraw-Hill, 316p.

Sinn, Hans-Werner. 1983, Economic decisions under uncertainty, North-Holland, 359p.

Varian, Hal R., 1984, Microeconomic analysis, 2nd ed., W. W. Norton & Company, 348p.

In Reply Refer To:
Mail Stop 905

May 16, 1990

Mr. Richard Bernknopf
U.S. Geological Survey
922 National Center
Reston, Virginia 22092

Dear Rich:

We appreciate your agreeing to provide some advice on expressing the results of an analysis of the probability of future earthquakes.

The National Earthquake Prediction Evaluation Council (NEPEC) is an advisory committee established to advise the Director of the U.S. Geological Survey (USGS) on earthquake predictions. In 1987, at the request of the Director, NEPEC established a Working Group on California Earthquake Probabilities to develop consensus estimates of the probabilities of large earthquakes in California. The report of that Working Group, "Probabilities of Large Earthquakes in California on the San Andreas Fault," was endorsed by NEPEC and released by the USGS in 1988. The report acknowledged significant uncertainties about data and the applicability of models, but reported estimates for earthquakes along several segments of the San Andreas and related faults. One of the segments accorded a high probability gave rise to the Loma Prieta earthquake of October 17, 1989.

Subsequent to the Loma Prieta earthquake, NEPEC established a new working group to reassess, in the light of new data, new interpretations, and any perceived physical changes, the probabilities of earthquakes in the San Francisco Bay area. A draft of the new report and a copy of the 1988 report are enclosed. NEPEC has begun its review of the new report. The methodology used by the new Working Group is essentially that used by the previous group, with what the current group perceives to be incremental improvements.

In the meantime, James Savage, a senior scientist at the USGS, has raised questions about the appropriateness of the approach used by both the previous and current working groups to express their results. (A comment from Savage and a rebuttal prepared by the Chairman of the Working Group are enclosed.)

In brief, we are dealing with what is effectively a renewal model with uncertain mean interarrival time, but known coefficient of variation. We have subjective prior distribution on this uncertain median, and we want to state something about the probability of an event in the next 30 years given an elapsed time. The Working Group and Savage agree on the proper way to analyze the model (including updating of the distribution on the median in light of elapsed time). Questions raised by Savage revolve around expressing the results of this analysis. Approaches range from stating the probability (i.e. posterior expectation of conditional probability) to displaying distributions on the conditional probability.

A peculiar aspect of this problem is that the breadth of this latter distribution depends strongly on the ratio of the parametric variability (i.e. prior standard deviation on uncertain median) to the known "intrinsic" variability (i.e. the standard deviation of interarrival times). Because the intrinsic variability appears to be poorly known, this characteristic confuses conventional intuitive interpretation.

While comments on any aspect of this subject would be appreciated, NEPEC especially seeks your comments on the following points:

(1) Confirm that the two presentations of the analysis are consistent with each other and are correct.

(2) Provide comments on the Working Group presentation and interpretation of results. In the context of public policy and as input to economic decisions is the decision of the Working Group to report the mean probability justified or is some alternate central measure, such as the mode or even the whole distribution (as suggested by Savage) more appropriate?

(3) The Working Group has preferred to report results to the public as a single measure, and in the interest of completeness to report to a subset of the audience "confidence bands" as quartiles in Appendix C. Savage prefers that the conditional probability be reported by 90 or 95 percent confidence intervals. Given that such intervals are to be presented, does the reviewer have comments on percentile levels?

We would greatly appreciate any comments you might have that would help us resolve this matter. NEPEC will be meeting again in early June, thus your comments would be most helpful if we were to receive them before the end of May.

Thank you very much.

Sincerely yours,

Thomas V. McEvilly
Chairman, National Earthquake
Prediction Evaluation Council

Robert L. Wesson
Vice-Chairman, National Earthquake
Prediction Evaluation Council

Enclosures

cc: Chron
File
Wesson
T. McEvilly

RLWesson:jac

Appendix T

Letter from J.Davis to J.Dieterich (Working Group)
regarding the Bay Region Earthquake Probabilities report,
May 18, 1990.

STATE OF CALIFORNIA—THE RESOURCES AGENCY GEORGE DEUKMEJIAN, Governor

DEPARTMENT OF CONSERVATION
DIVISION OF MINES AND GEOLOGY
DIVISION HEADQUARTERS
1416 NINTH STREET, ROOM 1341
SACRAMENTO, CA 95814
(Phone 916—445-1825)

May 18, 1990

James Dieterich
U.S. Geological Survey
345 Middlefield Road, MS 977
Menlo Park, CA 94025

Dear Jim:

We thank you and your colleagues for participating in the CEPEC meeting on May 11. We feel that the Working Group has done a commendable job of addressing damaging earthquake probabilities in the Bay Area. The new report addresses the parametric uncertainties which were not considered in the statistical analysis in the 1988. The exposition of methodology and use of the data base are very good in the 1990 report.

The following comments are provided for the consideration of the Working Group when it reconvenes on May 22.

- We concur with NEPEC that a publication for general public consumption should be a companion to the Working Group open-file report. This report should emphasize for public policy use the principal conclusions regarding the likelihood of damaging earthquakes in the Bay Area about which the members of the Working Group are all agreed. This can draw public attention to the importance of the conclusions and reduce distractions based upon any lack of consensus regarding secondary and tertiary issues in the study. The aggregated probabilities for the region should be stressed in the popular publication.

- Jim Savage's commentary should be acknowledged in the Working Group open-file report. We suggest that a brief discussion of Savage's method be presented together with the Working Group's critique in a new section just preceding the "Summary and Conclusions" portion of report rather than relegating this issue to an appendix.

- The forecasts of event probabilities for fault segments meet the definition of long-term earthquake predictions. As such there should be a brief discussion of their testability. The 1990 report includes Tables 2 and 6 which present the segment boundaries. It is also worth drawing attention to the circumstance that since the elapsed time is approximately two-thirds of the median recurrence time, the characteristic earthquake probabilities on most of the faults segments studied in the Bay Area are approaching equivalence to the Poisson model (page 3 of Appendix A). The Working Group should also present the brackets of moment magnitude values which will fulfill their long-term prediction conclusions. The discussion of the significance of the Loma Prieta earthquake to the south Santa Cruz mountain segment conclusions of the 1988 report demonstrates the value of including this type of material in the 1990 report.

- The rounding off of probabilities to the nearest tenth was supported by CEPEC in the 1988 report. We now suggest rounding off to the nearest five-hundredth in the 1990 report in order to draw attention to closer correspondence of some of the probability values than can be represented by use of tenths. We do not believe that this implies too great a confidence if the rationale is explained in the text.

- We recommend that the discussion of the reasons for the differences in the 1988 and 1990 conclusions be more prominently highlighted in the report.

- We suggest that the fact that not all active faults in the Bay Area are dealt with in the report be given greater emphasis. Discussion of the conventional wisdom regarding the seismic potential of the Calaveras fault would be useful. Are M7 events credible from any other structures in the Bay Area than those included in the study?

- The possibility of a single event occurring along the entire length of the Hayward fault should be explicitly stated in the Hayward section of the report.

- The illustration for the cover dramatizes the difference between the northern Hayward fault segment probability and probability conclusions reached by the group in the study area. Attention should be given to more accurate expression of the actual contrasts in these conclusions and their uncertainties in the way they are presented in cover illustration.

James Dieterich
Page 3
May 18, 1990

We thank you for the opportunity to comment on the 1990 report and look forward to its completion.

Sincerely,

James F. Davis
State Geologist

cc: Tom McEvilly
Rob Wesson
Dick Andrews
CEPEC Members

Appendix U

Letter from T.Heaton to T.McEvilly regarding the Bay Region Earthquake Probabilities report, May 17, 1990.

UNITED STATES
DEPARTMENT OF THE INTERIOR
GEOLOGICAL SURVEY

Prof. Thomas McEvilly
Chairman, NEPEC
Seismographic Station
University of California
Berkeley CA 94720

17 May 1990

Dear Tom,

I am writing to share several thoughts about the report from the Working Group on Probabilities in the San Francisco Bay Region. I would like to thank the working group for a thoughtful and carefully prepared document. However, as has become obvious from recent well publicized controversies, this report is likely to be very closely scrutinized and criticized, primarily by our colleagues (for years to come). Because this report must be "built to last," it must have a firm philosophical foundation that can be defended for years to come.

I feel that the report will be much easier to defend if the objectives of the report were more clearly stated right at the beginning. As it currently reads, one might conclude that this is an attempt to report on the results of a straight-forward application of an established method for estimating probabilities. Since both the technique (Nishenko-Buland) and the particular applications to Bay Area faults are still the subject of considerable scientific debate, this report may be attacked on the grounds that "they don't really know that." Furthermore, it may turn out that some of our basic assumptions (e.g., characteristic earthquake, earthquake cycle, or others) will later be proven wrong, which will lead to the untenable situation of trying to deal with a "scientific" report that we may later believe to be incorrect. I recommend that we make clear from the outset that the report is intended to provide <u>subjective</u> estimates of earthquake probabilities based upon the combined <u>judgements</u> of many researchers using a variety of arguments. We should make it clear that the primary motivation to formulate such probability estimates is to provide input for those who must prioritize key policy issues.

I feel that for such policy purposes, it is important to have a report that is resilient enough that it doesn't hinge on poorly justified key assumptions. We can cite several simple arguments that lead to the conclusion that there are significant chances of large earthquakes in the Bay Area (e.g., historic seismicity rates, time random models of earthquake occurrence on the known faults, geodetic strain vs. earthquake strain drop budgets, etc.) without having the report hinge upon a particular model of earthquake recurrence. In reality, it is only because there are multiple logic paths that lead towards the conclusion of significant risk, that I am reasonably comfortable with the probability estimates given by the working group. We should acknowledge that the detailed numbers and methods of analysis are likely to change in coming years, and we should emphasize the more obvious and robust parts of our knowledge. Although many of these statements are already interspersed throughout the report, I feel that the philosophy and the caveats should be more prominent in the introduction and conclusions.

As stated in the report's introduction, the occurrence of the Loma Prieta earthquake is the primary motivation for this update. Everyone wants to know how this earthquake has affected the earthquake probabilities (in the next several years). There is discussion (and a model) of how the Loma Prieta earthquake may have advanced the timing of the earthquake cycle on the Peninsula segment and these arguments look reasonable. However, I would feel more comfortable if we also discussed occurrence statistics for large crustal earthquake clusters (dimensions of tens of kilometers and several years) based upon a larger earthquake catalog. Lucy Jones did a quick count in southern California, and found that about 10 to 15 percent of significant earthquakes were followed by an adjacent significant earthquake within two years.

While on the subject of Loma Prieta, I feel that the discussion of that "prediction" and the ensuing earthquake is misleading to the point that we leave ourselves open to future criticism that we were not objective in our judgments. It seems quite clear that one interpretation of this sequence is that it did not occur on the same fault plane as that which daylights along the rift zone that geologists have called the San Andreas fault. Discussions with Clarence Allen and Dave Schwartz lead me to believe that there is probably a very active vertical strike-slip fault (which probably moved in 1906) beneath this rift zone that has always been called the San Andreas fault. Furthermore, the updip projection of the Loma Prieta earthquake coincides very well with an active reverse (probably oblique) fault called the Sargent fault. Considering the physiography of the area and the marine terrace arguments of Steve Ward, it seems plausible that the Loma Prieta earthquake occurred on the Sargent fault and that it has a long average recurrence interval (500 to 1,000 years). I acknowledge that it can be argued that there may be several strands of the San Andreas system (with different dips and slip angles) and that earthquakes on any of these strands change stress within some volume adjacent to the fault. However, because our understanding of the physics of strain accumulation and earthquake rupture physics is so incomplete, I believe that it is presumptuous for us to assert that we know that such distinctions are irrelevant. Furthermore, if this earthquake did occur on a fault whose surface trace has been called the Sargent fault, we will unnecessarily introduce confusion into geologic nomenclature and leave ourselves open to future criticism that we redefined the San Andreas fault to match our predictions. It is better to deal with these issues up front than have to deal later with a lot of grumbling and second guessing.

On pages 10 and 11 of the working groups report, they reevaluate the recurrence time for the Southern Santa Cruz Mountains segment of the San Andreas based upon the apparent 83-year recurrence time (1989-1906). The 1987 report listed an expected recurrence time of 136 years (Table 2), but the observed time of

83 years is highly unlikely using the Nishenko-Buland model and an average recurrence time of 136 years. From this, the working group concludes that the previous estimate of recurrence time was too long and the estimated slip rate for the fault was too low. However, this logic may be somewhat circular. Another conclusion is that the recurrence estimates were correct, but that the intrinsic uncertainty is larger than that assumed. As an aside, I am somewhat puzzled about how the the previous working group obtained a probability of 0.3 (for South Santa Cruz Mtns.) when the more recent analysis by both Dieterich and Savage indicates that a 136-year average recurrence time seems to long to be consistent with the Nishenko-Buland model. Perhaps this was one of those subjective judgements I mentioned at the beginning of this letter.

With regard to the recent discussion between Jim Dieterich and Jim Savage, they say that their analyses are equivalent, but they seem to have different interpretations of the resulting numbers (mean vs. mode, robust vs. meaningless, etc.). I must admit that I am somewhat baffled by what is the "best" interpretation of this analysis. It does appear that both analyses indicate that there are large uncertainties within the confines of the Nishenko-Buland model. I believe that it would be best to discuss both interpretations in an appendix. As far as I'm concerned, the real uncertainties lie in the fundamental applicability of this model in the first place. I feel that we should clearly state that use of this model helps to guide our overall estimation of earthquake probabilities, but that it is only one of several approaches that lead to similar conclusions.

One of the strongest results that comes from applying the Nishenko-Buland model is the conclusion that the probabilities for large earthquakes on the North Coast and South Santa Cruz Mountains segments of the San Andreas are very low because we are not yet far enough into their earthquake cycles. This is a strong conclusion and I fear that we do not have enough evidence to support it. I am particularly concerned that it is incompatible with Kerry Sieh's latest conclusions about the timing of events on the Mojave section of the San Andreas. I feel that we should add a baseline to probabilities on segments given a low probability by the Nishenko-Buland model (this is another one those subjective judgements I mentioned at the beginning of this letter).

According to the proposed report, the Hayward fault has the highest probability for a major earthquake in the Bay Area. However, evidence is cited that much of the fault is creeping at a rate (6 mm/yr) that is close to its estimated long-term slip rate (9 mm/yr, a poorly constrained number). This situation seems problematic to me. If there were no known large earthquakes on the Hayward fault, then I believe that we would have a very difficult time estimating the earthquake potential for this fault (it might be deemed to be similar to the creeping section of the San Andreas). Thus, arguments about the potential for the Hayward fault seem to hinge on the conclusion that the 1868 earthquake was a M 7 strike-slip earthquake on the Hayward fault. Given the paucity of information concerning this event, I am uncomfortable with this strong assumption regarding the source of the 1868 earthquake. The suggestion that the Hayward fault has 6 mm/yr of creep presents an additional problem. The 30 year probability was computed assuming that the entire long-term slip rate (9 mm/yr) is accumulating as elastic strain to be released in coming earthquakes. If only 3 mm/yr are accumulating as elastic strain, then we would obtain an average repeat time of several hundreds of years and we would conclude that a repeat of the 1868 earthquake is very unlikely in the next 30 years. I'm not sure how to deal with these uncertainties. Perhaps the logic-tree approach should be taken here. At the very least, there should be more said in the report about uncertainties regarding the mechanical behavior of the Hayward fault.

In conclusion, I feel that, as it stands, the report would greatly benefit from the addition of more discussion of the fundamental uncertainties in this type of analysis. I have included a suggested paragraph to explain philosophy in the preface of the report (see appendix to this letter). I don't believe that the overall probability estimates will change much if other approaches are considered (although they might come down slightly). I also feel that this report will be very valuable for assisting in the formulation of rational earthquake policies. The general public will probably not be too concerned about all of our scientific struggles with the methodologies used in the report. However, it is important for us to openly acknowledge these struggles in the report so that we can honestly defend the report to our colleagues.

Sincerely,

Thomas H. Heaton
U.S. Geological Survey
525 S. Wilson Ave.
Pasadena CA 91106
818-405-7814
FAX 818-405-7827

cc. J. Dieterich
J. Savage
R. Wesson
A. Johnston
J. Davis
J. Davies
H. Kanamori
K. Shedlock
J. Stock
R. Buland
K. Aki
W. Bakun
W. Prescott

APPENDIX

Suggested addition to the Preface

This report is intended to summarize the collective knowledge and judgments of many earthquake scientists to assist in the formulation of rational earthquake policies. Unfortunately, current knowledge of the earthquake process is insufficient to provide well constrained estimates of earthquake probabilities. However, there is considerable information about active faults in the San Francisco Bay region that leads to the conclusion that major earthquakes are likely within the next tens of years. Several techniques can be used to compute quantitative probabilities for future earthquakes, although there is considerable discussion within the scientific community about the validity of specific assumptions that must be made to apply these techniques. While the body of the report describes the detailed assumptions that led to specific probabilities for different fault segments, it is important to recognize that future advances in our understanding of earthquake physics may change the way that these probabilities are estimated. Even though there is uncertainty about the actual probability estimates, this report is consistent with current understanding of the occurrence of California earthquakes, and it provides a basis for the prioritization of earthquake hazard mitigation plans.

Appendix V

Memorandum from J.Dieterich to R.Wesson regarding the criticism from J.Savage on the Bay Region Earthquake Probabilities report, May 9, 1990.

United States Department of the Interior

GEOLOGICAL SURVEY

OFFICE OF EARTHQUAKES, VOLCANOES, AND ENGINEERING
Branch of Tectonophysics
345 Middlefield Road, MS/977
Menlo Park, CA 94025

TAKE PRIDE IN AMERICA

May 9, 1990

Memo

To: Rob Wesson
From: Jim Dieterich
Subject: Comments on Savage: "Criticisms of some forecasts of the National Earthquake Prediction Evaluation Council"

The following is a summary of points I expressed to NEPEC at the April 30 meeting of NEPEC in response to Jim Savage's "Criticisms of some forecasts of the National Earthquake Prediction Evaluation Council" which he presented at the same meeting. These comments are not intended to be a complete or a formal reply to Jim's criticisms. This is a second draft, containing some clarifications of points in the first version commented upon by Jim Savage.

There appears to be no disagreement with the mathematical procedure Savage has employed for obtaining the distribution of probabilities in his paper. I obtain similar distributions (to within ± a few percent) by updating the parametric distribution for elapsed time (see Appendix A of the draft report), and then directly integrating for the probability distributions (Jim uses a Monte Carlo simulation to draw times from the parametric distribution). The conditional probability is equivalent to the mean probability one obtains from this distribution of probabilities. Although I disagree with several of Savage's conclusions, this memo pertains only to the interpretation and significance of the distributions of probabilities he has employed.

My Points:

- Uncertainty in recurrence time is the reason we must express earthquake occurrence in probabilistic terms. The assumed model, lognormal distribution with median, $\widehat{T}$ and net uncertainty σ_N, summarizes our knowledge (and uncertainty) of recurrence time. To convey this information <u>and its uncertainty</u> (the uncertainty being on recurrence time) we compute a conditional probability from the net distribution. This probability is <u>the</u> appropriate measure of probability because it is based on all possible median recurrence times and their appropriate weights. The purpose of the exercise is to estimate the probability of an earthquake in some time interval, not as Savage claims, to find the most frequently occurring probability in a distribution of probabilities.

- o It would be nice if the so-called intrinsic uncertainty component of the net uncertainty were better understood and it could be argued that there are more appropriate distributions to employ (normal, Weibull etc.). I believe most of the Working Group would agree that the "intrinsic" uncertainty is less well known than the parametric uncertainty. In fact Savage has similarly argued that different segments may have different intrinsic uncertainties. However, as the draft report explains, neither the choice of the lognormal distribution nor the specific value of the intrinsic uncertainty (provided it is somewhat less than parametric uncertainty) has much effect on the mean probabilities we compute.

- o I believe the distributions of probabilities or related measures of dispersion as discussed by Savage to be misleading because the analysis fails to recognize that the intrinsic uncertainty is poorly known and in future applications of this approach different values may be employed. The dispersion of the probabilities (as computed by Savage) does not depend on the total uncertainty, σ_N, but on the ratio of the intrinsic uncertainty to parametric uncertainty, σ_I / σ_P. <u>If</u> σ_P <u>is larger than</u> σ_I <u>then the distributions are highly dispersed, independent of the magnitude of</u> σ_P.

- o Some characteristics of the distributions of probabilities are illustrated in the accompanying examples (see plots).

Example 1 gives a generic example that is typical of many of the segments considered in the draft report ($\widehat{T}$ = 150, T_e = 130, σ_I = 0.21, σ_P = 0.34, σ_N = 0.40). The parameters produce a distribution similar to that shown by Savage, Fig. 5, for the Southern Santa Cruz Mountains segment.

Example 2 has parameters identical to example 1 except the role of σ_I and σ_P have been reversed ($\hat{T}$ = 150, T_e = 130 σ_I = 0.34, σ_P = 0.21 , σ_N = 0.40). Note that the net uncertainty of recurrence time is identical to example 1, hence the probability is unchanged, but that the dispersion of the probabilities is greatly reduced.

Example 3 uses the same parameters as example 1 with the exception that the intrinsic uncertainty has been increased to equal the parametric uncertainty ($\hat{T}$ = 150, T_e = 130, σ_I = 0.34, σ_P = 0.34 , σ_N = 0.48). This example illustrates the type of result we would obtain if we increased the intrinsic uncertainty to respond to Savage's criticism of this parameter. This has the effect of somewhat increasing the net uncertainty but only slightly altering the probability. In this case increase in net uncertainty decreases the dispersion of the distribution of probabilities. Hence, the appearance of increased resolution of probability is actually obtained by a decrease in the resolution of the data. In fact time of occurrence is now less well-defined than before.

Example 4 further illustrates the point that greatly decreasing the resolution of recurrence time can lead to the appearance of improved resolution of probabilities. This is a pseudo-Poisson case where the intrinsic uncertainty is 1.0 ($\hat{T}$ = 150, T_e = 130, σ_I = 1.00, σ_P = 0.34 , σ_N = 1.06). The probabilities are very tightly clustered, but we know very little about the recurrence time.

Example 5 is the opposite extreme from 4. In this case the net uncertainty of recurrence time is very low, 0.11, but the apparent uncertainty of probabilities is very large simply because σ_I is small compared to σ_P . In this case the recurrence time is very well defined, but the probabilities appear to be either 0 or 1. The increased resolution of recurrence time results in mean probabilities that deviate more strongly from the Poisson case. The probabilities become larger than probabilities of segments with more uncertain distributions as the the median recurrence time is approached.

Conclusions: Intrinsic uncertainty not a well-defined quantity, but its numerical value has little effect on reported probabilities. A distribution of probabilities (as used by Savage) does not indicate how the mean probability is likely to change with improvement (narrowing) of net uncertainty of recurrence time, if one allows that changes in net uncertainty are likely to come about from a change of either the intrinsic uncertainty or parametric uncertainty. With increased resolution of recurrence time, distributions can broaden significantly. The distributions of probabilities as computed by Savage give the range of values one would obtain if the parametric uncertainty could be reduced to zero and if the intrinsic uncertainty remains unchanged. However, parametric uncertainty will always exist and the intrinsic uncertainty may be amenable to better analysis and modification. (On the latter point, I think it is possible that some portion intrinsic uncertainty arises from fault interactions that are not accounted for in the present model.) Hence, these distributions of probabilities and related measures of dispersion are meaningless if the goal of the exercise is to map out the range of possible future changes of probability estimates resulting from change of the net uncertainty.

Example 1

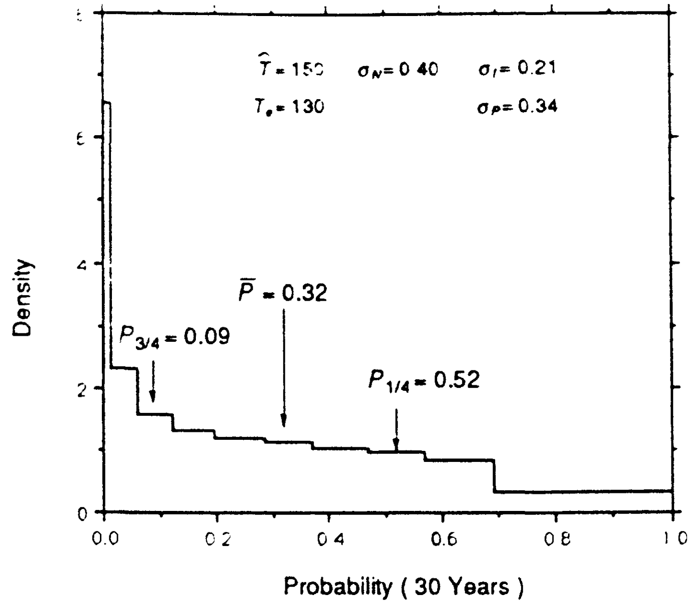

Example 2

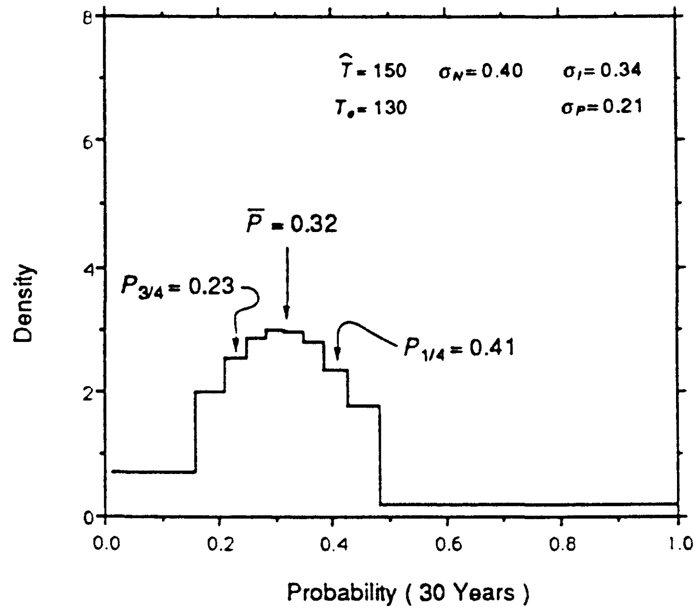

Example 3

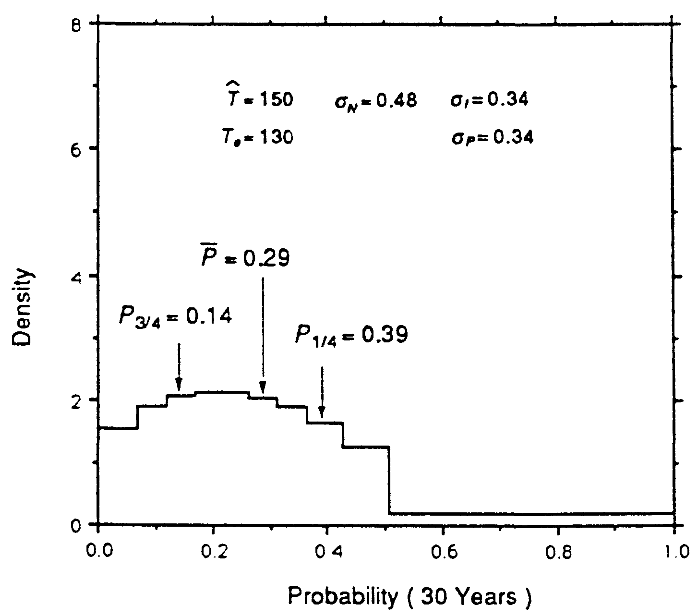

Example 4

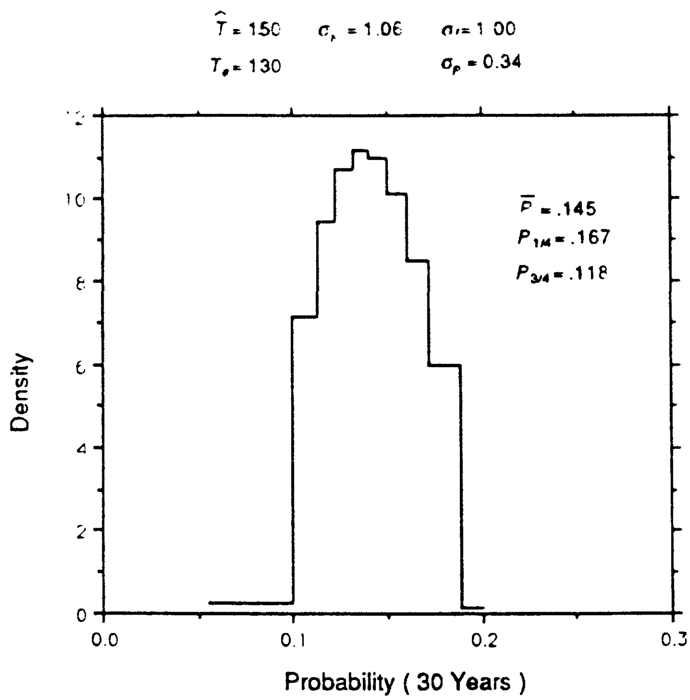

Example 5

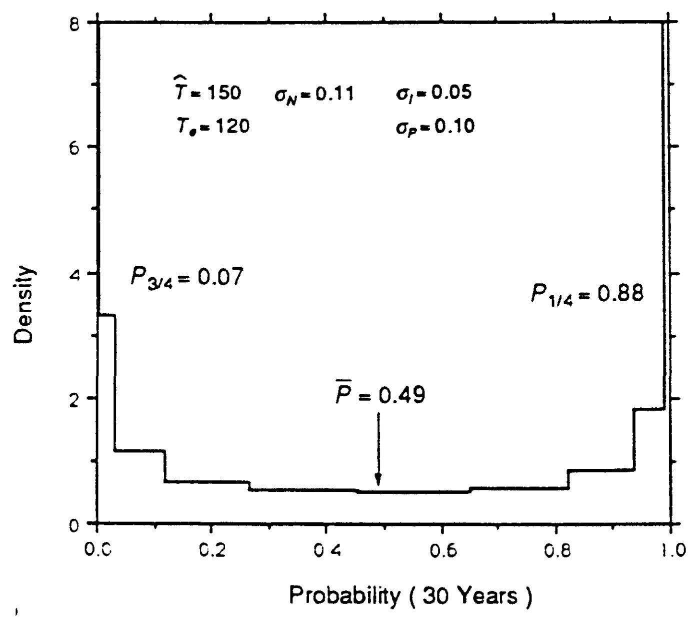

Appendix W

Memorandum from J.Savage to NEPEC regarding the Bay Region Earthquake Probabilities report, May 7, 1990.

United States Department of the Interior

GEOLOGICAL SURVEY
OFFICE OF EARTHQUAKES, VOLCANOES AND ENGINEERING
Branch of Tectonophysics
345 Middlefield Road, MS/977
Menlo Park, California 94025

May 7, 1990

Memorandum

To: NEPEC

From: Jim Savage

Subject: Rebuttal to Dieterich's Memo of 5/3/90

A point by point rebuttal to each of Dieterich's items follows:

Item 1. The purpose of the exercise should be to provide the best estimate of the conditional probability and its uncertainty. As can be seen by examining the distributions the best estimate in some cases may be the mode rather than the mean. At issue here, however, is the uncertainty. The letter reliability assigned by the Working Group is not very informative, whereas the distributions are quantitative and can be used to evaluate significance. Incidentally, what is this measure of uncertainty that Dieterich promises in this item?

Item 2. For the Mojave segment a change in σ_i from 0.21 to 0.7 changes the average probability from 0.32 to 0.19.

Item 3. The breadth of the distribution of the conditional probability does not depend upon σ_N but rather upon σ_P and to a lesser extent σ_i. If $\sigma_P = 0$, there is a unique probability for each σ_i (*i.e.*, the breadth of the probability distribution is zero in all cases, but the unique probability is different for different σ_i). As σ_P is increased the breadth of the probability distribution for fixed σ_i increases. Thus, Dieterich's underlined statement is wrong.

One goes to conditional probability to avoid the intrinsic uncertainty associated with σ_i. That is, given a lognormal distribution (median $\hat{T}$, shape factor σ_i), T is distributed with an uncertainty related to σ_i, but the conditional probability is uniquely defined. This is true independent of whose procedure (WGCEP or mine) is used.

Dieterich's conclusions: The distribution of probabilities has more information than does simply the mean. The mean can be calculated from the distribution. My understanding is that σ_i is intrinsic, not subject to improvement. Then any improvement in resolution comes from a decrease in σ_P which results in a narrowing of the probability distribution.

Appendix X

Memorandum to NEPEC from J.Dieterich regarding revision of the Bay Region Earthquake Probabilities report, May 31, 1990.

United States Department of the Interior

GEOLOGICAL SURVEY
OFFICE OF EARTHQUAKES, VOLCANOES, AND ENGINEERING
Branch of Tectonophysics
345 Middlefield Road, MS/977
Menlo Park, CA 94025

May 31, 1990

Memo

To: NEPEC and Working Group Members
From: Jim Dieterich
Subject: Revision of Probabilities Report:

The Working Group met May 22 to revise the report "Probabilities of large earthquakes in the San Francisco Bay region" based on comments and suggestions received from NEPEC, CEPEC and Working Group members. Major revisions are as follows:

1) Concern was expressed by NEPEC and CEPEC pertaining to the effect that rounding of probabilities might have on the perception of hazard posed by the Hayward fault. We reconsidered the issue of rounding and the report now gives all probabilities to two decimal places. Throughout the document, including the summary figures, the reader is reminded that differences of less than 0.10 are not considered meaningful. The height of the columns indicating probabilities in the summary figures are now plotted to the two digit accuracy and no longer accentuate the differences in probability due to rounding.

2) In response to suggestions from NEPEC, the summary figures (in the Executive Summary and Figure 9) now show other faults, in addition to those faults that have been evaluated. The Executive Summary (p. 5) and the Summary and Discussion (p.36) call attention to those faults and the note several reasons why the actual probability may be higher than we report. The need for additional studies is now stated (p.34).

3) Executive Summary. Jim Davis stressed the need to have an Executive Summary that represents a consensus and that will be supported by the Working Group. I believe it meets those criteria. The Executive Summary addresses the specific topics recommended in the NEPEC discussion:

Uncertainties and limitations of the method

Earthquake on any segments will have severe consequences for the entire region

Major revisions from the 1988 report
Listing of segment and aggregate probabilities
Other factors suggesting higher probabilities

4) Regional consequences of a M7 earthquake. The Executive Summary (p.4) and Summary and Discussion (p.35) now note that, in light of the Loma Prieta earthquake, an earthquake on any of the fault segments could have severe consequences for the entire region. This observation provides one basis for explaining the significance of the aggregated probabilities.

5) Uncertainties in model and supporting lines of evidence for principal conclusions. Tom Heaton's suggestions for a paragraph have been worked into the Preface. The Executive Summary (p.4) discusses uncertainty and other arguments for concluding the probability is high. The final paragraph of the introduction has been reworked (p.7, 8). Discussion of uncertainties and other arguments supporting the principal conclusions of the report have been retained and clarified in the Discussion and Summary (p.33-38).

6) Poisson probabilities. Related to the previous item, the Discussion and Summary now includes the discussion of Poisson probabilities (0.54 for 30 years) (see pages 5, 36-38).

7) At the suggestion of NEPEC we discussed our change from the 1988 Working Group's 1.4 m displacement estimates for the Hayward fault to 1.5 m. The Working Group elected to retained the 1.5 m estimate.

8) The potential for M≤7 along the North Coast segment is noted (p.28).

9) Treatment of the San Francisco Peninsula segment. The discussion of probabilities for the San Francisco Peninsula segment has been expanded and now includes results for the total probability of a magnitude 6.5 or 7 earthquake (p.28,29). The probability is also given in Table 5.

10) Loma Prieta Earthquake - Where did the previous forecasts fall short and how might differences between the earthquakes of 1906 and 1989 affect the probability estimates? The discussion of these topics has been expanded and clarified (p.16-18). A paragraph has been added (p.16, bottom) that acknowledges the differences between 1906 and 1989, notes the possibility of slip on different faults and discusses the presumed insensitivity of these factors to the stress cycle. The hypothesis test (was the Loma Prieta earthquake early?) has been reworked and simplified (p.17,18). The

possibility of vertical segmentation of the Southern Santa Cruz Mountains segment, giving a potential for a shallow M6.0-6.5 earthquake above the zone of the Loma earthquake is now discussed (p.28).

11) Tests of forecasts. CEPEC suggested that uncertainties in various forecast parameters be more fully specified to permit tests of the validity of the forecasts in the future. Several paragraphs (p.12, 13) have been added giving estimates of the uncertainties in segment boundaries, amount of slip and expected magnitude

12) Interpretation of creep and strain accumulation on Hayward fault. A discussion has been added (p.29, 30) dealing with the problem of interpreting the rate of strain accumulation given the high creep rates observed along the Hayward fault.

13) Potential for larger (2 segment) earthquake on the Hayward fault. CEPEC recommended that this possibility be explicitly stated. This possibility is recognized in the current report, but it is mentioned only in passing (p.30). It is an oversight of mine that this issue was not addressed. We will take this up before the report is finalized.

14) Criticisms of method by Savage. CEPEC recommended that we deal with the questions raised by Savage in the body of the report rather than relegating it to the appendices. We discussed this, but concluded that we would prefer not highlight these issues. Factors influencing this decision include: a) Savage's criticisms have undergone several changes and the final content of the paper is unknown. Hence, it is difficult to hit a moving target and specific responses cannot be made. b) We are in accord with Tom Heaton's comments that the report should not put undue emphasis on results that depend on the specific details of the model we have used to estimate probabilities. Uncertainties of probabilities depend on such details. Other models could give similar probabilities, but different uncertainties. A discussion of the interpretation of uncertainties has been added to Appendix C (p.2). c) We basically agree with Savage's analysis of uncertainty, but do not accept his interpretations. These differences are based on technical details that are out of place in the body of the report. Readers of the appendices are provided sufficient information to come to their own conclusions.

Appendix Y

Draft manuscript of public interest document prepared by P.Ward to inform the public of the Bay Region Earthquake Probabilities report, June 5, 1990.

Draft 1 p.m. 6/5/90

ARE YOU PREPARED FOR THE NEXT MAJOR EARTHQUAKE IN THE SAN FRANCISCO BAY REGION?

The odds are 2 to 1 than an earthquake considerably more damaging than the Loma Prieta earthquake of October 17, 1989, will strike the San Francisco Bay region within 30 years. Living with earthquakes can be made less hazardous than driving on a highway, if you take specific actions now to drastically reduce the hazards faced by you and your family.

Prepared by the United States Geological Survey
In cooperation with
Bay Area Regional Earthquake Preparedness Project
Association of Bay Area Governments
California Office of Emergency Services
California Division of Mines and Geology
California Seismic Safety Commission
Earthquake Engineering Research Institute
Applied Technology Council
Federal Emergency Management Agency
American Red Cross

Printed and Distributed with funds provided by
Give corporate names

(This document is planned to be a poster, about 17 by 28 inches, folded. The text will be read as you unfold the document much like a road map. The final unfolding will display, on the reverse side, a brightly colored map of the Bay region showing the likely ground shaking based on geology using the map prepared by Tim Hall for the Point Reyes Association. The fundamental purpose of this document is that it be released as a companion to the Open-File Report prepared by the Working Group on California Earthquake Probabilities in June, 1990, and that it put that report into a meaningful perspective for the average citizen. The point of the map is to emphasize that the level of potential hazard varies depending on where you live and work.)

1. THE MOST IMPORTANT MESSAGE

A national panel of scientists recently determined the odds to be 2 to 1 of a severe earthquake occurring in the San Francisco Bay region between the years 1990 and 2020.

This earthquake, with a magnitude of about 7, could occur at any time beginning today.

This earthquake will be located closer to major centers of population than the Loma Prieta earthquake of October 17, 1989, and is thus expected to cause more severe damage throughout the San Francisco Bay region.

You can live safely in earthquake country, if you understand the potential hazards and if you take a few practical steps to reduce these hazards.

This document explains what you need to know about earthquakes, what you should do to protect yourself and your family from earthquake hazards, and where you can get more information and help.

Keep this document in a safe place where you can refer to it often.

2. ABOUT THE ANTICIPATED EARTHQUAKE

An earthquake of magnitude 7 in the San Francisco Bay region is most likely to occur along one of four fault segments shown on the map on the reverse side of this pamphlet:

1. The San Andreas fault between Los Gatos and Hillsborough.
2. The Hayward fault between Fremont and San Leandro.
3. The Hayward fault between San Leandro and San Pablo Bay.
4. The Rodgers Creek fault between San Pablo Bay and Santa Rosa.

Similar earthquakes are considered less likely, but possible, on other faults such as the Calaveras, Concord, or San Gregorio.

A repeat of the magnitude 8.3 San Francisco earthquake of 1906 that broke along the San Andreas fault from south of San Jose to Cape Mendocino, is not likely during the next few decades.

While the odds are 2 to 1 that one of these earthquakes will occur within the next 30 years, all of these earthquakes are likely to occur within the next 100 to 150 years.

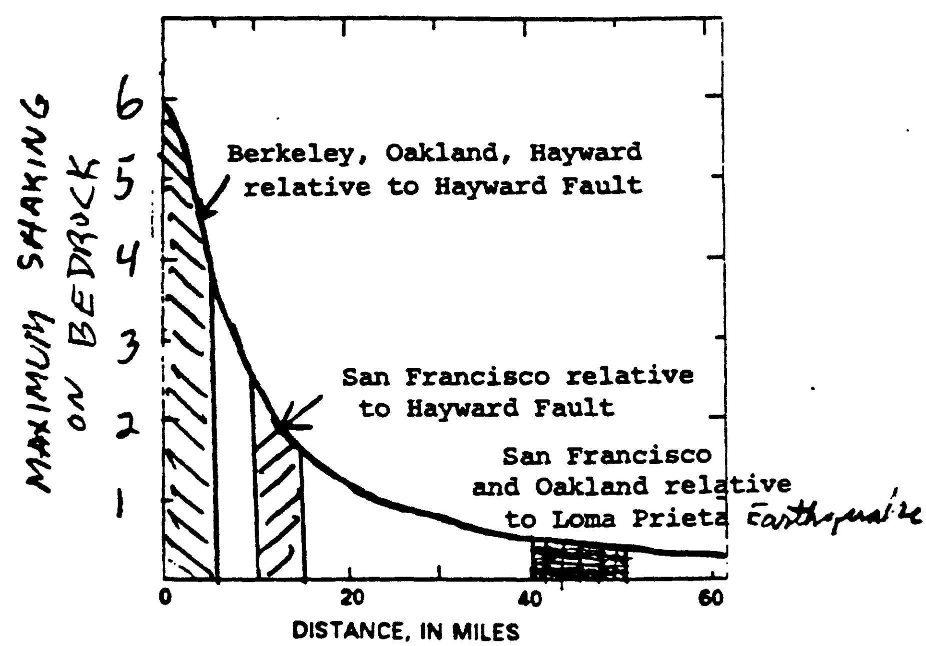

Most damage during earthquakes is caused by the horizontal (side-to-side) shaking of the ground. This shaking decreases rapidly with distance from the part of the fault where the earthquake occurred. The Loma Prieta earthquake was located in the rural Santa Cruz Mountains, about 50 miles to the south of Berkeley, Oakland, Hayward, and Fremont. The ground shaking was moderate in these areas. A similar earthquake of magnitude 7 on the Hayward fault will cause shaking that is about 10 times greater than experienced in these areas during the Loma Prieta earthquake. A similar earthquake on the Hayward fault or on the San Andreas fault along the San Francisco Peninsula will cause shaking in San Francisco that is about 5 times greater than felt within the city during the Loma Prieta earthquake.

The amount of shaking is magnified on soft soils and especially on mud and filled land. The map on the opposite side of this page shows areas in red where shaking will be increased several times compared to areas nearby on bedrock shown in green.

Damage may also be caused by landsliding in regions shown in orange and by ground rupture within fault zones shown in black.

Shaking during the anticipated earthquake will be particularly severe throughout the San Francisco Bay region from San Jose to San Rafael if the earthquake occurs on the Hayward or San Andreas faults and from San Francisco to north of Santa Rosa if the earthquake occurs on the Rodgers Creek fault. Damage will typically be greatest in regions of soft soil where the shaking will typically be strongest.

3. WHAT CAN YOU DO IMMEDIATELY TO PROTECT YOURSELF AND YOUR FAMILY?

Most people in the San Francisco Bay region will survive the anticipated earthquake with little loss. Some people will be severely affected. You can take actions now that will determine which group you and your family will be in.

Be prepared for the emergency during and after the quake.

FIRST: Practice "Duck, Cover, and Hold" drills with your family and at work.

Injuries and deaths during earthquakes are caused by falling objects and collapsing structures. Knowing instinctively how to protect yourself when the shaking starts may save your life. Duck under a strong table or stand in a sturdy doorway. Cover your head and face to protect from broken glass and falling objects. Hold you position until the shaking stops. **Do not run outside during the shaking or use the stairways or elevators.**

SECOND: Store emergency supplies.

After the anticipated earthquake, medical aid, transportation, water, electricity, and communication may be unavailable or severely restricted for several days to weeks throughout the bay region. Be prepared to take care of yourself, your family, and your neighbors. At home, at work, and in your car store flashlights, batteries, a battery operated radio, a first-aid kit and handbook, water, food, warm clothes and sturdy shoes. Make sure these supplies are located in a safe and readily available place. Make sure everyone in your family knows where these supplies are and how to use them.

THIRD: Develop an earthquake plan at home, in your neighborhood, at school, at work.

If the earthquake occurs during the day, family members may be separated for hours to several days. Plan for the various possibilities. Communication to points outside of northern California may be more available than local communication. Choose a relative or friend that family members may call to report their condition and location. Find out the policy of your local school concerning release of children after a quake. Arrange with neighbors to watch out for you family members and your property in case you are not home.

The most common cause of earthquake related fires is broken gas lines. Everyone should know how and when to turn off the gas supply at the meter in case of a leak.

Discuss the possibilities and make plans with your family, your neighbors, and at work. For more information look at the "First Aid and Survival Guide" in the introductory pages of most telephone directories. Your local Office of Emergency Service and American Red Cross Chapter can provide pamphlets, slide shows, video tapes, and speakers to help you organize self-help groups. Participate in earthquake drills. Ask your local library for more information. A one-hour video tape entitled **Surviving the Big One, How to prepare for a major earthquake** was developed for public television and is available from KCET Video, 4401 Sunset Boulevard, Los Angeles, California 90027, (800) 228-5238 ($19.95 + $3.50 P&H). Share a copy with your neighbors.

Discussing the options and making plans now will not only help your family deal with the emergency when it comes, but will also significantly reduce the fear and uncertainty your family and friends may feel until you all make contact after the quake.

4. REDUCE THE HAZARDS AND POTENTIAL LOSSES IN YOUR HOME, YOUR SCHOOL, AND YOUR OFFICE

Falling objects and toppling furniture are not only dangerous, but they will be the biggest loss for most residents.

Be sure there are no heavy items that could fall on your beds where you typically spend a third of each day.

Secure tall furniture and bookcases to the wall. Shelf lips may be added to help items remain on the shelves. Be sure adjustable shelves cannot slide off their supports.

Put strong latches on cabinet doors especially in your kitchen.

Fasten heavy or precious items to secured shelves or tables. Restrain file cabinets, computers, and machinery that may overturn during an earthquake.

Store potentially hazardous materials such cleaners, fertilizers, chemicals, and petroleum products in secure containers and sturdy cabinets fastened to the wall.

In your office, be sure heavy objects are fastened to the building structure and not just to a movable wall. Be sure light fixtures and modular ceiling systems are securely supported.

Broken gas mains are the primary cause of fires during earthquakes. Be sure your gas hot water heater is fastened to the wall and that all gas heaters and appliances are connected to the gas pipe through a short piece of flexible tubing.

Check with school officials to be sure building contents are properly secured.

The following references give more information on emergency preparedness and on how to reduce the potential damage to building contents:

General preparedness information (7 brochures covering personal preparedness in the home, apartments, mobile homes, high- rises, preparedness for the elderly or disabled, and a checklist), (ABAG P87059BAR, $2).

Home earthquake preparedness (Many cities have booklets of similar title describing how to prepare home and family for a major earthquake disaster in your neighborhood), check with your city Office of Public Safety or county Office of Emergency Services.

Getting ready for the big one, Health Plus, 694 Tennessee St., San Francisco, CA 94107, 1986, 45 pages $XXX.

Earthquake preparedness--for office, home, family, and community, Lafferty and Associates, Inc., P.O. Box 1026, La Canada, CA 91012, 1989, 32 pages, $5.00, (818) 952-5483.

Reducing losses from earthquakes through personal preparedness, W.J. Kockelman, 1984, U.S.G.S. Open-File Report 84-765, 21 pages ($2.75).

Earthquake preparedness: a key to small business survival, 1985, 8 pages (ABAG P85055BAR, $2.00 + $.90 P&H).

Living safely in your school building, Lawrence Hall of Science, University of California, Berkeley, CA 947201986, 9 pages, (415) 642-8718 ($2.00).

Guidebook for developing a school earthquake safety program, 1985, XXX pages, FEMA, $XXX.

Earthquake preparedness activities for child-care providers, 1989, 54 pages (ABAG P89002BAR, $7 + $2 P&H).

Reducing the risks of nonstructural earthquake damage: A practical guide, BAREPP number P87056BAR, $7.00 plus $1.60 postage and handling.

Hazardous materials problems in earthquakes: Background materials [preliminary version], 1990, 280 pages, ABAG cat #P900001EQK, $12.50 +$2.50 P&H.

Corporate comprehensive earthquake preparedness planning guidlines, 1985, 48 pages (ABAG P87054BAR, $8 + $1.50 P&H).

City comprehensive earthquake preparedness planning guidlines, 1985, 90 pages (ABAG P87052BAR, $8 + $1.80 P&H).

County comprehensive earthquake preparedness planning guidlines, 1985, 93 pages (ABAG P87052BAR, $8 + $1.80 P&H).

5. DECIDE HOW MUCH ACTION YOU SHOULD TAKE TO REDUCE EARTHQUAKE RISK

Earthquakes pose a risk that we accept as part of the price of enjoying the benefits of the San Francisco Bay region.

We face many hazards in our lives, and we have learned through science and technology that by taking certain actions, we can reduce many of these hazards to acceptable levels. For example, we have determined that by using seat-belts in our cars, we can reduce the chance of bodily injury during automobile accidents; by quitting smoking, we can reduce the likelihood of lung cancer; and by using metal detectors in airports, we can reduce the chance of hijacking. These are all actions that most people have come to accept as reasonable precautions.

Earthquake hazards are different from these other hazards because severe earthquakes occur infrequently and affect thousands of people at the same time when they do occur. Yet earthquake hazards can also be reduced significantly by taking appropriate action.

Such actions can be taken by individuals, businesses, and governments to change the consequences of future earthquakes. The basic actions described above are reasonable precautions that have proven effective and should be taken by all residents of the San Francisco Bay region.

Other actions such as strengthening or replacing a dangerous building, moving out of a dangerous building, or moving to a safer part of your city may involve significant expense and disruption. A key factor in choosing to take action and in determining how much action is appropriate, is to decide how imminent is the risk. Is life-safety a concern for occupants of a specific building or is the risk purely economic. What are the odds that time and money spent on action today will prove cost-effective within your lifetime and within the lifetimes of existing structures? If a structure will be replaced by normal development within 20 years, is strengthening it to resist earthquake damage cost-effective? Is such strengthening required by a governmental agency, is it legally reasonable or is it morally necessary?

These are difficult decisions. In addressing these issues you need to understand not only what is the potential for damaging earthquakes, but also what is the level of risk that you face. The amount of risk from earthquakes varies significantly from location to location, from structure to structure, from person to person. The following sections are designed to help you determine how much risk you and your family face.

Earthquakes are a hazard that we can live with safely by taking those precautions that are reasonable based on the risk we face. You can determine how much action on your part is appropriate. You will then know how to respond in the future if more specific earthquake forecasts or predictions are issued.

6. DETERMINE WHETHER YOU ARE LOCATED IN A POTENTIALLY HAZARDOUS REGION

The Loma Prieta earthquake caused severe damage in less than 1% of the San Francisco Bay region. While damage from future severe earthquakes is likely to be more widespread, most of the damage will also be concentrated in locations that can be identified in advance. The most hazardous regions include areas nearest to the earthquake, those regions where ground motion will be amplified in certain types of soil, and those areas where the ground surface may be ruptured by faulting, landsliding or soil failure.

The type of geologic material at a specific site has a controlling effect on the amount of shaking during an earthquake because it may increase or amplify the ground motion. The safest material is solid rock or bedrock. Thick deposits of mud, sand, and clay on the other hand may amplify shaking several times. The map on the other side of this page shows the general distribution of geologic materials throughout the San Francisco Bay region. Building new structures and reinforcing older structures in the more hazardous areas requires careful condsideration and attention to engineering design and construction quality, resulting in greater costs.

Particularly severe earthquake damage can result in the few areas where structures are built directly across active faults. The Alquist-Priolo Special Studies Zones Act of 1972 required the California Division of Mines and Geology to map all known active faults in California and to designate areas within 500 feet of these faults as Special

Study Zones. Substantial development within these zones can proceed only after geologic studies are done to ensure that structures are not placed directly on top of ground likely to rupture during major earthquakes. The Special Study Zones are shown on the map on the opposite side of this page. Most realtors have maps showing the location of these fault zones and of flood zones. Realtors are required to inform you if you are considering buying land within a Special Study Zone. You can learn more about these zones and how to obtain detailed maps by ordering Special Publication 42 of the California Division of Mines and Geology listed below. You may be able to examine these maps at your local planning office.

Landslides are likely to occur on steep slopes during earthquakes, especially if the earthquake occurs near the end of the rainy season. Ground failure is possible along margins of the bay that have been filled with "weak" soils, especially sand and water pumped through pipelines and sands deposited by local streams.

The enclosed map is meant to alert you to potential problems in your area. You can get more detailed information from maps listed below. Ask your local planning office if more detailed maps are available or if they are being produced in your area. If you suspect a serious hazard, you might wish to consult an engineering geologist for a detailed survey of your particular site.

The San Francisco Bay area–On shakey ground–San Francisco Map set and text, 1987, 32 pages, 7 maps at scale of 1:125,000 (includes Berkeley to Hayward)(ABAG P87001EQK, $8 +$2 P&H).

The San Francisco Bay area–On shakey ground–Alameda and Contra Costa Counties Map Set, 1988, 7 maps at scale of 1:125,000 only (Intended to be used with the San Francisco map set and text) (ABAG P88002EQK, $60 +$2 P&H).

The San Francisco Bay area–On shakey ground–Santa Clara County Map Set, 1987, 7 maps only 2 at scale of 1:125,000 (Intended to be used with the San Francisco map set and text) (ABAG P87002EQK, $60 +$2 P&H).

Map set (complete 20 map blue-line ozalid set for entire 9 county bay region to be used with the San Francisco–On Shakey Ground text), 20 maps @ 1:125,000 only (ABAG M80000EQK, $40 +$5 P&H). Map set includes maps of fault surface rupture, fault traces, geologic materials, anticipated ground shaking intensities for earthquakes from 10 different possible sections of fault, maximum ground shaking intensity, cumulative damage potential from ground shaking for 3 different types of buildings, dam-failure inundation areas, and liquefaction susceptibility and potential maps. (Intended to be used with the San Francisco map set and text.)

Eight-map mini-set (part of the above set), (ABAG M80001EQK, $20 +$5 P&H). Set includes maps of fault surface rupture, geologic materials, anticipated ground shaking intensities for San Andreas and Hayward faults only, maximum ground shaking intensities, and cumulative damage potential from ground shaking for 3 different types of buildings. (Intended to be used with the San Francisco map set and text).

Fault-rupture hazard zones in California, Alquist-Priolo Special Studies Zones Act of 1972 with index to special studies zones maps, California Division of Mines and Geology Special Publication 42, 24 pages, revised 1988, ($1.00 from P.O. Box 2980, Sacramento, CA 95812).

Living on the fault: A field guide to the visible evidence of the Hayward fault, 16 pages, 1988 (ABAG P88004BAR, $2.00 + $1.00 P&H)

Maps showing maximum earthquake intensity predicted in the southern San Francisco Bay region, California, for large earthquakes on the San Andreas and Hayward faults by R.D. Borcherdt, J.F. Gibbs, and K.R. Lajoie, U.S. Geological Survey Miscellaneous Field Studies Map MF-709, 1975 (USGS, $4.50).

The following 5 maps for San Mateo County are prototypes of the kind of detailed work that is now possible and could be carried out by state, county, or local workers or consultants.

Map showing slope stability during earthquakes in San Mateo County, California, by G.F. Wieczorek, R.C. Wilson, and E.L. Harp, Geological Survey Miscellaneous Investigations Series Map I-1257-E, 1985 (USGS, $3.10).

Map showing faults and earthquake epicenters in San Mateo County, California, by E.A. Brabb and J.A. Olsen, Geological Survey Miscellaneous Investigations Series Map I-1257-F, 1986 (USGS, $5.50).

Map showing liquefaction susceptibility of San Mateo County, California, by T.L. Youd and J.B. Perkins, Geological Survey Miscellaneous Investigations Series Map I-1257-G, 1987 (USGS, $3.10).

Map showing predicted seismic-shaking intensities of an earthquake in San Mateo County, California, comparable in magnitude to the 1906 San Francisco earthquake, by J.M. Thomson and J.F. Evernden, Geological Survey Miscellaneous Investigations Series Map I-1257-H, 1986 (USGS, $3.10).

Maps showing cumulative damage potential from earthquake ground shaking, San Mateo County, California, by J.B. Perkins, Geological Survey Miscellaneous Investigations Series Map I-1257-I, 1987 (USGS, $9.30).

7. DETERMINE WHETHER YOU LIVE OR WORK IN A POTENTIALLY HAZARDOUS BUILDING

The number of deaths during earthquakes in California has been kept small because most structures in California do not collapse during the shaking. Structures that are damaged typically do not have sufficient strength and stiffness to resist the horizontal shaking. Potentially hazardous buildings, often designed and built before we understood how earthquakes affect buildings, can be readily identified by engineers.

Modern criteria for seismic design are included in the 1988 Uniform Building Code that is now required throughout California. The code provides minimum requirements. Structures placed in particularly hazardous regions should be built to higher standards.

Most people in California are quite safe at home if they live in a one or two floor wood-frame building. These buildings rarely collapse during earthquakes. The most common damage involves the brick chimney that may crack or topple. Chimneys can be braced with steel bands to prevent toppling. After an earthquake, a cracked chimney should not be used until inspected by an expert.

Unfortunately, seismic design for wood-frame buildings prior to about 1950 has often proven inadequate. These structures often fail at or near ground level because they are not adequately bolted to the foundation or because the short "cripple" walls between the foundation and the first floor are not adequately braced. Instructions for adding foundation bolts and bracing the cripple wall are available through you local office of emergency service.

Excessive termite damage and dry rot could have seriously weakened wooden structures. You may wish to consider having a termite inspection if your building has not been inspected within the past few decades.

Public elementary and high school buildings are typically safe. Following severe damage to several schools during the Long Beach earthquake of 1933, the Field Act (Education Code Section 39140) was passed requiring special seismic strengthening of public school buildings. Knowledge about proper strengthening has been increasing rapidly. If your school building was built or strengthened before 1971, you should ask the school district whether the seismic strength of the building has been reassessed in light of modern building codes. You should ask school officials in private schools and colleges whether the school buildings have been evaluated for earthquake resistance.

Mobile homes need to have supports that resist horizontal forces from earthquakes. If mobile homes are used as temporary classrooms at your local school, you should ask the school district whether they are properly anchored.

Older unreinforced brick buildings pose a hazard in even moderate earthquakes. Unbraced parapets and walls that are inadequately tied to the floors and roof can topple onto sidewalks or adjacent buildings. Many such buildings are currently used for low income housing and commercial space in the San Francisco Bay region. Senate Bill 547 required all local governments to inventory existing unreinforced masonry buildings and to develop a mitigation plan by January, 1990. If you are concerned about these buildings, contact your local building department to see what is being done with this inventory.

Brittle concrete-frame structures built before 1973 also pose a hazard during moderate earthquakes. This design was commonly used for mid-rise office and commercial buildings in our cities. These structures are too inflexible to absorb repeated cycles of horizontal movement caused by earthquake shaking and can collapse catastrophically. The collapse of a single mid-rise, brittle concrete structure in an earthquake in California could result in a greater loss of life in a single building than the total loss of life during all earthquakes in California since 1906.

"Tilt-up" buildings built before 1973 are another type of concrete structure that has proven particularly vulnerable to damage during moderate or larger earthquakes. These buildings are constructed of concrete precast on the ground and then tilted vertically into place. They often fail at the connections between the walls, the floor, and the roof. While the occupancy of these buildings is usually low, such buildings do house many of the major industrial activities of the San Francisco Bay region, posing the potential for severe economic loss and spill of hazardous materials. Strengthening the connections is a relatively inexpensive procedure.

Major damage during earthquakes often occurs in buildings with a "soft" first story. What this means is that the first floor does not have shear strength adequate to resist the horizontal shaking of the upper parts of the building, usually because the first floor consists of garages or is of an open, columnar design often used for stores or large offices. Similarly, rooms added over garages of private homes may not be adequately supported.

Damage to all these types of buildings pose a threat to both life and property during earthquakes. These losses can be avoided by strengthening structures before the earthquakes occur. Investment in structural strengthening can be very cost-effective by reducing the structural and non-structural damage during earthquakes and allowing continuation of your business after the earthquake.

These brief descriptions are meant to alert you to the most common types of failures in buildings during earthquakes. The following references provide more detailed information. If you believe a structure that you or your family uses is hazardous, ask the building owner what consideration has been given to seismic design and strengthening. Your local building department may be able to provide information. Structural engineers can examine potentially dangerous buildings and recommend appropriate action. Can you see that such action is taken or should you consider moving to safer structures?

Getting ready for a big quake, Special Report, Sunset Magazine, March, p. 104-111, 1982 ($0.25 from Earthquake Reprint, Sunset Magazine, 80 Willow Road, Menlo Park, CA 94025).

Peace of mind in earthquake country, by Peter Yanev, Chronicle Books, San Francisco, California, 304 pages, 1974 ($XXX).

Building stock and earthquake losses -- San Francisco Bay area example by J.B. Perkins and R. Moreland, 68 pages, 1986. (ABAG P86005EQK, $8.00 + $2.00 P&H)

Rapid visual screening of buildings for potential seismic hazards: A handbook, Federal Emergency Management Agency, FEMA-154, 185 pages, 1988 (Free).

Earthquake hazards and wood frame houses: What You Should Know and Can Do, M. Comerio and H. Levin, 1982, 46 pages($6.44 from Center for Environmental Design Research, 390 Wurster Hall, University of California, Berkeley, CA 94720 (415)642-2896. Make check payable to "U.C. Regents).

8. REGIONAL PLANNING TO REDUCE EARTHQUAKE HAZARDS

Earthquake hazards vary throughout your community depending on the type of soil, the potential for ground failure, the closeness to active faults, and the age and design of existing structures. Recognizing these differences can provide a basis for guiding future development to minimize earthquake hazards. Clearly, critical facilities such as hospitals and fire stations should be located in the safest regions and the most hazardous regions might best be designated for parks or other low-density uses.

In the early 1970s, counties and cities were required to develop a Safety Element for their General Plan that included consideration of earthquake hazard. Citizens interested in the future development of their community may wish to consult this plan at their local planning office and to encourage update of this plan in the near future. The following references would be of interest to regional planners and concerned citizens:

California at risk--Steps to earthquake safety for local governments, California Seismic Safety Commission Report SSC 88-01, G.G. Mader and M. Blair-Tyler, 1988, 56 pages ($10.00).

Seismic hazards and land-use planning, D.R. Nichols and J.M. Buchanan-Banks, 1974, 33 pages, U.S. Geological Survey Circular 690 (USGS, free).

Geology for decisionmakers--Protecting life, property, and resources, R.D. Brown and W.J. Kockelman, 1985, 11 pages, Bulletin of the Institute of Governmental Studies, Regents of the University of California, Berkeley (Free from W.J. Kockelman, U.S.G.S., Mail Stop 977, 345 Middlefield Road, Menlo Park, CA 94025).

Seismic safety and land-use planning--Selected examples from California, M.L. Blair and W.E. Spangle, 1979, 82 pages, U.S. Geological Survey Professional Paper 941B (USGS, $6.50).

Examples of seismic zonation in the San Francisco Bay Region, U.S. Geological Survey Circular 807, W.J. Kockelman and E. A. Brabb, 1979, page 73-84 (USGS, free).

Putting seismic safety policies to work, M. Blair-Tyler and P.A. Gregory, 1988, 44 pages (ABAG P88006BAR, $8.00 + $1.75 P&H).

Evaluating earthquake hazards in the Los Angeles region: U.S. Geological Survey Professional Paper 1360, J.I. Ziony ed., 1985, 505 pages (USGS, $24.00).

Flatland deposits -- their geology and engineering properties and their importance to comprehensive planning: Selected examples from the San Francisco Bay region, California, by E.J. Helley, K.R. LaJoie, W.E. Spangle, and M.L. Blair, U.S. Geological Survey Professional Paper 943, 88 pages, 1979 ($6.00).

Relative slope stability and land-use planning: Selected examples from the San Francisco Bay region, California, by T.H. Nilsen, R.H. Wright, T.C. Vlasic and W.E. Spangle, U.S. Geological Survey Professional Paper 944, 96 pages, 1979 ($6.00).

Quantitative land-capability analysis: Selected examples from the San Francisco Bay region, California, by R.T. Laird, J.B. Perkins, D.A. Bainbridge, D.A. Baker, J.B. Boyd, R.T. Huntsman, P.E. Staub, and M.B. Zucker, U.S. Geological Survey Professional Paper 945, 115 pages, 1979 ($6.50).

Geologic principles for prudent land-use: A decisionmakers guide for the San Francisco Bay region, by R.D. Brown, Jr., and W.J. Kockelman, U.S. Geological Survey Professional Paper 946, 97 pages, 1983 ($XXX).

One way to anticipate emergency needs during future earthquakes and to plan our communities to minimize earthquake hazards, is to develop scenarios of what the effects of specific earthquakes are likely to be. The following references provide a great deal of specific information:

San Francisco: Earthquake planning scenario for a magnitude 7.5 earthquake on the Hayward fault in the San Francisco Bay area, California Department of Conservation, Division of Mines and Geology, Special Publication 78, 260 pages, 1987 (CDMG, $30.00).

San Francisco: Earthquake planning scenario for a magnitude 8.3 earthquake on the San Andreas fault in the San Francisco Bay area, California Department of Conservation, Division of Mines and Geology, Special Publication 61, 160 pages, 1982 (CDMG, $8.00).

9. WHY EARTHQUAKES ARE INEVITABLE IN THE SAN FRANCISCO BAY REGION

Geologists know that the surface of the earth is made up of a dozen or so large plates, most of which cover millions of square miles and each of which is at least 40 miles thick. These plates are in continual motion relative to each other. The San Francisco Bay region lies in the boundary between two of them, the North American plate to the east and the Pacific plate to the west.

The North American and Pacific plates are sliding by each other at a rate of about 2 inches per year as the Pacific plate moves to the northwest. Most of this sliding motion in northern California takes place along the San Andreas fault west of San Francisco Bay and along smaller faults east of the Bay including the Hayward, Calaveras, and Rodgers Creek faults.

But this sliding motion is neither smooth nor constant because slip does not occur continuously along most faults. The motion of the plates strains or deforms the ground along the plate boundaries much like the stretching of an elastic band. When the ground can no longer withstand the strain, sudden slip occurs along the major cracks in the ground that we call faults. The elastic energy stored in the strained ground is released as earthquake shaking.

Sudden slip and accompanying earthquakes occur on different parts or segments of these faults at different times. For example, in the great magnitude 8.3 San Francisco earthquake of 1906, a 270-mile segment of the San Andreas fault from south of San Jose northwestward to Cape Mendocino slipped about 15 feet. During the magnitude 7.1 Loma Prieta earthquake of 1989, a 25-mile segment of the San Andreas fault southwest of San Jose slipped about 7½ feet.

Geologists have matched up similar rocks on either side of the San Andreas fault to show that land in California to the west of the fault has moved nearly 200 miles to the northwest relative to land east of the fault during the last several million years. This motion has been producing major earthquakes for millions of years and will most likely continue to do so.

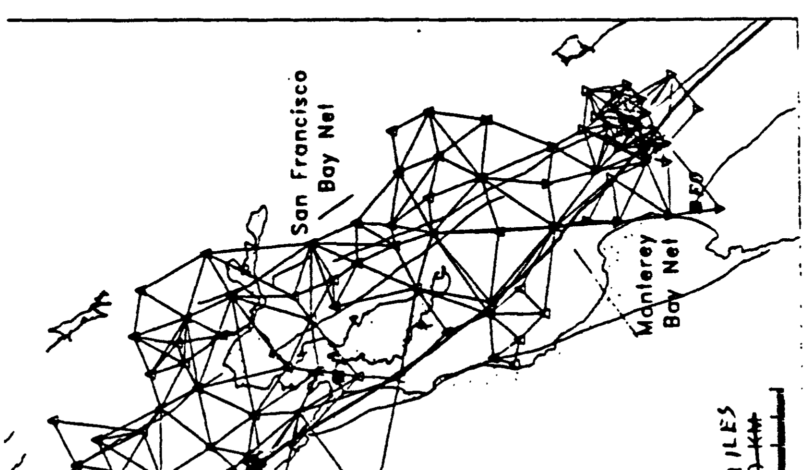

The average rate of strain build up and the amount of slip during earthquakes can be measured by precise surveying between mountain tops in the San Francisco Bay region. Accurate surveys since 1851 show that the average slip across the San Andreas, Hayward, Calaveras, and related faults is approximately 1½ inches per year. Additional movement of about ½ inch per year occurs on still other faults, including some in eastern California and western Nevada.

10. HOW SCIENTISTS DETERMINE THE PROBABILITY OF FUTURE EARTHQUAKES

One simple approach to determining the chance of another earthquake is to count the number of earthquakes that occurred in the past. Since 1836, there have been 5 earthquakes in the San Francisco Bay region with a magnitude of 6¾ or greater. If earthquakes occurred randomly over time, the region would experience another earthquake of this same magnitude in the next 30 years with a 50% probability. That is, there would be an even chance that an earthquake of this magnitude would occur sometime within the next 30 years.

But scientists know that earthquakes are **not** randomly spread over time. Studies show that earthquakes are **clustered** in time. An example of this clustering can be seen in the time line to the right. There were 16 earthquakes of magnitude 6 or larger throughout the San Francisco Bay region during the 70 years prior to 1906 and there were no events greater than magnitude 5½ during the 68 years between 1911 and 1979.

Apparently the amount of movement that occurred at the time of the 1906 earthquake was large enough to reduce strain throughout the region, reducing the likelihood that large earthquakes would occur. Since 1979, there have been six earthquakes greater than magnitude 5½, leading up to the recent Loma Prieta earthquake. Geologists are now concerned that the strain along the fault has built up again and that another major earthquake could occur.

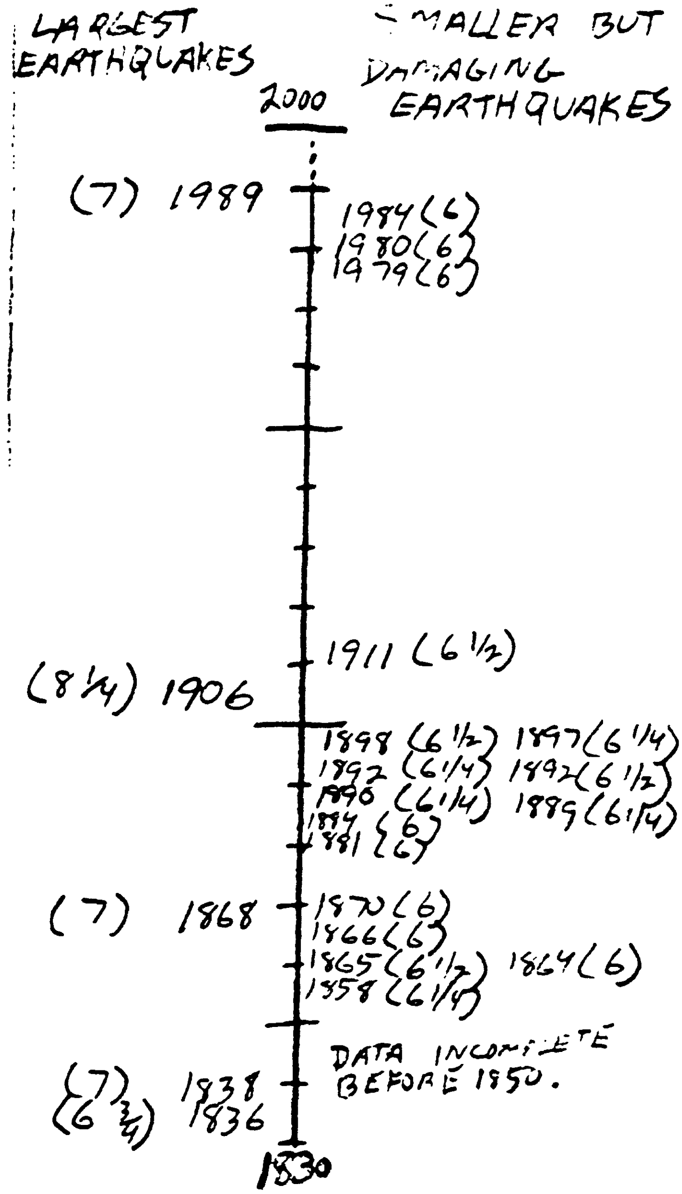

Earthquakes occur when a segment of a fault slips. The points where segments begin and end are often associated with changes in the direction of the fault, changes in the geology along the fault, and the intersection or interaction with nearby faults. The first step in anticipating future earthquakes is to determine which fault segments have slipped in the past. By determining the length of the segment, you can estimate the potential magnitude of the anticipated earthquake. For example, a magnitude 7 earthquake in California occurs when there is sudden slip on a fault segment 25 to 50 miles long. A magnitude 8 earthquake occurs when there is slip on connected segments whose total length is 200 or more miles.

Scientists have discovered that when the strain builds to a critical level, sudden slip occurs during an earthquake. The more slip during one earthquake, the longer, on average, until the next earthquake.

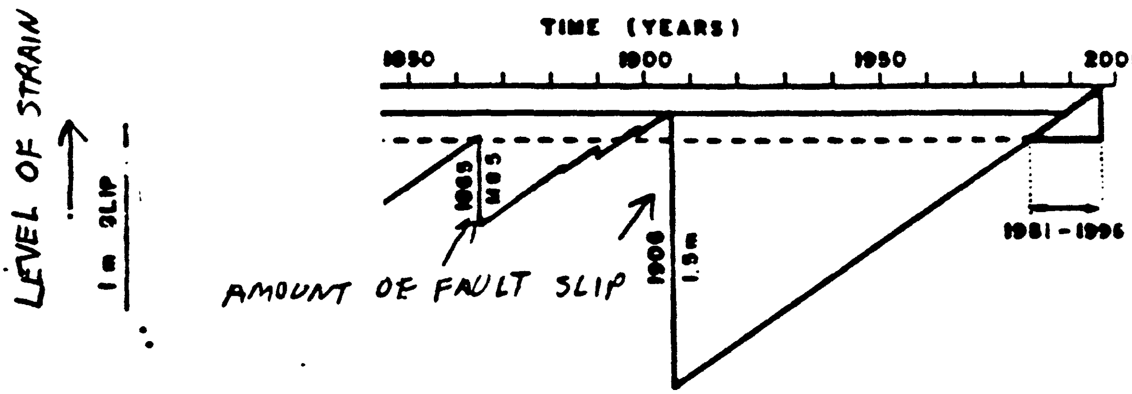

This graph shows how the strain increased at an average rate along the Loma Prieta segment of the San Andreas fault. Sudden slip that reduces the level of strain is believed to have occured along this segment during earthquakes in 1865, and 1906. The slip in 1906 was only about 5 feet, much less than the 15 feet of slip measured along parts of the San Andreas fault to the north. For these reasons scientists suggested in 1981 that another damaging earthquake might recur between then and 1996. The Loma Prieta earthquake of 1989 proved their projections correct.

Anticipating when the next earthquake will strike along a given fault segment involves determining how much strain was released in the last earthquake, how fast the strain is building up along the segment, and how long it has been since the last earthquake. With this information, scientists calculate the time required to rebuild the strain, or the recurrence time. Recurrence times for fault segments in the San Francisco Bay region are estimated to range from 70 to 280 years. Written history in California is less than 250 years long, but detailed studies of fault zones have allowed dating of a few prehistoric earthquakes.

Although the model is relatively simple, the information about strain is incomplete. Thus judgement is needed in interpreting the data.

In 1987, a national panel of experts was convened by the National Earthquake Prediction Evaluation Council for the sole purpose of determining the probabilities of future earthquakes along major faults in California. In 1988, this panel issued a report which is referenced below. The panel concluded that the probability of an earthquake of magnitude 7 or larger occurring in the San Francisco Bay region within 30 years was 50%. The panel also concluded that the most likely severe earthquake to occur in the San Francisco Bay region during the next 30 years was an event of magnitude 6½ or larger in the Santa Cruz Mountains.

This anticipated earthquake, the Loma Prieta earthquake, occurred one year later on October 17, 1989. The national panel of experts then reconvened to determine how the occurrence of that event changed the probabilities of future earthquakes. Their report, issued in June 1990 and referenced below, gives the following probabilities for individual fault segments:

Probabilities of Individual Earthquakes				
Fault Segment	Previous Event	Expected Magnitude	Average Recurrence Time	Probability
San Andreas SF Peninsula	1906	7	About 128±38	23%
Southern Hayward fault	1868	7	167±67	23%
Northern Hayward fault	1836	7	167±67	28%
Rodgers Creek fault	≥1808	7	≥222±74	22%

The panel concluded that when the probabilities of all likely earthquakes are combined in the most reasonable way, **there is a 2 to 1 chance that at least one earthquake of magnitude 7 or larger will occur in the San Francisco Bay region between 1990 and 2020.** Such an earthquake is just as likely to occur today as on any particular day 30 years hence.

Many details leading to the calculated probabilities are still being debated by scientists. These details include exactly where fault segments begin and end, the average recurrence time for each segment, the magnitude of anticipated earthquakes, the magnitude and amount of slip for some earthquakes in the 19th century that were not recorded by instruments, and the best statistical methods to use in calculating the probabilities.

Some scientists believe that the probability estimates may be too low. They are concerned because earthquakes of magnitude 6½ or larger in northern California have often occurred in pairs. An earthquake in 1865, similar to the earthquake of October 17, 1989, was followed 3 years later by a major earthquake on the Hayward fault. Other pairs occurred in 1836 and 1838, in 1892 and 1898, and in 1906 and 1911. Scientists do not understand why such pairing should exist.

Scientists have also noted an increase in the number of magnitude 5 earthquakes along the southern part of the Calaveras fault east of San Jose since 1979. A similar pattern of activity may have preceeded the Hayward fault earthquake of 1868.

The probability analysis does not account for these observations and it does not account for all of the slip anticipated between the plates in northern California. **Thus it**

seems prudent to consider the 2 to 1 chance as a minimum estimate.

While there is some debate among scientists over how to estimate probability, there is fundamental agreement that earthquakes of magnitude 7 and larger will occur in the future in the San Francisco Bay region and that each of these events has the potential to cause significantly more damage than the earthquake of October 17, 1989, because each will be located closer to densely populated areas.

There is also fundamental agreement that actions can be taken now that will dramatically reduce the amount of damage and death likely to occur during future earthquakes. **Such protective actions are very important, given that a severe earthquake is twice as likely as not to occur within the San Francisco Bay region at some time before the year 2020.**

A primary goal of continuing research on earthquakes is to be able to make these probability estimates more specific in the future, especially by reducing the time period within which each earthquake is expected to occur. Scientists are making progress, but they are still working with many unknowns. There are likely to be some surprises.

It may eventually be possible to predict hours to days in advance when a major earthquake is anticipated. If such predictions can be made, they will be released through the California Office of Emergency Services with an evaluation of their reliability after rapid but careful review by the California and National Earthquake Prediction Evaluation Councils. Such reviewed predictions should not be confused with predictions made by individuals. If you understand your relative risk from earthquakes, you will be in a good position to decide how to respond to such information.

We cannot control earthquakes, but we can control how much damage will occur during future earthquakes. We still have a great deal to learn about earthquakes, earthquake engineering, and earthquake hazard reduction. Yet enough is already known that we can take meaningful and cost-effective action now to reduce earthquake risk to an acceptable level.

Probabilities of large earthquakes occurring in California on the San Andreas fault, The Working Group on California Earthquake Probabilities, U.S. Geological Survey Open-File Report 88-398, 62 pages, 1988.

Probabilities of large earthquakes in the San Francisco Bay region, The Working Group on California Earthquake Probabilities, U.S. Geological Survey Open-File Report 90-XXX, 84 pages, 1990.

11. SOURCES FOR MORE INFORMATION

Your community library

Your county or city planning department

BAREPP, Bay Area Regional Earthquake Preparedness Project, MetroCenter, 101 8th Street, Suite 152, Oakland, CA 94607, (415) 540-2713.

ABAG, Association of Bay Area Governments, P.O. Box 2050, Oakland, CA 94604-2050, located at MetroCenter, 101 8th Street, Suite 152, (415) 464-7900.

Earth Science Information Centers, U.S. Geological Survey,

Menlo Park, CA 94025, 345 Middlefield Road, (415) 329-4390.

San Francisco, CA 94111, 555 Battery Street, Room 504 Customs House, (415) 705-1010.

FEMA, Federal Emergency Management Agency, Building 105, The Presideo, San Francisco, CA 94129, (415) 923-7100.

CDMG, California Department of Conservation, Division of Mines and Geology, P.O. Box 2980, Sacramento, CA 95812-2980, (916) 445-5716.

California Seismic Safety Commission, 1900 K Street, Suite 100, Sacramento, CA 95814-4186, (916)322-4917.

12. ENGINEERING ORGANIZATIONS PRIMARILY OF INTEREST TO PRACTICING ENGINEERS

Applied Technology Council, 3 Twin Dolphin Drive, Redwood City, CA 94065 (415) 595-1542.

EERI, Earthquake Engineering Research Institute, 6431 Fairmount Avenue, Suite 7, El Cerrito, CA 94530-3624, (415) 525-3668.

NISEE, Earthquake Engineering Research Center, University of California Berkeley, 1301 South 46th Street, Richmond, CA 94804, (415) 231-9554.

John A. Blume Earthquake Center, Department of Civil Engineering, Stanford University, Stanford, CA 94305, (415) 723-3074

13. SOME BOOKS ABOUT EARTHQUAKES AND EARTHQUAKE PREPAREDNESS

Earthquake preparedness and public information: An annotated bibliography (includes a listing of 245 books, pamphlets, and audio-visual publications divided into 16 topical areas for the non-technical audience), 1985, 86 pages (ABAG P87058BAR $8 +$1.60 P&H).

Earthquake ready, by Virginia Kimball, Roundtable Publishing, Inc., Santa Monica, California, 225 pages, 1988 ($13.95).

Earthquakes, by Bruce Bolt, W.H. Freeman, New York, 282 pages, 1988 ($13.95)XXX.

Earthquakes, by Don DeNevi, Celestial Arts, Millbrae, California, 230 pages, 1977 (out of print).

Earthquakes, by Bryce Walker, Time-Life Books, Alexandria, Virginia, 176 pages, 1982 (out of print).

On shaky ground: America's earthquake alert, by John J. Nance, Avon Books, New York, 440 pages, 1989 ($4.95).

Predicting the next great earthquake in California by R.L. Wesson and R.E. Wallace, Scientific American, v. 252, no. 2, p.35-43, 1985.

Terra non firma, by J.M. Gere and H.C. Shah, W.H. Freeman, New York, 203 pages, 1984 ($12.95).

The San Francisco Bay area--On shaky ground by J.B. Perkins, Association of Bay Area Governments, Oakland, California, 32 pages, 1987. (ABAG P87001EQK $8.00+$2.00PH)

14. MAGAZINES ABOUT EARTHQUAKES AND EARTHQUAKE PREPAREDNESS

Networks, earthquake preparedness news, Periodic Publication of BAREPP. Free.

Earthquakes and volcanoes, A bimonthly publication of the U.S. Geological Survey available yearly for $9.00 from the Superintendent of Documents, U.S. Government Printing Office, Washington, D.C. 20402, or by credit card at 202-783-3238.

15. ABOUT ORDERING BOOKS AND MAPS

Ask you local library to see the publications listed in this document. If you want to order copies, send an order to the institution listed in parentheses including the full reference, the money for the publication and postage and handling charges listed, and 7.25% sales tax. USGS orders by mail must include $1.00 P&H.

List OES and Red CRoss Offices???

This document was written by Peter L. Ward, USGS, with significant input from Richard Eisner, BAREPP; Jeanne Perkins, ABAG; Jim Davis, CDMG; Dennis Mileti, Colorado State University; Joanne Nigg, University of Delaware; Bill Bakun, Bob Brown, Bill Ellsworth, Tom Hanks, Tom Holzer, Bill Kockelman, Al Lindh, Will Prescott, Bob Wallace, and Randy White USGS.

Editing by Helen Gibbons, USGS.